Electronically distinctive cyclic phosphanes: synthesis and structural modifications toward the control of chemical and electronic properties.

Kyle Gaia Pearce

Department of Chemistry

School of Life Sciences

University of Sussex

A thesis submitted for the degree of Doctor of Philosophy

April 2021

Declaration

I hereby declare that this thesis has not been and will not be, submitted in whole or in part to another University for the award of any other degree.

Signed ……..

Kyle Gaia Pearce

Publications

Work from this thesis, and carried out in the duration of the PhD have been included in the following publications:

Controlled Reactivity of Terminal Cyaphide Complexes: Isolation of the 5-Coordinate $[Ru(dppe)_2(C{\equiv}P)]^+$

Madeleine C. Levis, Kyle G. Pearce and Ian R. Crossley, *Inorg. Chem.*, 2019, **58**, 14800-14807.

Phosphacycloalkyldiones: synthesis and coordinative behaviour of 6- and 7-member cyclic diketophosphanyls

Kyle G. Pearce, Vladimir Simenok and Ian R. Crossley, *Dalton Trans.*, 2020, **49**, 5482-5492.

Diphosphametacyclophanes: Structural and Electronic Influences of Substituent Variation within a Family of Bis(diketophosphanyl) Macrocycles

Kyle G. Pearce and Ian R. Crossley, *J. Org. Chem.*, 2020, **85**, 14697-14707.

A Benzodiphosphaborolediide

Kyle G. Pearce, Elinor P. F. Canham, John F. Nixon and Ian R. Crossley, 2021, *Submitted.*

Acknowledgements

There are almost too many people to thank! First and foremost, I would like to thank my supervisor Ian for accepting me for this PhD, putting up with my excessive enthusiasm and helping me throughout the whole process. Your passion for chemistry is infectious and I am truly indebted to you for all of your guidance. I would also like to thank Ewan for sparking my interest in research during my time at Kent and making me believe in myself.

I have thoroughly enjoyed my time at Sussex and I leave with a heavy heart, though I'm sure I'll be back to visit! Anyone who has had the pleasure of working in Lab 14 knows it's a special place, with a lot of chemical history to its name…and the scars to tell it, but past the bricks and mortar, it's the spirit of those who work within that really make it. On that note, I'd like to thank the Crossley group as a whole, with a special mention to Sam for making me feel welcome from the very beginning and checking up on me till the bitter end, to ensure all was going well and Maddie, for all of the tea breaks. I'd also like to thank Nikos, a legend of the lab, for all of the crystallography discussions; Rick, James and Siobhan, although you all only arrived in L14 toward the end of my PhD, its been a pleasure to work with you all and thanks for keeping me entertained, well fed (Siobhan) and introducing me to squash (R & J). Thanks to all of the masters/summer students and everyone else from Lab 14, it would not have been the same without any of you.

I'd also like to give thanks to Geoff, John and John (Turner and Spencer) for their continued support, encouragement and advice in my thesis committees. I'd also like to thank the service providers Dr Iain Day, Dr Alla Abdul-Sada, Dr Mark Roe and Verity Holmes for their invaluable assistance.

Last but not least, thank you to my family and friends for their continued support and encouragement, especially Amy, without your support this whole journey would not have been possible. Thanks for always being there for me.

P.S. I won't judge you if you stop reading now.

Abbreviations

The following abbreviations have been used in this thesis:

δ	Chemical Shift
$\{^1H\}$	Proton Decoupled
°	Degrees
°C	Degrees Celcius
Å	Angstrom
Ar	Arene
cm^{-1}	Wavenumber
COD	1,5-Cyclooctadiene
Cp	Cyclopentadienyl
CV	Cyclic Voltammetry
br	Broad
d	Doublet
DBU	1,8-Diazabicyclo[5.4.0]undec-7-ene
DCM	Dichloromethane
DFT	Density Functional Theory
DME	Dimethoxyethane
DMSO	Dimethylsulfoxide
dppe	1,2-bis(diphenylphosphino)ethane
E½	Half-Wave Potential
EI	Electron Ionisation
ESI-MS	Electro-spray Ionisation Mass Spectrometry

Et	Ethyl
eV	Electronvolt
E_{pa}	Oxidation Peak Potential
E_{pc}	Reduction Peak Potential
Fc	Ferrocenyl
Hz	Hertz
HMBC	Heteronuclear Multiple Bond Correlation
HOMO	Highest Occupied Molecular Orbital
HSQC	Heteronuclear Single-Quantum Coherence
i-	Ipso
^{i}Pr	Isopropyl
IR	Infrared
^{x}J	Scalar Coupling (*J*), Coupling Constant Over x Bonds (^{X}J)
K	Kelvin
L	Ligand
LUMO	Lowest Occupied Molecular Orbital
M	Molar
m	Multiplet
m-	Meta
m/z	Mass/Charge Ratio
mbar	Millibar
Me	Methyl
Mes	Mesitylene

MS	Mass Spectrometry
^{n}Bu	n-Butyl
NBO	Natural Bond Order
NICS	Nucleus-Independent Chemical Shift
nm	Nanometers
NMR	Nuclear Magnetic Resonance
o-	Ortho
OLED	Organic Light Emitting Diode
OTf	Triflate
p-	Para
Ph	Phenyl
ppm	Parts Per Million
PPV	Poly(-phenylenevinylene)
q	Quartet
quin	Quintet
s	Singlet
t	Triplet
TBAF	Tetrabutylammonium Fluoride
^{t}Bu	Tert-butyl
THF	Tetrahydrofuran
TMS	Trimethylsilyl
UV/Vis	Ultraviolet/Visible

Abstract

This thesis describes the synthesis and development of novel cyclic phosphanes, with the intent to exploit their electronic character and subsequently explore their respective reactivities.

A family of diphosphametacyclophanes bearing the electronically distinctive diketophosphanyl functionality are prepared from reacting $RP(SiMe_3)_2$ (R = Me, Ph) with the respective diacyl chloride and were characterised spectroscopically and unequivocally by single-crystal X-Ray diffraction. The aromatic 5-R substituent can influence the displacement angle between π-systems, allowing control over the cavity size, which could hold promise for metal sequestration. Electronically, it was found that the LUMO was more stabilised for weaker donating substituents and overall exhibit no delocalisation/conjugation around the macrocyclic core; instead the two diketophosphanyl units are essentially discretely isolated. Attempts to enhance their electron acceptor character *via* oxidation was unsuccessful, yet these macrocycles coordinate to transition metals, facilitating the synthesis of $[M(\eta^4\text{-}C_8H_{12})Cl\{3\text{-}C(O)\text{-}C_6H_4\text{-}(C(O)PMe)\}_2]$ (M = Rh, Ir) and $[\{Pt(PEt_3)Cl_2\}_2\{3\text{-}C(O)\text{-}C_6H_4\text{-}(C(O)PPh)\}_2]$.

The first examples of 6- and 7-membered saturated phosphorus heterocycles bearing the diketo-functionality, $RP\{C(O)\}_2C_nH_{2n}$ (n = 3, 4; R= aryl, alkyl) have been synthesised and fully characterised. The coordination chemistry of these species has been explored including a series of tungsten-pentacarbonyl complexes, which were prepared and elucidated spectroscopically and by X-Ray diffraction. Data suggest these heterocycles are relatively weak σ-donors, placing them between traditional phosphanes and phosphites in this regard.

In tangential studies, novel trifluorophosphalkenes ($RP{=}C(OSiMe_3)CF_3$) are pursued by reacting the respective bis-silylated phosphane, $RP(SiMe_3)_2$ (R = Ph, ^{t}Bu, Mes, $SiMe_3$) with one equivalent of trifluoroacetic anhydride, leading to the isolation of both the E- and Z-isomers. The reactivity of these phosphaalkenes has been explored, including [4+2] cyclicadditions to afford cyclic species such as $Me_3SiPCH_2CHCHCH_2C(OSiMe_3)(CF_3)$, which was tentatively identified. Similarly, reactions with $LiN(SiMe_3)_2$ afford a range of complex products at ambient temperature, but with evidence for trifluoromethylphosphaalkyne below −20 °C, respectively. Efforts to effect coordination are outlined, demonstrating an unexpected variability in coordination mode.

Finally, the first dianionic diphosphaboracycles ($[C_6P_2BC_6H_5]^{2-}$ $2[Li(THF)_{1.5}]^{2+}$, $[C_6P_2BC_6H_5]^{2-}$ $2[Li(TMEDA)]^{2+}$) are synthesised from the reaction between 1,2-bis(phosphino)benzene and dichlorophenylborane. The reactivity and coordination chemistry of which has been extensively explored leading to a series of novel compounds, including a η^5, η^1, η^1-trimolybdenum complex, confirming that the diphosphaboracycle can act as a π-ligand with metals other than lithium.

Contents

Chapter 1 - Introduction

"The chemists are a strange class of mortals, impelled by an almost insane impulse to seek their pleasures amid smoke and vapour, soot and flame, poisons and poverty; yet among all these evils I seem to live so sweetly that may I die if I were to change places with the Persian king."

--Johann Joachim Becher 1635-1682

This introduction aims to broadly cover the importance of phosphorus chemistry, with a particular focus upon the incorporation of electronically distinctive phosphorus motifs within π-conjugated materials, a subject of relevance for both **Chapters 2** and **3**. In contrast, a more relevant introduction is included at the start of **Chapters 4** and **5**.

1.1 Phosphorus "The Philosopher's Stone"

Phosphorus, also known as 'the devil's element', was first discovered in 1669 by alchemist Hennig Brandt;[1] it was first isolated by the putrefaction of urine for several days and then boiling down to a paste which was subsequently distilled at higher temperatures, the vapour from which was condensed under water to give the element as "a white waxy substance that glowed in the dark when exposed to air".[2] The source of white phosphorus has since been improved, involving the heating of phosphate rock (calcium phosphate) to 1200-1500 °C in the presence of sand and refined coal to produce P_4 vapour, which is condensed under water to afford P_4 as a white solid.[3] Phosphorus is the 11th most abundant element on earth and exhibits an extensive and varied chemistry with applications ranging from fertilisers and fire retardants to the crucial role it plays In the biochemistry of all living things.[4,5]

Within the realms of inorganic chemistry, phosphorus exhibits reactivity with elements from across the periodic table; more specifically, organophosphorus chemistry is diverse, phosphorus being able to adopt a range of different coordination numbers (σ), valencies (λ) and geometries.[6] For organophosphorus chemistry these can be divided into the categories in **Figure 1**, **Table 1**.[7]

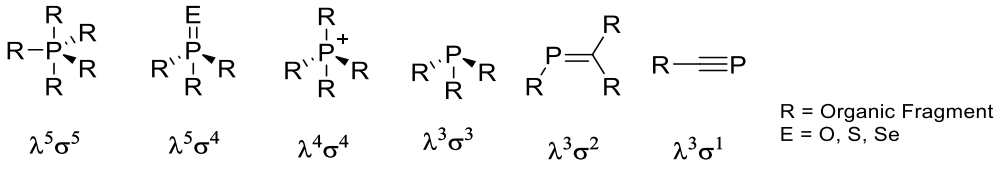

Figure 1. *Different categories of organophosphorus compounds.*

Table 1. *Organophosphorus categories and relevant examples of each.*

Organophosphorus Categories	***Relevant Examples***
λ^5, σ^5	*PR_5, $P(OR)_5$*
λ^5, σ^4	*OPR_3, $OP(OR)_3$, EPR_3 (E = S, Se, Te)*
λ^4, σ^4	*$[PR_4]^+[X]^-$*
λ^3, σ^3	*PR_3, $P(OR)_3$*
λ^3, σ^2	*RP=R,*
λ^3, σ^1	*P≡R,*

This thesis focuses primarily on tri- and di-coordinate organophosphorus species, therefore literature regarding tertiaryphosphanes and phosphaalkenes will be reviewed, including defining characteristics, synthetic methodologies and applications.

1.2 Phosphanes

The most commonly documented phosphorus-containing species are phosphanes, they are neutral two-electron donor compounds (L-type ligands), adopting a trigonal-pyramidal geometry.[8] Phosphanes can be divided into the sub-categories: primary (**1.1a**), secondary (**1.1b**) and tertiary (**1.1c**), with the last of these having numerous sub classes, for example: phosphomides (**1.2a**), diphosphanes (**1.2b**), cyclic-phosphanes (**1.2c**) and phosphites (**1.2d**; **Figure 2**). This thesis investigates tertiary phosphanes, with a particular interest in phosphomides, aryl diphosphanes and cyclic-phosphanes.

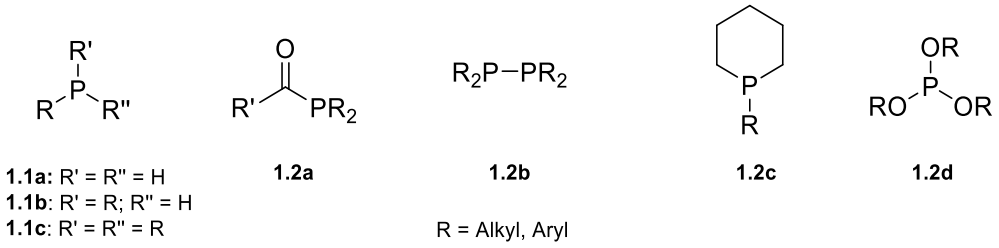

1.1a: R' = R" = H
1.1b: R' = R; R" = H
1.1c: R' = R" = R

1.2a **1.2b** **1.2c** **1.2d**

R = Alkyl, Aryl

Figure 2. *Sub-categories of phosphanes.*

1.2.1 Preparation of Tertiary Phosphanes

There are a variety of different routes to synthesise tertiary phosphanes (PR_3), though some feature in the literature more frequently than others. Classical methods involve the use of phosphane (PH_3), PCl_3 or $P(SiMe_3)_3$. Phosphane gas is produced on an industrial scale from the reaction of P_4 with MOH (M = Na, K), while PCl_3 is synthesised from P_4 and Cl_2.[1] Alternatively, $P(SiMe_3)_3$ is prepared by heating P_4 or red phosphorus at reflux with Na and Me_3SiCl (**Scheme 1**).[9] After workup both PCl_3 and $P(SiMe_3)_3$ are subsequently purified by distillation.

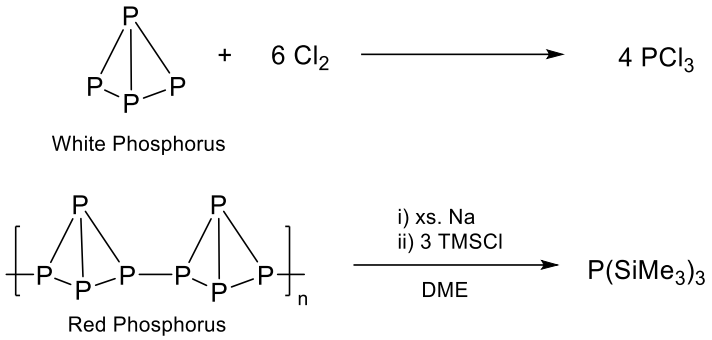

Scheme 1. *Preparation of PCl_3 and $P(SiMe_3)_3$.*

The preparation of tertiary phosphanes is then undertaken *via* several general reactions, for example phosphane gas (PH_3) can be reacted with NaO^tBu to generate the corresponding metal phosphide, the addition of RX to this species affords the desired tertiary phosphane (illustrated in **Scheme 2a** with 1-bromonapththalene).[10] Other methods include generating a lithium phosphide and subsequently reacting with a halogenated substrate such as an alkylhalide (**Scheme 2b**).[11,12] In contrast, lithiated organic substrates such as lithium alkynyls can be reacted with halophosphanes to functionalise the phosphorus centre (**Scheme 2c**).[13] Alternatively, treating halophosphanes with Grignard reagents, such as the addition of PhMgX to PCl_3, affords PPh_3 (**Scheme 2d),** though tertiary phosphanes can also be prepared by catalytic dehydrocoupling of primary phosphanes (**Scheme 2e**), *via* radical reactions (**Scheme 2f**)[14] and even from the photolytic reaction of P_4 and ArX (**Scheme 2g**).[15]

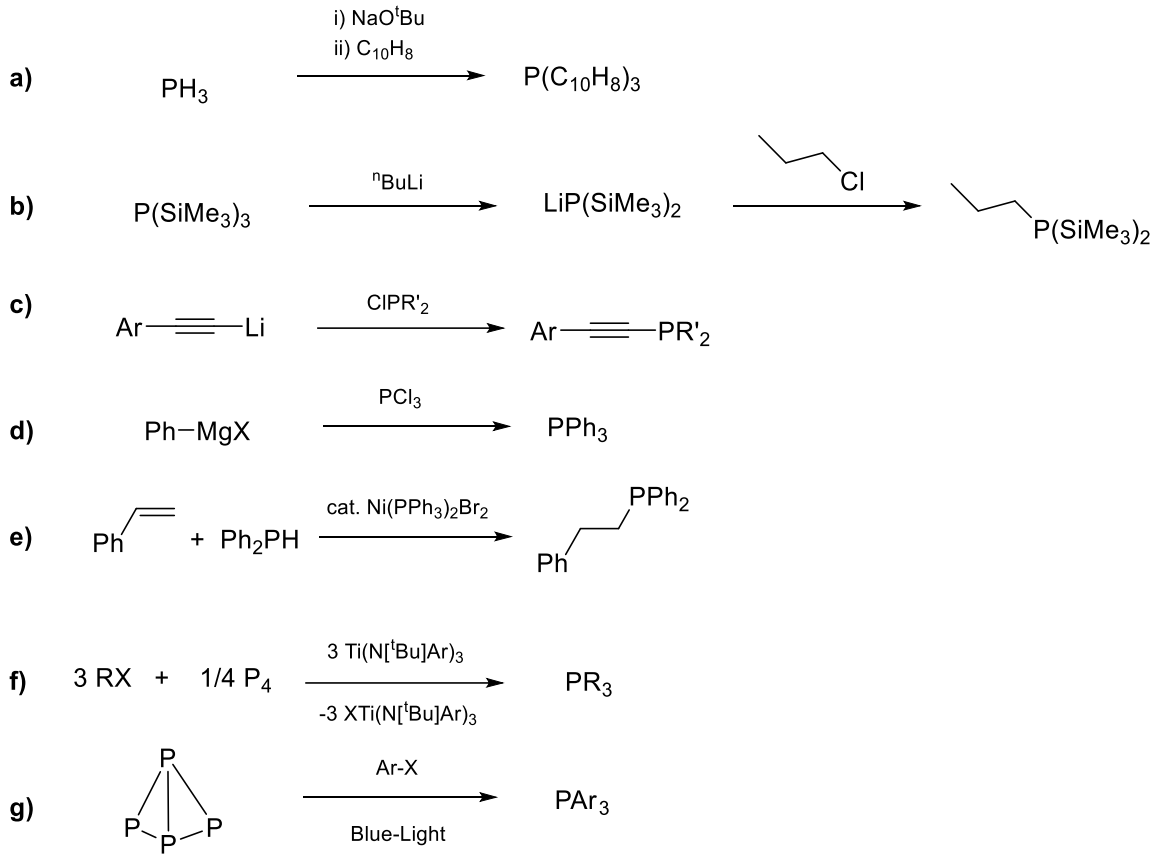

Scheme 2. *Selected examples for the synthesis of phosphanes.*[11-15]

1.3 Applications of Phosphanes

1.3.1 Steric and Electronic Properties

Phosphanes of all types play a major role in coordination and organometallic chemistry.[16] Phosphanes are commonly employed as ancillary ligands as a result of their capacity to augment and control reactivity due to the tunability of their electronic and steric properties. In 1977, Tolman documented a quantitative way to measure the electron donating or withdrawing ability of a ligand (L), by measuring and comparing the A_1 CO vibrational mode (ν_{CO}) for complexes of the type $[LNi(CO)_3]$, exhibiting C_{3v} symmetry,[17] the resulting carbonyl stretch now being known as the Tolman electronic parameter (TEP). However, Tolman noted that the coordination behaviour of $[R_3PNi(CO)_3]$ complexes could not be explained purely by electronic effects and discussed the relationship between steric and electronic parameters. This led Tolman define an additional measure, to assess the steric bulk of a ligand in a $[LNi(CO)_3]$ complex, defined as "the solid angle formed with the metal at the vertex and the outermost edge of the van der Waals spheres of the ligand atoms at the perimeter of the cone" (**Figure 3**, **Table 2**), now known as the Tolman cone angle. Though this method is based on $[LNi(CO)_3]$ complexes, there are conversion factors which can be used for alternative metal complexes.[18]

One example that highlights the relationship between sterics and electronic features, is the competing reactivities of PMe_3 and P^tBu_3 toward $[Ni(CO)_4]$; PMe_3 is found to coordinate to $[Ni(CO)_4]$ preferentially, despite the greater basicity of P^tBu_3, as assessed on the basis of their respective A_1 stretching frequencies ($[Ni(CO)_3P^tBu_3]$; ν_{CO} 2056 cm^{-1}, $[Ni(CO)_3PMe_3]$; ν_{CO} 2064 cm^{-1}). This effect was explained as a result of steric hindrance, the bulky tertiary-butyl substituents clashing (cone angle 106◦, *cf*. 98.9◦ ($[Ni(CO)_3PMe_3]$) with the CO ligands of the metal complex, in comparison to the less sterically crowded methyl groups. Together, the TEP and Tolman cone angle have become powerful tools for assessing the steric and electronic properties of different phosphanes, which are important characteristics for catalysis.

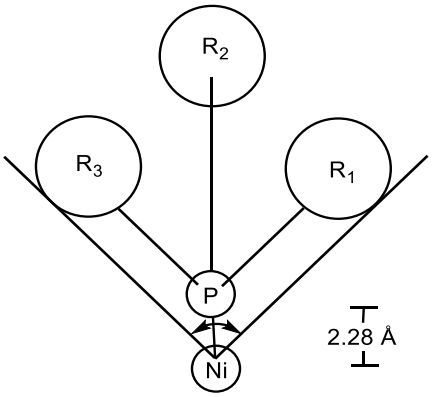

Figure 3. *Example of the Tolman cone angle.*[17,18]

Table 2. *Tolman electronic parameters and Tolman cone angles of common phosphane complexes $[Ni(CO)_3PR_3]$.*[17]

Phosphorus Ligand	***ν_{CO} (cm^{-1})***	***Cone Angle (◦)***
P^tBu_3	*2056*	*106*
PMe_3	*2064*	*98.9*
PPh_3	*2069*	*103*
PH_3	*2083*	*93.8*
PCl_3	*2097*	*100*

1.3.2 Catalysis

The size of a phosphane ligand has been shown to affect the reactivity of the metal centre to which it is coordinated, enabling catalytic control. For example, gold catalysed cycloaddition reactions with a P^tBu_2(o-biPh) (o-biPh = 2-biphenyl) supporting ligand follow a 1,2-H-shift pathway, whilst the same reaction with the smaller $(PhO)_3P$ ligated system alternatively undergoes a 1,2-alkyl-shift (**Scheme 3**).[19] Another example is the hydroformylation of styrene using 2,2'-dimethyl-1,1'-binaphthyl phosphanes in the presence of $[Rh(CO)_2(acac)]$, in this instance the enhanced basicity at phosphorus upon the

introduction of more electron donating substituents on phosphorus (NMe_2-C_6H_4), results in a higher enantiomeric excess (ee = 48 % (R)) than for alkyl and aryl analogues (ee = 20 % (R)).[20,21]

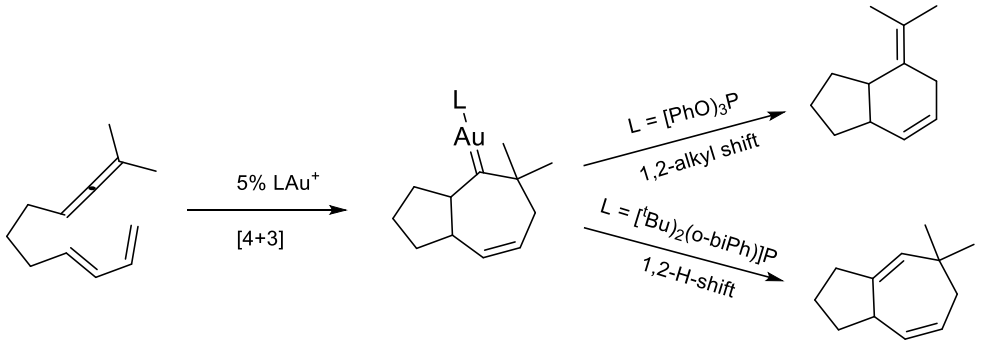

Scheme 3. *Reactivity differences between $(PhO)_3P$ and $(^tBu)_2$(o-biPh)P ligands in gold(I)-catalysed cycloaddition.*[19]

Phosphane ligands are now ubiquitous in catalysis and some important complexes which stand out for their prevalent use include Wilkinson's catalyst [$RhCl(PPh_3)_3$], widely used for the hydrogenation of alkenes, the mechanism of which has been described as the most extensively studied in catalytic research (**Scheme 4**).[22,23,24] Other common examples include Vaska's complex ([$IrCl(CO)(PPh_3)_2$]) which is also utilised for the hydrogenation of unsaturated organic substrates,[25] the first generation Grubbs catalyst [$RuCl_2(CHPh)(PCy_3)_2$],[26] which is famously employed to catalyse ring opening metathesis,[27]and [$Pd(PPh_3]_4$], widely used for carbon-carbon bond formation within the Heck reaction,[28] Suzuki-,[29] Stille-,[30] Sonogashira- and Negishi-coupling.[31,32]

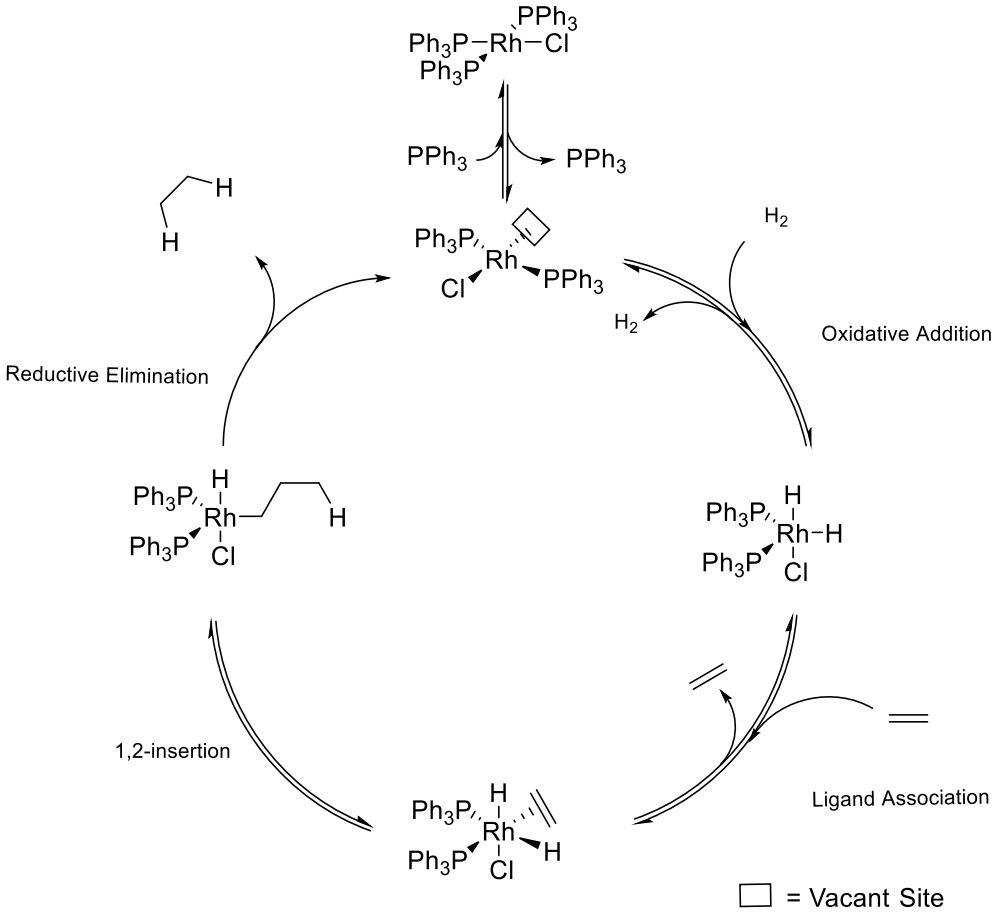

Scheme 4. *Mechanism for the hydrogenation of alkenes using Wilkinson's catalyst.*[24]

Chiral phosphane ligands have been incorporated into metal complexes leading to asymmetric catalysis,[33] and since the first report of asymmetric hydrogenation by Knowles and co-workers in 1968, a library of chiral mono- and diphosphanes has been reported; **Figure 4** highlights some early examples.[33] Of the chiral phosphanes, it has been noted that the use of diphosphane ligands yields efficient enantioselective catalysis, for example the asymmetric hydrogenation of alkenes exhibiting over 95% ee.[33]

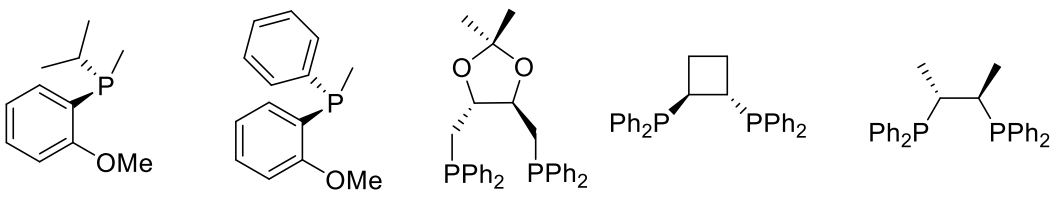

Figure 4. *Early examples of chiral mono- and diphosphanes used in asymmetric hydrogenation.*[33]

One chiral diphosphane ligand that is widely used in asymmetric catalysis is 2,2'-bis(diphenylphosphino))-1,1'-binaphthyl (BINAP; **1.3a**). For example BINAP is used in Noyori asymmetric hydrogenations, in which ketones and related functional groups are enantioselectively reduced. These hydrogenations are used in the production of several drugs including the antibacterial levofloxin and antibiotic carbapenem.[34] Since the discovery of BINAP the field of asymmetric catalysis and the pool of chiral-phosphanes has been ever expanding, initially by the structural modification of the BINAP ligand itself to improve enantioselectivity; common modifications included variation of the aryl substituent at phosphorus as well as alterations to the biaryl skeleton. Subsequently, inspired by the BINAP ligand, novel chiral diphosphanes were developed, one such example being the disubstituted-cyclophane PHANEPHOS (**Figure 5**; **1.3b**),[35] which exhibits enhanced selectivity over its carbon-based analogues. PHANEPHOS locks the catalytically active species (**1.3c**) into a specific conformation, thus affording the product as a single enantiomer, for example the hydrogenation of dehydroamino acid methyl esters results in 99% ee with complete conversion.[36,37]

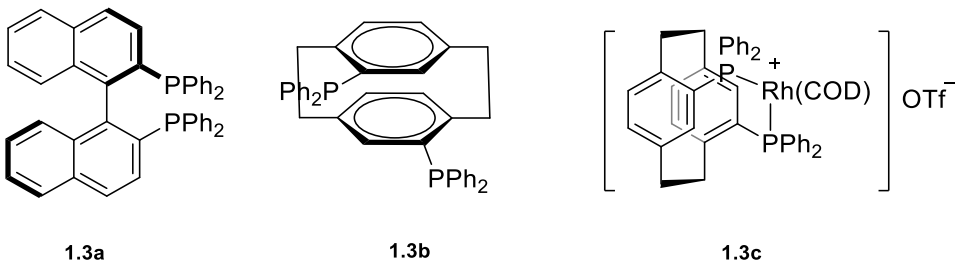

1.3a **1.3b** **1.3c**

Figure 5. *BINAP, PHANEPHOS, and the BINAP catalytically active species.*[35-37]

The application and general importance of phosphane chemistry extends further than catalysis,[33] another common application of phosphanes includes their use as reducing agents, such as in the Staudinger- and Wittig-reactions, where the ease with which phosphanes are oxidised is exploited. The Staudinger reaction enables the reduction of azide functionalities *via* an iminophosphorane intermediate, generating amines or amides without the requirement of harsh conditions (**Scheme 5a**).[38,39] Similarly, in the Wittig-reaction alkenes are prepared from their respective aldehyde or ketone starting materials *via* a phosphaylid (**Scheme 5b**). This method is advantageous over more conventional reducing agents as even sterically hindered ketones can be converted to their alkene derivatives.[40] Phosphanes are also employed as reducing agents in the Mitsunobu reaction, in which primary and secondary alcohols are converted to esters, ethers, thioethers, imides or azides with PPh_3 and an azodicarboylate (typically DEAD or DIAD; **Scheme 5c**).[41] However, phosphorus chemistry is not limited to purely synthetic applications, phosphanes also find use within materials chemistry, for

example within organic light-emitting diodes (OLEDs) and organic photovoltaic cells (OPV cells); phosphanes are also used in the preparation of π-conjugated materials more generally, a subject of significance for this thesis.[42,43,44,45]

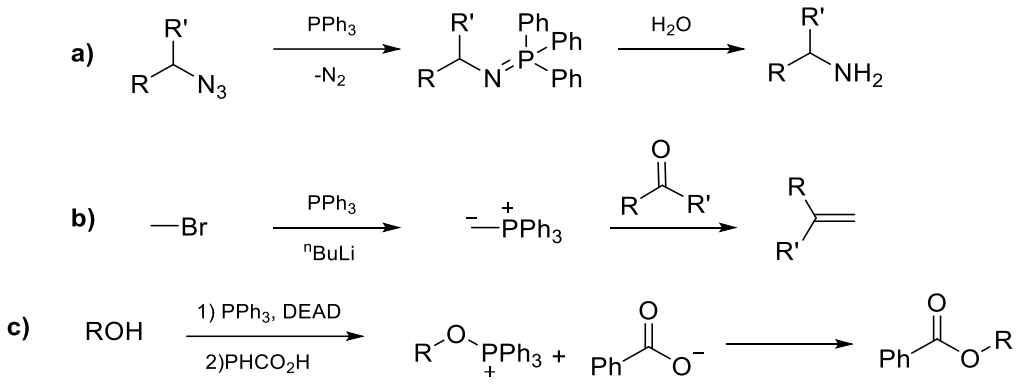

***Scheme 5**. The Staudinger, Wittig and Mitsunobu Reactions.*[38,40,41]

1.4 π-Conjugated Materials

One area of particular prominence in modern chemical science is molecular electronics, which offers the possibility of efficient light-weight and flexible electronic devices which are significantly reduced in size relative to conventional electronic components.[46] Organic π-conjugated polymers such as polyaniline, polypyrrole and polyacetylene have been explored in this regard as they exhibit electron delocalisation along the polymeric chain which acts as a path for charge transport, resulting in semi-conducting properties (**Figure 6**).[47] These functionalities have therefore been utilised within high-performance electronic devices such as organic light emitting diodes (OLEDs),[48,49] photovoltaic cells,[50] electrochromic windows and polymeric sensors.[51,52]

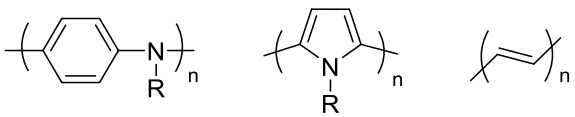

***Figure 6.** Poly(aniline), poly(pyrrole) and poly(acetylene).*

It has been well documented that the performance of these organic π-conjugated materials is predominantly controlled by their chemical structure, augmented by intermolecular interactions such as π-π-stacking.[53] Research has therefore focused on making subtle structural modifications to tune the optoelectronic behaviour of π-conjugated materials by altering their electronic properties (e.g.

band gap),[54,55] these structural modifications include the incorporation of electron donating or withdrawing groups to influence the electronics of the system. Similarly, the planarity of the molecule as well as the packing arrangement in the solid state have been shown to influence the nature and extent of intermolecular interactions and thus alter the electronic properties; the degree of steric bulk present is a key feature in this regard. Another important approach is to increase the degree of conjugation present in the system, enhancing electron delocalisation and thus lowering the energy of the LUMO, affording red-shifted absorptions.[56]

The incorporation of organophosphorus building blocks (**Figure 7**)[51] has recently been used as a method for tailoring the properties of π-conjugated systems. The presence of phosphorus results in an n-π* transition from the phosphorus lone pair which is therefore not observed for carbocentric analogues, affording markedly different HOMO-LUMO energies and thus electronic properties. In addition to this, much-like carbon-based systems the frontier molecular orbitals are predominantly controlled by the chemical structure and the structural dependence in this regard has been investigated for phosphorus-based building blocks, including arylphosphanes, phospholes, phosphaalkenes and diphosphenes.[51]

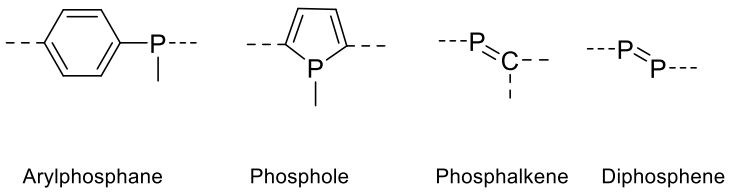

Figure 7. *Phosphorus-based building blocks for π-conjugation.*[51]

1.4.2 Phosphorus Incorporation into π-Conjugated Materials

The incorporation of phosphorus (**Figure 7**) into π-conjugated materials was first reported in the 1990s; these compounds exhibit notably different properties to their nitrogen based analogues.[57] This difference stems from nitrogen possessing a lower inversion barrier (*ca*2-5 kcal mol^{-1}), thus being able to achieve an optimum planar configuration facilitating the interaction of its lone pair with neighbouring carbon p-orbitals, whereas for phosphorus the inversion barrier is much higher (30-35 kcal mol^{-1}) and consequently planar geometry is harder to achieve.[51,58,59] However, the pyramidal geometry of phosphorus allows for negative hyperconjugation upon oxidation and thus pronounced electron acceptor character (pentavalent phosphoryl species; *vide infra*). Moreover, the lone pair is more accessible for further functionalisation (e.g. metal coordination), a useful method for tuning the electronic properties.

The incorporation of unsaturated phosphorus functionalities into π-conjugates promotes electron delocalisation of the π-system, whereas the inclusion of a reactive heteroatom allows for post-synthetic modifications and thus the tuning of the frontier molecular orbitals. These properties highlight why phospholes are currently the most extensively studied phosphorus-based building block for π-conjugated materials. Another method to 'tune' the electronics of phospholes is to alter the substituents in the 2,5-positions; for example incorporating the electron-rich 2-thienyl functionality (**1.4a; Figure 8**) results in notably red-shifted absorptions ($\Delta\lambda_{max}$ = 58 nm) relative to compound **1.4b**.[60] Similarly, compound **1.4a** exhibits an even more pronounced redshift than when incorporating 2-pyridyl groups (**1.4c**; $\Delta\lambda_{max}$ = 36 nm). It has been calculated that the HOMO-LUMO separation decreases for the series in the order: **1.4b** > **1.4c** > **1.4a**, with the pronounced π-conjugation observed for **1.4a** resulting from a "better interaction between the HOMO of the phosphole and thiophene units, compared to that with pyridine", though compounds **1.4a**-**1.4c** all exhibit fluorescence, **1.4b** and **1.4c** exhibiting emission at 463-466 nm, whereas compound **1.4a** is significantly red-shifted emitting at 501 nm.[44]

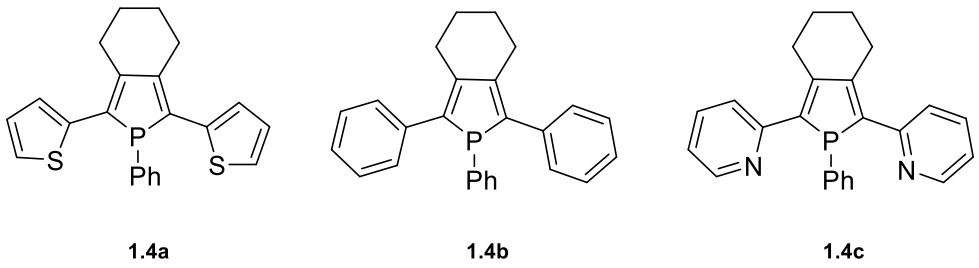

1.4a **1.4b** **1.4c**

***Figure 8**. Phospholes with varied 2,5-aryl substituents (**1.4a**-**1.4c**).[60]*

Incorporating an isoelectronic analogue of C=C (P=C) has a drastic effect on the electronic behaviour, as exemplified by compound **1.5**, which exhibits intense blue fluorescence.[61] The fluorescence can be modified by altering the substituent at the 2-position, for example changing the aryl unit to an alkyl resulted in a higher LUMO energy and thus a blue-shift.[62] Phosphorus building blocks are now being embedded into extended π-conjugated frameworks, common examples including poly(p-phenylenediethynylene phosphane)s (PPYPs; **Figure 10**), which can exhibit luminescence in both solution and in the solid-state.[63] The incorporation of dialkyloxy groups (**1.6c**) results in a slight blue-shift relative to compound **1.6b** (Δλ = 4 nm) with comparable absorptions noted for compound **1.6d**,

alternatively, the incorporation of a fluorene group (**1.6e**) results in a red shift of 24 nm relative to **1.6b**. The photo-physical properties of polymer **1.6a** could not be analysed due to its insoluble nature.

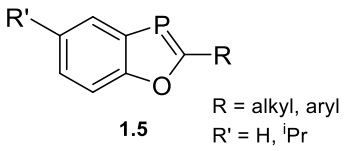

Figure 9. *1,3-Benzoxaphospholes.*[61]

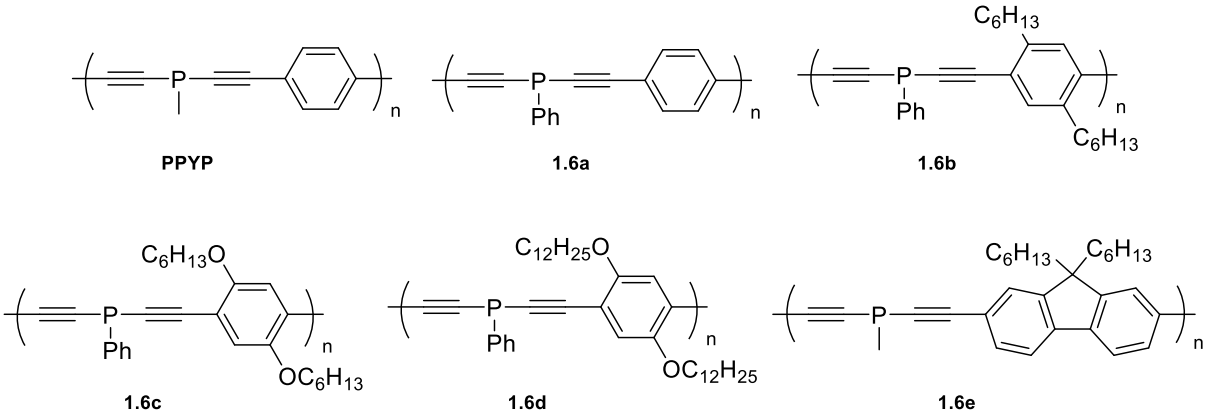

Figure 10. *Generic structure of a PPYP and series of PPYPs.*[63]

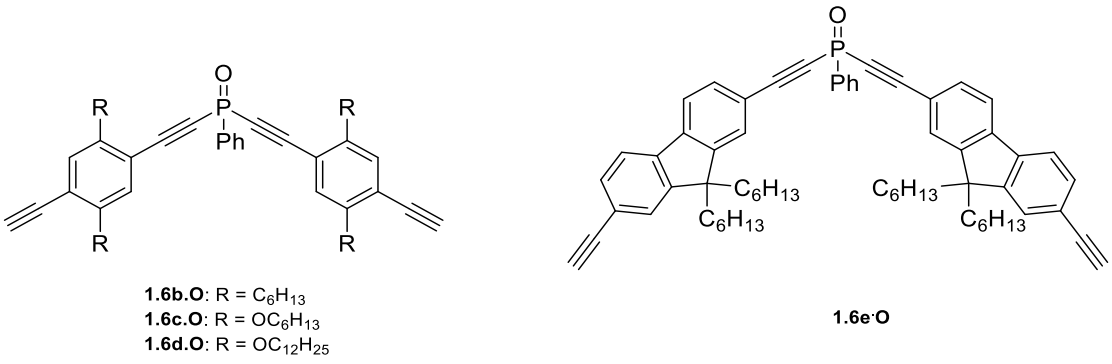

Figure 11. *Alkynylphosphane oxides from compounds **1.6b**-**1.6e**.*[63]

Compounds **1.6b**-**1.6e** exhibit little to no emission in solution, which is often observed for P(III) species as a consequence of the phosphorus lone pair quenching fluorescence.[64] One method to counter this effect is to form a phosphane oxide (P=O), thus sequestering the lone pair and preventing this fluorescence quenching mechanism. In this instance treating compounds **1.6b**-**1.6e** with hydrogen peroxide resulted in clean oxidation and afforded compounds **1.6b·O**-**1.6e·O** (**Figure 11**), all of which exhibit blue fluorescence, though a slight redshift was noted as conjugation was increased, consistent with a reduction in the HOMO-LUMO band gap. These compounds exhibit what is commonly termed

'turn-on fluorescence' as emission is only observed upon functionalisation of phosphorus. Beyond such applications, the oxidation of phosphanes more generally is a useful and important method for altering the energy level of the LUMO and thus changing the electron-accepting capabilities of the phosphorus moiety.[65]

1.4.3 Post-Synthetic Functionalisation of Phosphanes in π-Conjugated Materials

1.4.3.1 Oxidation of Phosphorus Centres

In addition to being employed as a means of preventing fluorescence quenching (*vide supra*) oxidation of tertiary phosphanes with chalcogens sequesters the lone pair and creates a hypervalent environment, therefore increasing the relative electronegativity of the phosphorus centre and altering its character from electron donor to an electron acceptor.[66] The P=E bond (where typically E = O, S, Se; **Figure 12**) is strongly polarised and best described as involving π back-donation from a filled p-orbital (lone pair at E) into an antibonding σ^*_{PE} and σ^*_{PC} orbital; this interaction has been defined as negative-hyperconjugation, for which the trigonal-pyramidal geometry of phosphorus is considered a key feature.[67] As a consequence of the increased electronegativity of phosphorus, it becomes an inductively withdrawing substituent that can alter the frontier molecular orbitals of a π-conjugated system, commonly resulting in a lowering of LUMO energies.[51,68]

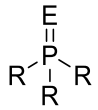

***Figure 12**. Product from oxidising a tertiary phosphane.*

Fluorescence is a common consequence of oxidation, as illustrated by the oxidation of trianthryl phosphane (**1.7a**; **Figure 13**), resulting in compound **1.7b** which exhibits fluorescence, where **1.7a** exhibited none.[69] The general red-shifted absorptions is exemplified by compound **1.8a** (**Figure 13**), relative to **1.8b** (e.g. λ_{max}: 245 and 258 nm, respectively).[70] In addition to oxidation, the degree of conjugation also allows for simple control of the absorptive and emissive properties, for example, in the phosphepines (**1.9a** and **1.9b**; **Figure 14)**,[71] the introduction of a saturated 5-membered ring in **1.9b** results in a red-shifted absorption maximum (λ_{max}), emission maximum (λ_{em}) and an increased quantum yield (ϕ), **1.9a**: λ_{max} = 347 nm, λ_{em} = 446, ϕ = 0.43; **1.9b**: λ_{max} = 363 nm, λ_{em} = 449, ϕ = 0.51, though both compounds emit in the blue-region. It has also been documented that the position of an

endocyclic sulfur atom results in starkly contrasting absorptive behaviours, as demonstrated in compounds **1.10a** and **1.10b**,[72] the former exhibiting a higher energy absorption at 266 nm and several lower energy features at 385, 405 and 428 nm, while **1.10b** only displays the lower energy bands 366, 385, 406 nm, which are blue shifted relative to **1.10a**.

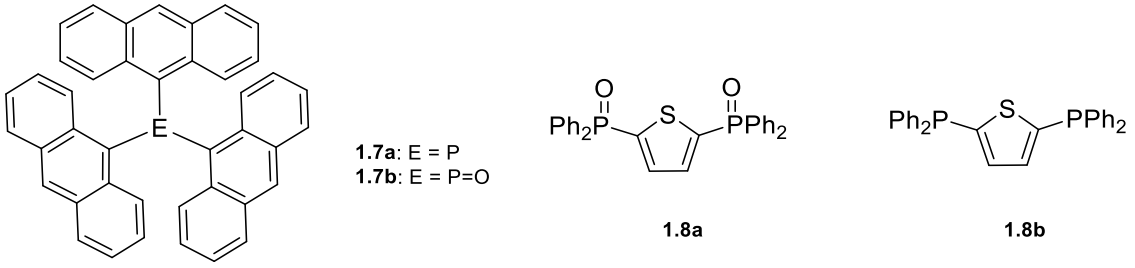

***Figure 13**. Trianthryl phosphane and functionalised trianthryl phosphanes (**1.7**), 2,5-bis(diphenylphosphino)thiophene (**1.8a**) and 2,5-bis(diphenylphosphane oxide)thiophene (**1.8b**) (PTP and PTPO).[69,70]*

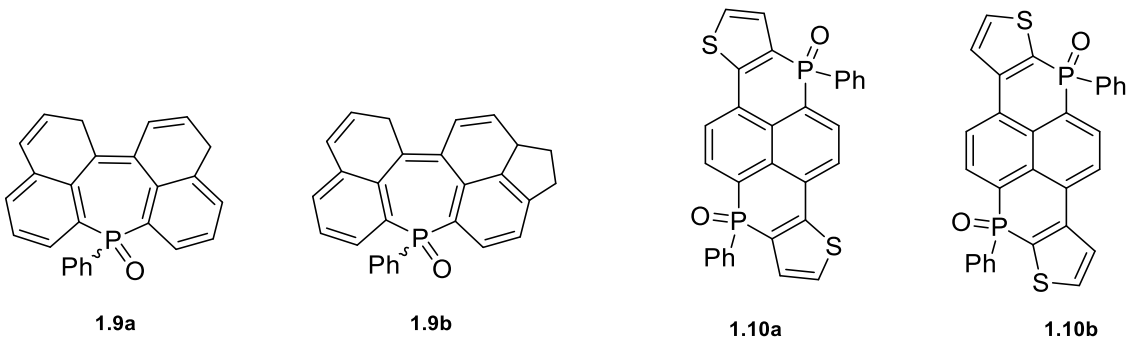

***Figure 14.** Examples of phosphepines (**1.9a**-**1.9b**) and phosphapyrenes (**1.10a**-**1.10b**).[71,72]*

Notably, the chalcogen present in a P=E bond (E = O, S, Se) can influence the compounds' effectiveness for optoelectronic devices. One property of interest in this regard is the electron mobility, which is defined as the measured value of drift velocity (average velocity attained by charged partiles) per unit of electric field strength, typically within a semi-conductor.[73] For example, the sulfur-containing system **1.11a (Figure 15**) exhibits enhanced electron mobility relative to oxide **1.11b** (**12a** = $2x10^{-3}$ cm^2 $V\ s^{-1}$; **1.11b** = $5x10^{-6}$ cm^2 $V\ s^{-1}$ under $2.5x10^{-5}$ $V\ cm^{-1}$).[73] Both **1.11a** and **1.11b** could successfully be used within OLEDs, however, **1.11a** is notably more efficient electron transport material, exhibiting lower driving voltage*,[74] and higher luminosity.[68,73] In contrast, the incorporation of heavier chalcogens

* Driving voltage is the maximum voltage you can apply without the risk of immediately damaging the material.

typically results in an increased rate of both radiative and non-radiative decay, leading to short lived excited states and thus quenches emission.[75,76]

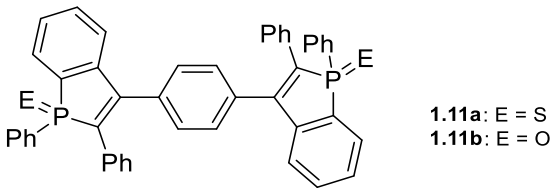

Figure 15. *Di(benzophosphole oxide)benzene (**1.11a**) and di(benzophosphole sulfide) benzene (**1.11b**), Benzo[b]phosphole sulfides. highly electron-transporting materials for organic semiconductor devices.[73]*

In addition to the use of chalcogens, coordination to metal centres such as gold is another commonly employed method to generally reduce LUMO energies. The series of benzophosphole derivatives **1.12a-d** (**Figure 16**) illustrate the typical post-synthetic approaches used to modify the absorptive/emissive properties of phosphanes more generally.[77] Compound **1.12a** can be readily oxidised to compound **1.12b** or **1.12c** *via* exposure to air or by heating in the presence of S_8;[78] compound **1.12d** is prepared from the reaction between **1.12a** and $Au(SMe_2)Cl$.[79] Compounds **1.12b**-**1.12d** exhibit comparable absorptive profiles, though a slight red-shifted absorption is observed for the Au(I)-complex (**1.12d**; 333 nm, $\Delta\lambda max$ = 3 nm), similarly they are all photoluminescent and emit in the UV-region (ϕ: **1.12b** = 4.2; **1.12c** = 0.2; **1.12d** = 13.4), however, compound **1.12d** exhibits a significantly higher quantum yield than **1.12b**, which is in-turn somewhat higher than **1.12c**. The quantum yields appear to be heavily perturbed upon functionalisation of phosphorus,[51] for **1.12d** this is believed to be a result of gold altering the packing arrangement in the solid state resulting in increased π-π interactions.[80] Gold complexes generally exhibit more red-shifted absorptions than observed for compound **1.12d**, for example compounds **1.13** and **1.14a**-**c** exhibit red shifted absorptions of $\Delta\lambda$ = 50 nm and 32-97 nm compared to their uncoordinated analogues.[81]

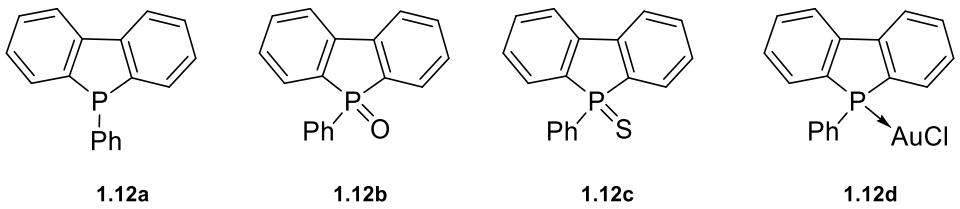

Figure 16. *Benzophosphole Derivatives.[77]*

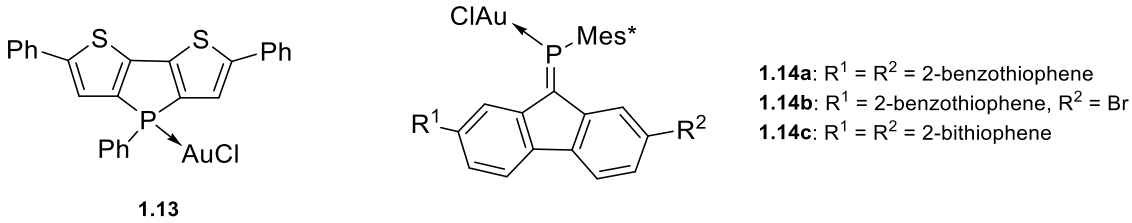

Figure 17. *AuCl functionalised phosphole and phosphaalkenes.*[81,80]

1.5 In Pursuit of New Electronically Active Phosphanes

The majority of the phosphorus-based building blocks mentioned throughout the preceding sections are based on phosphorus functionalities which have been extensively explored, in some cases since as early as the 1950s.[78] As such the introduction and exploration of novel functionalities is clearly a basis for further tailoring π-conjugated systems, not simple just to prepare new conjugated materials but to introduce motifs that exhibit properties not currently available from well-established building blocks, with the intent to prepare compounds possessing unique electronic properties.

1.5.1 The Incorporation of Electron Accepting Moieties

One active area of interest for the development of novel phosphorus-building blocks has been enhancing their electron accepting nature by including electron-withdrawing groups. A recent approach toward this has been the incorporation of carbonyl functionalities in order to reduce the energy of the LUMO and thus enhance electron acceptor character.[82] This effect is illustrated by **1.15** (**Scheme 6**) the introduction of a single carbonyl unit in the para-position of the six-membered phosphinine ring (**1.15**) resulting in a red-shift relative to its diacetal starting material (**1.16**; $\Delta\lambda_{max}$ = 10 nm).[83]

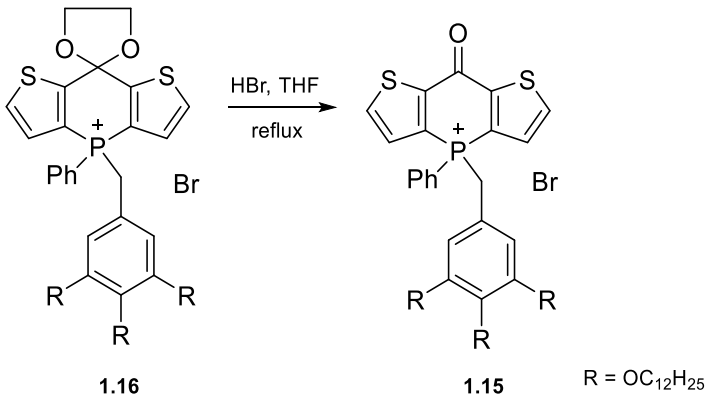

Scheme 6*. Synthesis of dithieno[2,3-b;3',2'-e]-4-keto-1,4-dihydrophosphinines.*[83]

In an extension of this concept, Baumgartner incorporated a second carbonyl unit into a 7-membered phosphacycle (**Figure 18**), preparing a diketophosphanyl (-C(=O)-PR-C(=O)-) with the intent to further reduce LUMO energies.[84] Relative to compound **1.15**, compounds **1.17a** and **1.17b** exhibit lower energy absorptions and higher absorption coefficients (ε) (λ_{max}: **1.15** = 270 nm, **1.17a** = 468 nm, **1.17b** = 492 nm), consistent with reduced LUMO energies. In addition to this, both **1.17a** and **1.17b** demonstrate blue-to-green emissions, where **1.15** exhibits none.[84]

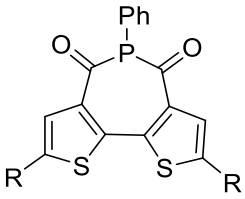

1.17a: R = H
1.17b: R = CCH

Figure 18. *Dithieno[3,2-c:2',3'-e]-2,7-diketophosphepins.*[84]

Compounds **1.17a-b** illustrate the advantages associated with incorporating another carbonyl functionality, especially as an acyl phosphane unit. Much like precedent phosphorus-based systems, the phosphorus centre can be functionalised (**Scheme 7**), compound **1.18a-O** exhibiting a more red-shifted absorbance than in **1.18a**, by *ca* 7 and 32 nm for the two different absorption bands. Coordination of **1.18** to gold (**1.18-AuCl**) results in a similar red-shift to 1.18-a, however, **1.18a-AuCl** also displays dual-emission, not observed for **1.18a** or **1.18a-O**, the second emission is believed to be a result of charge transfer from the lone pair of the gold-bound chloride atom to the diketophosphanyl core.[84]

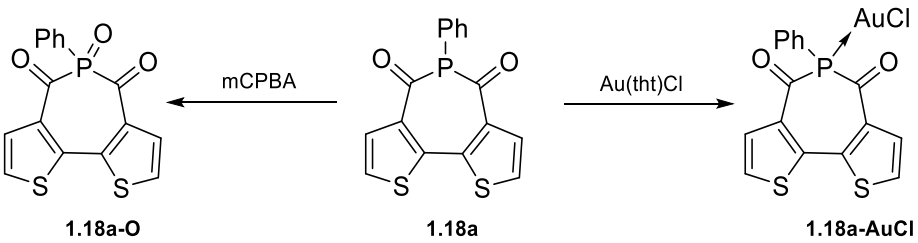

1.18a-O **1.18a** **1.18a-AuCl**

Scheme 7*. Functionalisation of compound* ***1.18a****.*[84]

Diketophosphanyl systems fall within the general class of acyl phosphanes, which are explored more generally for their fundamental chemistry as well as catalytic properties.[85,86] Acyl phosphanes can be synthesised *via* the Becker condensation which involves the addition of a silylated phosphane (R_2PSiMe_3) to an acyl chloride, resulting in the formation of an acyl phosphane. However, in the presence of a second P-silyl function many are prone to a facile 1,3-silatropic shift affording prefentially phosphaalkenes (see **Chapter 4**). More typically, acyl phosphanes are synthesised by reacting a secondary phosphane with an acyl chloride, some instances requiring the addition of base (**Scheme 8**).[87,88]

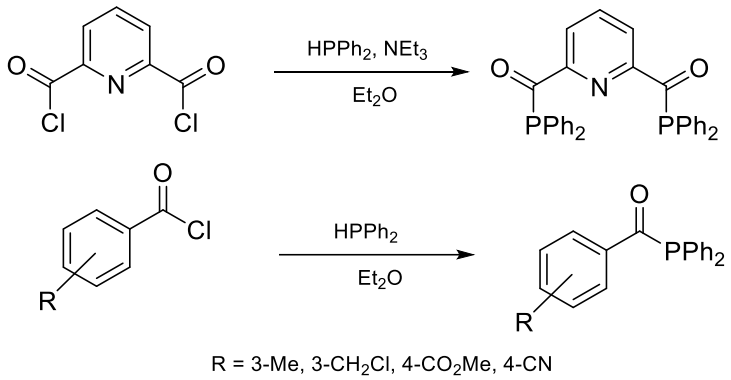

Scheme 8. *Representative synthetic strategies for Acyl-phosphanes.*[87,88]

Acyl phosphanes can exhibit hyperconjugation between the π_{PO} and σ^*_{PC} orbitals resulting in a reduction of double bond character for the carbonyl unit,[89] and thus delocalisation of the phosphorus lone pair. This delocalisation is comparable to that of the nitrogen lone pair in amides and these species are described as 'phosphomides', exhibiting the resonance structure illustrated in **Figure 19** as first postulated by Kostyanovky.[90] Phosphomides are more strictly defined as acyl phosphanes that exhibit carbonyl stretches in the region ν_{CO} 1630-1650 cm^{-1},[91] reminiscent with those of amides.[86] At present, no aliphatic acyl phosphanes have been shown to exhibit 'phosphomide character',[92] though a number of aryl-based systems have been reported. Nevertheless, acyl-phosphanes in general have been shown to stabilise LUMOs, especially for heavily conjugated systems, rendering them a desirably functionality to incorporate into π-conjugated materials.

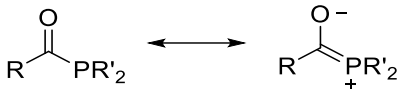

Figure 19. *Resonance forms of acyl phosphanes.*[90]

1.5.2 Cyclophanes

The incorporation of chromophores into molecular architectures is a key feature within the investigation of π-conjugated materials for optoelectronic applications, highlighting cyclophanes as a desirable functionality in that regard.[93] Initially, researchers such as Cram investigated cyclophanes for the synthetic challenge of discovering molecules which "skirt the fine line between isolability and self-destruction" and **Figure 20** illustrates a few of their examples.[94,95]

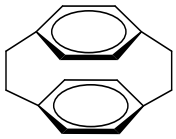

1.19

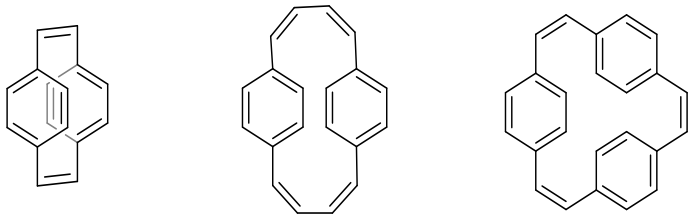

Figure 20. *[2.2] Paracyclophane and some examples of cyclophanes made by Cram.*[93,95]

Cyclophanes now find application within optoelectronic devices, exhibiting interesting absorptive and emissive properties as a consequence of the aromatic π-system being fixed in a rigid arrangement, the intra-arene distances of which are lower than typical aryl organic moieties. For paracyclophane (pCp; **1.19**) absorbance bands were detected at 225, 244, 286 and 302 nm; the long-wavelength band has been termed the "cyclophanes band" as it exceeds the typical absorption of simple alkyl-substituted aromatics,[96,97] with a broad emissive band is observed at 365 nm. These spectroscopic properties are believed to result from strong σ-π interactions between the alkyl-bridge and aromatic unit, as well as through-space π-π interactions, resulting in energy-transfer around the entire cyclophane core.[96] The electronic communication between chromophoric units in general depends on their relative orientations as well as inter-ring distance, the interactions of which can be altered *via* modifications to the aromatic group and bridge length, or by extending the conjugation (**Figure 21**).[98]

The effect of conjugation is illustrated in compounds **1.20a-c**, **1.20a** exhibiting the shortest conjugation (relative to **1.20b** and **1.20c**) and a red shifted emission relative to pCp (356 nm), while the increased conjugation in **1.20b** leads to a blue-shifted absorption as well as a red shifted emission relative to pCp and compound **1.20a**.[96] In contrast, removing the alkene substituents and instead incorporating an unsaturated bond in the bridging chain (**1.20d**)[98] results in similar absorptive features to compound **1.20a**. It has also been observed that elongation of the saturated bridging chain (**1.21a** and **1.21b**), results in blue-shifted absorptions (Δλ = 10 nm).[98]

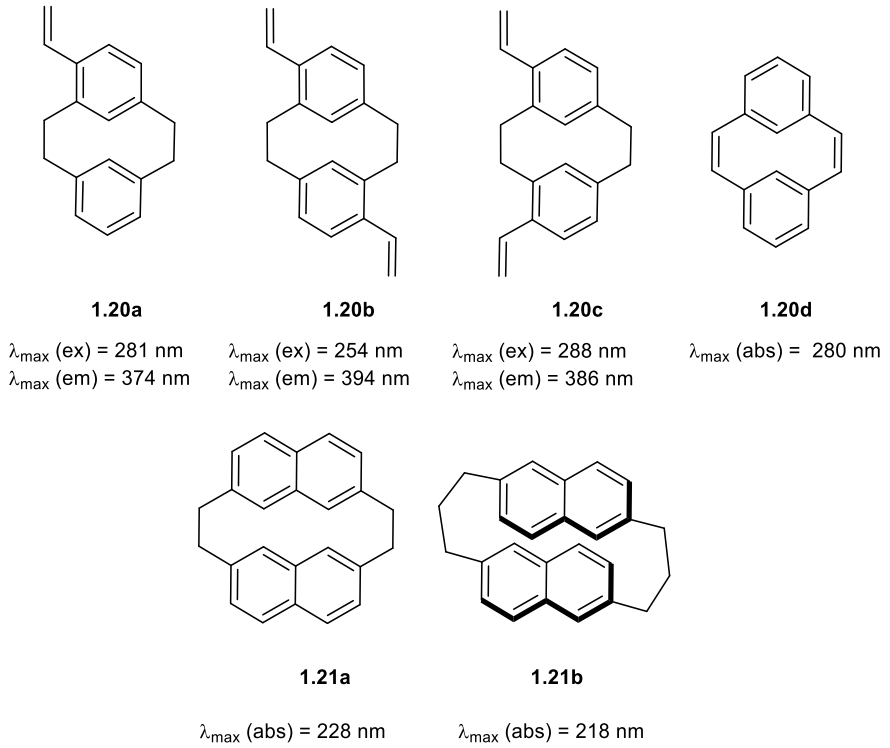

Figure 21. *Varying optical properties via modifications of the aromatic or bridging moieties.*[96,98]

1.5.3 Heterophanes

Carbocentric cyclophanes highlighted the potential these macrocyclic structures possess and consequently led to the development of heterophanes incorporating an endocyclic donor atom such as nitrogen. The first example of a heterophane was [2.2](2,6)pyridinophane (**1.22**),[99] which inspired the preparation of similar species (**Figure 22**) and the first review of parapyridinophanes was published in 1986 by Czuchajowski and co-workers.[100,101] The incorporation of nitrogen into the basic [2.2]paracyclophane skeleton (**1.23**) resulted in red-shifted absorptions, with a π-π* transition at 308 nm, reduced in energy relative to that of **1.19** (302 nm); this is a generally observed feature for the

incorporation of nitrogen, lowering the LUMO energy and thus red-shifting absorptions relative to precedent carbocentric systems.[102,103]

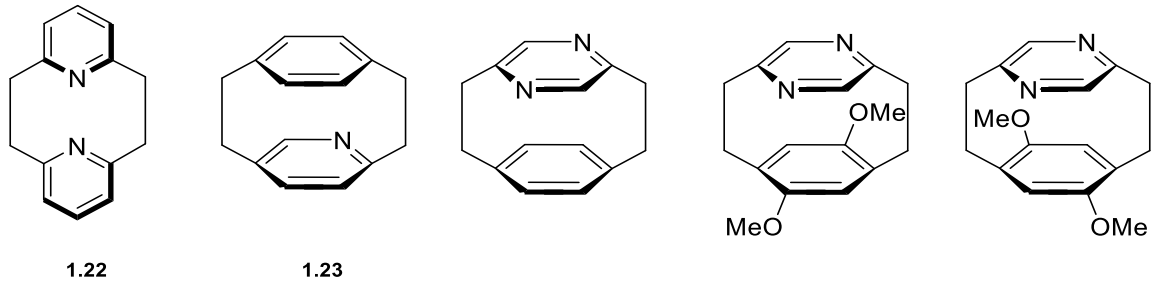

1.22 **1.23**

Figure 22. *A range of parapyridinophanes.*[99-103]

Heterophanes are not limited to nitrogen, both oxygen and sulfur being extensively documented as part of the bridging unit (**1.24**);[104] there are also examples of oxygen and sulfur being incorporated into the aromatic unit, such as in [2.2](2,5)-furanophane (**1.25a**) and -thiophenophane (**1.25b**), which are isoelectronic with pyrrolophane (**1.25c**; **Figure 23**).[105,106] Compound **1.25b** exhibits a red-shifted absorptive band relative to **1.25c**, which is in turn red-shifted from that of **1.25a** (λ_{max}: 275 (**1.25b**), 240-250 (**1.25c**) and 222 nm (**1.25a**) respectively); this is a consequence of conformational rigidity which was found to increase with heteroatom size: **1.25b** > **1.25c** > **1.25a**.[107]

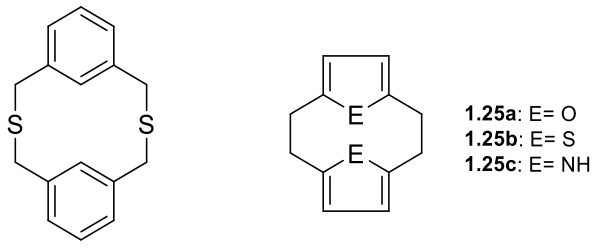

1.24

Figure 23. *2,1-Dithia-[3,3]-metacyclophane (**1.24**) and [2.2](2,5)-furanophane, -pyrrolophane and thiophenophane (**1.25a-c**).*[104-107]

Although phosphorus has previously been incorporated into the skeleton of π-conjugated materials, which exhibit notably different absorptive/emissive properties relative to nitrogen and carbon based analogues (*vide supra* **Section 1.4.2**), there are only a handful of known phosphacyclophanes, all of which incorporate a P-O-C linkage within the skeleton in each case (**Figure 24**).[108,109,110] More elusive still are the phosphmetacyclophanes of which the first, 1,10-dimethyl-1,10-diphospha-[3.3]-

metacyclophane-2,9,11,18-tetraone (**1.26**),[111] was prepared in 2012 *via* a simple condensation route (**Scheme 9**). However, despite the recent work highlighting the interesting emissive properties seen for precedent cyclophanes along with the electron accepting capabilities of the diketophosphanyl unit, only the coordination chemistry of **1.26** has been briefly investigated, leaving the photo-absorptive properties entirely unexplored.

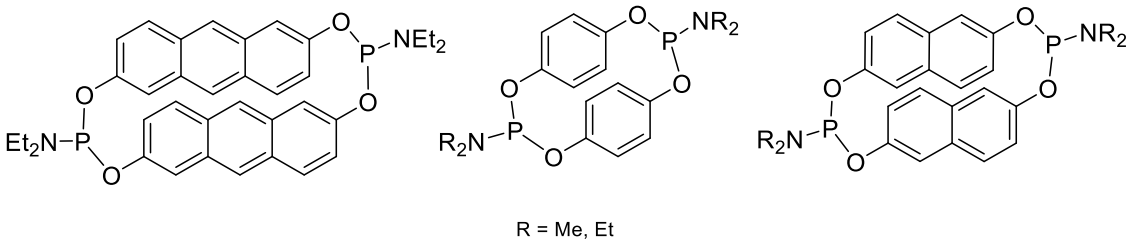

Figure 24. *Phosphacyclophanes.*[108-110]

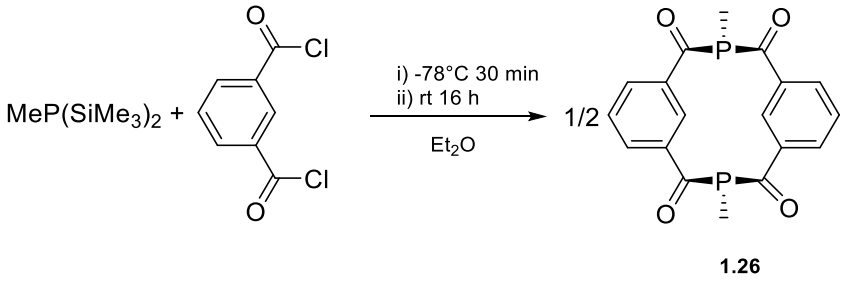

Scheme 9. *Synthesis of the first Diphosphametacyclophane: 1,10-dimetyl-1,10-diphospha-[3.3]-metacyclophane-2,9,11,18-tetraone (**1.26**).*

1.6 Concluding Remarks

The investigation of phosphorus-containing species for optoelectronic applications is clearly an intriguing topic, allowing for the fine tuning of absorptive and emissive properties *via* structural modifications both pre- and post-synthetically. The incorporation of acyl phosphanes, specifically the diketophosphanyl unit, possesses potential for new optoelectronic materials, though very few examples have been explored. Similarly, there is a notable lack of phosphacyclophanes reported in the literature, systems which could potentially possess interesting emissive properties with the clear potential for electronic tuning by post-synthetic modifications. Even more elusive are the diphosphametacyclophanes, which incorporate the electron accepting diketophosphanyl moiety into a cyclophanic scaffold, though the photophysical properties have not yet been investigated.

1.7 Aims and Objectives

Herein, a family of phosphacyclophanes incorporating two diketophosphanyl units will be explored, this study will examine the relationship between dimer, trimer and tetramer formation, alongside investigating the cyclophanes' photophysical properties and how these are influenced by structural modifications. Furthermore, this work will explore electronically distinctive 6- and 7-membered phosphorus heterocycles, trifluoromethylphosphaalkenes and diphosphaboracycles, exploring their coordination chemistry and respective reactivity, leading to the synthesis of a range of novel compounds and complexes thereof with an additional investigation into the unusual electronics of the diphosphaboracycles *via* cyclic voltammetry.

Chapter 2 – The Synthesis and Electronic Behaviour of the Diphosphametacyclophanes

"I'm going on an adventure!"

-- *The Hobbit: An Unexpected Journey (2012)*

2.1 Introduction

Unlike carbocentric and nitrogenous cyclophanes, phosphacyclophanes are sparsely reported in the literature, with none exhibiting direct C-P bonds (*vide supra* **Section 1.5.3**).[108,109,110] More elusive still are phosphametayclophanes of which the first, (1,10-dimethyl-1,10-diphospha-[3.3]-metacyclophane-2,9,11,18-tetraone) **2.1**, was discovered in 2012 by Saunders *et al*.[111]

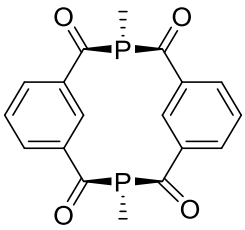

2.1

Scheme 10. *Synthesis of the first diphosphametacyclophane.*[111]

Compound **2.1** incorporates the 'diketophosphanyl' functionality (-C(=O)-PR)-C(=O)-) which has previously been incorporated into π-conjugated materials as a method of reducing LUMO energies and thus red-shifting absorptions (see **Chapter 1**).[84] In addition, from diketophosphanyl moieties a phosphanoyl and benzoyl radical pair can be generated *via* bond cleavage (**Scheme 11**), the former serves as an effective initiator for radical polymerisation(photoinitiator),[112] overcoming the inefficient polymerisation seen for carbocentric congeners.[113]

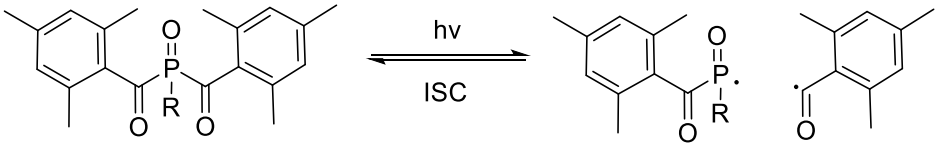

Scheme 11. *Photolysis of BAPOs, generating a primary phosphanoyl and benzoyl radical pair from bond cleavage..*[112]

Following the development of the diketophosphanyl functionality, Balakrishna and co-workers attempted to synthesise an analogue of **2.1** based on a pyridyl skeleton,[114] however, trimeric (**2.2**) and tetrameric (**2.3**) species were instead obtained (**Figure 25**), these being identified and distinguished on the basis of mass spectrometric and structural data, given their apparently identical $^{31}P\{^{1}H\}$ NMR resonances, δ_p 23.3. Balakrishna proposed the higher oligomer formation is a result of intramolecular

π-π interactions between the phosphorus-bound phenyl substituents (CH-π, π-π) and concluded the methyl derivative will favour dimer formation due to its inability to "facilitate CH-π or π-π intramolecular interactions".[114] Their conclusions were supported by DFT calculations at the M062X/6-31G** level of theory, which suggest that the trimeric and tetrameric structures possess significant stability relative to their dimeric analogue (ΔG = −6.7 kcal mol^{-1}, −12.8 kcal mol^{-1} respectively), whereas the dimeric structure of the methyl derivative was found to be lower in energy compared to the trimeric and tetrameric derivatives (ΔG = +4.4 kcal mol^{-1}, +5.5 kcal mol^{-1} respectively).

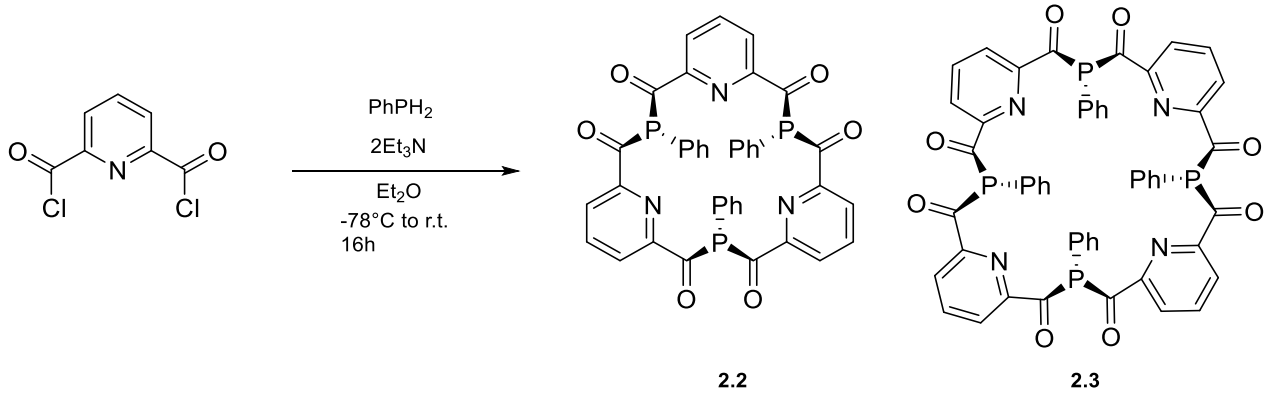

Figure 25. *Work by Balakrishna and Co-workers.*[114]

Relative to compound **2.1**, Balakrishna's trimeric and tetrameric oligomers (**2.2** and **2.3**, respectively) incorporate a pyridyl unit and are accessed *via* an alternative synthetic pathway.[114] Therefore, these phosphametacyclophanes warrant further investigation to determine if the size of the macrocycle (dimer, trimer and tetramer) can be controlled, whilst simultaneously exploring their absorptive/emissive properties.

2.2 Synthesis and Characterisation of the Diphosphametacyclophanes

2.2.1 Investigating Dimeric, Trimeric and Tetrameric Phosphametacyclophanes

In order to determine the generality of Balakrishna's conclusion, pyridyl-free analogues of **2.1** were sought, applying a modification of their methodology. Thus, isophthaloyl chloride was reacted with phenyl phosphane in the presence of triethylamine (**Scheme 12**) with the aim of producing *m*-{-C(O)-C_6H_4(C(O)PPh)}$_2$ (**2.4**). However, in contrast to Balakrishna's work, more than one product formed with resonances observed in the $^{31}P\{^1H\}$ NMR spectrum at δ_P 30.3 (>3 peaks overlapping), 41 (s) and −29 (m) (**Figure 26**), with only broad resonances observed in the aromatic region of the ^1H NMR spectrum. However, the resonance at δ_P −29 gives rise to a doublet of multiplets in the proton-coupled spectrum,

the magnitude of coupling being consistent with a P-H species (J_{PH} = 230 Hz). Repeated synthetic attempts fail to afford consistency in the number of resonances in this region, though the impurities at δ_P 41 (unidentified) and δ_P −29 (unidentified P-H species) are always present.

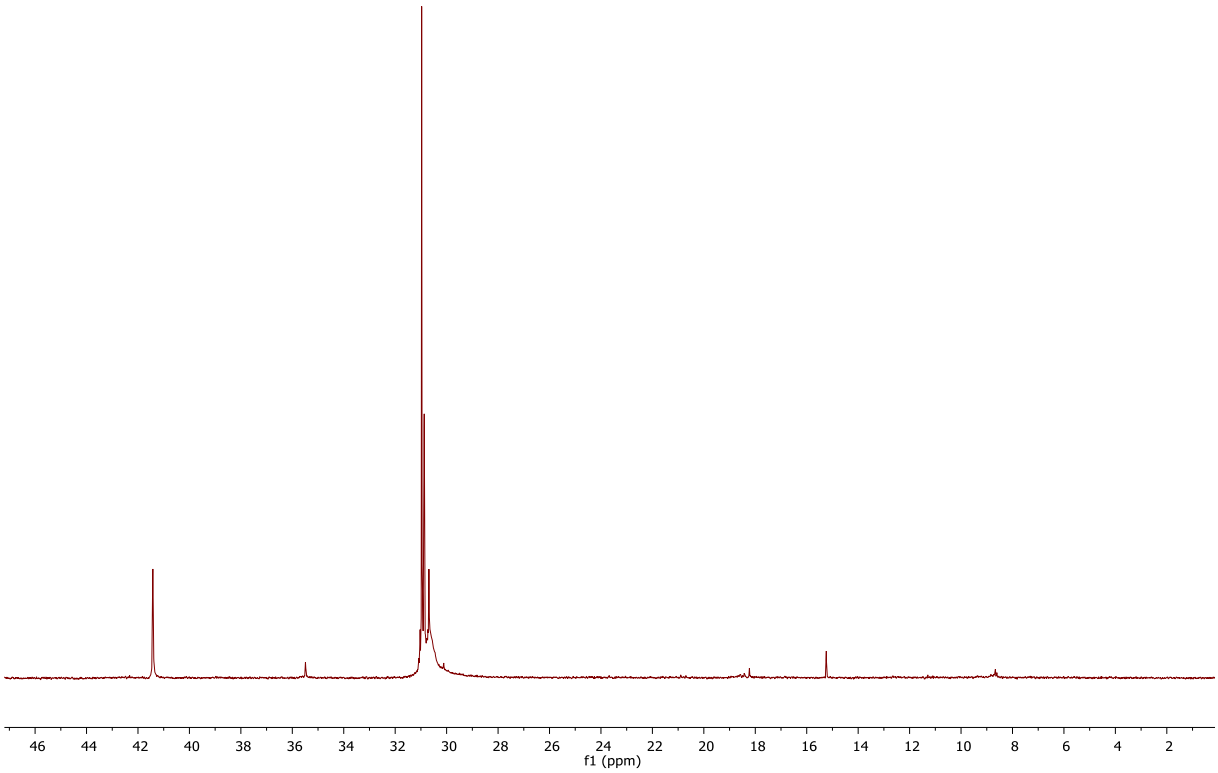

Figure 26. *^{31}P NMR spectrum (C_6D_6, 161.72 MHz) from trying to prepare **2.4** from $PhPH_2$.*

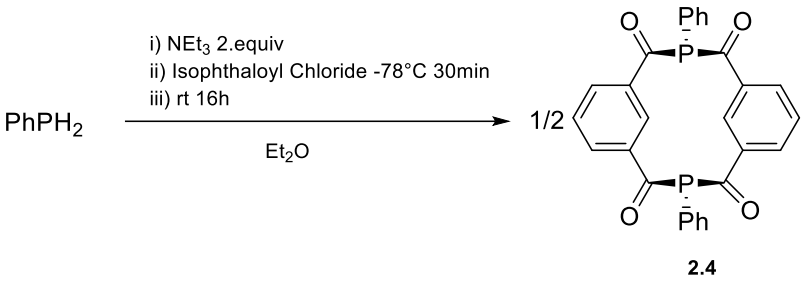

2.4

Scheme 12. *Attempted Synthesis of **2.4** from a primary phosphane.*

Repeating the reaction without the presence of base, initially resulted in the observation of a doublet resonance in the ^{31}P NMR spectrum at −29 ppm (J_{PH} = 230 Hz), though 35% of $PhPH_2$ still remained. After stirring for a further 3 days a yellow solid was isolated, exhibiting a doublet at δ_P 25, J_{PH} = 573 Hz alongside numerous unresolved signals.

The final approach to access compound **2.4** starts from the bis-silylated phosphane, $PhP(SiMe_3)_2$, which when reacted with isophthaloyl chloride in a 1:1 ratio (**Scheme 13**), afforded **2.4** as a yellow solid, exhibiting a phosphorus resonance at δ_p 30.5 ($w_{1/2}$ = 17 Hz). It is worth noting the importance of

reaction conditions for this synthesis, as the product distribution between **2.4** and by-products appears directly related to the concentration of reagents being added; optimal conversion was achieved by adding a 0.4 M solution of isophthaloyl chloride to a dilute ethereal solution of $PhP(SiMe_3)_2$ (0.13 M), which afforded the cleanest conversion and highest crude yield (**Table 3**). The synthesis of **2.4** is appreciably less facile than that of **2.1**, which could suggest that the electronic nature of the phosphorus substituent and thus the basicity of the phosphorus centre plays a key role in the reaction, i.e. the reaction is slower with reduced basicity (**2.4**) and possibly more scope for side reactions.

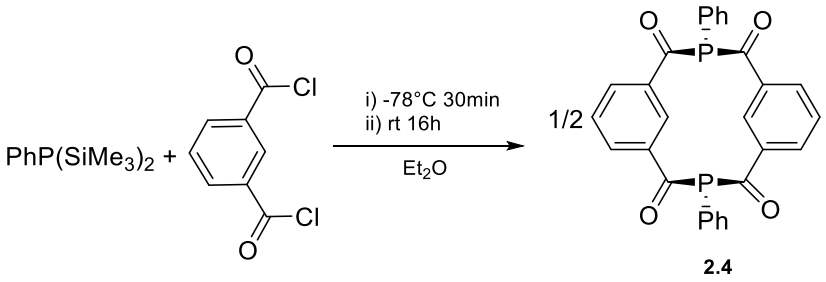

Scheme 13. *The synthesis of **2.4** from $PhP(SiMe_3)_2$, the yield of which shows appreciable concentration dependence.*

Table 3. *Condition optimisation for the synthesis of **2.4**.*

[$PhP(SiMe_3)_2$]/ mol dm^{-3}	[Isopthaloyl Chloride]/ mol dm^{-3}	Product Distribution from ^{31}P and ^{1}H NMR (%).[a]	Crude Yield (%)
0.01	0.01	85 (**2.4**), 13 (**A**), 1.5 (**B**)	-
0.60	0.60	**2.4** +^{1}H impurities	4
0.12	0.12	80 (**2.4**), 20 (**A**)	3.5
0.22	0.22	86 (**2.4**), 7 (**A**), 7 (**B**)	-
0.08	0.08	75 (**2.4**), 25 (**C**)	-
0.25	0.25	62 (**2.4**), 21 (**A**), 17 (**B**)	-
0.34	0.562	98 (**2.4**), 2 (**A**)	31
0.13	0.41	**2.4**	31
0.50	0.50	94 (**2.4**), 1 (**A**), 5(**B**)	11
1	1	74 (**2.4**), 2.(**A**), 8 (**D**), 15 (**B**)	50
0.50	0.50	94 (**2.4**), 6(**A**)	14
0.5 (–78 °C filtration)[b]	0.5 (–78 °C filtration)[b]	**2.4** + ^{1}H impurities	-

*a. δ_P: 30.5 = **2.4**, 41 = **A**, –30 = **B**, 19.3 = **C**, -1.5 = **D**. b. The yellow solid and solution were analysed, this was the only filtration performed cold.*

The ^{1}H NMR spectrum of compound **2.4** exhibits five broad aromatic environments which integrate for 18 protons, consistent with the formation of **2.4;** furthermore a single C=O resonance is observed in the $^{13}C\{^{1}H\}$ NMR spectrum. The broad resonances and poorly resolved spectra could be indicative of fluxionality in solution, though no appreciable change was observed between −80 °C and 60 °C.

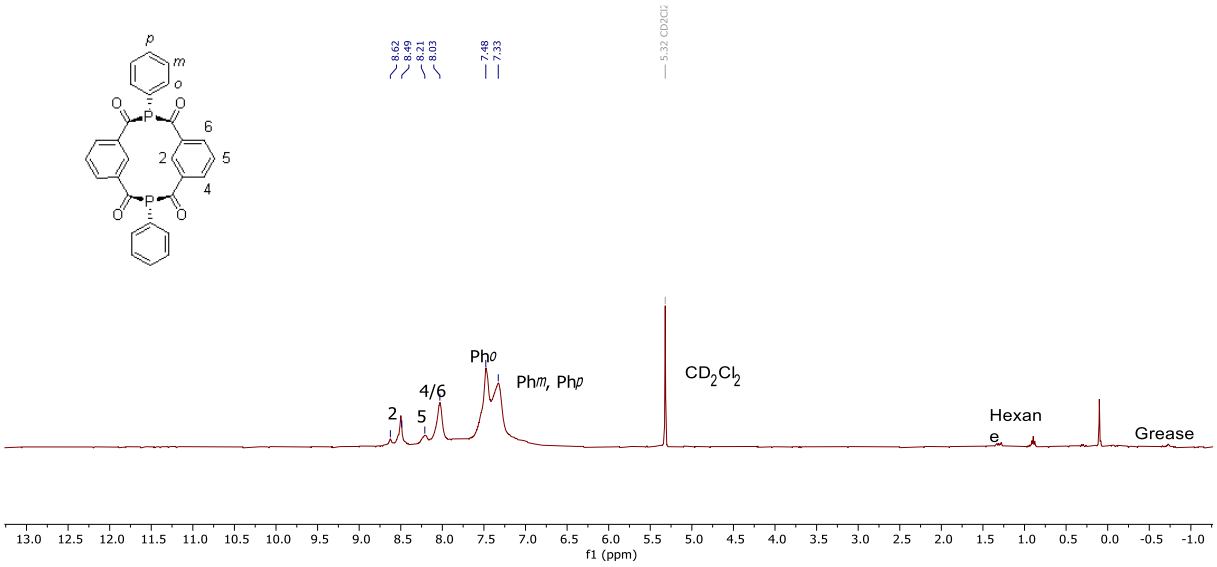

***Figure 27**. ^{1}H NMR Spectrum (CD_2Cl_2, 303K, 399.49 MHz) of **2.4**.*

Despite the complex solution-state behaviour, the presence of **2.4** was confirmed by the observation of the molecular ion (480.0699 *m/z*) in the electron ionisation mass spectrum, and ultimately by X-Ray diffraction (**Figure 28**; **Table 4**, *vide infra*). Overall, the data for **2.4** show no evidence for the formation of trimeric or tetrameric species, in spite of the predicted thermodynamic preference of higher oligomers on the basis of Balakrishna's DFT studies.[114] This would seem to question the impetus for formation of higher oligomers, perhaps suggesting either higher oligomer formation must be driven by the incorporation of the pyridyl group, or alternatively the synthetic route itself.

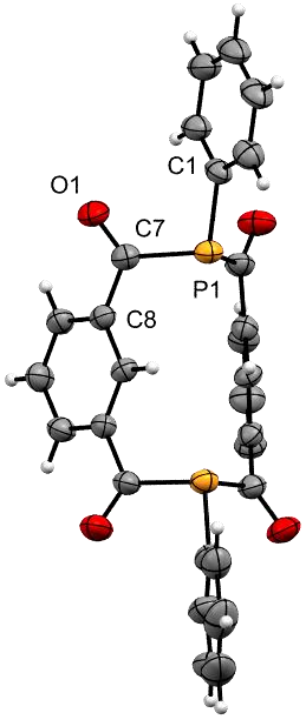

Figure 28. *Molecular structure of* ***2.4*** *with thermal ellipsoids at the 50 % probability level; solvent molecules omitted for clarity.*

In order to determine the relative influence of the pyridyl moiety upon the formation of higher oligomers, the reaction between $MeP(SiMe_3)_2$ and 2,6-pyridinedicarbonyl chloride was explored, resulting in the formation of **2.5**. Compound **2.5** was characterised by a single resonance in the $^{31}P\{^1H\}$ NMR spectrum, δ_P 30.1, and characteristic $^{13}C\{^1H\}$ and ^1H resonances associated with the acyl carbon and aromatic moieties. Confirmation of the dimeric structure of **2.5** was obtained from X-Ray diffraction (**Figure 29**); a number of repeat syntheses were untaken and screened with no indication of higher oligomer formation demonstrating consistency in the products obtained.

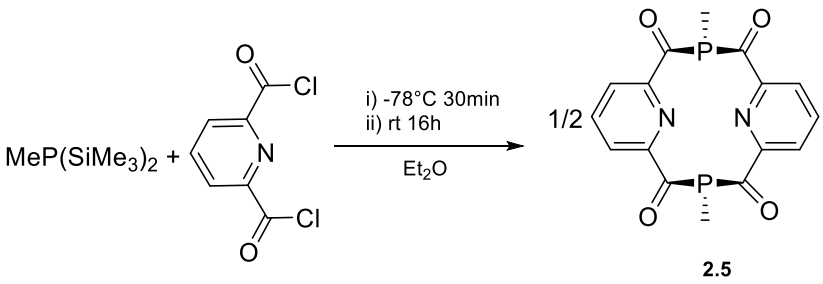

Scheme 14*. The synthesis of* ***2.5*** *from* $MeP(SiMe_3)_2$ *and 2,6-pyridinedicarbonyl chloride.*

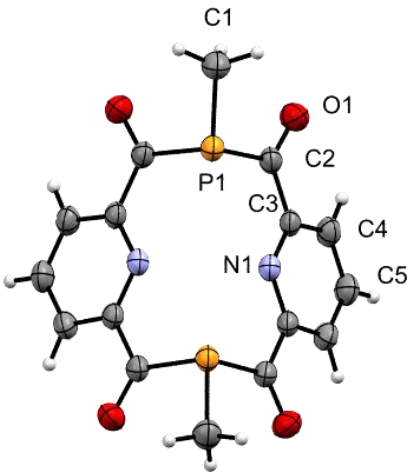

Figure 29. *Molecular structure of* ***2.5*** *with thermal ellipsoids at the 50 % probability level.*

Compound **2.5** was only observed as a dimer and thus would seem to suggest that pyridine incorporation is not the cause for higher oligomer formation, thus leaving the synthetic route as the likely key factor. However, numerous efforts to replicate Balakrishna's work, including with a range of substrates, resulted only in intractable mixtures of polymeric materials, thus preventing verification of the conclusion.

2.2.1 Variation of The Phosphametacyclophanes Aromatic Substituents

The relationship between dimer, trimer and tetramer formation is clearly not a result of π-stacking between P-aryl substituents, or incorporation of a pyridyl unit and thus presumably is a consequence of the synthetic route; this opens a range of options for the development of the general diphosphametacyclophane motif. One key question is how variation of substituents about the cyclophane skeleton might influence their photophysical properties. In order to probe this, a series of 5-substituted isophthaloyl chlorides were prepared, either by literature methods or *via* modifications thereof (**Scheme 15**). Subsequently, $MeP(SiMe_3)_2$ was reacted with each respective 5-substituted isophthaloyl chloride, in a 1:1 ratio (**Scheme 16**), leading to the formation of **2.6**-**2.10**. Compounds **2.6**-**2.10** were characterised spectroscopically *via* their single phosphorus NMR resonance and associated acyl and aromatic signatures, with the carbonyl moieties further confirmed by their infrared absorbances associated with the carbonyl moiety (**Table 4**). The growth of single crystals led to structural confirmation (**Figure 31**), with key parameters outlined in **Table 5** (*vide infra*).

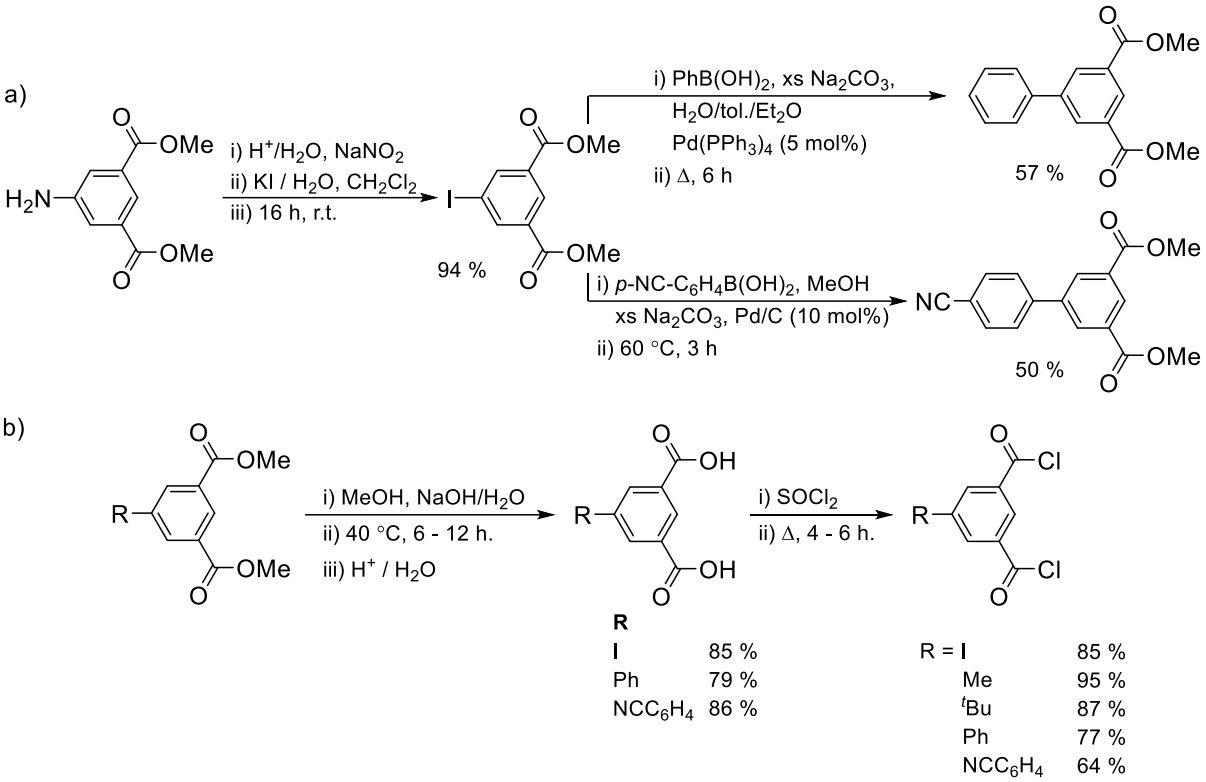

Scheme 15. *Synthesis of 5-R-isophthaloyl derivatives. a) 5-Aryl-isophthaloyl esters; b) 5-R-isophthaloyl chlorides by modifications of literature procedures for R= I.*

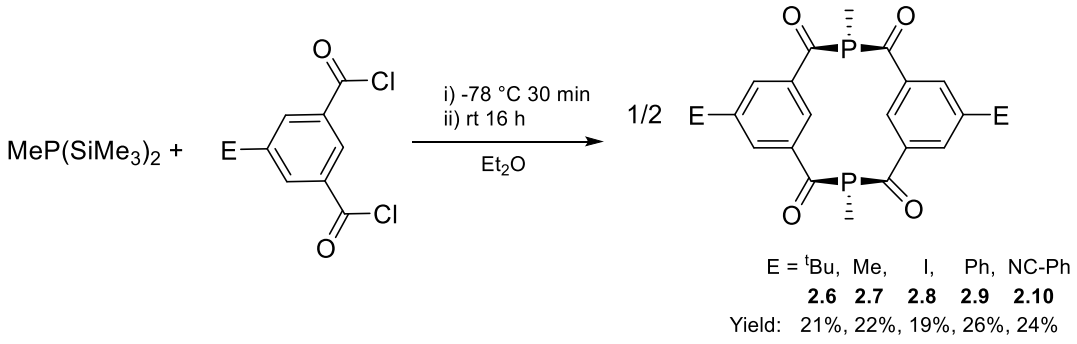

Scheme 16. *General reaction scheme for para-substituted phosphacyclophane derivatives.*

Table 4. *Selected Spectroscopic Data for* ***2.1***, ***2.4***-***2.10*** *(^{1}H 399.5 MHz, ^{13}C 100.46 MHz, ^{31}P 161.71 MHz).*

	δ_P[a]	C=O δ_C ($^1J_{CP}$[b])	δ_H ($^2J_{HP}$[b])	ν_{CO} / cm^{-1}
2.1[111]	*32.7*	*206.9 (46)*	*1.58 (3.1)*	*1654, 1637*
2.4	*30.5*	*208.5 (35)*[c]	*-*	*1639*
2.5	*30.1*	*209.1 (51)*	*1.63 (6.2)*	*1656, 1640*
2.6	*34.5*	*207.2 (46)*[d]	*1.65 (2.7)*[d]	*1657, 1614*
2.7	*32.3*	*207.3 (46)*[c]	*1.58 (2.7)*[c]	*1653, 1640*
2.8	*36.1*	*205.4 (47)*[c]	*1.61 (3.0)*[c]	*1640*[d]
2.9	*35.7*	*207.4 (46)*[c]	*1.66 (2.3)*[c]	*1658, 1639*
2.10	*35.2*	*205.9 (46)*	*1.66 (3.1)*	*1648,*[d] *2227*[e]

[a]as C_6D_6 solution. [b]in Hz. [c]as CD_2Cl_2 solution. [d]as $CDCl_3$ solution. [e]symmetric mode not observed. [f] ν_{CN} Stretch.

Attempts to access macrocycles bearing C≡N or C≡CH substituents by reacting $MeP(SiMe_3)_2$ with 5-ethylnyl or 5-cyanoisophthaloyl chloride were unsuccessful, resulting only in the formation of $MePH_2$ *in situ*, (δ_P −163 ($^1J_{PH}$ = 188 Hz)).[115] Efforts to access these macrocycles by cross-coupling reactions or indeed halide abstraction with **2.8** were also unsuccessful.

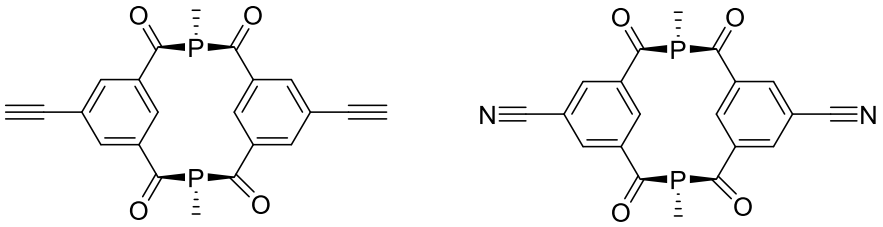

Figure 30. *Desired ethynyl- and cyano-phosphametacyclophanes.*

2.2.3 Spectroscopic and Structural Features of the Diphosphametacyclophanes

The $^{31}P\{^1H\}$ NMR spectra for compounds **2.4**-**2.10** each exhibit a single resonance in the region 30-36 ppm (vide supra, **Table 4**), consistent with that observed for **2.1** and within the range of most precedent diketophosphanyl derivatives (68-30 ppm).[84,111,116] It is notable that Balakrishna's systems (**2.2**, **2.3**) are observed at significantly lower frequency (δ_P 23), which would seem a simple diagnostic tool for identifying the di- over tri- and tetra-meric systems. The acyl moieties of **2.4-2.10** are apparent from a single acyl resonance in the $^{13}C\{^1H\}$ NMR spectra and their infrared absorbances, which are consistent with the symmetry of the systems. This is also reflected in the ^{1}H NMR spectra, resonances

associated with the aromatic and p-methyl moieties (*ca* 1.6 ppm (d, $^{2}J_{HP}$ = 2-6 Hz)) integrating consistently.

The spectroscopic data are broadly consistent across the series (**2.4**-**2.10**), though changes to the aromatic substituent lead to variation of δ_P; the highest shift is observed for **2.8** presumably as a consequence of the electronegativity of iodine. In each case, the acyl carbon couples to phosphorus, with **2.4** exhibiting the weakest $^{1}J_{CP}$ coupling, presumably due to reduced *s*-character at phosphorus as a consequence of the phenyl donor.[117,118] In contrast, **2.5** possesses the strongest $^{1}J_{CP}$ and $^{2}J_{HP}$ coupling across the series, which could feasibly be as a result of the electronegative pyridyl group. The molecular geometries of the phosphametacyclophanes **2.4**-**2.10** are illustrated in **Figure 28**, **Figure 29** and **Figure 31** (*vide supra*), with selected parameters summarised in **Table 5**.

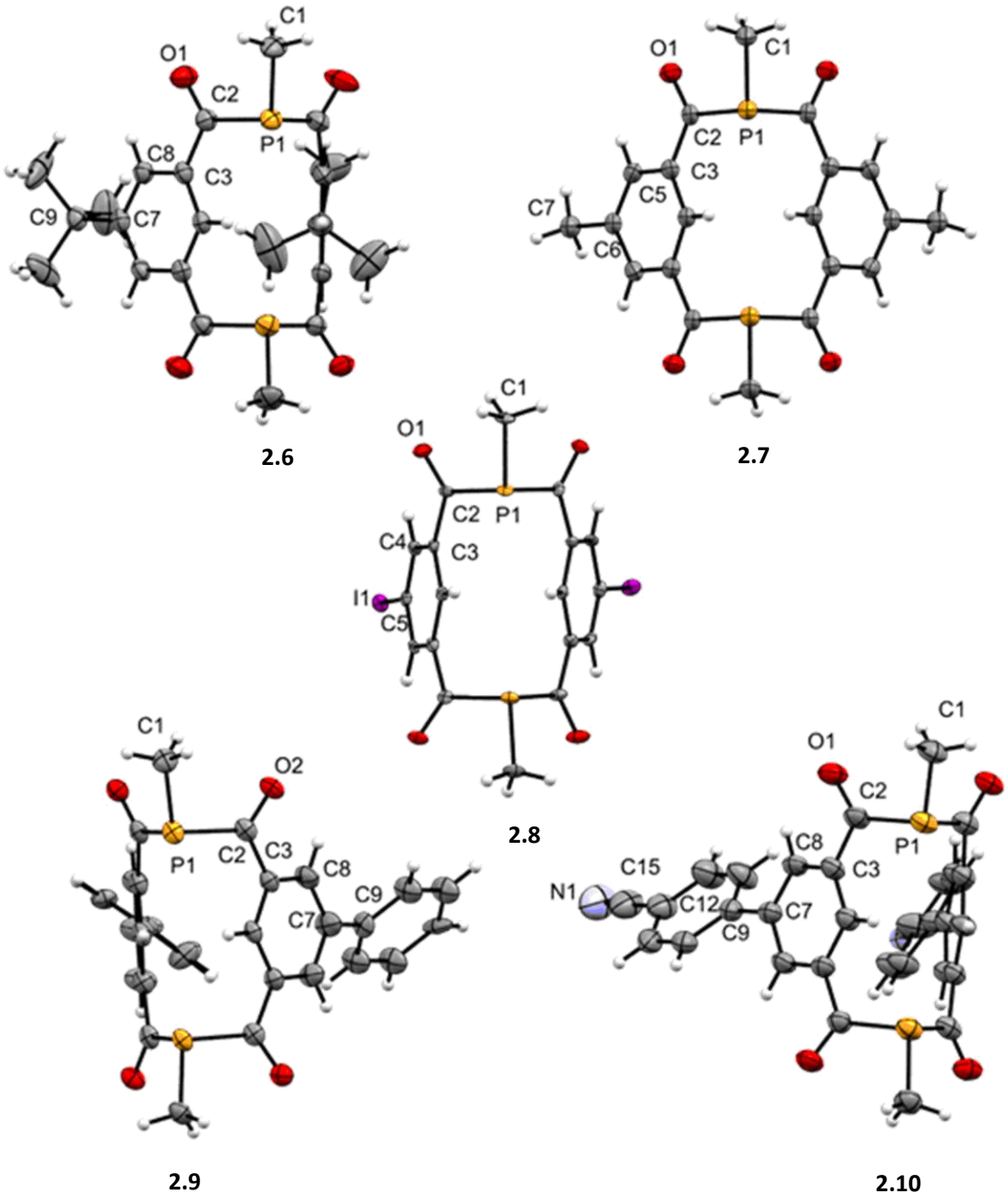

Figure 31. *Molecular structures of **2.6**-**2.10** with thermal ellipsoids at the 50 % probability level; the modelled disorder (**2.6**: ^{t}Bu, **2.9**: Ph) and solvent of crystallisation (**2.6**, **2.9**, **2.10**) omitted for clarity.*

Table 5. Selected bond lengths (Å) and angles (°) for compounds **2.1** and **2.4**-**2.10** with estimated standard uncertainties in parentheses.

	2.1[111]	***2.4***	***2.5***	***2.6***	***2.7***	***2.8***	***2.9***	***2.10***
P-C(O)	*1.894(3)*	*1.892(5)*	*1.892(2)*	*1.892(1)*	*1.910(3)*	*1.898(4)*	*1.890(2)*	*1.881(5)*
P-C(R) [a]	*1.816(4)*	*1.816(4)*	*1.835(4)*	*1.818(2)*	*1.825(5)*	*1.810(4)*	*1.821(2)*	*1.820(5)*
C=O	*1.202(3)*	*1.201(6)*	*1.215(3)*	*1.212(2)*	*1.207(4)*	*1.207(5)*	*1.214(3)*	*1.224(5)*
C(O)-C(Ar)	*1.494(4)*	*1.491(6)*	*1.491(3)*	*1.484(2)*	*1.486(4)*	*1.496(5)*	*1.490(3)*	*1.485(6)*
C(Ar)-E [b]	*1.390(3)*	*1.401(6)*	*1.334(2)*	*1.391(2)*	*1.392(4)*	*1.390(6)*	*1.390(3)*	*1.395(6)*
C^{exo}-E' [c]	-	-	-	*1.531(2)*	*1.499(7)*	*2.098(4)*	*1.555(4)*	*1.478(7)*
N-C	-	-	-	-	-	-	-	*1.150(8)*
C(N)-C	-	-	-	-	-	-	-	*1.437(8)*
P—P	*5.111(1)*	*5.147(1)*	*4.751(1)*	*5.050(7)*	*5.073(2)*	*5.090(1)*	*5.089(4)*	*5.067(1)*
Centroid	*3.930(1)*	*3.923(6)*	*4.832(5)*	*4.027(6)*	*4.897(6)*	*3.865(2)*	*3.976(3)*	*3.750(1)*
Displacement	*41.64(10)*	*41.53(16)*	*86.24(12)*	*45.49(6)*	*83.8(2)*	*38.11(3)*	*43.65(5)*	*34.26(16)*
C(R)-P-C(O)	*98.76(14)*	*102.0(2)*	*96.91(11)*	*99.15(9)*	*97.90(16)*	*99.5(2)*	*99.02(10)*	*99.8(2)*
C(O)-P-C(O)	*95.73(13)*	*96.9(2)*	*97.07(13)*	*100.33(10)*	*97.8(2)*	*98.8(2)*	*96.65(9)*	*93.5(2)*
P-C(O)-C(Ar)	*117.6(2)*	*116.7(3)*	*119.80(15)*	*119.23(12)*	*119.1(2)*	*116.1(3)*	*117.90(15)*	*118.4(3)*
E-C(Ar)-C(O)	*121.9(3)*	*121.1(4)*	*117.42(18)*	*121.71(15)*	*122.2(3)*	*120.8(4)*	*120.92(18)*	*119.9(4)*
O=C-P	*120.6(2)*	*121.1(4)*	*119.57(17)*	*119.12(14)*	*118.5(2)*	*121.3(3)*	*120.12(17)*	*120.2(4)*
E'-C^{i}-C^{o}	-	-	-	*120.39(16)*	*120.8(2)*	*120.2(3)*	*125.1(3)*	*121.4(4)*
N-C-C	-	-	-	-	-	-	-	*179.4(9)*

[a] *R = Me **2.1**, **2.5**-**2.10**; Ph **2.4**.* [b] *E = CH **2.1**, **2.4**, **2.6**-**2.10**; N **2.5**.* [c] *E' = H **2.1**, **2.4**, **2.5**; C **2.6**, **2.7**, **2.9**, **2.10**; I **2.8**.*

The phosphametacyclophanes adopt a 'butterfly' conformation with a P--P separation in the range of 5.050(7)-5.147(1) Å, apart from **2.5** which exhibits a reduced distance of 4.751(1) Å. The C=O bond lengths are consistent with standard ketones (e.g. 1.21 Å for acetone),[119] and are comparable to precedent diketophosphanyl compounds,[84,111,116] The P-C(O) distance for these macrocycles is notably longer than most acylphosphanes (1.79-1.85 Å),[120] though **2.10** exhibits a reduced distance relative to the series. In addition, the phenyl rings in **2.10** are not co-planar, exhibiting a torsion angle of 27 ° relative to one another, suggesting reduced conjugation relative to co-planar systems,[121] this loss of planarity has previously been seen as a result of steric repulsion between ortho-hydrogens.[122,123,124,125] Similar behaviour is observed for **2.9**, though the three-fold disorder about the distal phenyl rings impedes quantitative discussion.

The C(O)-P-C(O) angles marginally deviate across the series, being largest for **2.5** and **2.7**; similarly, they both exhibit an *ca* 1 Å longer centroid-centroid separation than the other macrocycles. More notably, the skeletal benzene rings are displaced from co-planarity by 34.26(16) ° and 86.24(12) ° in the smallest (**2.10**) and largest (**2.5**) cases respectively; the nature of the aromatic 5-R substituent is clearly influential, where significantly smaller displacement angles are observed for more electron withdrawing 5-R substituents.[126] In the case of compound **2.7**, a network of hydrogen bonding is observed between the 5-Me substituent and the carbonyl groups on the adjacent molecule (**Figure 32**), leading to a significantly larger displacement angle, a similar packing arrangement is also observed for compound **2.5**. Insight into the displacement angle is provided by DFT studies (B3LYP/6-311G(3d, 3p)), which indicate **2.1**, **2.4** and **2.6**-**2.10** possess an inter-ring bonding interaction constraining their proximity and disposition within the macrocyclic core; in contrast, the equivalent interaction within **2.5** is localised to the nitrogen centres, leading to significant widening of the inter-ring angle (**Figure 33**).

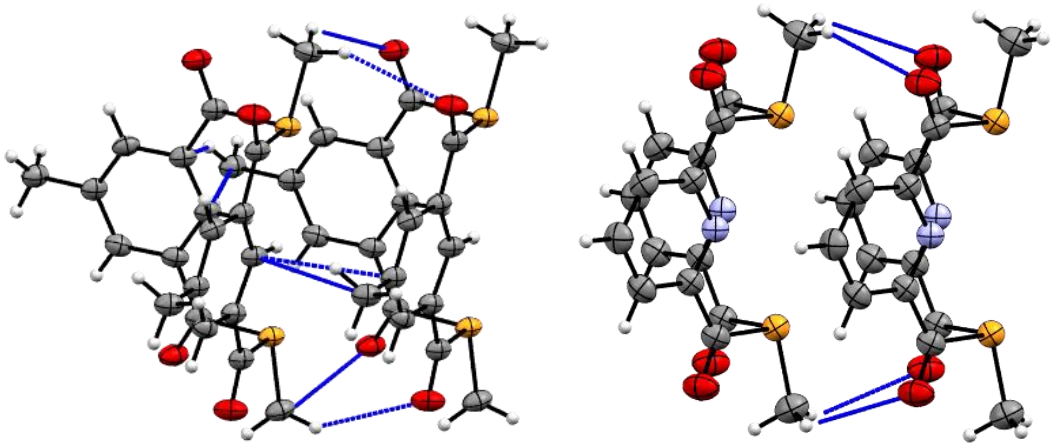

Figure 32. *Solid-state packing arrangement of **2.7** (left) and **2.5** (right) illustrating H-bonding and π-H interactions constraining the conformation.*

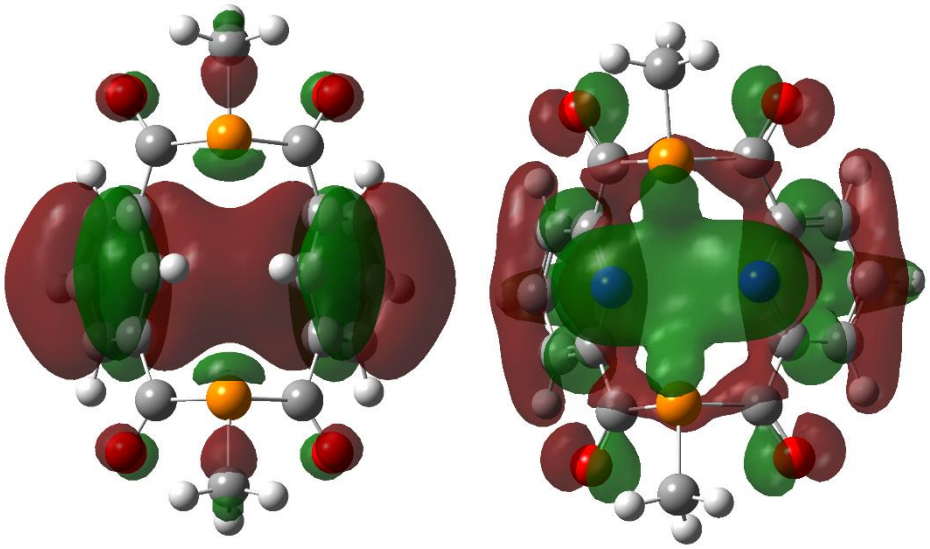

Figure 33. *Molecular orbitals for* ***2.1*** *(left) and* ***2.5*** *(right), illustrating the inter-ring bonding interaction.*

The DFT studies also provide insight into the frontier molecular orbitals, and reveal that in each case both the HOMO and HOMO-1 are predominantly associated with the phosphorus lone pair and carbonyl fragments (46-50 and 38-46 %, respectively (HOMO)), with the aromatic moieties featuring in lower lying orbitals (typically, HOMO-3 and -4); for compound **2.10** the cyanide functionality is not significantly involved until HOMO-14, whereas the LUMO-LUMO+3 are primarily associated with the aromatic and carbonyl units ($\pi^*_{(CO/Ar)}$). These data suggest the HOMO is predominantly associated with the phosphorus lone pair (**Figure 34**), suggesting preferential coordination through phosphorus over the π-system (see **Section 2.4**).[111]

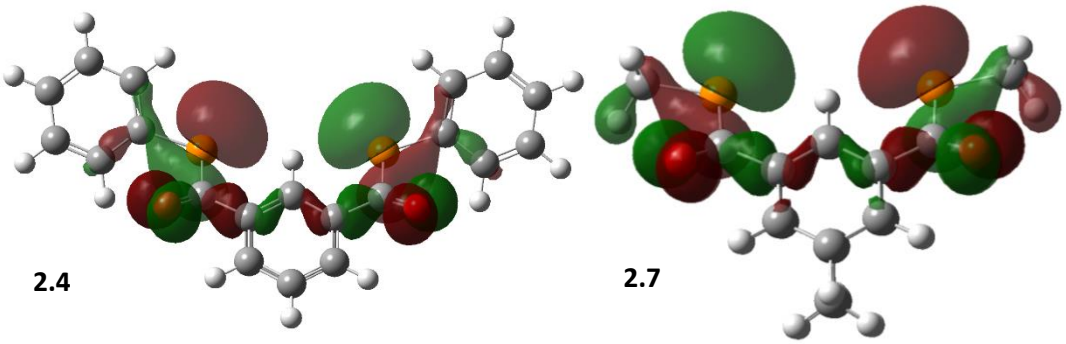

Figure 34. *Calculated HOMOs of* ***2.5*** *and* ***2.7****.*

2.3 UV-Vis Spectroscopy and Electrochemical Studies

The photophysical properties of **2.1** and **2.4**-**2.10** were investigated using UV-Vis spectroscopy to explore how structural variations perturb the absorptive features; the spectra were measured between 220-800 nm, data are presented in **Figure 35** (exemplar spectrum **Figure 37**), λ_{max} and molar absorptivity values have been tabulated (**Table 6**). The sharp absorption at *ca* 225 nm is a real feature, the spectra being recorded across several concentrations and different path lengths to equivalent effect.

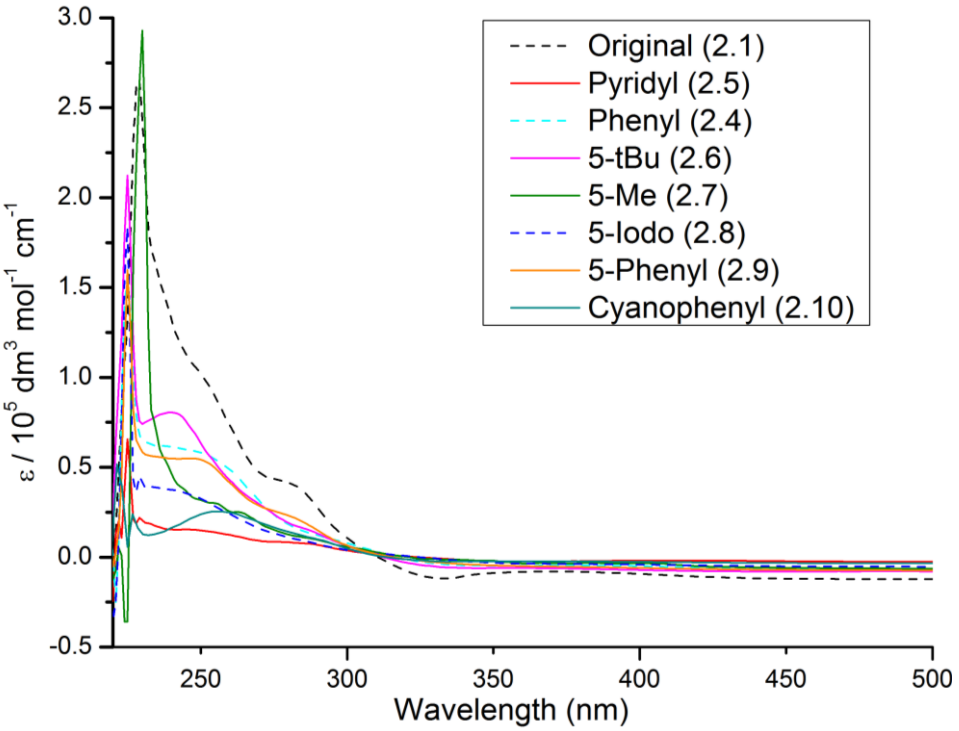

Figure 35. *Stacked UV-Vis Spectra of* ***2.1, 2.4-2.10*** *220-500 nm, omitted 200-220 nm. 1.0x10^{-5} mol dm^{-3} in CH_2Cl_2, path length 1 cm.*

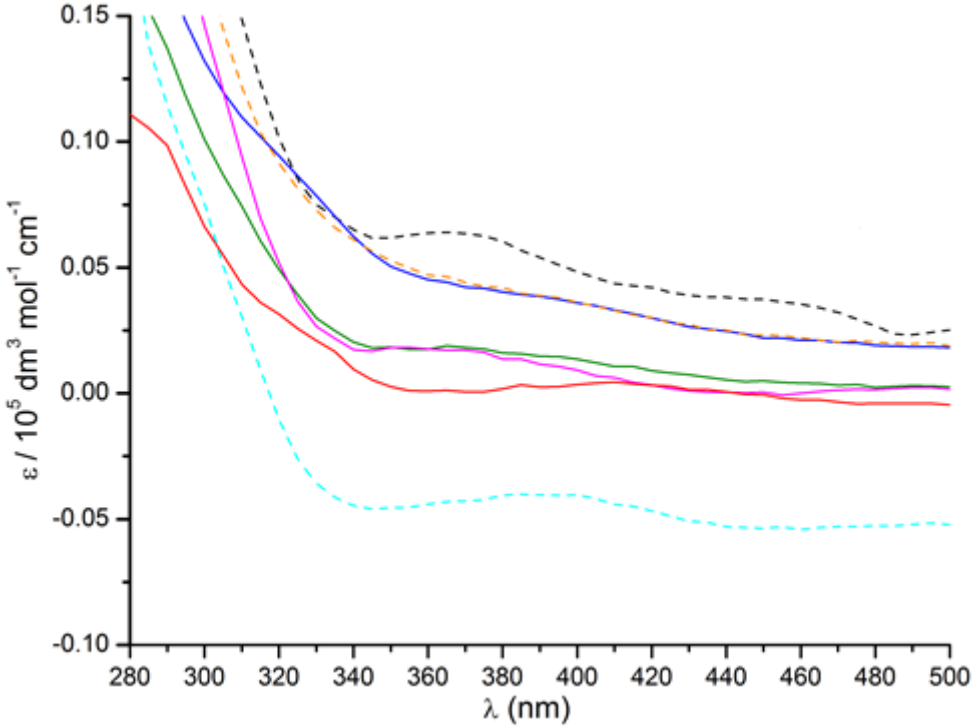

Figure 36. *Stacked Experimental UV/Vis Spectra 280-500 nm, 1.0 x 10^{-5} mol dm^{-3} in CH_2Cl_2, 1 cm path.*

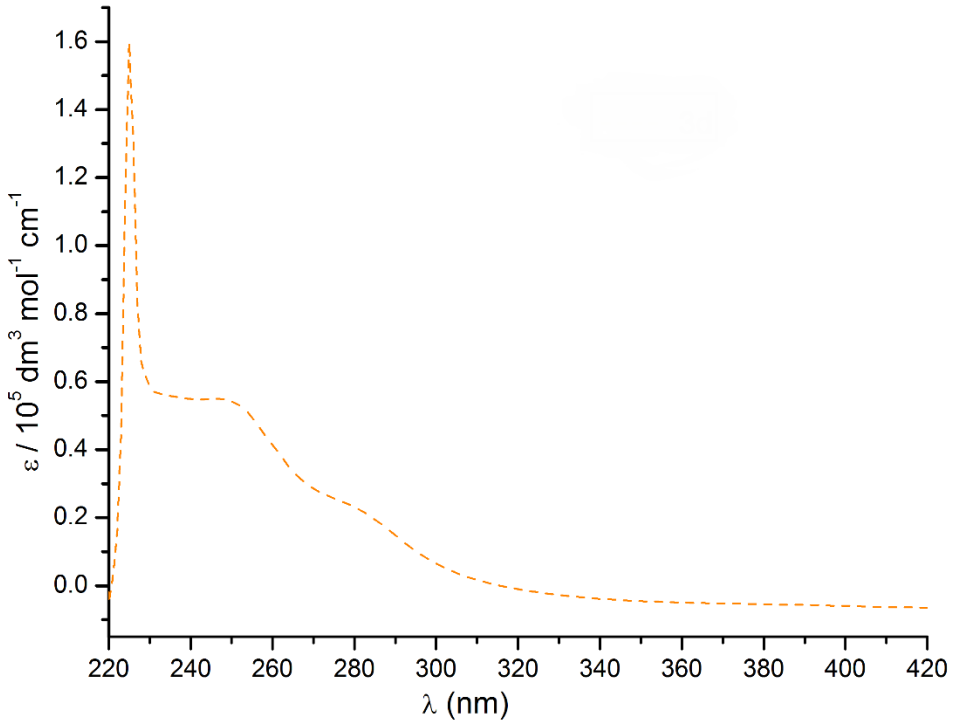

Figure 37. *Exemplar UV-Vis Spectrum of* ***2.9****. 1.0x10^{-5} mol dm^{-3} in DCM, path length 1 cm.*

Table 6. *λ_{max} and molar absorptivity values for* ***2.1, 2.4-2.10.***

	λ_{max} / nm [ε / 10^4 dm^3 mol^{-1} cm^{-1}]				
2.1	*229 [26.52]*	*250 [10.21]*	*279 [4.24]*	*365 [0.64]*	*415 [0.43]*
2.4	*225 [15.52]*	*255 [5.43]*	*294 [1.05]*		
2.5	*225 [6.56]*	*245 [1.54]*	*281 [0.82]*	*322 [0.02]*	*415 [0.04]*
2.6	*225 [21.24]*	*240 [8.05]*	*286 [1.56]*	*330 [0.27]*	*370 [0.17]*
2.7	*230 [29.30]*	*256 [2.96]*	*290 [0.96]*	*303 [0.51]*	*365 [0.19]*
2.8	*225 [18.35]*	*250 [3.25]*	*283 [0.99]*	*319 [0.10]*	*395 [0.37]*
2.9	*225 [15.97]*	*246 [5.49]*	*280 [2.37]*	*380 [0.42]*	*415 [0.31]*
2.10	*221 [5.16]*	*256 [2.54]*	*290 [0.99]*		

The UV-Spectra all exhibit three distinct features, including a high-energy absorption at *ca* 221-230 nm, with subsequent lower-energy bands observed around 250 and 280 nm. Additionally, much weaker broad features are observed around 300-350 nm and 400 nm, though these were not convincingly detected for **2.4** or **2.10**. In order to aid explanation of the observed photochemical transitions, the first 150 excited states were calculated using TD-DFT (e.g. **Figure 38**) with the B3LYP functional and 6-311G(3d,3p) basis set for P,C,H and O, with the LANL2DZ basis set used for I; these calculations included a CPCM (CH_2Cl_2) solvent model.

The highest energy feature (225-230 nm) is in each case associated with a $\pi_{Ar} \rightarrow \pi^*_{(CO/Ar)}$ transition from the HOMO-5/HOMO-8 levels into low-lying acceptor orbitals (LUMO to LUMO+3). In the case of **2.6** and **2.9** there is also a small $n \rightarrow \pi^*_{(CO/Ar)}$ contribution from the phosphorus lone pair (HOMO-8 $\rightarrow$ LUMO+2 and HOMO-11 $\rightarrow$ LUMO+1 respectively). The sharp high energy feature is most prominent for **2.1** and **2.7**, displaying a slight red shift (5 nm), in contrast **2.10** displays a weaker, blue-shifted transition (221 nm). More generally, the remaining compounds exhibit comparable spectra, though notably **2.5** displays much lower intensity absorptions across the full spectrum. The subsequent higher energy bands (*ca* 250, 280 nm) consist of $\pi \rightarrow \pi^*$ transitions from low lying occupied orbitals to the LUMO/LUMO+1 levels, with increasing contributions from $n \rightarrow \pi^*$ from the phosphorus lone pairs (HOMO/HOMO-1) to LUMO+3. The weaker broader features (*ca* 300-350, 400 nm) are associated with transitions between the frontier molecular orbitals, HOMO $\rightarrow$ LUMO, HOMO-1 $\rightarrow$ LUMO and HOMO $\rightarrow$ LUMO+1, which are predominantly $n \rightarrow \pi^*_{(CO/Ar)}$ in nature.

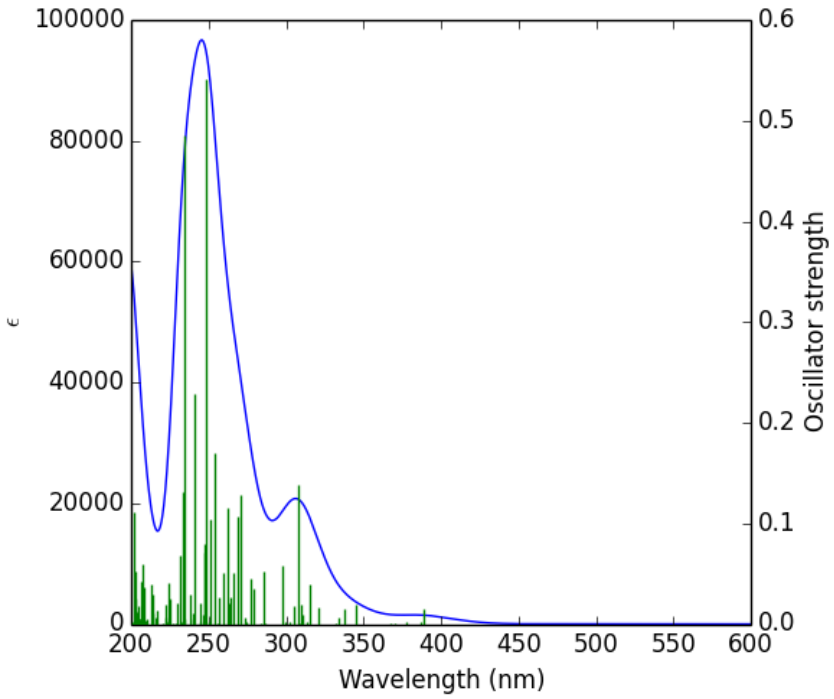

Figure 38. *Simulated UV/Vis Spectrum for* ***2.9****, derived from TD-DFT.*

In comparison, Baumgartner's diketophosphepins (**2.11**, **2.12**) show two distinct features at 270-290 and 390-460 nm,[84] significantly red shifted relative to the diphosphametacyclophanes. However, **2.1**, **2.4**-**2.10** exhibit comparable photophysical behaviour to Takeda's diphosphaindacenetetraone (**2.13**),[120] which is surprising considering the two diketophosphanyl units present in the phosphametacyclophanes, which would be anticipated to lead to reduced LUMO energies and thus red-shifted absorptions.

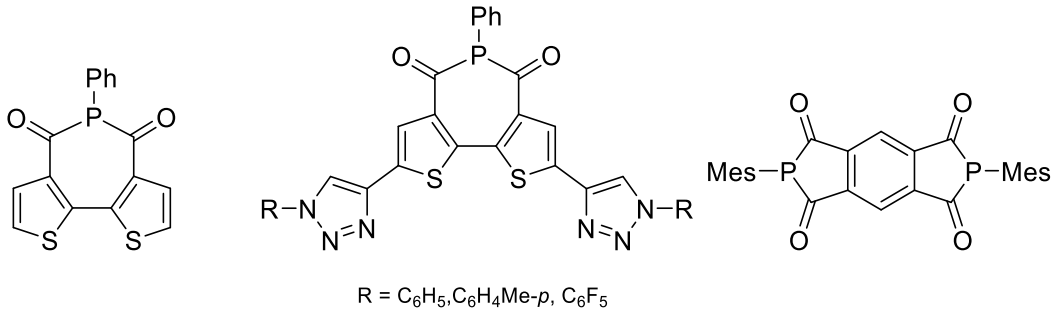

2.11 **2.12** **2.13**

Figure 39. *Diketophosphepins,* ***2.11, 2.12*** *and Diphosphaindacenetetrone,* ***2.13****.*[84,120]

To assess the electron accepting abilities of these phosphametacyclophanes their redox chemistry was probed *via* cyclic voltammetry in CH_2Cl_2, at a Pt or Au disk working electrode (1 mm) with [$^nBu_4N$][PF_6]

or [$^{n}Bu_4N$][BAr^{F}_{24}] supporting electrolyte. Notably the reductive events were not significant for compound **2.7** and **2.4**, while only one reductive event was observed for compound **2.9**. The electrochemical data for compounds **2.1** and **2.4**-**2.10** at 0.1 V s^{-1} scan rate has been tabulated (**Table 7**).

Table 7. *Electrochemical data for compounds **2.1** and **2.5**-**2.10**.0.5 mM, solvent: CH_2Cl_2; supporting electrolyte: 0.1 M tetrabutylammonium hexafluorophosphate) recorded using a Pt working electrode, Pt wire counter electrode and Ag pseudo-reference electrode (potentials are given vs. Fc+/Fc(0.00 V)).*

	Reduction 1 (V)				***Reduction 2 (V)***		
	$^{1}E_{pc}$	$^{1}E_{1/2}$	$^{1}\Delta E_p$	$^{1}E_{LUMO}$(eV)[a]	$^{2}E_{pc}$	$^{2}E_{1/2}$	$^{2}\Delta E_p$
2.1	*-1.96*	*-1.835*	*0.25*	*-2.965*	*-2.24*	*-2.15*	*0.18*
2.5	*-1.84*	*-1.735*	*0.21*	*-3.065*	*-2.21*	*-2.115*	*0.17*
2.6	*-1.965*	*-1.885*	*0.16*	*-2.915*	*-2.245*	*-2.225*	*0.2*
2.8	*-1.625*	*-1.605*	*0.04*	*-3.195*	-	-	-
2.9	*-1.815*	*-1.725*	*0.18*	*-3.075*	*-2.185*	*-2.035*	*0.22*
2.10	*-1.81*	*-1.735*	*0.1*	*-3.065*	*-2.15*	*-2.11*	*0.18*

[a] $E_{LUMO} = -(4.8 + {}^{1}E_{1/2}/V)$ eV

Generally, two distinct reductive events were observed (e.g. **Figure 40**) at E_{pc} = -1.71 to -1.98 V and -2.15 to -2.25 V vs Fc^{+}/Fc, the peak-to-peak separation (ΔE_p) being indicative of a quasi-reversible process, consistent with previously described diketophosphanyl compounds.[120,127] The E_{LUMO} values are similar to the small number of diketophosphanyls (-3.02 to -4.04 V), albeit only just, indicating a decreased electron accepting capability relative to most. The notably lower reduction potential for **2.9** indicates a more stabilised LUMO for weaker donating substituents, with **2.9** lying *ca* 0.15 eV lower in energy than the rest of the series, whereas the LUMO of **2.6** (which bears the most electron donating substituent) is 0.25 eV higher in energy.

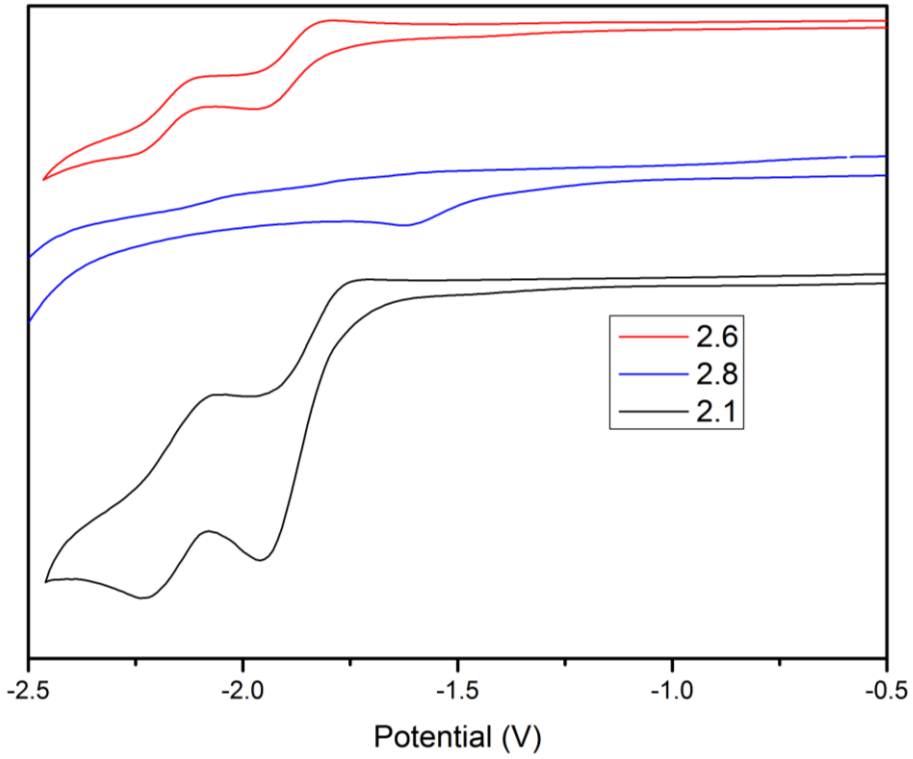

Figure 40. *Cyclic voltammogram of* ***2.1, 2.6*** *and* ***2.8*** *(0.5 mM, solvent: CH_2Cl_2; supporting electrolyte: 0.1 M tetrabutylammonium hexafluorophosphate) recorded using a Pt working electrode, Pt wire counter electrode and Ag pseudo-reference electrode (potentials are given vs. Fc+/Fc(0.00 V)).*

The quasi-reversible nature of these reductive events suggests the radical anions should be rather persistent, furthermore, the first reductive event is comparable to those of bis(acyl)phosphane oxides (BAPOs), $E_{1/2}$ = *ca* −1.8V, E_{LUMO} = −3.0 eV, which are used as effective initiators for polymerisation.[127] Overall these phosphacyclophanes exhibit comparable redox behaviour to that of simpler aromatic diketophosphanyls,[120] exhibiting no further stabilisation of the LUMO upon the introduction of the second diketophosphanyl moiety. This behaviour could suggest that the two diketophosphanyl units are essentially two distinct functionalities, which may be inferred (*vide supra*) from the HOMO and HOMO-1, which are dominated by the phosphorus lone pairs rather than the aromatic cores, the frontier molecular orbitals more generally do not appear to exhibit a fully delocalised system, indicating no conjugation between the two diketophosphanyl units and thus the two units are essentially isolated.

2.4 Coordination of The Diphosphametacyclophanes

The oxidation of phosphanes within π-conjugated systems has previously been shown to reduce the E_{LUMO} of the system and thus enhance electron acceptor character.[84,128] The oxidation of the

phosphametacyclophanes with chalcogens (S, Se or Te) was therefore attempted, though resulted in the recovery of the free macrocycle. Further attempts using Woolins-reagent,[129] hydrogen peroxide or *meta*-chloroperoxybenzoic acid (mCPBA) resulted only in decomposition or the formation of $MePH_2$.

Reacting **2.1** with $[M(\eta^4\text{-}C_8H_{12})Cl]_2$ (M = Ir, Rh) results in the formation of $[M(\eta^4\text{-}C_8H_{12})Cl\{3\text{-}C(O)\text{-}C_6H_4\text{-}(C(O)PMe)\}_2]$ (M = Ir (**2.14**), Rh (**2.15**)). However, some residual metal dimer is always present in the product and due to the similar solubilities of reagent and product bulk recrystallisation is difficult, though it is possible to grow single crystals of the products preferentially (**Figure 41**; **Table 8**), albeit at low isolated yield.

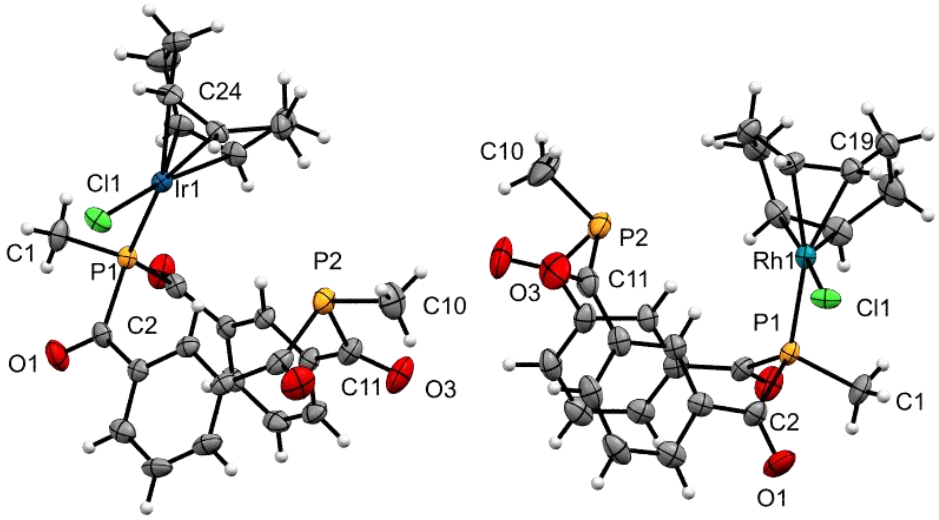

Figure 41. *Molecular Structure of $[M(\eta^4\text{-}C_8H_{12})Cl\{3\text{-}C(O)\text{-}C_6H_4\text{-}(C(O)PMe)\}_2]$ with thermal ellipsoids at the 50 % probability level. M = Ir (left) and Rh (right).*

Table 8. *Selected bond lengths (Å) and angles (°) for **2.14** and **2.15** with estimated standard uncertainties in parentheses.*

	2.14	***2.15***
P(M)-CH_3[a]	*1.804 (4)*	*1.806 (6)*
P-CH_3	*1.826 (5)*	*1.825 (8)*
P-M[a]	*2.2733 (9)*	*2.2730 (16)*
P(M)-C(O)[a]	*1.911 (4)*	*1.900 (7)*
P-C(O)	*1.895 (4)*	*1.876 (8)*
C=O	*1.209 (5)*	*1.211 (8)*
M-Cl[a]	*2.3792 (8)*	*2.4646 (13)*
M-C=C[a]	*2.209 (3)*	*2.223 (6)*

[a]*M = Ir (**2.14**) and Rh (**2.15**).*

The parameters of the macrocyclic core in complexes **2.14** and **2.15** are generally consistent with data for free **2.1**, though a slight contraction is noted for the P(M)-CH_3 distances. More generally, the bond lengths of **2.14** and **2.15** are comparable, only the M-Cl bond distance displaying a significant difference, albeit consistent with expectation between Ir/Rh systems.[130] The P-Rh bond length is somewhat shorter than [RhCl(COD)PPh_3] (2.308 (7) Å),[131] and longer than the bisphosphomide complex [RhCl{2,6-{$Ph_2PC(O)$}$_2$(C_5H_3N)}] (2.2523 (6) Å),[116] which may suggest weaker binding than in the latter case.

Compound **2.4** was reacted with [Pt(PEt_3)Cl_2]$_2$ to afford [{Pt(PEt_3)Cl_2}$_2$}{3-C(O)-C_6H_4-(C(O)PPh}$_2$] (**Figure 43**). The $^{31}P\{^1H\}$ spectrum exhibits two doublets, δ_p 40 and 16 ($^2J_{P\text{-}P}$ = 425 Hz), with associated ^{195}Pt satellites, the magnitude of coupling ($^1J_{P\text{-}Pt}$ = 2010 and 2770 Hz; **Figure 42**) being suggestive of *trans*-coordination.[111] This is consistent with the previously reported coordination of **2.1,** reaction with [Pt(PEt_3)Cl_2]$_2$,[111] affording a product with two doublets at δ_P 15.9 and 51.3, bearing comparable P-P ($^2J_{PP}$ 441 Hz) and Pt-P ($^1J_{PPt}$ 2813 and 1951 Hz respectively) coupling, in accordance with trans-coordination. Crystals suitable for X-Ray diffraction from reactions with both **2.1** and **2.4** remain elusive.

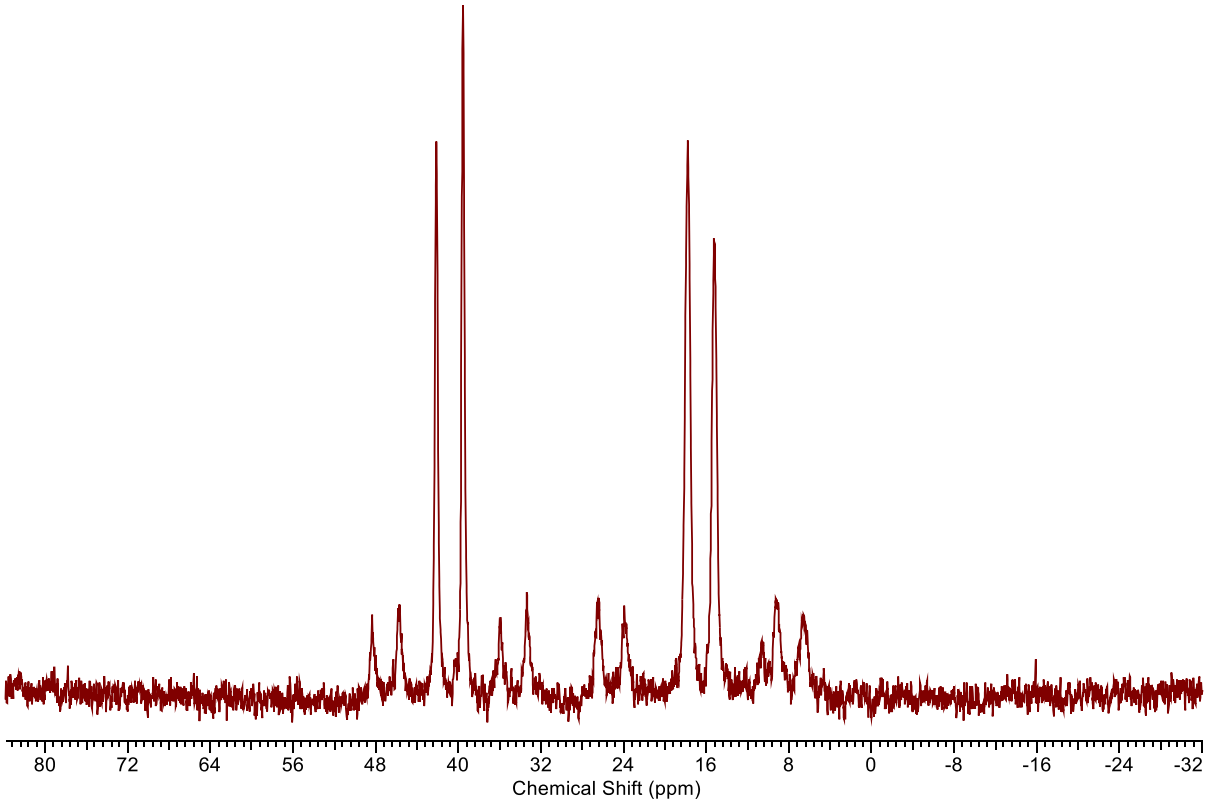

Figure 42. *^{31}P NMR spectrum (C_6D_6, 161.72 MHz) of [{Pt(PEt_3)Cl_2}$_2$}{3-C(O)-C_6H_4-(C(O)PPh)}$_2$].*

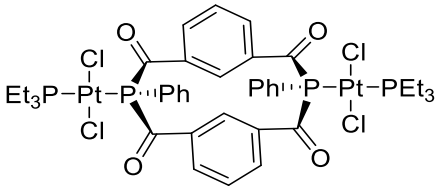

Figure 43. *[{Pt(PEt$_3$)Cl$_2$}$_2${3-C(O)-C$_6$H$_4$-(C(O)PPh)}$_2$].*

In an analogous reaction with *m*-{-C(O)-C$_5$N$_1$H$_4$(C(O)PMe)}$_2$ (**2.5**; **Scheme 17**), P-C bond cleavage occurred, resulting in the formation of a pincer complex (**2.16**) as identified from X-Ray diffraction (**Figure 44**). This is similar to the reactions observed for Balakrishna's tetramer (**2.2**) when reacted with [Pd(allyl)Cl]$_2$,[114] however, the reaction with **2.5** does not display such clean conversion, with multiple species being observed by ^{31}P NMR. These include three ^{31}P resonances, a doublet of doublets at δ_P 32 (*J* = 400 Hz, 32 Hz), a doublet at 11.6 (*J* = 400 Hz) and a triplet at 5.8 (*J* = 32 Hz), the comparable coupling suggests these resonances are associated with one another and could be consistent with the formation of **2.16**, which was identified by X-Ray diffraction, though the low-quality data deems the bond metrics unreliable, thus only permitting connectivity to be confirmed.

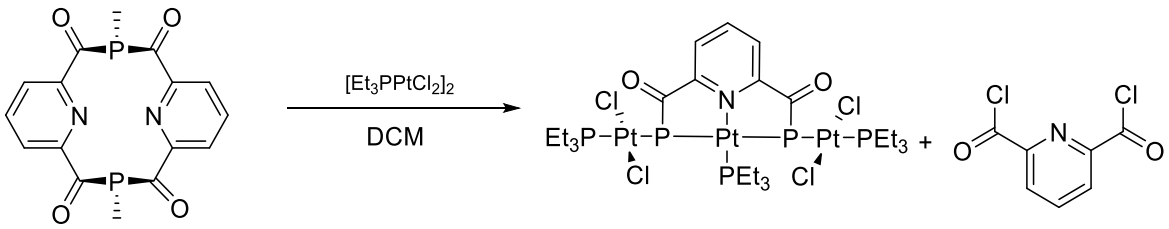

Scheme 17. *Proposed reaction scheme for compound* ***2.16****.*

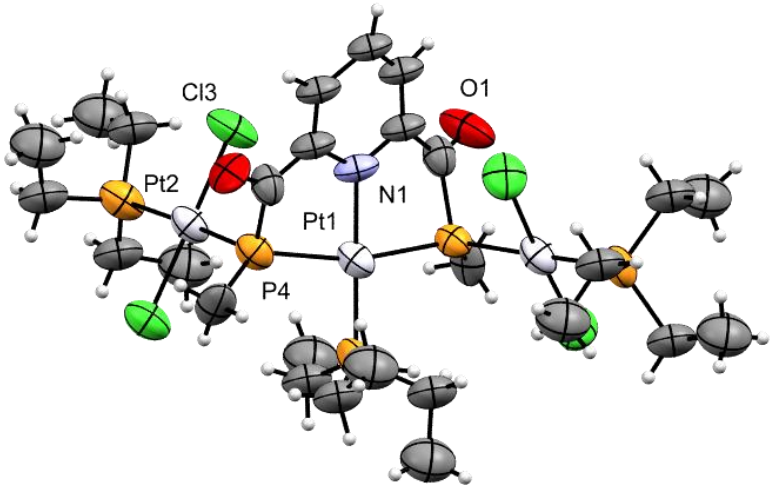

Figure 44*. Molecular structure of* ***2.16*** *with thermal ellipsoids at the 50 % probability level; the crystallisation solvent omitted for clarity.*

Despite the coordination chemistry of the phosphametacyclophanes not being extensively studied, the formation of **2.14**-**2.16** and [{Pt(PEt_3)Cl_2}$_2${3-C(O)-C_6H_4-(C(O)PPh)}$_2$] demonstrate that phosphorus coordination is achievable, despite the apparent resistance to oxidation.

2.5 Nitrogenous Analogues of the Phosphametacyclophanes

Though nitrogen-based cyclophanes are notably more common than phosphacyclophanes, they are typically prepared *via* multi-step, complex syntheses. In comparison, *via* a simple condensation route the diphosphametacyclophanes were prepared in a facile manner, which should be able to facilitate the preparation of nitrogen analogues as well. Therefore, in seeking a direct nitrogen analogue of the phosphametacyclophanes with which to compare, $MeN(SiMe_3)_2$ was reacted with isophthaloyl chloride under comparable conditions in an effort to prepare *m*-{-C(O)-C_6H_4(C(O)NMe)}$_2$ (**2.17**; **Scheme 18**), however, no reaction occurred after 7 days. The reaction was repeated in toluene and brought to reflux, resulting in multiple unidentified species in the ^{1}H NMR spectrum, though none was consistent with the formation of **2.17**.

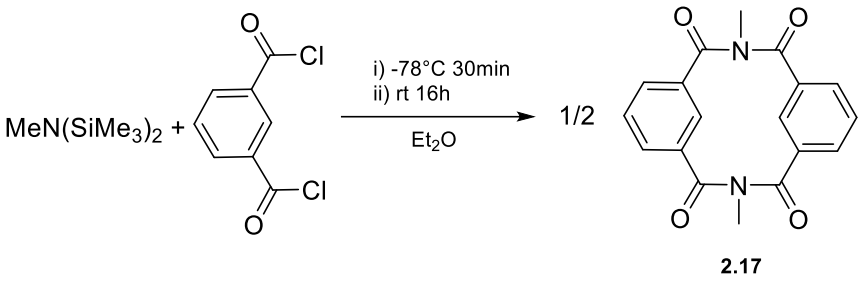

Scheme 18. *Attempted synthetic route to prepare* ***2.17****.*

Given unsuccessful attempts to synthesise **2.17** from $MeN(SiMe_3)_2$, an alternative approach was considered. $MeNH_2$ was disregarded due to being a gas under ambient conditions and instead aniline was used in an attempt to make the nitrogen congener of **2.4** (**2.18**). Therefore, aniline was reacted with isophthaloyl chloride in the presence of triethyl amine (**Scheme 19**); seemingly the reaction stopped once diphenylisophthalamide (**2.19**) was formed, initially thought to be a consequence of low solubility. A second equivalent of isophthaloyl chloride was added in the presence of ^{n}BuLi, however, even after reflux, compound **2.19**, was recovered unchanged.

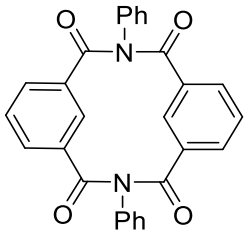

2.18

Figure 45. *m-{-C(O)-C_6H_4(C(O)NPh)}$_2$ (**2.18**).*

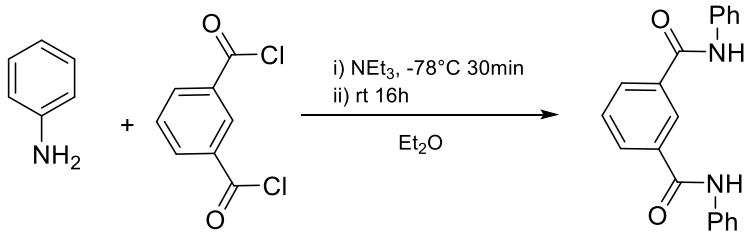

2.19

Scheme 19. *Attempted reaction to form 2.18, which stopped after forming diphenylisophthalamide (**2.19**).*

Notably, the post-synthetic modification of **2.19** is significantly less facile than its phosphorus congener, which could be a consequence of the greater delocalisation of the amide lone pair compared with phosphorus analogues. Nevertheless, a similar compound, **2.20**, has previously been prepared,[132] suggesting the problem may instead lie with the size of the substrate. Therefore **2.19** was reacted with glutaryl chloride in the presence of base, however, only starting material was recovered, despite testing a multitude of temperatures as well as varying the order of addition. Similar reactions with benzoyl chloride, resulted in the formation of {$C_6H_4C(O)NC(O)C_6H_5$}$_2$ (**2.21; Figure 47**), ultimately confirmed by X-Ray diffraction (**Figure 48**).

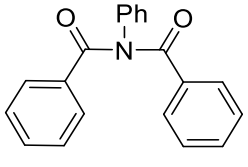

2.20

Figure 46. *Specific example that the amide functionality can be further functionalised.*

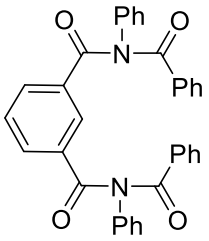

2.21

Figure 47. *$\{C_6H_4C(O)NC(O)C_6H_5\}_2$.*

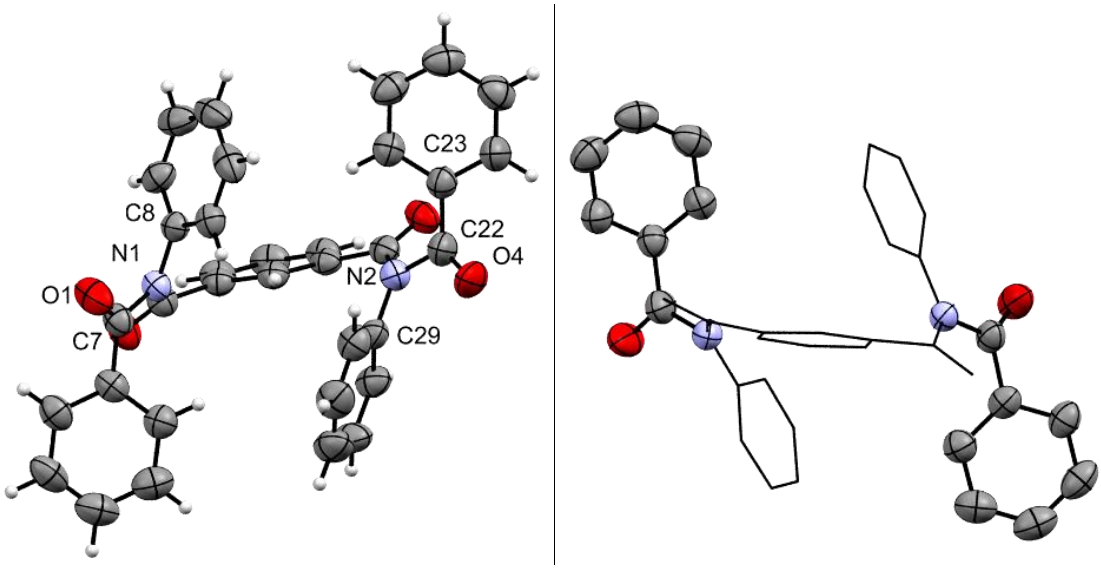

Figure 48. *Molecular structure of **2.21**, with thermal ellipsoids at the 50 % probability level. Selected bond lengths (Å) and angles (°): N1-C8 1.443(2), N1-C14 1.414(2), N1-C7 1.412(2), N2-C21 1.397(2), N2-C29 1.442(2), N2-C22 1.430(3), O1-C7 1.207(2), O3-C21 1.216(2), O2-C14 1.208(2), O4-C22 1.186(18). C14-N1-C8 119.01(13), C7-N1-C8 118.09(15), C7-N1-C14 120.58(14), C21-N2-C29 12.71(15), C21-N2-C22 116.92(15), C22-N2-C29 116.91(15).*

Notably in compound **2.21** the two benzoyl substituents are situated in opposing directions, presumably due to steric constraints. This relative geometry is also observed in **2.19**, where the hydrogen atoms on nitrogen are positioned in alternate directions,[133] which could reasonably underpin the lack of reactivity seen with isophthaloyl chloride, as the relative positions of the phenyl substituents would limit the size of substrates able to approach the nitrogen centres as a result of steric hinderance.

2.6 Investigating the Relationship Between Phosphaalkene and Macrocycle formation

Isolation of the cyclophanes **2.1**, **2.4**-**2.10** from simple condensation of $RP(SiMe_3)_2$ and the respective diacyl chloride is remarkable, given that comparable reactions with alkyl and many aryl acid chlorides typically favour the Becker condensation pathway to afford phosphaalkenes (**Scheme 20**). This results

from an acyl phosphane undergoing a spontaneous 1,3-silatropic rearrangement driven by the oxophilicity of silicon, to afford the phosphaalkene.

If a bulkier phosphane is reacted with isophthaloyl chloride, $RP(SiMe_3)_2$ (R = ^{t}Bu or Mes), new spectroscopic signatures are detected at δ_P 197 (^{t}Bu) and 153 (Mes) in the ^{31}P NMR spectrum, which lie in regions consistent with phosphaalkenes.[134,135,136] In addition, the ^{1}H NMR spectra exhibit peaks consistent with the aromatic backbone, 'R' substituent and the trimethylsilyl group (TMS), integrating in a 1:1:1 manner, suggesting the latter has been retained and the corresponding phosphaalkene has formed (**Scheme 21**).

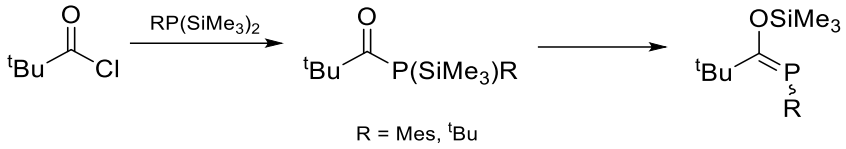

Scheme 20. *The Becker condensation pathway.*

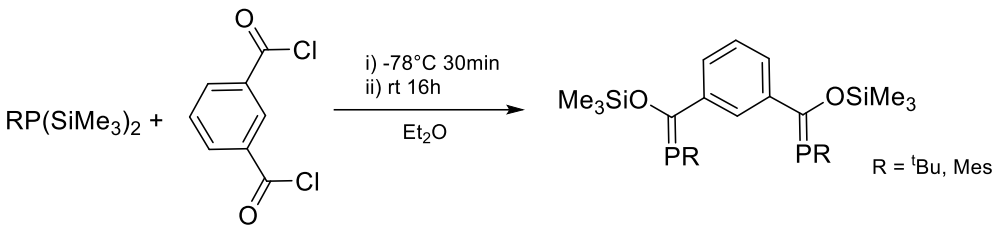

Scheme 21. *Proposed phosphaalkene formation.*

Although spectroscopic data are consistent with phosphaalkene formation, attempts to isolate the product *via* vac-transfer, distillation, solvent removal and trituration were unsuccessful. Upon exposure to vacuum, only a single phosphorus resonance at δ_P 26 (^{t}Bu) and 25 (Mes) is observed, though this species has not been identified.

The mesityl-substituted phosphaalkene is somewhat more 'stable', therefore coordination to $W(CO)_5(THF)$ was attempted, resulting in a significant shift of the phosphorus NMR resonance to δ_P 110 alongside the manifestation of tungsten satellites (^{183}W, I = ½, 14 %; J_{PW} = 255 Hz), confirming coordination of the phosphorus centre, albeit this species could only be observed *in situ*. The reaction of the proposed mesityl phosphaalkene with $[Pt(PEt_3)Cl_2]$ led to the decomposition of the phosphaalkene, though the Pt centre did react with a minor hydrolysed impurity, yielding two sets of doublets ($^2J_{PP}$ = 464 Hz, J_{PPt} = 2864, 2058 Hz) in the ^{31}P{^{1}H} NMR spectrum, the latter becoming a

doublet of doublets in the coupled spectrum ($^1J_{PH}$ = 378 Hz). Crystals suitable for X-Ray diffraction were grown, confirming the structure of [{Pt(PEt_3)Cl_2}$_2${3-C(O)(Cl)-C_6H_4-(C(O)P(H)Mes)}] (**Figure 49**).

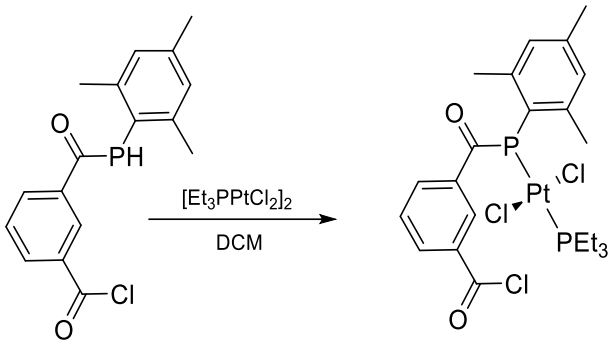

Scheme 22. *Believed impurity and reaction which led to the observation of [{Pt(PEt_3)Cl_2}$_2${3-C(O)(Cl)-C_6H_4-(C(O)P(H)Mes)}]*

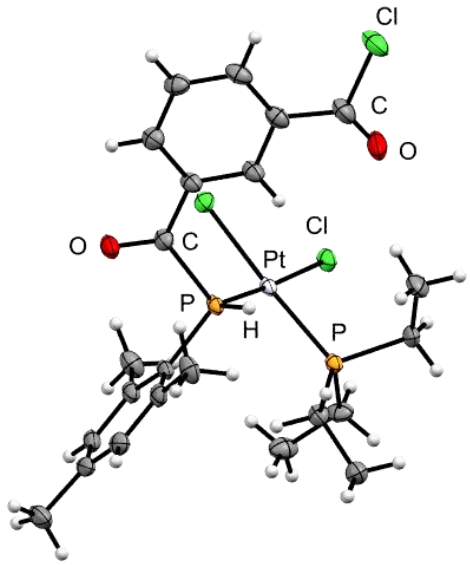

Figure 49. *Molecular Structure of [{Pt(PEt_3)Cl_2}$_2${3-C(O)(Cl)-C_6H_4-(C(O)P(H)Mes)}] with thermal ellipsoids at the 50 % probability level*. Selected bond lengths (Å) and angles (°): Pt1-Cl2 2.3804(9), Pt1-Cl3 2.3261(8), Pt1-P1 2.2272(8), Pt1-P2 2.2476(9), P1-C4 1.816(3), P1-C11 1.897(4), P2-C26 1.823(4), P2-C28 1.822(4), P2-C30 1.822(4).Cl3-Pt1-Cl2 88.79(3), P1-Pt1-Cl2 89.49(3), P1-Pt1-Cl3 175.44(3).*

*This platinum complex was isolated whilst working with a summer JRA student, Vladimir Simenok.

2.7 Summary

A series of phosphametacyclophanes (**2.4**-**2.10**) have been synthesised and characterised by heteronuclear NMR spectroscopy and their characteristic carbonyl stretches. Structural data confirm these phosphacyclophanes are dimeric in nature, in comparison to work by Balakrishna and co-workers who observe tri- and tetrameric structures, which can reasonably conclude to be a facet of the synthetic route, rather than the incorporation of phenyl or pyridyl units.

The structural data obtained (**Table 5**) highlight the influence the 5-R substituent has upon the displacement angle between π-systems, with significantly smaller displacement angles being observed for more electron withdrawing substituents, allowing control over the cavity size.

The electronic properties of these macrocycles were probed *via* UV-Vis spectroscopy and cyclic voltammetry. Overall, it was found that E_{LUMO} was more stabilised for weaker donating substituents on the aromatic ring (e.g. I) and indeed that the macrocycles photophysical and redox behaviour was comparable to that of simpler aromatic diketophosphanyls, exhibiting no further stabilisation of the LUMO with the second diketophosphanyl moiety, suggesting that the two diketophosphanyl units are essentially two distinct functionalities possessing no delocalisation/conjugation between the two units.

Attempts to further reduce the E_{LUMO} of the system and thus enhance their electron acceptor character *via* oxidation were unsuccessful. However, these macrocycles readily coordinate to transition metals, facilitating the synthesis of $[M(\eta^4\text{-}C_8H_{12})Cl\{3\text{-}C(O)\text{-}C_6H_4\text{-}(C(O)PMe)\}_2]$ (M = Rh, Ir) and $[\{Pt(PEt_3)Cl_2\}_2\{3\text{-}C(O)\text{-}C_6H_4\text{-}(C(O)PPh)\}_2]$.

Attempts to access nitrogenous analogues of **2.1** and **2.4** were unsuccessful, however, a benzoyl substituted derivative (**2.21**) was prepared. Finally, unlike Me and Ph substituted bis-silylated phosphanes ($RP(SiMe_3)_2$), ^{t}Bu and Mes analogues form phosphaalkenes *via* Becker-type condensation when reacted with isophthaloyl chloride, the Mes-Phosphaalkene coordinates tungsten pentacarbonyl (J_{PW} = 255 Hz), though only stable in solution.

Chapter 3 - Phosphacycloalkyldiones: Synthesis and coordinative behaviour of 6- and 7-member cyclic diketophosphanyls

"I am fire! I am…death!"

--The Hobbit: The Desolation of Smaug (2013)

3.1 Introduction

Despite the increasing exploitation of diketophosphanyl derivatives in organic opto-electronics (**Chapter 2**), the exploration of α-acyl phosphanes more generally remains sparse. Although a number of such compounds have been reported, their lack of use presumably stems from the inherent weakness of the phosphomide linkage (P-C(O)) rendering them prone to hydrolytic and/or oxidative cleavage,[137] though a small number have been investigated for ruthenium-catalysed hydrogenations,[138] rhodium-catalysed hydroformylation[86] and the coordination chemistry of $C_6H_4\{C(O)PPh_2\}_2$-1,3 and $C_5H_3N\{C(O)PPh_2\}_2$-2,6 has also been described.[87,88]

The diketophosphanyl functionality (-C(=O)-PR-C(=O)-) has recently become established as a desirable moiety for opto-electronically active species, leading to an upsurge of interest in bis(acyl)phosphanes. The 'diketo' motif exhibits reduced LUMO energies compared with precedent carbon and nitrogen systems,[84] thus a range of derivatives based upon aromatic backbones have been investigated,[84,116,139] with the intent to enhance their n-type properties, consequently improving the performance of organic optoelectronic devices (e.g. OLEDS, POVs).

Acyclic derivatives have also shown promise as photoinitiators, with bis(acyl) phosphane oxides (BAPOs) overcoming the inefficient UV curing seen for carbocentric congeners.[113] The P-C(O) bond cleavage produces a phosphanoyl and benzoyl radical pair, which serves as an effective initiator for radical polymerisation (*vide supra* **Scheme 11**).[112]

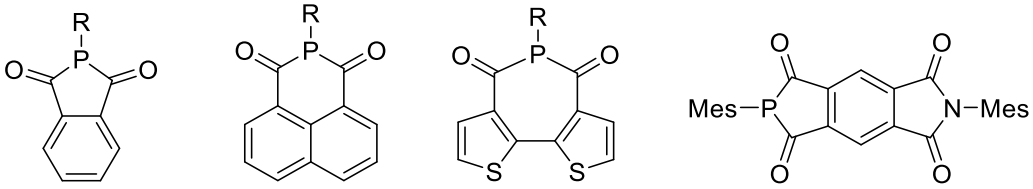

Figure 50. *Examples of diketophosphanyl compounds.*[84,116,120]

No examples of cyclic bis(acyl)phosphanes based upon fully saturated backbones exist and indeed saturated phosphacycles more generally are somewhat less studied, the first being discovered by Grüttner in 1915 (**3.1; Figure 51**),[140] with only a handful being reported since.[141,142,143] Among the small collection of saturated phosphacycles, only a few bear an acyl functionality (**Figure 52**);[144,145,146] the coordination chemistry of these compounds has briefly been explored,[144] with a particular focus on catalytic applications.[147,148]

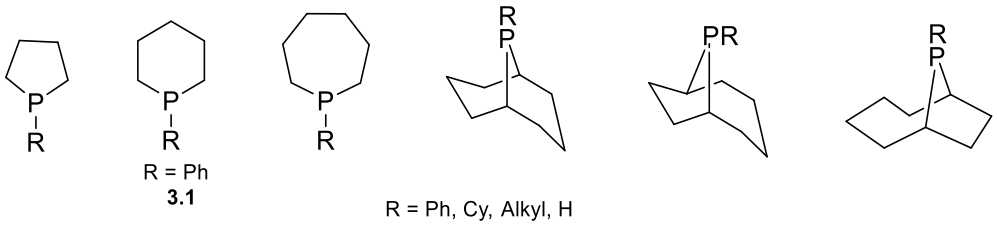

Figure 51. *Reported saturated phosphacycles.*[141-146]

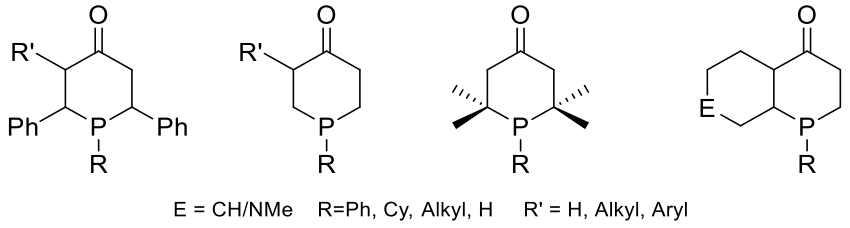

Figure 52. *Representative acyl functionalised saturated phosphacycles.*[144-146]

Following the synthesis, isolation and systematic study of phosphametacyclophanes (**Chapter 2**), analogous materials based upon a saturated cyclic motif were sought. This chapter describes the synthesis of 6- and 7-member cyclic bis(phosphomides) $RP\{C(O)\}_2C_nH_{2n}$ (n = 3, 4; R= aryl, alkyl) and investigates their donor behaviour *via* coordinative and computational studies.

3.2 Synthesis and Characterisation of the Phosphacycloalkyldiones

Phosphinanes **3.2** and phosphepanes **3.3** were obtained from the condensation reaction of the respective bis-silylated phosphane ($RP(SiMe_3)_2$, R = Me, ^{n}Bu, ^{t}Bu, Ph) and acyl chlorides $\{C(O)Cl\}_2\{(CH_2)_n\}$ (n = 3, 4; **Scheme 23**). In each case, compound identity was elucidated from spectroscopic data (**Table 9**), the observation of consistent molecular ions in the mass spectra, and in the case of **3.2d** and **3.2e**[*], X-Ray structural data (**Table 9**). The observed $^{31}P\{^1H\}$ NMR shifts δ_P 68-31 are in line with the standard range of trialkyl phosphanes,[149] in addition a single P-C(O) environment is observed in the $^{13}C\{^1H\}$ NMR spectra δ_C 221-216, with a doublet multiplicity ($^1J_{CP}$ = 40-50 Hz) which is in agreement with precedent acyl phosphanes, while no signals suggestive of phosphaalkene formation are observed.[150] Additionally, the retention of P-alkyl/aryl substituents were also observed in the ^1H NMR spectra, which integrate with broad consistency.

[*] Initial synthesis of **3.2e** was performed alongside summer student Vladamir Simenok.

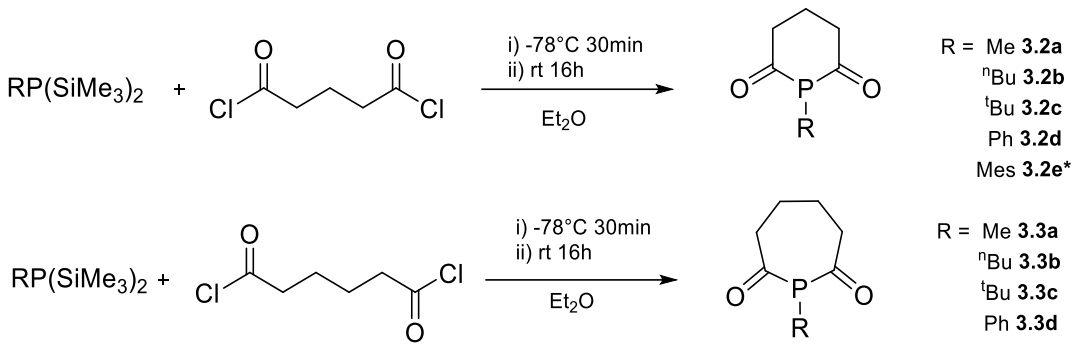

Scheme 23. *Synthesis of phosphacycloalkyldiones **3.2a-e** and **3.3a-d**.*

Table 9. *Selected Spectroscopic data for **3.2a-e*** and **3.3a-d** (^{13}C 100.46 MHz, ^{31}P 161.71 MHz)..*

	δ_P[a]	δ_C ($^1J_{CP}$[b])	ν_{CO}[c] / cm^{-1}
3.2a	*36.9*	*220.5 (42)*[d]	*1739 (w), 1668 (s)*
3.2b	*47.7*	*219.6 (43)*[a]	*1768 (w), 1660 (s)*
3.2c	*68.2*	*218.8 (48)*[a]	*1736 (w), 1655 (s)*
3.2d	*49.2*	*218.5 (44)*[e]	*1737 (w), 1667 (s)*
3.2e	*31.3*	*217.0 (41)*[a]	*1738 (w), 1659 (s)*
3.3a	*39.7*	*217.7 (48)*[a]	*1659 (s)*[f]
3.3b	*48.9*	*218.5 (48)*[a]	*1736 (w), 1657 (s)*
3.3c	*60.9*	*221.5 (50)*[d]	*1736 (m), 1652 (s)*
3.3d	*49.0*	*218.1 (47)*[d]	*1735 (w), 1665 (s)*

[a]as C_6D_6 Solution. [b]in Hz. [C]as THF solution. [d]as $CDCl_3$ solution. [e]as CD_2Cl_2 solution. [f]symmetric mode not observed.

The ^{31}P NMR spectral shifts are in line with precedent diketophosphanyl derivatives (δ_P 30–67),[84,139] though the phosphane substituent 'R' appears to have a more notable influence on δ_P for **3.2** and **3.3** than was observed for phosphametacyclophanes (δ_P 32.7 (Me), 30.5 (Ph)). The phosphacycles **3.2** and **3.3** exhibit higher frequency phosphorus shifts relative to their fully saturated comparators (δ_P –34.3 to 2.1; **Figure 51**, *vide supra*), presumably as a consequence of the flanking carbonyls deshielding the phosphorus centre. The shift of the associated P-C(O) resonance in the $^{13}C\{^1H\}$ NMR is comparable to similar 'diketo' containing compounds (δ_C 199-209; $^1J_{CP}$ = 35-51 Hz), though somewhat lower than the acyl(chloro)phosphane RC(O)P(Cl)(*t*-Bu) (R = $C_{14}H_{10}$), δ_C 211 ($^1J_{CP}$ = 67 Hz).[151]

The ^1H resonances observed for **3.2** and **3.3** generally integrate consistently, however, those associated with the cyclic skeleton display poor resolution, suggestive of conformational non-rigidity

* Initial synthesis of **3.2e** was performed alongside summer student Vladamir Simenok.

in solution (**Figure 54**, 30 °C), presumably resulting from chair-boat interconversion (**Figure 53**). This is most pronounced in the case of compound **3.2a**, in which the associated proton signals are barely distinguishable at ambient temperature, however, the four unique environments become well resolved at −40 °C (**Figure 55**) allowing the inequivalent protons to be assigned, though the complex splitting patterns observed in **3.2a** hinder the extraction of coupling constants. Lower temperatures led to loss of resolution due to slow-tumbling,[117] while the slow exchange limit could not be reached. The molecular composition of **3.2** and **3.3** was confirmed by high-resolution mass spectrometry and the structure of these heterocycles was ultimately confirmed by X-Ray diffraction (**Figure 56**, **Figure 57**); structural parameters are outlined in (**Table 10**).

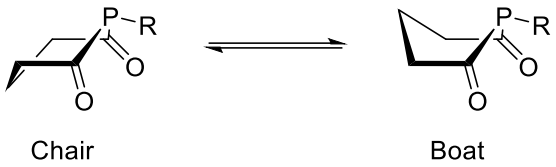

Figure 53. *Chair-Boat phosphacycle interconversion.*

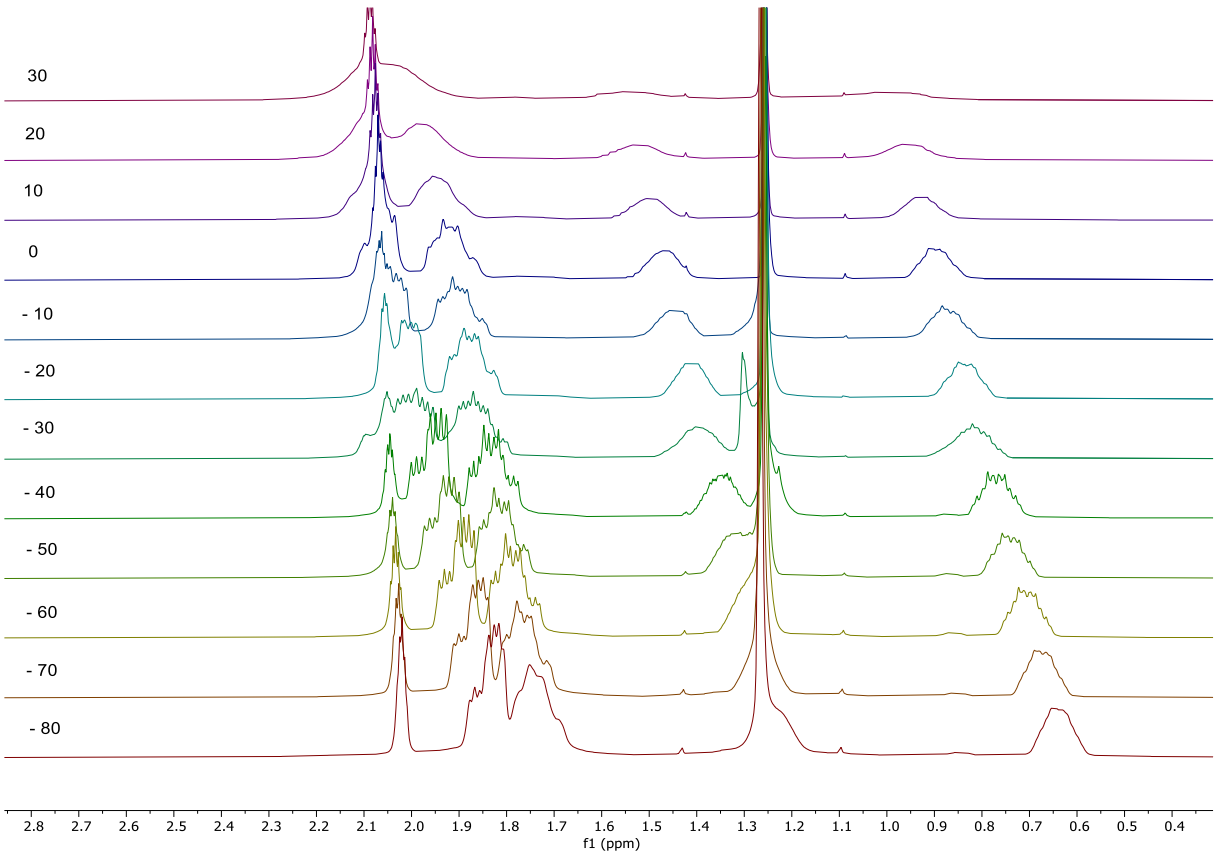

Figure 54. *Variable temperature ^{1}H NMR (C_7D_8, 303-238 K, 399.49 MHz) spectra for compound **3.2a** for the alkyl region.*

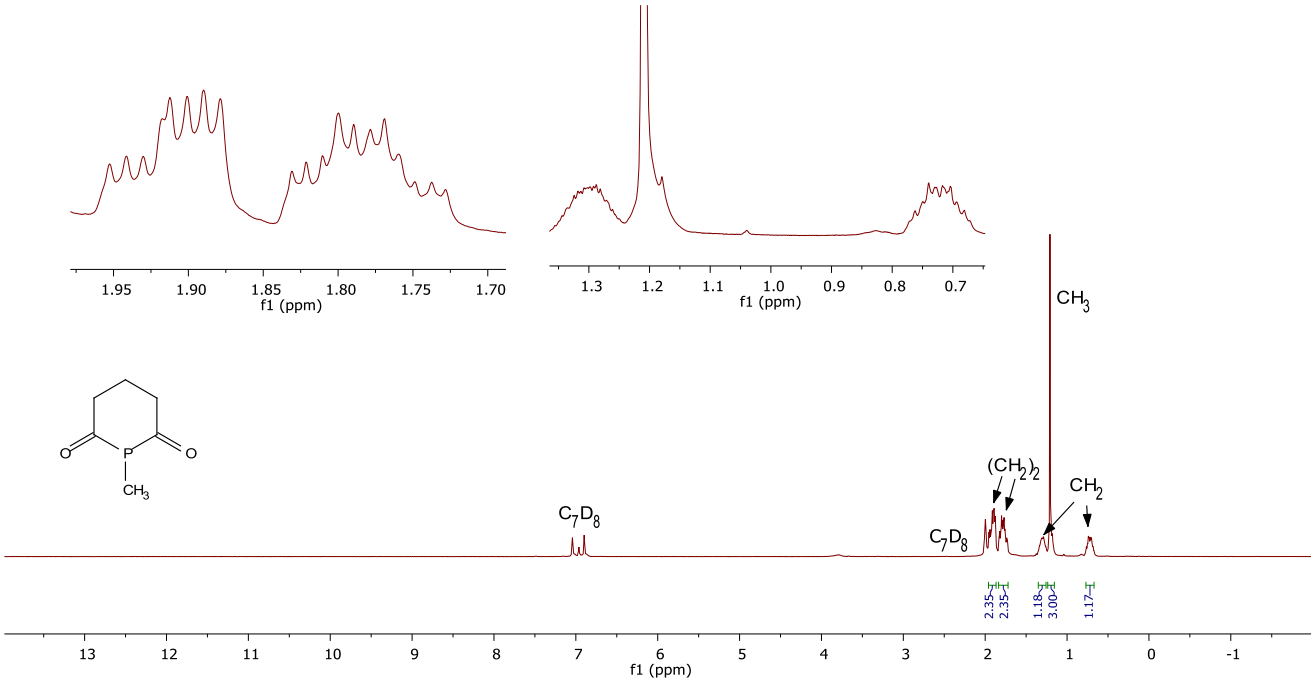

***Figure 55**. [1]H NMR Spectrum (C_7D_8, 238 K, 399.49 MHz) for compound **3.2a**.*

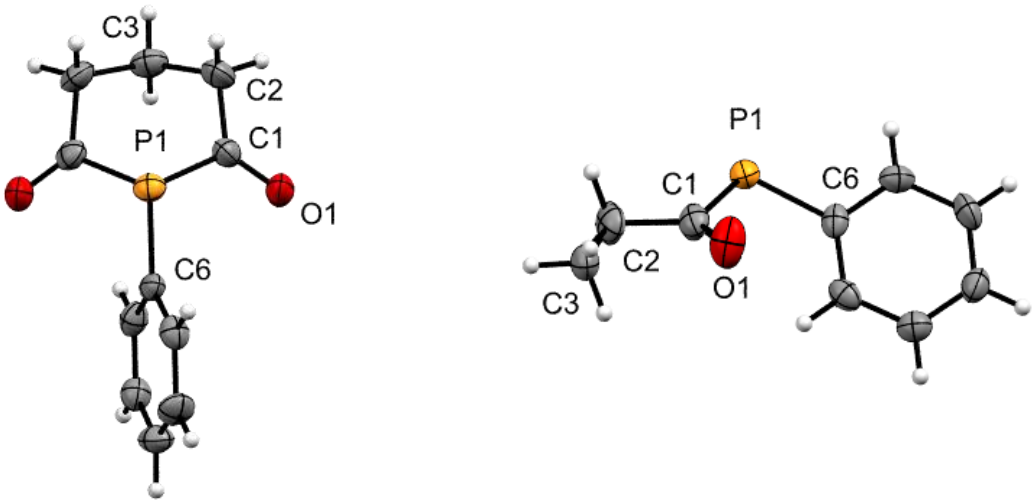

***Figure 56.** Two orientations of the molecular structure of **3.2d** with thermal ellipsoids at the 50% probability level. The left hand side orientation is to display the conformation of the phosphacyclic backbone.*

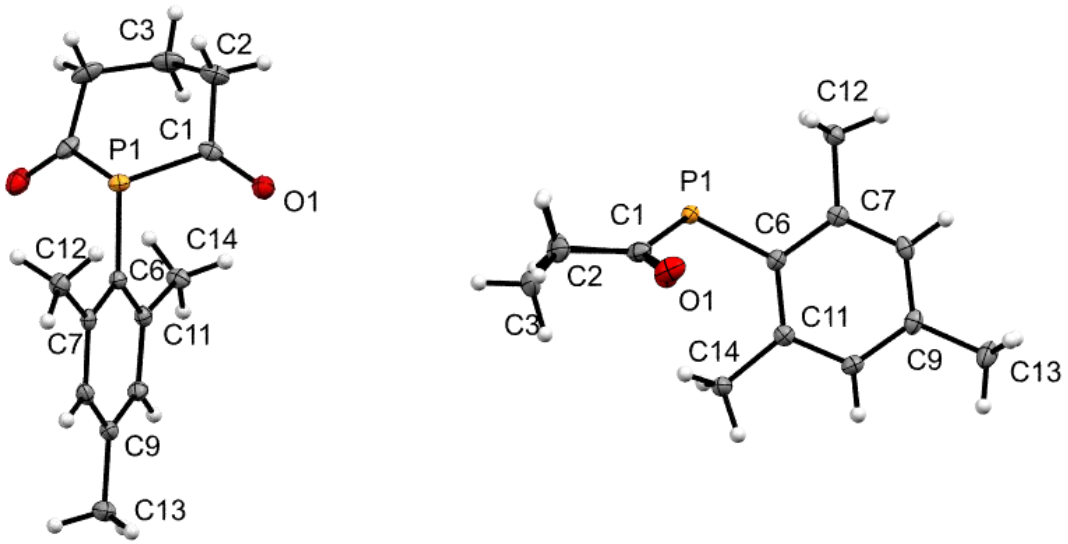

Figure 57. *Two orientations of the molecular structure of* ***3.2e*** *with thermal ellipsoids at the 50 % probability level. The left hand side orientation is to display the conformation of the phosphacyclic backbone.*

Table 10. *Selected bond lengths (Å) and angles (°) for compounds* ***3.2d*** *and* ***3.2e****, with estimated standard uncertainties in parentheses.*

Bond/Angle	***3.2d***	***3.2e***
P1-C1	*1.865 (6)*	*1.853 (2)*
P1-C5	*1.888 (6)*	*1.857 (2)*
P1-C6	*1.825 (5)*	*1.816 (2)*
C1-O1	*1.202 (7)*	*1.208 (2)*
C5-O2	*1.192 (8)*	*1.214 (2)*
C6-C7	*1.398 (8)*	*1.412 (2)*
C7-C12	-	*1.513 (2)*
C1-P1-C5	*97.0 (3)*	*100.11 (7)*
C1-P1-C6	*102.8 (3)*	*107.89 (7)*
C5-P1-C6	*103.5 (3)*	*105.41 (7)*
P1-C1-O1	*121.2 (4)*	*121.80 (12)*
P1-C5-O2	*120.0 (5)*	*120.62 (13)*
C1-C2-C3	*112.4 (5)*	*112.59 (14)*
C6-C7-C12	-	*122.96 (14)*

Structural data for compounds **3.2d** and **3.2e**, confirm that the phosphacycles adopt chair-like conformations, with the respective aryl groups (Ph, Mes) aligned almost orthogonally to the plane of the heterocycle (77.48 °, 89.98 ° respectively). Although, no direct comparators for these heterocycles exist, the 'diketo' parameters can be compared against the small number of precedent aromatic diketophosphanyls (e.g. **Figure 50**, *vide supra* **Chapter 2**). The C=O bond lengths are within the standard range of ketones (*ca* 1.21 Å),[119] and are comparable with previously reported diketophosphanyl compounds (1.20-1.23 Å).[139] The P-C(O) distance in **3.2e** is somewhat shorter than that of **3.2d**, as well as the average distance for mono-acyl phosphanes in the CCDC (by *ca* 0.02 Å).[152] In comparison, **3.2e** and **3.2d** exhibit significantly shorter P-C(O) bond lengths than the previously reported phosphametacyclophanes **2.1**, **2.5**-**2.11** (1.881(5)-1.910 (3) Å, **Chapter 2**). The C1-C2-C3 bond angle is in line with similar 6-member phosphacycles (vide supra, **Figure 51**),[141] displaying a slightly larger angle than carbocentric congeners (109.5 °).[153] It is also noted that the P-Aryl bond lengths are slightly shorter than that of their triarylphosphane analogues (PPh_3 and $PMes_3$, 1.834(2), 1.837 Å),[154,155,156] but significantly shortened relative to $MesP(SiMe_3)_2$ (1.851 (2) Å; **Figure 58**),* as well as the small range of precedent $ArP(SiR_3)_2$ (Ar = $C_6H_3{}^iPr^2$-2,6,[157] Mes*,[158] $C_6H_2{}^iPr_2$-2,4,6,[159] Ph[160], R = alkyl) and their complexes (1.829 – 1.884 Å)[161,162].

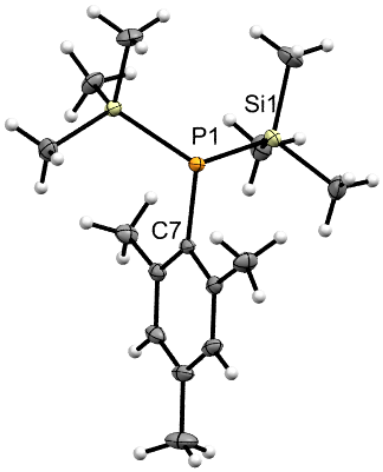

Figure 58. *Molecular Structure of $MesP(SiMe_3)_2$ with thermal ellipsoids at the 50 % probability level. The asymmetric unit comprises two molecules, the second of which has been omitted for clarity. Selected bond distances (Å) and angles (°): P1-Si1 2.2465(5), P1-Si2 2.2529(4), P1-C7 1.8505(13), Si1-C1 1.8729 (16), Si2-C4 1.8727 (15), C7-C8 1.4158(18), C8-C15 1.5109(19). Si1-P1-Si2 111.039(18), C7-P1-Si1 103.08(4), C7-P1-Si2 114.58(4), C15-C8-C7 122.48(12), P1-C7-C8 115.82(10).*

* Initial synthesis of $MesP(SiMe_3)_2$ was performed alongside summer student Vladamir Simenok.

3.3 Coordination of the Phosphacycloalkyldiones

Upon exposure to air both **3.2** and **3.3** readily decompose as noted previously for phosphomide containing species,[137] though the products in this case were not determined. Even so, attempts to oxidise **3.2** and **3.3** *via* heating solutions of the free heterocycle with chalcogens (S, Se, Te) resulted only in the recovery of the unreacted heterocycle; this is presumably an influence of the flanking carbonyls, leading to some inductive stabilisation of the lone pair.

To determine if metal coordination was possible, **3.2d** was reacted with half an equivalent of $[Cl_2PtPEt_3]_2$ in DCM, affording *cis*-$[PEt_3PtCl_2(Ph)P\{C(O)(CH_2)_3C(O)\}]$ (**3.4; Scheme 24**) as yellow plate like crystals in high yield (83%). Compound **3.4** was first characterised spectroscopically, the $^{31}P\{^1H\}$ NMR spectrum exhibiting two sets of doublets at δ_P 26.8 ($(Ph)P\{C(O)(CH_2)_3C(O)\}$], $^2J_{PP}$ = 15 Hz) and δ_P 9.0 (PEt_3, $^2J_{PP}$ = 15 Hz) (**Figure 59**), with associated Pt satellites ($J_{(PtP)}$ = 3413 Hz and 3166 Hz respectively). The corresponding ^{195}Pt NMR spectrum displays a doublet of doublets δ_{Pt} –4432 ($^1J_{PtP}$ = 3412 Hz, 3164 Hz), the magnitude of the Pt-P coupling being consistent with a *cis*-coordination geometry,[163,164] as confirmed by X-Ray diffraction studies (**Figure 60**). It is noted that metal coordination imparts some aerobic stability, permitting bulk purity to be confirmed by microanalysis.

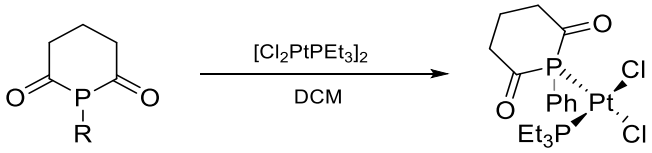

***Scheme 24**. Synthesis of cis-[$PEt_3PtCl_2(Ph)P\{C(O)(CH_2)_3C(O)\}$](**3.4**).*

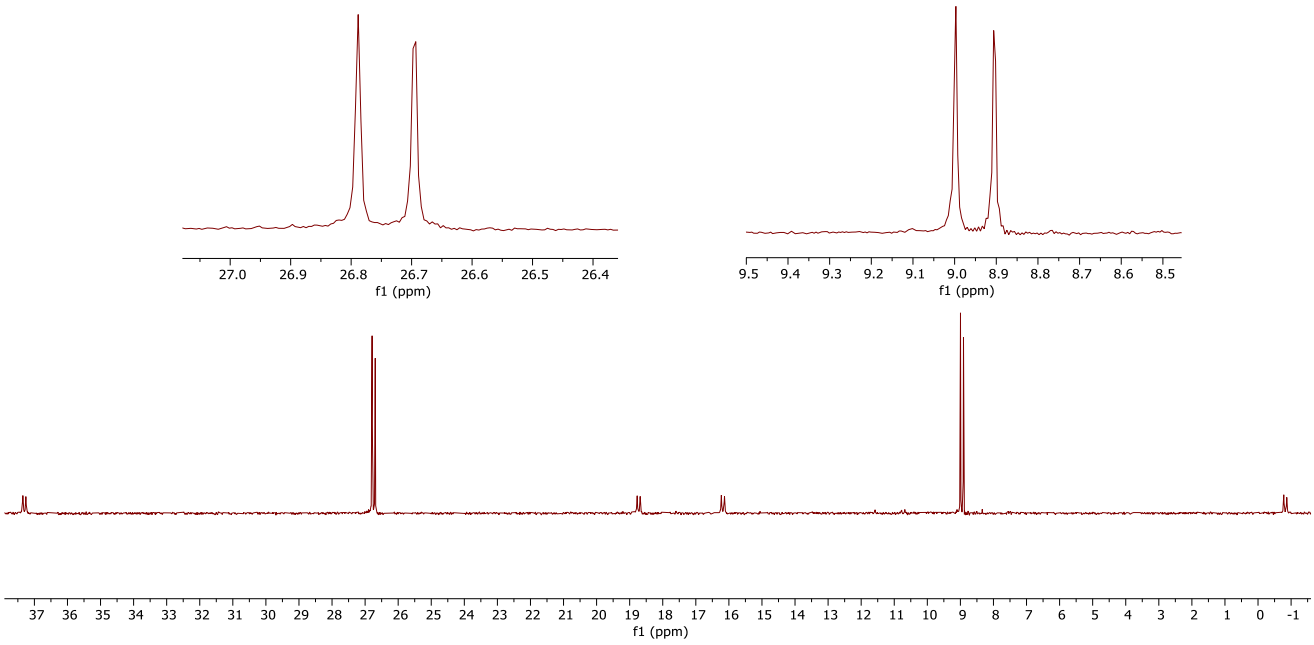

Figure 59. *$^{31}P\{^{1}H\}$ NMR Spectrum (CD_2Cl_2, 303 K, 161.72 MHz, D1 = 30 s) for compound* ***3.4.***

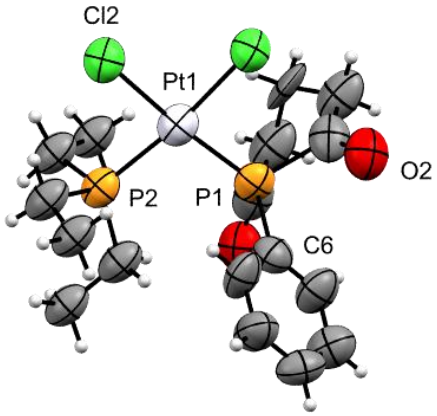

Figure 60. *Molecular Structure of* ***3.4*** *with thermal ellipsoids at the 50% probability level.*

The weakly diffracting nature of the crystals of **3.4** only allow connectivity to be determined. Interestingly, the phosphacyclic core appears to have inverted into the boat conformation compared to the free heterocycles which possesses the chair conformer in the solid state (**Figure 56**, **Figure 57**).

In seeking to determine if this is a general feature of coordination, **3.2d** was reacted with $[Rh(\eta^4\text{-}C_8H_{12})Cl]_2$, the product from which exhibits a single resonance in the $^{31}P\{^{1}H\}$ NMR spectrum (δ_P 49.2) at 30 °C, identical to the free heterocycle, though the red colouration and presence of broad C_8H_{12} resonances in the ^{1}H NMR spectrum suggest coordination has occurred. Upon cooling to temperatures below –50 °C, P-Rh coupling is resolved, δ_P 55.7 ($^{1}J_{P\text{-}Rh}$ = 137 Hz; **Figure 61**), suggesting the formation of $[(\eta^4\text{-}C_8H_{12})RhCl(Ph)P\{C(O)(CH_2)_3C(O)\}]$ (**3.5**), the phosphorus resonance is at a somewhat higher frequency than that of comparative trialkyl/aryl complexes $[RhCl(COD)(PR_3)]$ (R = Ph_3, Et_3, $^{n}Pr_3$, $^{i}Pr_3$,

$^{n}Bu_3$, Cy_3; δ_P 13.0-38.6),[165] and in the upper range of the fluoride analogues [RhF(COD)(PR_3)] (R = Ph_3, Et_3, $^{i}Pr_3$, Cy_3; δ_P 24.7-59.2).[166] However, the P-Rh coupling lies between those of trialkyl/aryl phosphane and phosphite comparators ($^{1}J_{P\text{-}Rh}$ = 144-162 Hz and 249 Hz, respectively)[167] and the bisphosphomide complex [RhCl{2,6-{Ph_2PCO)}$_2$(C_5H_3N)}] ($^{1}J_{P\text{-}Rh}$ = 104 Hz),[88] and are in line with Rh(L)$_2$Cl (L= dpe, dpp, dpb, diop) complexes, $^{1}J_{P\text{-}Rh}$ = 132-134 Hz.[168] These data might suggest the *s*-density of phosphorus in the free heterocycles is between that of classic phosphanes and phosphomides. Crystals of **2.15** were grown from DCM/Pentane, permitting structural characterisation (**Figure 63**, **Table 11**).

As seen for the free heterocycles, the broad ^{1}H resonances become resolved upon cooling (**Figure 62**), allowing the inequivalent CH_2 protons to be assigned. This dynamic behaviour is reminiscent of chair-boat isomerisation as seen for the free heterocycles (**Figure 53**), though coordination/free heterocycle exchange cannot be excluded.

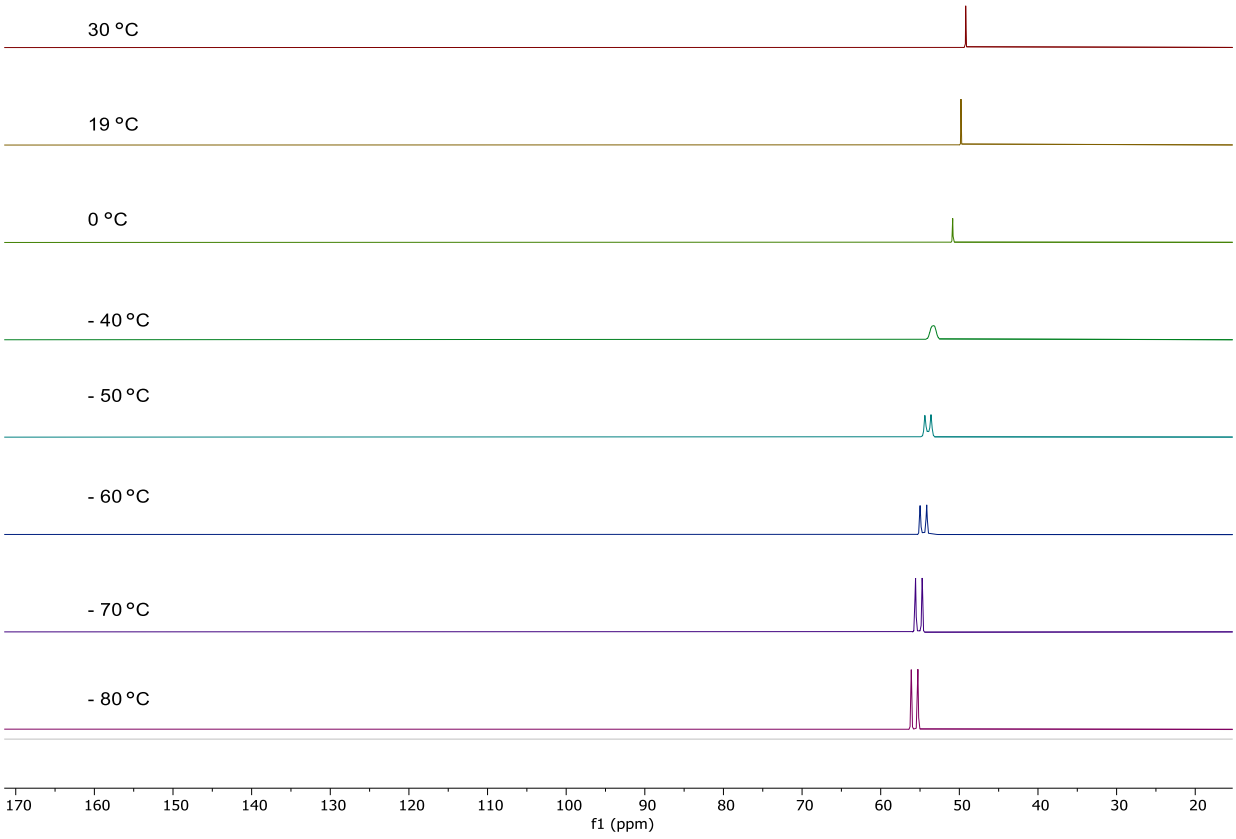

Figure 61. *Variable temperature $^{31}P\{^{1}H\}$ NMR (CD_2Cl_2, 161.72 MHz) spectra for **3.5**.*

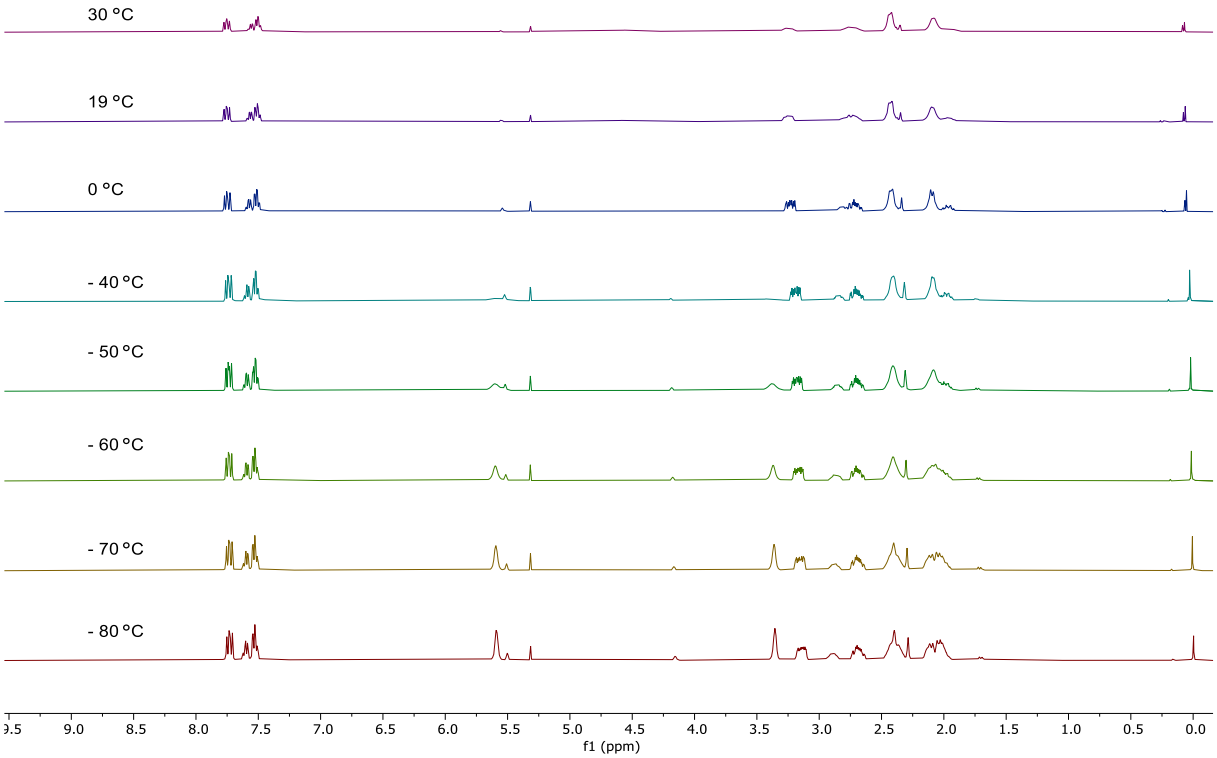

Figure 62. *Variable temperature ^{1}H NMR (CD_2Cl_2, 399.5 MHz) spectra for* ***3.5.***

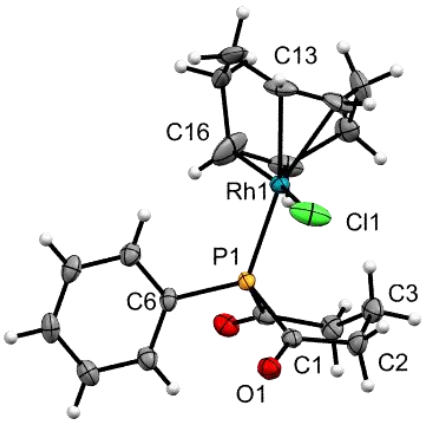

Figure 63. *Molecular structure of* ***3.5*** *with thermal ellipsoids at the 50% probability level. The modelled disorder about the COD unit has been omitted for clarity.*

Table 11. *Selected bond lengths (Å) and angles (°) for compound **3.5**, with estimated standard uncertainties in parentheses.*

Bond Length (Å)		***Bond Angle (°)***	
P1-Rh1	*2.272 (4)*	*C1-P1-C5*	*95.0 (3)*
P1-C1	*1.887 (6)*	*C1-P1-C6*	*104.9 (3)*
P1-C5	*1.887 (6)*	*C5-P1-C6*	*106.9 (3)*
P1-C6	*1.804 (6)*	*O1-C1-P1*	*121.5 (4)*
C1-O1	*1.200 (7)*	*O2-C5-P1*	*122.2 (5)*
C5-O2	*1.203 (8)*	*C6-P1-Rh1*	*119.51 (19)*
Rh1-Cl1	*2.363 (6)*	*Rh1-P1-C1*	*112.53 (18)*
Rh1-C13	*2.216 (6)*	*Rh1-P1-C5*	*114.87 (18)*
Rh1-C16	*2.137 (7)*	*P1-Rh1-Cl1*	*87.38 (5)*

Within both complexes **3.4** and **3.5** the phosphacyclic ligand adopts a boat conformation, where the free heterocycles only display the chair conformer. This behaviour has previously been observed by Pringle *et al.* (*vide supra*; **Figure 52**), concluding that "occupation of pseudo-axial sites by bulky substituents (which would be inevitable in a chair conformation) is avoided" leading to the preferential formation of the boat conformer.[144] For **3.5**, close contacts are also observed between the oxygen and proximal CH of the phosphacycle in the adjacent molecule (**Figure 64**), these H-bonding interactions could also facilitate preferential boat formation.

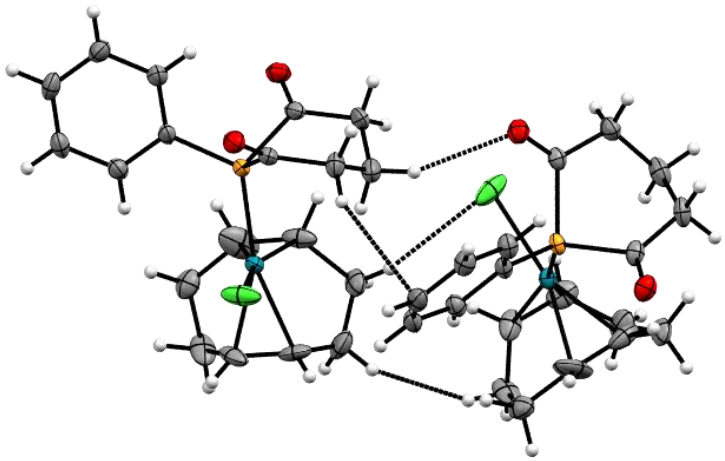

Figure 64. *Solid-state packing arrangement of **3.5** illustrating H-bonding interactions, potentially favouring boat conformation.*

Compound **3.5** exhibits comparable P-C(O) and C=O bond lengths to those of **3.2d**; similarly the Rh-C bond distances are in line with comparative $Rh(COD)PR_3$ complexes,[166] though slightly elongated relative to $[Rh(\eta^4\text{-}C_8H_{12})Cl]_2$ (2.07 (4) Å).[169] A somewhat contracted P-Aryl bond distance is noted for

3.5 relative to **3.2d**, suggesting a stronger P-Ph bond for **3.5**. Although typically upon coordination the elongation of the P-R bond length from backbonding into the σ* orbital and contraction from decreased P(Lonepair)-R(bonding pair) repulsions balance out,[170] in this instance the latter effect appears to be of more significance. The P-Rh bond length is shorter than trialkyl phosphane analogues (e.g. [RhCl(COD)(PPh_3] 2.308 (7) Å),[131] and slightly longer than in the bisphosphomide complex [RhCl{2,6-{$Ph_2PC(O)$}$_2$(C_5H_3N)}] (2.2523 (6) Å);[88] though it would be expected that the more strongly donating trialkyl phosphanes would be more tightly bound, an inverse relationship is observed.

3.4 The Preparation and Electronic Exploration of Tungsten Pentacarbonyl Complexes

In seeking a more detailed understanding of the coordinative behaviour of the 6- and 7-membered phosphacycles, their respective tungsten pentacarbonyl complexes were synthesised (**3.6a**-**3.6d**, **3.7**; **Scheme 25**). Upon reacting **3.2** or **3.3b** with $W(CO)_5$(THF) a coordination shift for the phosphorus centre to lower frequency ($\Delta\delta_P$ = 10-20 ppm) was observed alongside the manifestation of ^{183}W satellites (I = ½, 14 %) (**Table 12**). The magnitude of tungsten-phosphorus coupling ($^1J_{WP}$) can be indicative of the *s*-character at phosphorus,[171,172] the coupling being reported to increase as a function of π-acidity, thus higher coupling constants are typically observed for more electronegative substituents on phosphorus (**Table 13**), as their σ_{PC}* orbitals are lower in energy.[173,174]

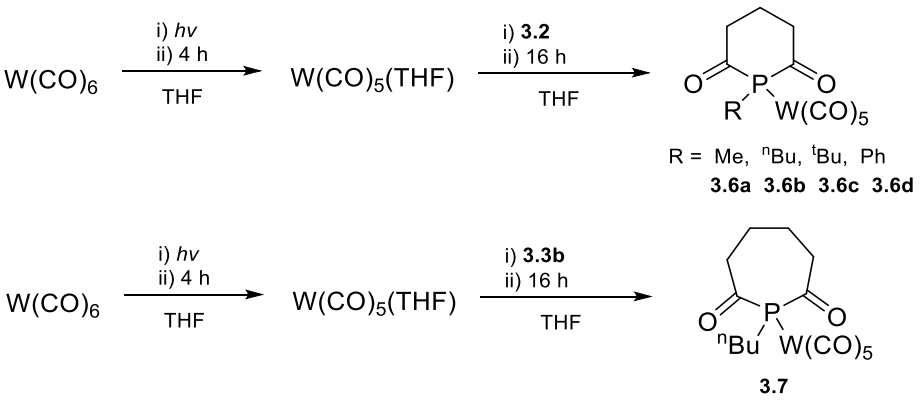

Scheme 25. *Synthesis of tungsten complexes **3.6** and **3.7**.*

Table 12. *Selected NMR Spectroscopic data for* ***3.6*** *and* ***3.7****.*[a]

	δ_P ($^1J_{WP}$[b])	$\Delta\delta_P$	δ_C WC(O)$_{cis}$ ($^1J_{CW}$[b])	δ_C WC(O)$_{trans}$ ($^1J_{CW}$[b])
3.6a	*20.7 (203)*	*-16.2*	*195.4 (125)*	*197.9 (149)*
3.6b	*33.1 (202)*	*-14.6*	*195.4 (125)*	*197.9 (148)*
3.6c	*51.3 (207)*	*-16.9*	*196.0 (125)*	*197.2 (146)*
3.6d	*28.9 (214)*	*-20.3*	*195.7 (125)*	*197.8 (148)*
3.7	*39.2 (216)*	*-9.7*	*195.8 (125)*	*198.0 (147)*

[a]*as* C_6D_6 *solution.* [b]*in Hz.*

The coupling constants of $[W(CO)_5(L)]$ (L = **3.2**, **3.3b**) are considerably lower in magnitude than those of phosphites (378-411 Hz) and generally somewhat lower than trialkyl/aryl phosphanes, though it is noted that P^nBu_3 exhibits a somewhat lower coupling (200 Hz).[171,175,176] From the small number of phosphomide complexes in the literature, $[\{H_4C_4P(C(O)Me)\}W(CO)_5]$ is the only comparable example (215 Hz),[177] while others (e.g. $[PhC(O)P(X)W(CO)_5]$ (X = Cl, F, OMe, $O(CH_2)_2OMe$)) exhibit coupling in the range of 230-280 Hz.[178,179] Though, the magnitude of $^1J_{WP}$ for **3.6a**-**3.6d** follow the correlation Ph > ^{t}Bu > Me > ^{n}Bu, they are not situated between phosphite and phosphane comparators as expected. X-Ray quality crystals were grown from saturated benzene solutions permitting comparative structural analyses (**Figure 65**-**Figure 67**; **Table 14**).

Table 13. *Phosphorus-tungsten coupling constant for* ***3.6a*****-3.6d**, **3.7** and related analogues.

Ligand (L)	$^{1}J_{WP}{}^{a}$	***Ref***
$P(OPh)_3$	411	171
$P(OMe)_3$	398	171
$P(O^nBu)_3$	390	171
PPh_3	280	171
P^tBu_3	232	176
PMe_3	230	175
H_2PMe	225	180
PH_3	216	180
$^nBuP\{C(O)\}_2C_4H_8$ (***3.7***)	216	
$H_4C_4PC(O)Me$	215	177
$PhP\{C(O)\}_2C_3H_6$ (***3.6d***)	214	
$HP(SiMe_3)_2$	212	180
$^tBu\ P\{C(O)\}_2C_3H_6$ (***3.6c***)	207	
$MeP\{C(O)\}_2C_3H_6$ (***3.6a***)	203	
$^nBuP\{C(O)\}_2C_3H_6$ (***3.6b***)	202	
P^nBu_3	200	171
$P(SiMe_3)_3$	157	181

[a] *in Hz*

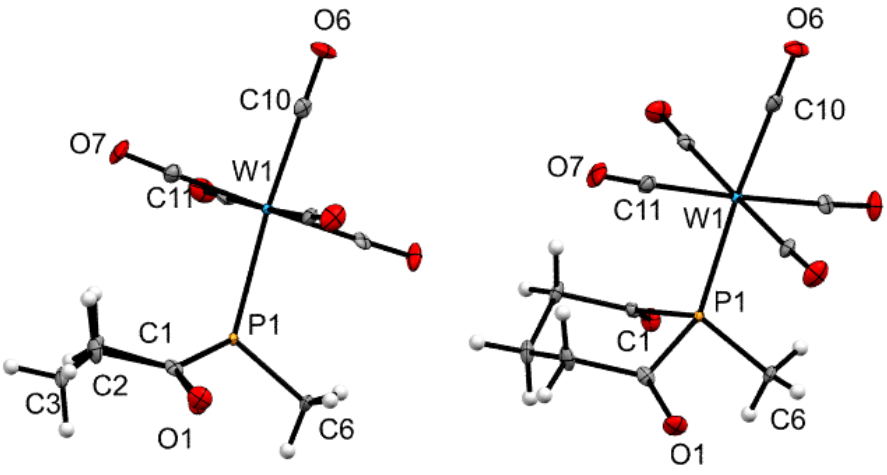

Figure 65. *Two orientations of the molecular structure of* ***3.6a*** *with thermal ellipsoids at the 50% probability level.*

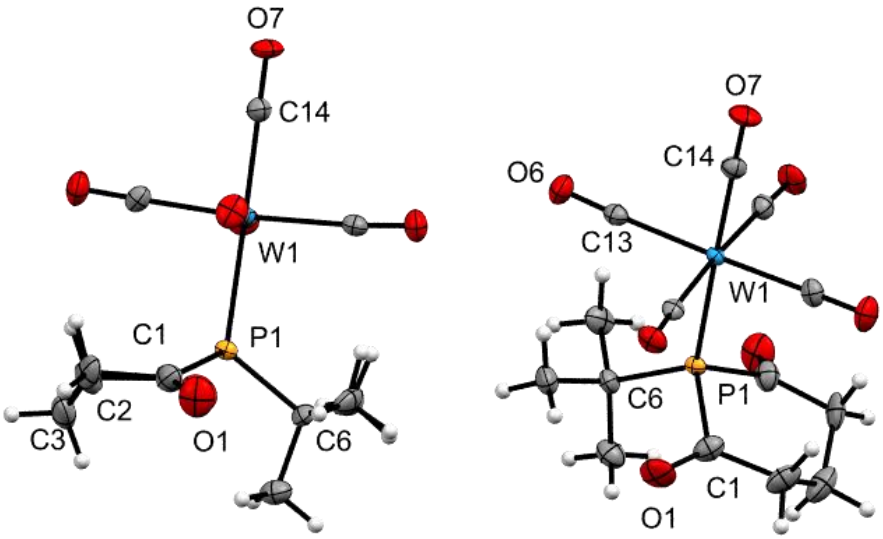

Figure 66. *Two orientations of the molecular structure of* ***3.6c*** *with thermal ellipsoids at the 50% probability level.*

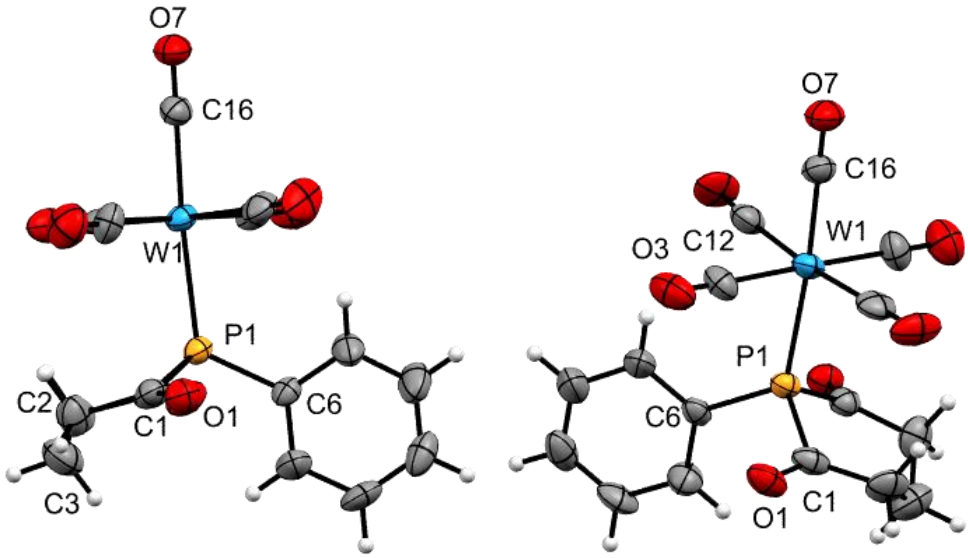

Figure 67. *Two orientations of the molecular structure of* ***3.6d*** *with thermal ellipsoids at the 50% probability level. The asymmetric unit comprises two units, the disordered second unit has been omitted for clarity.*

Table 14. *Selected bond lengths (Å) and angles (°) for compounds* ***3.6a, 3.6c*** *and* ***3.6d*** *with estimated standard uncertainties in parentheses.*

	3.6a	***3.6c***	***3.6d***
P1-C1	*1.880 (3)*	*1.879 (5)*	*1.882 (10)*
P1-C5	*1.881 (4)*	*1.883 (5)*	*1.889 (12)*
P1-C6	*1.815 (3)*	*1.882 (5)*	*1.818 (10)*
C1-O1	*1.202 (4)*	*1.209 (7)*	*1.212 (13)*
C5-O2	*1.206 (4)*	*1.203 (6)*	*1.205 (10)*
W1-P1	*2.5065 (7)*	*2.5149 (10)*	*2.490 (3)*
W-CO$_{trans}$	*1.998 (3)*	*2.007 (3)*	*2.009 (11)*
W-CO$_{cis}$	*2.045 (3) - 2.064 (4)*	*2.024 (5) – 2.060 (5)*	*2.02 (1) – 2.05 (1)*
C≡O$_{trans}$	*1.145 (4)*	*1.147 (6)*	*1.14 (2)*
C≡O$_{cis}$	*1.133 (5) – 1.143 (4)*	*1.133 (6) – 1.144 (6)*	*1.13 (1) – 1.17(2)*
W1-P1-C1	*117.00 (10)*	*109.84 (16)*	*111.5 (3)*
W1-P1-C5	*114.19 (10)*	*111.69 (17)*	*111.9 (3)*
W1-P1-C6	*116.72 (11)*	*122.04 (17)*	*121.9 (3)*
C1-P1-C5	*97.81 (14)*	*101.9 (2)*	*102.6 (5)*
C1-P1-C6	*103.41 (15)*	*104.7 (3)*	*103.1 (5)*
C5-P1-C6	*105.36 (15)*	*104.7 (2)*	*103.8 (5)*
C1-C2-C3	*113.9 (3)*	*113.1 (4)*	*113.0 (11)*

The phosphacyclic backbones in compounds **3.6a, 3.6c** and **3.6d** retain the chair-like conformations and exhibit comparable bond lengths and angles to the free heterocycles with the corresponding aryl substituent (**3.6d**), adopting a similar angle (C-P-C; 77.46 °) to that observed for **3.2d**. The comparable CO_{cis} and CO_{trans} bond lengths for compounds **3.6** suggest the alkyl/aryl substituent has limited effect on the σ-donor strength of these heterocycles. In contrast, the W-P bond distances reflect substituent donor strength ^{t}Bu > Me > Ph and are in-line with $[W(CO)_5P(CH(SiMe_3)_2(X)C(O)Ph]$ (**Figure 68**; X = Cl, F, OMe, $O(CH_2)_2OMe$) (X = Cl, 2.506 (1) Å),[179] though notably shorter than trialkyl/aryl phosphane analogues $[W(CO)_5PMe_3]$ (2.516 (2) Å),[182] $[W(CO)_5P^tBu_3]$ (2.686 (2) Å)[183] and $[W(CO)_5PPh_3]$ (2.545 (1) Å)[184], which is likely to be a facet of steric hinderance.[185] The *trans*-W-CO distances are shorter than for the *cis* carbonyls, and indeed those within free $W(CO)_6$ (2.036-2.066 Å),[186] implying **3.2a**, **3.2c** and **3.2d** have a lower trans-influence than CO, whereas the respective trialkyl/aryl phosphanes $[W(CO)_5PR_3]$ (R = Ph, tBu, Me) exhibit comparable trans-W-CO distances (2.00(1) - 2.006(5) Å).[182-184] Notwithstanding, their associated carbon shifts and C-W coupling constants suggest **3.6** exhibit

reduced σ-donor character relative to PPh_3 (δ_C 199 , $^1J_{CW}$ 140), PMe_3 (δ_C 200, $^1J_{CW}$ 145) and $P(OPh)_3$ (δ_C 196, $^1J_{CW}$ 137 Hz).[187]

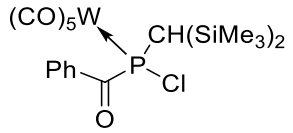

Figure 68. *Acyl(chloro)phosphane complex.*

The carbonyl stretching frequencies of **3.6** and **3.7** were analysed, the *trans*-carbonyl (pseudo-A_1) mode being clearly distinguishable at higher frequency relative to other absorptions (**Table 15**). Across the series of tungsten complexes little variation in this *trans*-carbonyl mode was observed, suggesting the phosphorus substituent has little effect on the donating capabilities of these heterocycles and are therefore predominantly driven by the diketophosphanyl. In addition, compounds **3.6** and **3.7** exhibit a slight increase in the *trans*-carbonyl stretching mode relative to PR_3 comparators, and a decrease relative to $P(OR)_3$ analogues (**Table 15**).

Table 15. Carbonyl *stretches of compounds **3.6**, **3.7** and related analogues, obtained using a solution cell.*

	***trans*-ν_{CO} / cm^{-1}**	**ν_{CO} / cm^{-1}**
$W(CO)_5(PMe_3)$[a]	2069	1976, 1942, 1932
$W(CO)_5(P^nBu_3)$[a]	2068	1932
$W(CO)_5(PPh_3)$[a]	2071	1976, 1940
3.6a[a]	2076	1946, 1933
3.6b[a]	2075	1953, 1950, 1942
3.6c[a]	2075	1955, 1940
3.6d[a]	2076	1949 (br)
3.7[a]	2075	1951, 1946, 1938
$W(CO)_5(P\{OMe\}_3)$[a]	2079	1962, 1948
$W(CO)_5(P\{OPh\}_3)$[b]	2083	1968, 1959

[a]as solution in THF. [b]as solution in hexane.

Overall, the coordinative behaviour of these heterocycles establishes them as relatively weak σ-donors, supported by the shortened Pt-Cl bond length (2.307 (11)Å) observed for **3.4** relative to triaryl phosphane analogues (2.346 Å);[188] this implies a lower *trans*-influence of **3.2d** relative to traditional triaryl phosphanes.* Similarly, the magnitude of P-Rh coupling ($^{1}J_{P\text{-}Rh}$) could suggest the phosphorus centre in the free heterocycles possesses reduced *s*-density relative to classic phosphanes, though this can only be confirmed for the phenyl substituted heterocycle (**3.2d**). Furthermore, infrared analyses of the tungsten complexes place heterocycles **3.2** and **3.3** between conventional phosphane and phosphite compounds in ligand space,[189] supporting prior observations, suggestive of relatively weak σ-donor character.

3.5 Computational Studies of The Phosphacycloalkyldiones

In order to gain insight into the fundamental electronics of **3.2a-e**, **3.6a** and **3.6d**, computational analyses were performed. Initial calculations for the free 6-membered heterocycles (**3.2a**-**e**) were performed at the B3LYP level of theory with the 6-311G(3d,3p) basis set, while the LanL2DZ[190] effective core potential (ECP) basis set was implemented to model the tungsten atoms in their respective complexes. Geometry optimisation and frequency calculations were performed, key structural parameters have been summarised in **Table 16**.

Table 16. *Selected bond lengths (Å), angles (°) and HOMO energies for the computed **3.2a**-**e** structures.*

	3.2a	***3.2b***	***3.2c***	***3.2d***	***3.2e***
P-R[a]	*1.838*	*1.849*	*1.888*	*1.819*	*1.825*
P-C(O)	*1.877*	*1.867*	*1.873*	*1.883*	*1.866*
C=O	*1.206*	*1.208*	*1.208*	*1.204*	*1.207*
C(O)-P1-C(O)	*95.9*	*98.9*	*97.4*	*96.1*	*100.1*
C(O)-P1-R[a]	*102.8*	*104.6*	*106.8*	*105.0*	*108.6*
P-C=O	*121.5*	*121.2*	*122.5*	*122.3*	*122.3*
C(O)-CH_2-CH_2	*112.1*	*112.8*	*112.7*	*112.3*	*113.2*
HOMO Energy (eV)	*-0.245*	*-0.240*	*-0.240*	*-0.242*	*-0.237*

[a]R: a = CH_3, b = ^{n}Bu, c = ^{t}Bu, d = Phenyl and e = Mesityl.

* This can only be loosely stated due to the weakly diffracting nature of the crystal.

The computed structures all exhibit the chair-conformer and the bond lengths for **3.2d** and **3.2e** are in agreement with the solid state (± 0.02 Å),[◊] with the larger C(O)-P-C(O) angle for **3.2e** relative to **3.2d** also observed. In each case the C=O distances are relatively consistent, where the P-C(O) distances and C(O)-P-C(O) angles showing the largest deviation across the series; in comparison **3.2a** possesses the smallest angle, potentially as a consequence of the weak bonding interaction between the carbonyl and CH_3 group, though the CH_3 group only contributes 4% to the HOMO. It is worth noting that in each case the HOMO is predominantly associated with the phosphorus lone pair and carbonyl moiety (42-47 % and 43-48 % respectively).

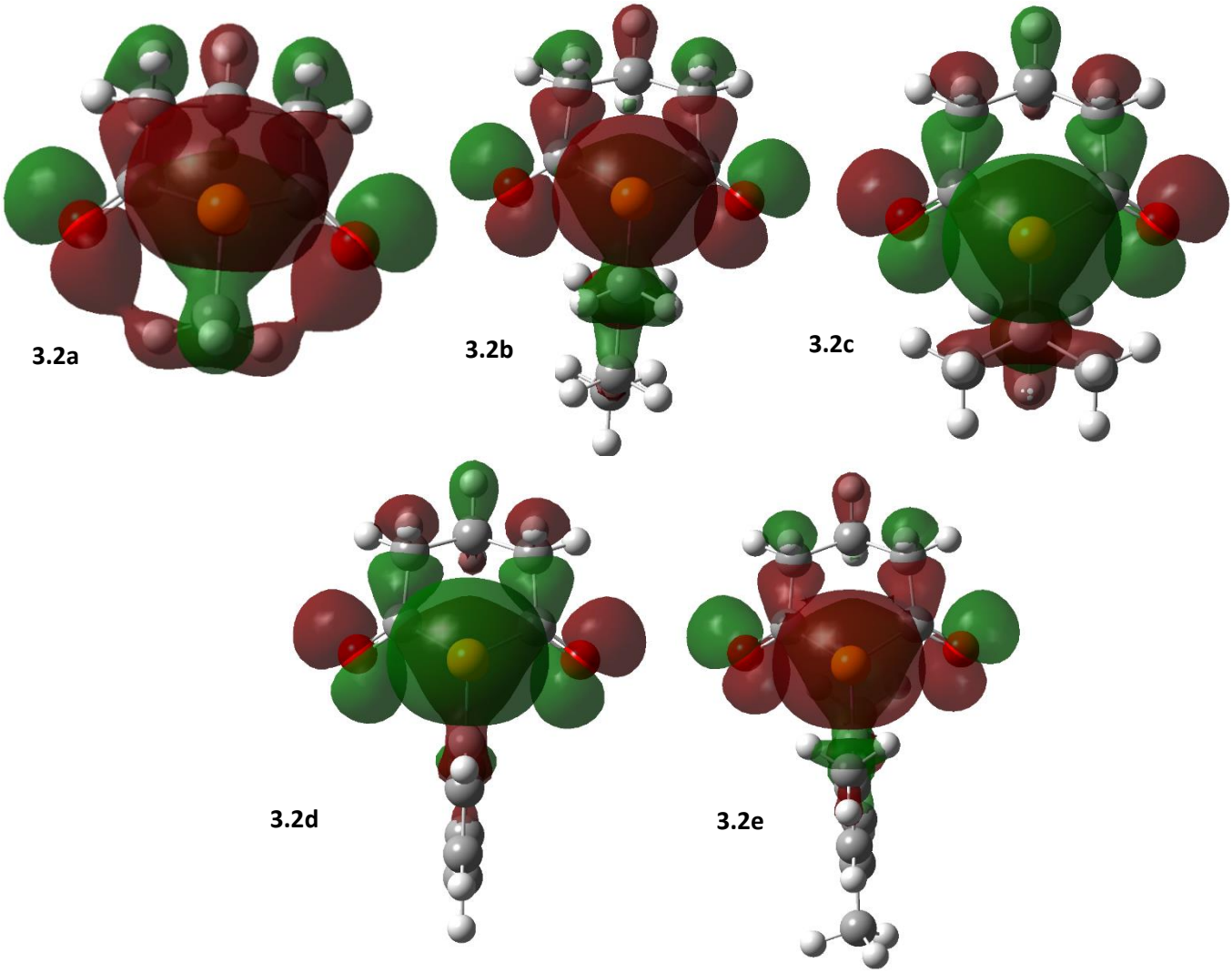

Figure 69. *Visualisation of the HOMO orbitals for* ***3.2a-e****.*

[◊] Starting geometries were derived from experimental structural data for **3.2d** and modified accordingly.

The computed tungsten complexes exhibit somewhat elongated W-P bond distances relative to experiment, though the experimental values were shorter than expected (**Table 14**). Overall, the bond distances are generally comparable to experiment (**Table 17**) and the HOMO is in each case associated with tungsten.

Table 17. *Selected bond lengths (Å) and angles (°) for the computed tungsten complexes* ***3.6a*** *and* ***3.6d*** *vs experimental solid-state data.*

	3.6a	***3.6a*** $_{(experimental)}$	***3.6d***	***3.6d*** $_{(experimental)}$
P-R[a]	*1.827*	*1.815 (3)*	*1.825*	*1.818 (10)*
P-C(O)	*1.891*	*1.880 (3)*	*1.894*	*1.882 (10)*
C=O	*1.203*	*1.202 (4)*	*1.202*	*1.205 (10)*
W-P	*2.551*	*2.5065 (7)*	*2.5706*	*2.490 (3)*
W-CO$_{trans}$	*2.026*	*1.998 (3)*	*2.022*	*2.009 (11)*
W-CO$_{cis}$	*2.066*	*2.045 (3)*	*2.049*	*2.02 (1)*
C≡O$_{trans}$	*1.145*	*1.145 (4)*	*1.145*	*1.14 (2)*
C≡O$_{cis}$	*1.142*	*1.143 (4)*	*1.141*	*1.13 (1)*

[a]*R:* ***3.6a*** *=* CH_3*,* ***3.6d*** *= Phenyl*

Natural bond orbital (NBO) analysis has previously been utilised for the quantitative determination of *s*-character of phosphanes, therefore, similar analyses were performed for heterocycles **3.2a**-**e** alongside the mono-acylated (**3.8**) and fully saturated (**3.9**) analogues as well as PMe_3 for comparative purposes. However, in this instance no clear conclusions could be drawn from the computed *s*- and *p*-orbital components of the phosphorus lone-pair.

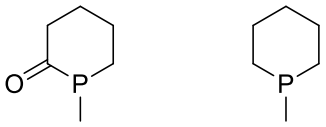

3.8 **3.9**

Figure 70. *Monoacylated and fully saturated analogues of* ***3.2a****.*

Tungsten complexes **3.6a** and **3.6d,** and the PMe_3 analogue ($[W(CO)_5(PMe_3)]$) were analysed to examine the nature of the W-P bond (**Table 18**). The phosphorus *s*-character in **3.6d** is decreased

relative to **3.6a**, indicative of a weaker bond which correlates with experimental results. In addition, the calculated IR stretches display a similar trend to those observed experimentally, [$(CO)_5WPMe_3$] possessing a lower energy *trans*-carbonyl (pseudo-A_1) stretch, indicative of a more strongly donating phosphane substituent.

Table 18. *NBO components of tungsten pentacarbonyl complexes* ***3.6a***, ***3.6d*** *and* [$(CO)_5WPMe_3$].

			Tungsten			Phosphorus	
	%W	**%P**	**%s**	**%p**	**%d**	**%s**	**%p**
3.6a	29.5	70.5	25.4	55.4	30.3	37.3	62.7
3.6d	28.7	71.3	14.6	56.4	29.0	35.8	64.2
PMe_3	31.1	68.9	14.4	56.4	29.2	36.2	63.4

3.6 Summary

A series of 6- and 7-member cyclic bis(phosphomides) have been successfully synthesised and fully characterised. The fluxionality of these systems was confirmed by variable temperature NMR spectroscopy, allowing the inequivalent proton resonances to be resolved below −40 °C. The attempted oxidation of the phosphacycloalkyldiones with chalcogens (Se, S and Te) resulted in the recovery of starting material, which could result from an inductive stabilisation effect from the carbonyls. However, this effect does not preclude coordination as demonstrated by the Pt (**3.4**) and Rh (**3.5**) complexes.

Tungsten pentacarbonyl complexes were prepared and characterised by NMR spectroscopy, X-Ray diffraction and microanalytical methods. The associated carbon shifts and C-W couplings for the trans-carbonyl ligand suggest compounds **3.2** possess reduced σ-donor character relative to traditional phosphanes, which was supported by structural data. Infrared analysis of these complexes found the heterocycles to be relatively weak σ-donors, the 'A_1' stretching modes lying between those of respective PR_3 and $P(OR)_3$ analogues, which is in line with conclusions from NMR and structural data. It is worth noting that the alkyl/aryl substituent ('R') appears to have little influence on the infrared stretching frequencies, suggesting the 'diketo' unit dominates the electronics of these heterocycles.

Alongside experimental investigations, *in-silico* studies were performed, the computed structures of which were in good agreement with the solid state. In addition, NBO calculations were performed for the tungsten complexes, the phosphorus *s*-character in the W-P bond for the phenyl system (**3.6d**) was decreased relative to methyl (**3.6a**), indicative of a weaker bond, in-line with experimental results.

Overall, experimental and computational observations identify these heterocycles as relatively weak σ-donors, finding their electronic behaviour between that of traditional phosphanes (PR_3) and phosphites (POR_3).

Chapter 4 - Trifluoromethylphosphaalkenes: Synthetic and Reactivity Studies

"I am sorry that I made you a part of my perils…"

--The Hobbit: The Battle of the Five Armies

4.1 Introduction

Phosphorus has the capability to 'mimic' carbon, silicon or nitrogen depending on its coordinated state.[7] It has been established that phosphorus is more similar to its diagonal relative, carbon, than to nitrogen and indeed it has been stated that the "vertical nitrogen-phosphorus analogy sheds no light upon low-coordinate phosphorus chemistry".[191] The similar electronegativities of carbon and phosphorus (C: 2.5; P: 2.2)[192,193] lead to somewhat comparable reactivity between isoelectronic functionalities such as phosphaalkenes ($R_2C{=}PR$) and alkenes ($R_2C{=}CR_2$), which are also isolobal. In contrast the HOMO of imines corresponds to the lone-pair, with the π-bond lying much lower in energy. Where for phosphaethylene ($H_2C{=}PH$) the HOMO is the π-bond, which is substantially higher in energy than that of imine, while the lone pair of phosphaethylene is only 0.40 eV more stable than the π-HOMO (**Figure 71**).[194] This small HOMO – HOMO-1 energy gap allows phosphaalkenes to react at both the π-system and the lone-pair, whereas imines typically react *via* the nitrogen lone-pair alone.[191] Although a lot of recognisable alkene-like chemistry is observed for phosphaalkenes, the reactive lone pair can interfere with further transformations. This can, however, be shut down by coordination of the lone pair, allowing reactivity to proceed exclusively at the π-system thus making phosphaalkenes essentially direct analogues of alkenes. This relationship has led to phosphorus being termed 'the carbon-copy' and these parallels are exemplified by phospha-variants of common olefinic reactions, e.g. the phospha-Wittig,[195] cycloaddition,[196] and η^2-coordination to metals.[197]

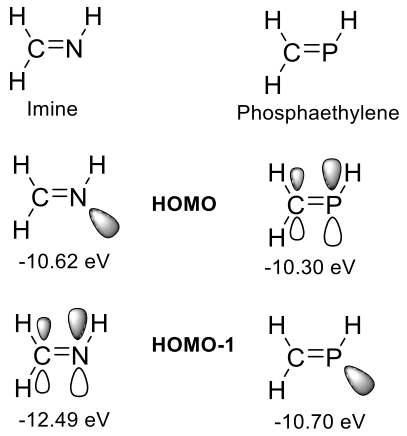

Figure 71. *Frontier Orbitals of Imine and Phosphaethylene.*[191]

Phosphaalkenes are typically synthesised *via* the Becker-condensation, which involves the addition of a silylated phosphane $RP(SiMe_3)_2$ (R = Me, Ph) to an acyl chloride (e.g. ^{t}BuCOCl; **Scheme 26**) initially forming an acyl phosphane that undergoes a spontaneous 1,3-silatropic rearrangement ([1,3] SR),

driven by the oxophilicity of silicon, to afford the phosphaalkene.[87] While the phosphaalkene is typically the energetically favoured product, there are instances where the acyl phosphane can be isolated as was the case in the preceding chapters.[198,199]

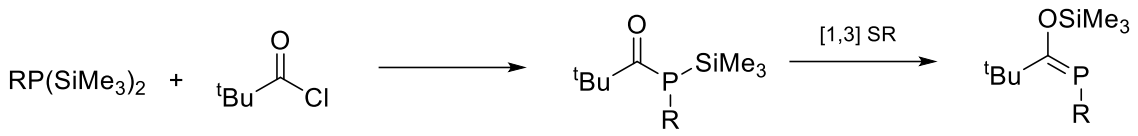

Scheme 26. *Synthesis of phosphaalkenes via the Becker condensation.*

Phosphaalkenes can also be prepared by the Phospha-Peterson reaction, which is essentially an extension of the Becker condensation, whereby $ArPH_2$ is treated with $^{n}BuLi$ and $ClSiMe_2{}^{t}Bu$ to afford the respective lithium salt $[(Me_3Si)_2P(Ar)^{t}Bu][Li]$. The subsequent addition of R(H)C=O affords the desired phosphaalkene *via* a 1,3-silatropic shift, affording hexamethyldisiloxane as by-product (**Scheme 27a**).[200] Alternatively, phosphaalkenes can be synthesised by dehydrohalogenation, for example by reacting $RP(Cl)C(H)Ph_2$ with a base such as DBU (**Scheme 27b**); this method was used by Bickelhaupt in 1978 to synthesise the first thermally stable phosphaalkene, $MesP{=}CPh_2$,[201] and has since been used to access a range of novel phosphaalkenes, including $Me_3SiC{\equiv}PCl$, a valuable synthon for preparing a wide variety of further phosphaalkenes.[202]

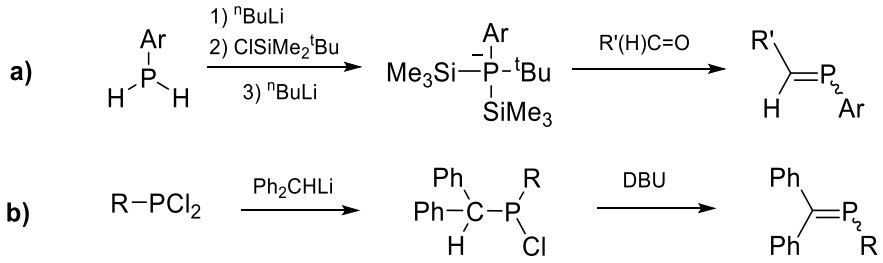

Scheme 27. *Synthesis of phosphaalkenes by dehydrohalogenation and the Phospha-Peterson reaction.*[200,201]

Phosphaalkenes now find a multitude of uses, ranging from ligands within coordination chemistry to new inorganic polymers (**Figure 72**). The latter find use as π-conjugated materials, due to their tendency to exhibit red-shifted absorptions relative to carbocentric analogues, due to reduced LUMO energies.[7] Despite this prevelant activity, pursuit of novel-phosphaalkenes remains an active area of research, especially as they are convenient precursors to access phosphalkynes (RC≡P).[203] The initial

syntheses of phosphaalkynes required harsh conditions, the first example (HC≡P) being synthesised *via* electrical discharge between graphite electrodes within a phosphane atmosphere.[204] Since this discovery, more adaptable synthetic routes have been reported, with phosphaalkynes now typically prepared *via* 1,2-elimination reactions from phosphaalkenes (**Scheme 28**).[205]

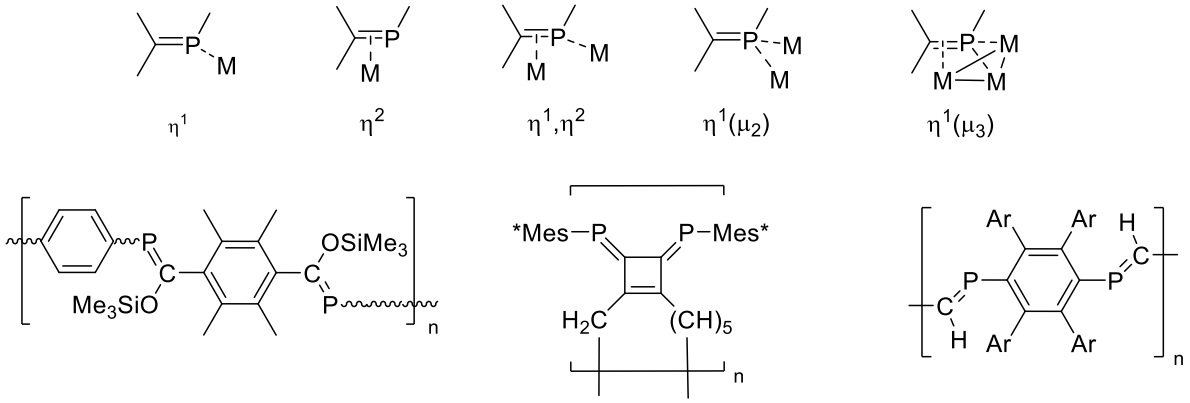

***Figure 72**. Coordination modes of phosphaalkenes and exemplar phosphaalkene polymers.*

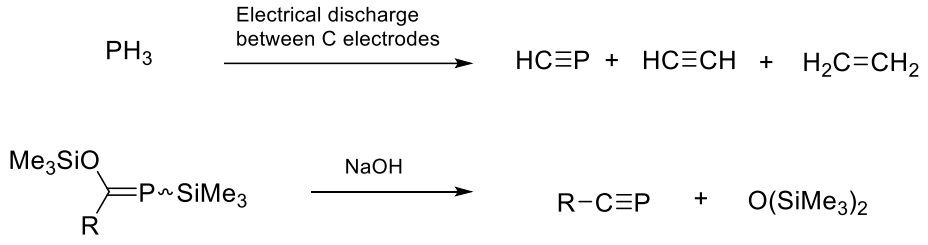

***Scheme 28.** Synthesis of Phosphaalkynes.[206]*

A surprising omission from the range of known phosphaalkynes is trifluoromethylphosphaalkyne (**4.1**; **Figure 73**), the closest analogue being FC≡P, which was observed in the gas phase by Nixon and Kroto.[207] Similarly, the precursor to **4.1** and trifluoromethylphosphaalkenes more generally would be interesting compounds in their own right, but no such species have been explored. This chapter describes the synthesis and reactivity of a series of trifluoromethyl-substituted phosphaalkenes and the pursuit of the elusive trifluoromethylphosphaalkyne (**4.1**), a potentially useful compound to incorporate into π-conjugated materials.

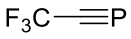

4.1

***Figure 73.** Trifluoromethylphosphalkyne.*

4.2 Synthesis and Characterisation

The synthesis of trifluoromethylphosphaalkenes was pursued by a modified Becker condensation route, using trifluoroacetic anhydride in place of an acid chloride. Compounds **4.2a**-**4.2d** were thus obtained from the respective bis-silylated phosphane, $RP(SiMe_3)_2$ (R= Ph, ^tBu, Mes, $SiMe_3$) (**Scheme 29**). The $^{31}P\{^1H\}$ NMR spectrum in each case exhibited a quartet in the range δ_P 228-153 (**Table 19**), a region in which phosphaalkenes are commonly observed (e.g. $Ar_FP(H)C(R)=CH_2$ and Poly(p-phenylenephosphaalkene) (**PPP**s; *vide supra* **Chapter 1**)).[56,208] The formulation of **4.2a**-**4.2d** is substantiated by the observation of a doublet in the ^{19}F NMR spectrum ($^2J_{FP}$ = 47-37 Hz), with the associated R and TMS substituents apparent from the ^1H and $^{13}C\{^1H\}$ spectra. Much-like many precedent phosphaalkenes **4.2d** is obtained as a mixture of E- and Z-isomers (**Figure 74**), apparent as two resonances in the ^{31}P NMR spectrum, a quartet at δ_P 161 (J_{PF} = 39 Hz) and a broad quartet resonance at δ_P 153.6; a doublet and broad singlet resonance were apparent in the corresponding ^{19}F NMR spectrum at δ_F −67.1 (J_{FP} = 39 Hz), −66.9, respectively. The $^{29}Si\{^1H\}$ NMR spectrum exhibits four resonances, consistent with both isomers forming, these signals include a doublet at δ_{Si} 26 (J = 4 Hz), singlets at δ_{Si} 24 and 7 along with a doublet of quartets at δ_{Si} −0.5 (J = 44, 3 Hz), the latter presumably being coupled by phosphorus and the CF_3 group, whereas the doublet (δ_{Si} 26) only experiences coupling from phosphorus, which would support the formation of **4.2d**. Compounds **4.2a** and **4.2c** exhibit only one resonance in the ^{31}P NMR spectrum, suggesting either the E- and Z-isomers have an identical signal or only one isomer has formed.

For **4.2d**, the higher frequency species with a δ_P 161.3 is likely to be the E-isomer as it has generally been observed that Z-isomers exhibit lower frequency shifts in both the $^{13}C\{^1H\}$ and ^{31}P NMR spectra.[209] In addition to this, the E-isomer of fluorovinyl phosphanes generally exhibits larger P-F coupling ($^3J_{PF}$ = 39 Hz),[117] which can be augmented by interactions between overlapping lone pair orbitals (P and F) known as through-space coupling.[209] The magnitude of coupling *via* the through-space mechanism varies according to the element present and in the case of P-F species, if in close enough proximity this has generally been shown to increase the coupling constant, for example in o-trifluoromethylsubstituted triphenylphosphane derivatives.[210]

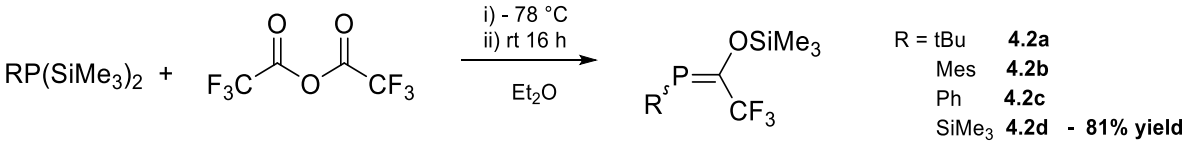

Scheme 29. *Synthesis of the trifluoromethylphosphaalkenes (**4.2**). Only compound **4.2d** could be isolated.*

Table 19. *Selected Spectroscopic data for compounds* ***4.2a***-***d****.*

	$\delta_P{}^a$ ($^3J_{PF}$)^b	$\delta_F{}^a$ ($^3J_{PF}$)^b
4.2a	*211.5 (47)*	*–68.3 (47)*
4.2b	*228.4 (38)*	*–69.4 (38)*
4.2c	*168.2 (46)*	*–70.6 (46)*
4.2d	*161.3 (39)*	*–67.1 (39)*

c. as C_6D_6 solution. d. in Hz.

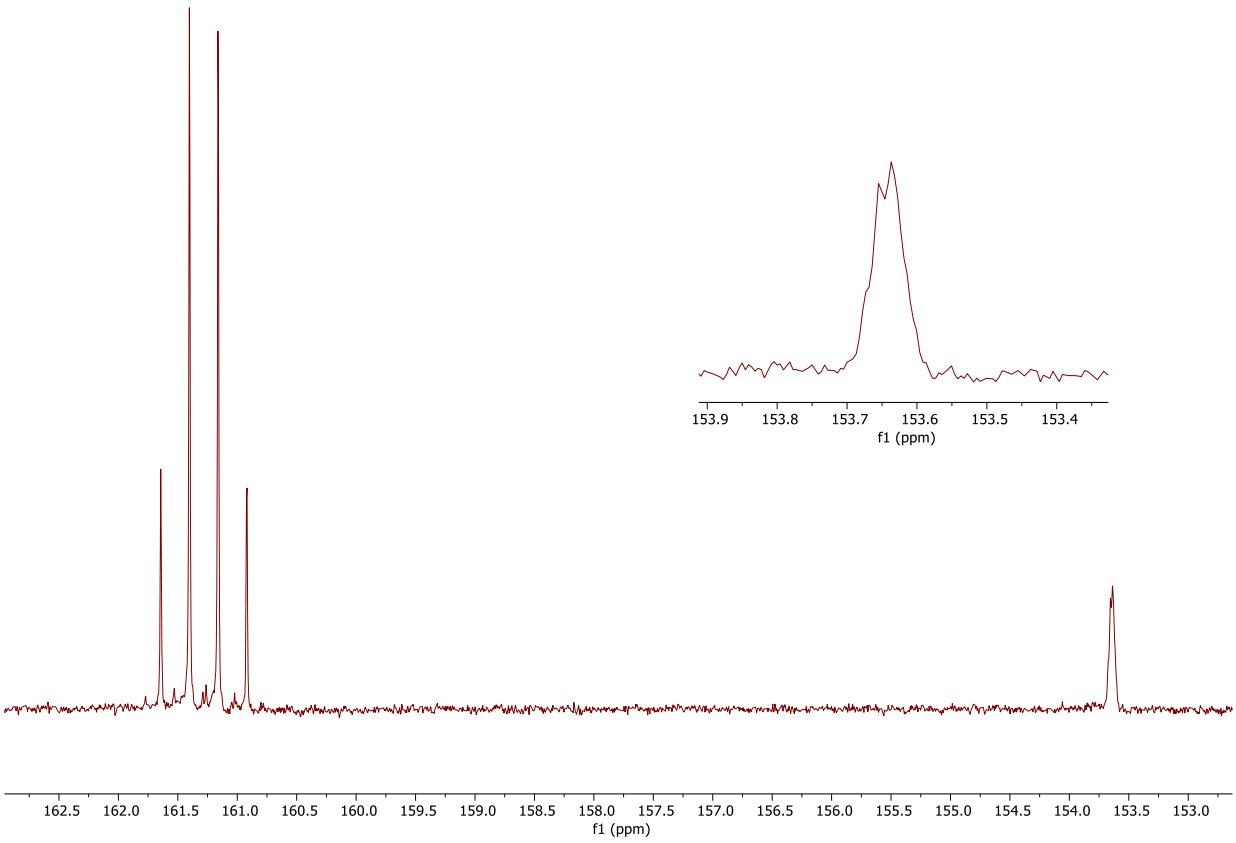

Figure 74. *$^{31}P\{^1H\}$ NMR (C_6D_6, 161.72 MHz) spectrum for* ***4.2d****.*

Compound **4.2d** is readily isolated *via* static vacuum distillation, albeit with some loss of product due to its volatility, however, the isolation of **4.2a**-**4.2c** proved more challenging. Compounds **4.2a** and **4.2b** appear unstable to removal of volatiles, including *via* static-vacuum distillation, whereas volatiles can be removed from compound **4.2c**. However, even when cooled to –40 °C, **4.2c** slowly converts to a new species, apparent from a new resonance at δ_P 30 in the ^{31}P NMR spectrum (septet, J_{PF} = 13 Hz; **Figure 75**), with an apparent doublet observed in the corresponding ^{19}F NMR spectrum at δ_F –76.5 (J_{FP} = 13 Hz). The J_{PF} coupling could be consistent with phosphorus coupling to two separate CF_3 groups,

though in very similar or indeed equivalent environments, with a comparable shift to that of [1,3]-diphosphacyclobutane (**4.3**; δ_P 34.5) observed.[211,212] However, the head-to-tail dimer, **4.4**, can be excluded, since both of the two CF_3 groups would experience coupling to both phosphorus centres and thus result in a resonance with triplet multiplicity.

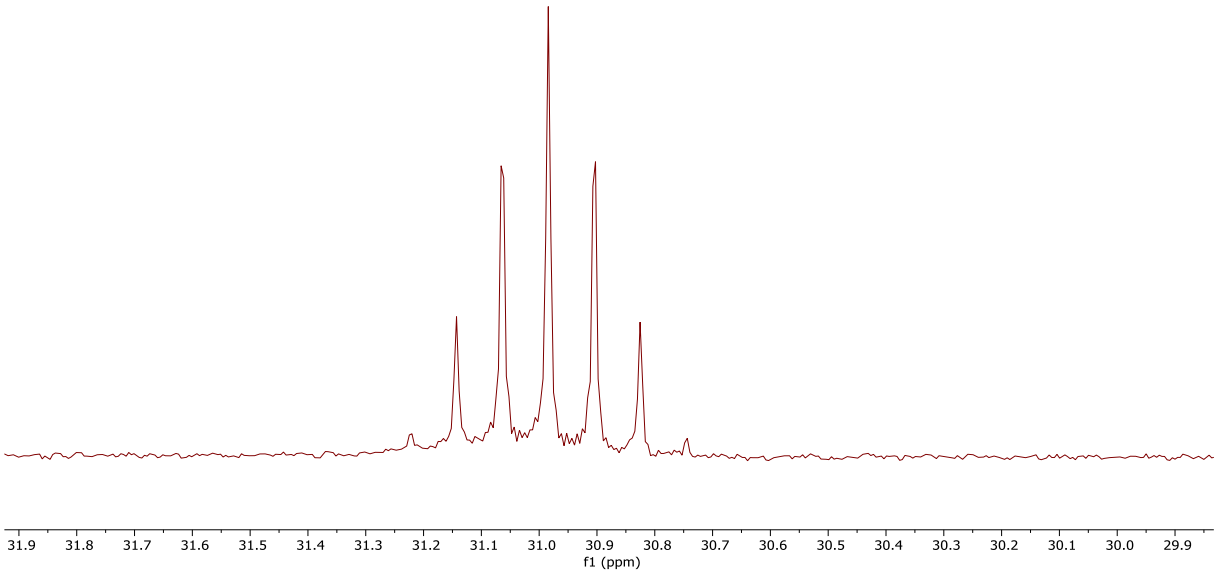

***Figure 75**. $^{31}P\{^1H\}$ NMR (C_6D_6, 161.72 MHz) spectrum for potential dimer of **4.2c**.*

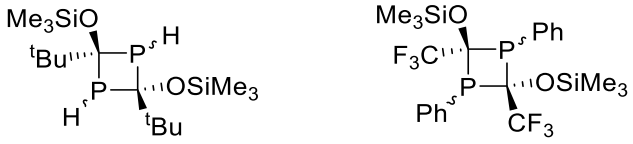

4.3 **4.4**

***Figure 76.** [1,3]-Diphosphacyclobutane (**4.3**) and the compound **4.4** (the dimer of **4.2c**).*

4.3 Reactivity Studies of the Trifluoromethylphosphaalkenes

4.3.1 Diels-Alder (4+2) Cycloaddition Reactions

In common with their carbon congeners, phosphaalkenes have previously been shown to undergo [4+2] cycloadditions with butadiene.[211] Therefore, compound **4.2d** was reacted with an atmosphere of butadiene (**Scheme 30**), resulting in the observation of four new resonances in the ^{31}P NMR spectrum as those for **4.2d** were lost. The new resonances all exhibit characteristic CF_3 coupling (**Figure 77**), with four associated doublets in the corresponding ^{19}F NMR spectrum, the proportions of which suggest four discrete species. Notably, these species are observed at significantly lower frequency than for **4.2d** and in a region often attributed to fully saturated phosphorus compounds.[213] Heating

the reaction resulted in the loss of all four resonances, though it is noted that thermal degradation is also apparent upon heating **4.2d** in isolation. Two of the species initially observed were found to be volatile in nature and could be separated from the mixture by static-vacuum distillation (**Figure 78**). Attempts to identify these two species by mass spectrometry resulted in the observation of a single molecular ion peak of 328 *m/z*, raising the possibility that they are diastereoisomers of **4.5** (**Scheme 30**).

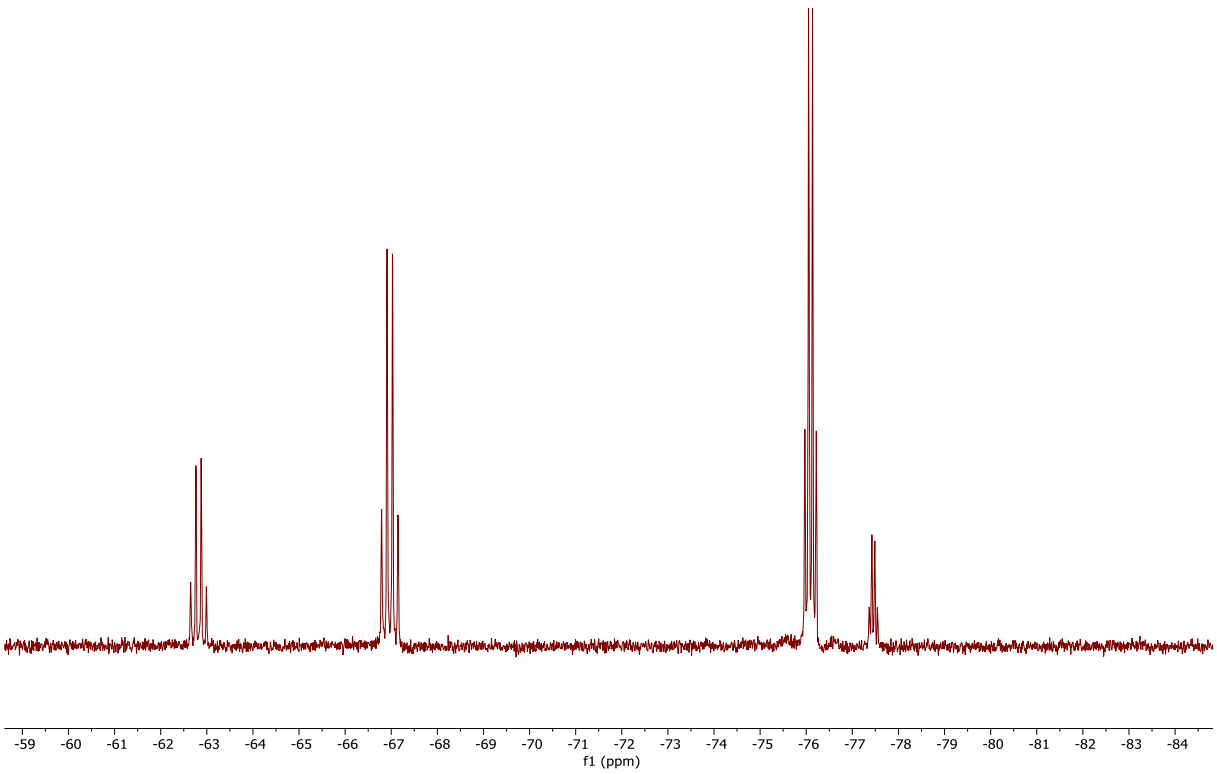

Figure 77. *^{31}P NMR (C_6D_6, 161.72 MHz) for reaction mixture of* ***4.2d*** *+ butadiene.*

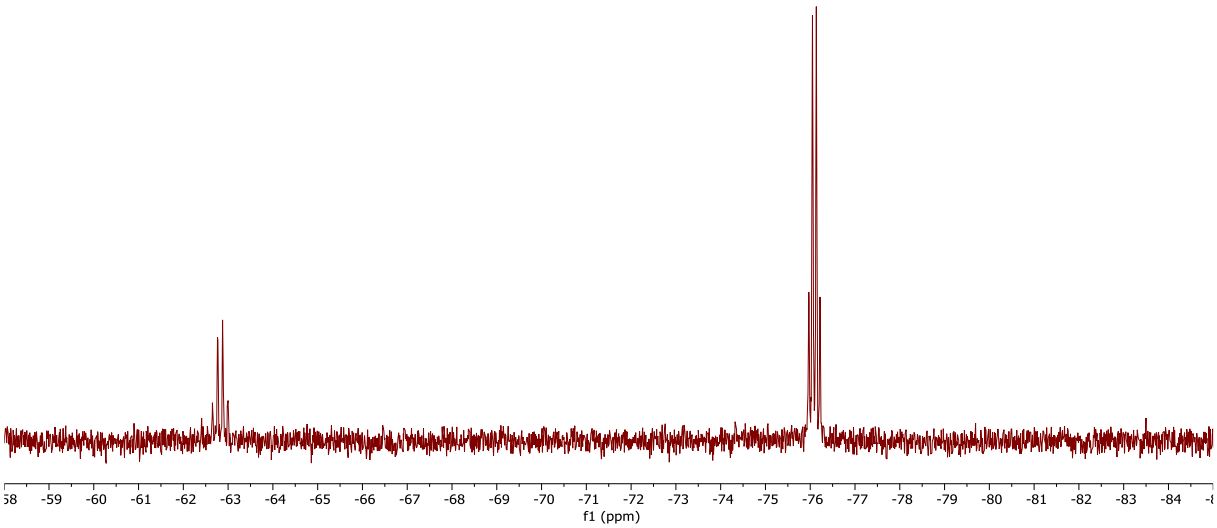

Figure 78. *^{31}P NMR (C_6D_6, 161.72 MHz) for destination flask, after static-vacuum distillation of* ***4.5****.*

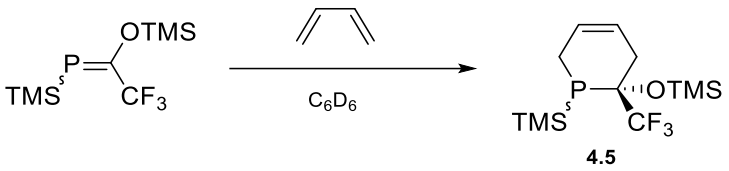

Scheme 30. *[4+2] Cycloaddition reaction between* ***4.2d*** *and butadiene, potentially affording the cyclic-phosphane (****4.5****).*

In an attempt to confirm the structure of **4.5**, reactions were performed with $W(CO)_5(THF)$, the product being characterised by a quartet resonance at δ_P −40 (J_{PF} = Hz), which exhibited tungsten satellites ($J_{(PW)}$ = 238 Hz; **Figure 79**) and two broad singlets in the ^{19}F NMR spectrum (δ_F −74 ($w_{1/2}$ = 19 Hz), −75 ($w_{1/2}$ = 15 Hz)). Attempts to crystallise this complex from benzene resulted only in the observation of $W(CO)_3(\eta^6\text{-}C_6H_6)$ by X-Ray diffraction, the only source of C_6H_6 is the solvent.

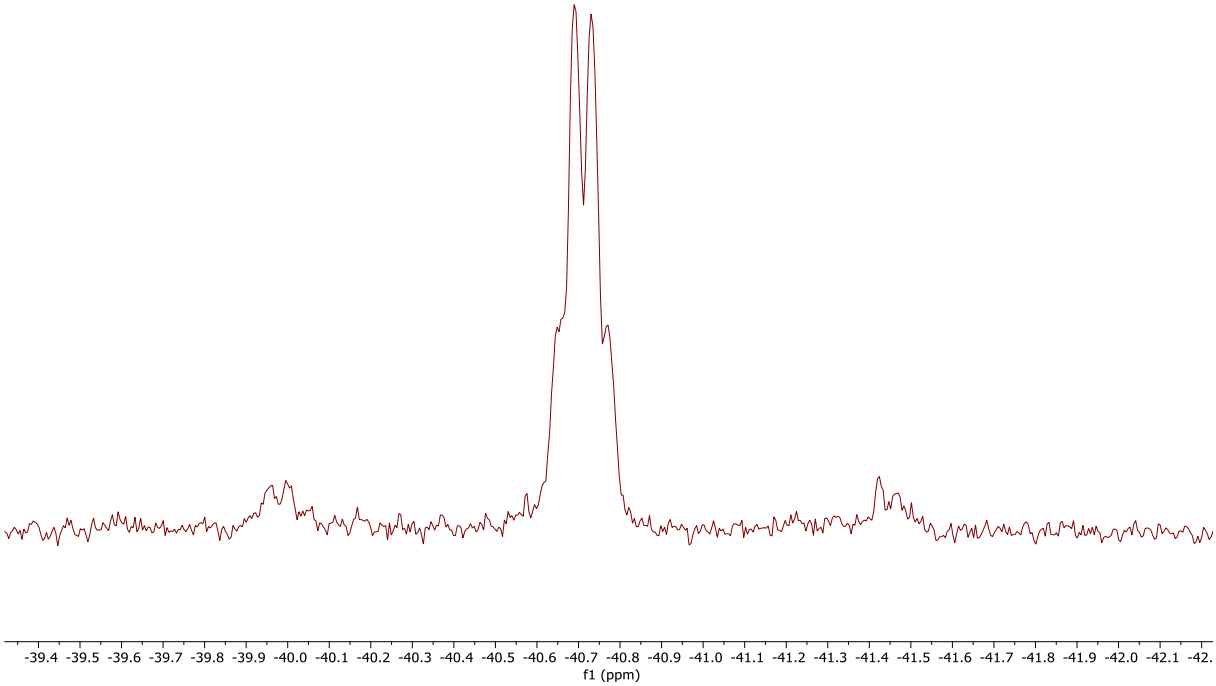

Figure 79. *^{31}P NMR (C_6D_6, 161.72 MHz) for **4.5** + $W(CO)_5$(THF).*

In an attempt to prepare a less-volatile product, compound **4.2d** was reacted with the bulkier 1,4-diphenyl-1,3-butadiene. Although four new species were again observed, this time in the region 46-27 ppm in the $^{31}P\{^1H\}$ NMR spectrum, they were accompanied with a large amount of unreacted **4.2d**, which persisted even after several days. Given the thermal sensitivity of **4.2d**, photolytic activation was employed to potentially result in either [2+2] cycloaddition (dimerization) or accelerate the reaction as a small amount of heat is also given out. Irradiation with a high-pressure Hg lamp resulting in a significant increase in the intensity of the resonance at δ_P 46.3 (**Figure 80**), though a significant amount of **4.2d** remained. Multiple other species are present in both the $^{31}P\{^1H\}$ (**Figure 81**) and ^{19}F NMR spectra, hindering structural assignment, though the species observed at δ_P −80, has an associated doublet of doublets in the ^{19}F NMR spectrum, (J_{FP} = 16 Hz, J = 2 Hz), the coupling from which could suggest an interaction from two phosphorus centres, one in closer proximity, though there does not appear to be a second phosphorus environment exhibiting mutual coupling with that of δ_P −80 (130 Hz, J_{PF} = 16 Hz).* Nonetheless, the associated molecular ion peak for the desired product was observed (**4.6**; 480 m/z), alongside that for the dimer of **4.2d** (**4.7**; 548 *m/z*), which may account for the multiplet at δ_P 46.3, which exhibits an apparently higher order pattern, suggestive of closely related but magnetically inequivalent centres. Volatiles could be removed from these species *via*

* Not observed between 300 and -300 ppm, though the corresponding peak could have been outside of that window.

static-vacuum distillation, though notably reactions with 1,4-diphenyl-1,3-butadiene are significantly less clean than butadiene itself.

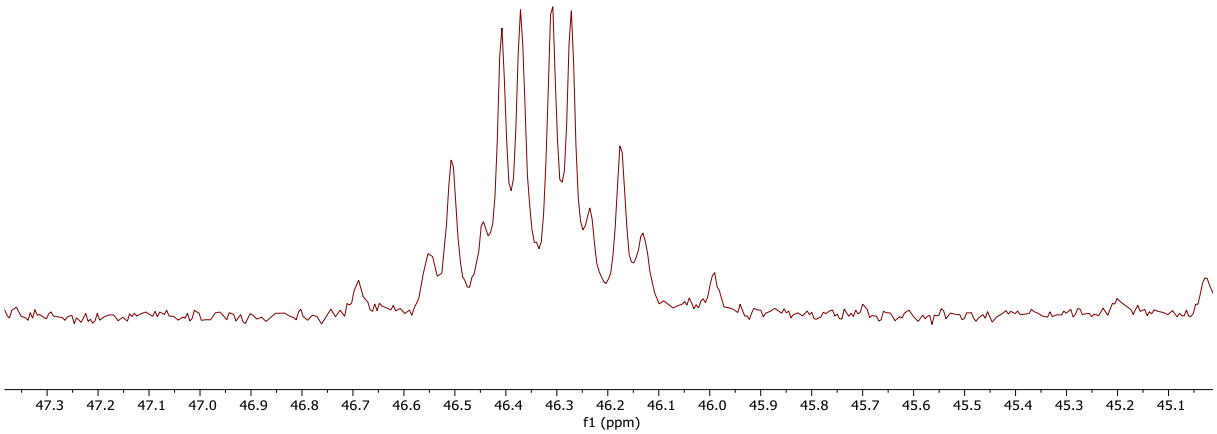

Figure 80. *Dominant species by $^{31}P\{^{1}H\}$ NMR (C_6D_6, 161.72 MHz) for* ***4.2d*** *+ 1,4-diphenyl-1,3-butadiene.*

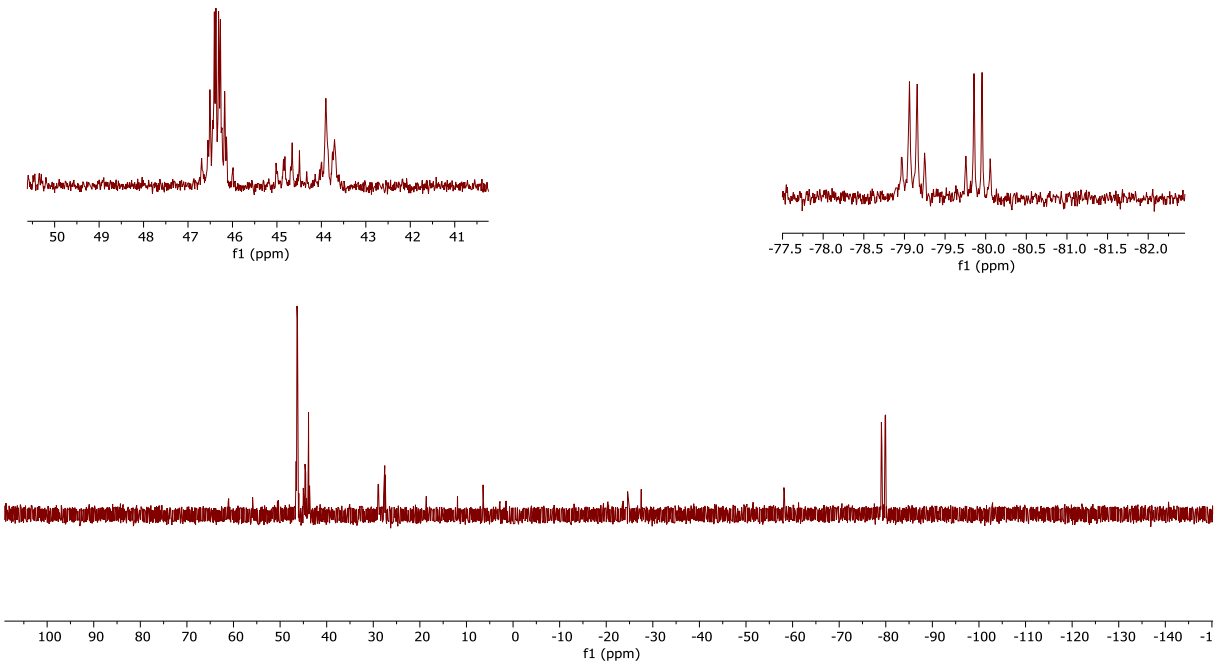

Figure 81. *$^{31}P\{^{1}H\}$ NMR (C_6D_6, 161.72 MHz) for* ***4.2d*** *+ 1,4-diphenyl-1,3-butadiene.*

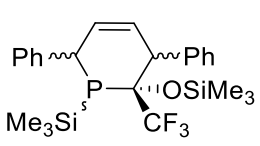

4.6

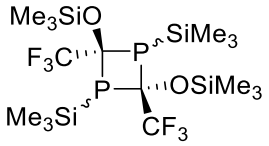

4.7

Figure 82. *The products from the* ***4.2d*** *+ 1,4-diphenyl-1,3-butadiene reaction.*

To further investigate [2+2] cycloadditions, compound **4.2d** was reacted with 1 equivalent of phenylisocyanate (PhNCO). Under ambient conditions essentially only **4.2d** was observed in the ^{31}P NMR spectrum, therefore, the reaction mixture was irradiated with a high-pressure Hg lamp. The resulting ^{31}P NMR spectrum exhibits five new resonances, the dominant new species being at δ_P 46.3, though a significant amount of **4.2d** still remains (**Figure 83**). The resonance at δ_P 46.3 has previously been observed upon irradiation of **4.2d** with other substrates (*vide supra*), which could suggest this species results from **4.2d** itself. A molecular ion peak consistent with compound **4.8** (**Figure 84**) was observed by mass-spectrometry (393 *m/z*), though specifics of the structure remain undetermined. Similar attempts to react compound **4.2d** with 1-hexyne resulted in an intractable mixture, while with furan and carbon monoxide (CO) no reaction was observed.

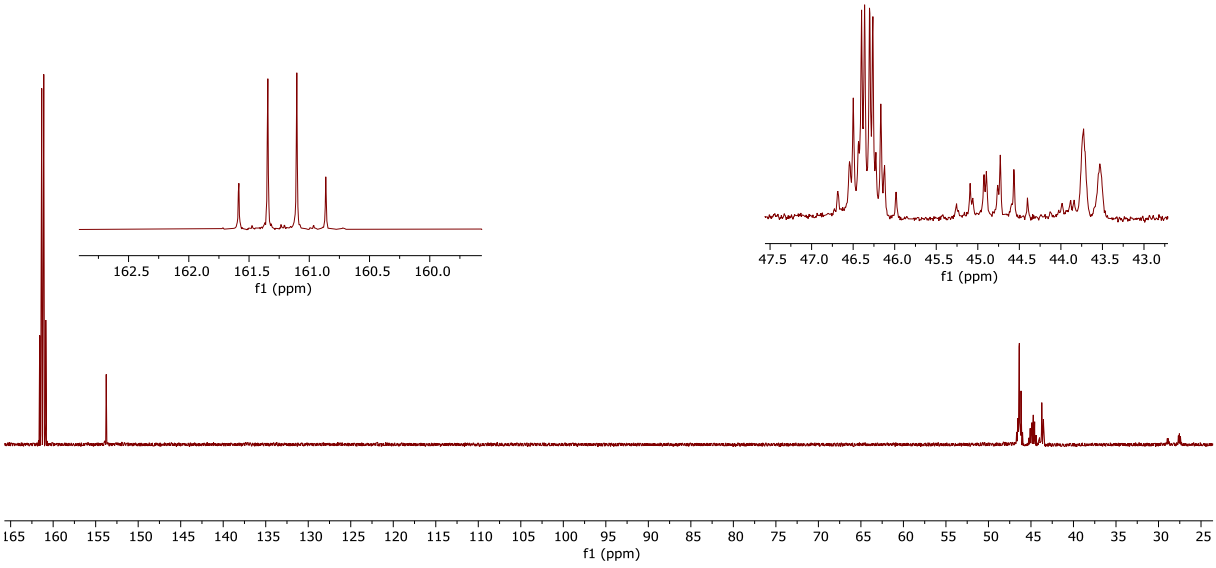

Figure 83. *$^{31}P\{^1H\}$ NMR (C_6D_6, 161.72 MHz) for **4.2d** + PhNCO.*

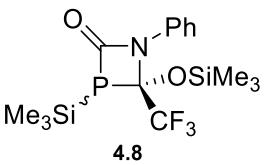

4.8

Figure 84. *Desired product from reacting compound **4.2d** with PhNCO.*

4.3.2 Coordination Reactions of the Trifluoromethylphosphaalkenes

Low-coordinate phosphorus species have previously often been stabilised by coordination to the -$W(CO)_5$ fragment, allowing for isolation and subsequent structural characterisation.[214] Therefore

compound **4.2d** was added to a $W(CO)_5(THF)$ solution, though only the tentatively assigned E-isomer (δ_P 161.3) reacted, resulting in a new phosphorus resonance at δ_P 173 (**4.9a**; **Figure 85**). This species also exhibits tungsten satellites, with an associated resonance observed in the ^{19}F NMR spectrum (−61 ppm (15 Hz)), consistent with the formation of $[(CO)_5WP(TMS)=(OTMS)CF_3]$. Interestingly, after stirring for an hour a new species started to form, characterised by a lower frequency phosphorus resonance (δ_P 162; **4.9b**, **Figure 86**), which ultimately became the only species present after 16 hours, again exhibiting an associated resonance in the ^{19}F NMR spectrum (−64 ppm (28 Hz)).

Compound **4.9a** exhibits a slightly larger phosphorus-tungsten coupling ($^1J_{PW}$: **4.9a** = 272 Hz, **4.9b** = 260 Hz), but smaller J_{PF} coupling than **4.9b** (Δ11 Hz; **Table 20**), whereas both **4.9a** and **4.9b** exhibit a smaller J_{PF} coupling than **4.2d**. This is presumably a result of coordination, which has been reported to decrease the magnitude of coupling constants by virtue of the lone pair becoming involved in bonding to the metal.[210] The extent of the coupling generally depends upon the coordination mode, where the lone pair is more intimately involved with bonding to the metal in η^1-coordination, relative to η^2, due to the increased directional interaction in the former and direct P-M bond.[117] The coupling differences between **4.9a** and **4.9b** could feasibly result from different coordination modes, with the larger P-M coupling for **4.9a** potentially the result of η^1 coordination,[185] where the increased s-contact to the metal results in an increased magnitude of P-W coupling at the expense of *s*-character in the internal ligand bonding, reducing J_{PF} interactions, as seen for similar systems such as $[(F_3P)_2Mo(CO)_4]$.[215,216] However, the differences between **4.9a** and **4.9b** are subtle and thus further evidence would be required to unequivocally confirm which coordination mode is present in each case (**Figure 87**); attempts to isolate these complexes led to decomposition and loss of phosphorus NMR signals.

If the reaction was repeated and solvent immediately removed after the addition of $W(CO)_5(THF)$. This time a single multiplet is observed at δ_P 135.8 (**4.9c**; **Figure 88**), with a doublet observed in the ^{19}F NMR spectrum (J_{PF} = 25 Hz). Unlike **4.9a** and **4.9b** this species was stable after exposure to vacuum, though specifics of the structure of **4.9c** remain undetermined, the acquisition of single crystals having thus far proven elusive.

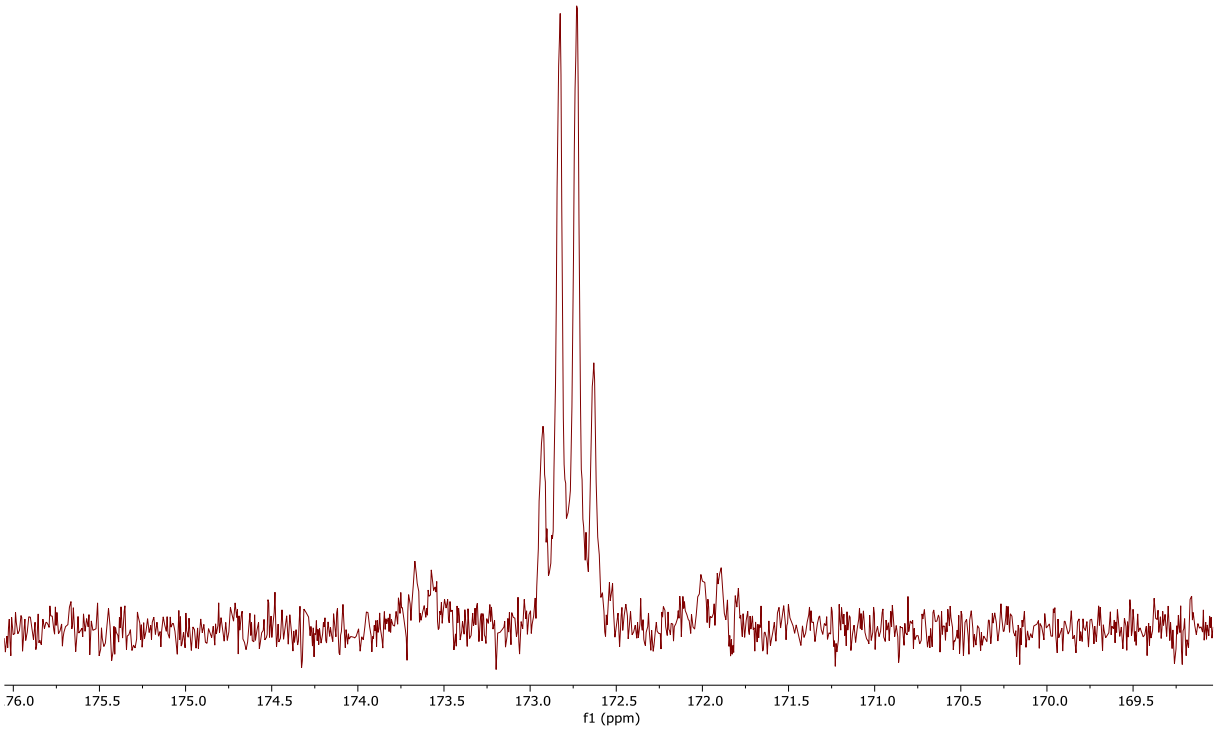

Figure 85. *Initial $^{31}P\{^{1}H\}$ NMR (C_6D_6 capillary, 161.72 MHz) spectrum of $[(CO)_5WP(TMS)=(OTMS)CF_3$.*

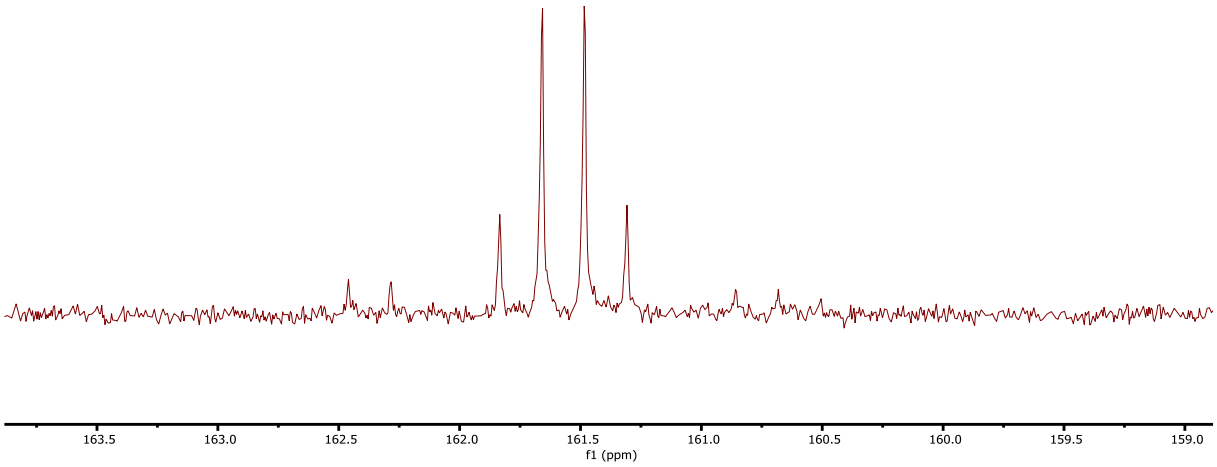

Figure 86. *$^{31}P\{^{1}H\}$ NMR (C_6D_6 capillary, 161.72 MHz) spectrum of $[(CO)_5WP(TMS)=(OTMS)CF_3$ after 16 hours.*

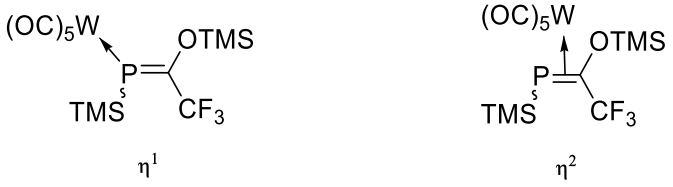

Figure 87. *Potential coordination modes for **4.9a** and **4.9b**.*

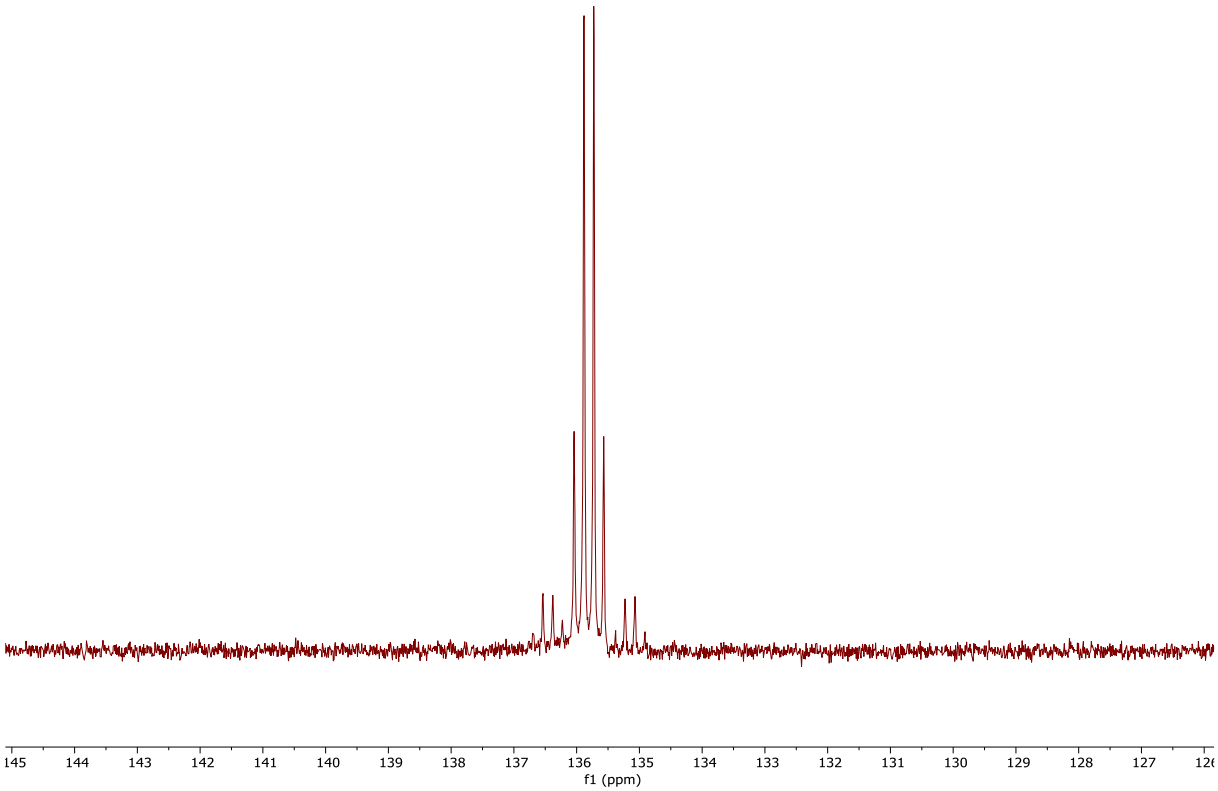

Figure 88. *$^{31}P\{^{1}H\}$ NMR (C_6D_6, 161.72 MHz) spectrum of **4.2d** + $W(CO)_5(THF)$ after instantly removing solvent.*

Table 20. *Selected Spectroscopic data for **4.9a-c**.*

	δ_P (ppm)	J_{PF} (Hz)	J_{PW} (Hz)	$\delta_F{}^a$ (J_{PF})^b
4.9a	*173*	*15*	*272*	*–61 (15)*
4.9b	*162*	*28*	*260*	*–64 (28)*
4.9c	*136*	*25*	*211*	*–62 (25)*

a. In ppm. b. In Hz.

Phosphaalkenes have previously been coordinated to a metal centre in an η^2-arrangement and subsequently treated with base, resulting in base-induced desilylation to afford the respective coordinated phosphaalkyne.[217] With this in mind, **4.9b** was reacted with an equivalent of $LiN(SiMe_3)_2$, affording an extremely viscous oil, which upon concentrating formed a sticky film. The associated ^{31}P NMR spectrum exhibits 3 poorly resolved resonances (δ_P 205, 102, 9.4), though these species have not been identified. Compound **4.2d** was also reacted with a range of Pt complexes, bis(triphenylphosphane)platinum-ethylene yielding no reaction, while 1:1 reactions with Pt(COD)MeCl, $Pt(dppe)_2$ or $[Pt(PEt_3)Cl_2]_2$ led to decomposition. In the latter two cases only the platinum starting material was observed in the ^{31}P NMR spectrum (δ_P 32 and 11, respectively).[218,219]

Similarly, reactions with $[PdCl(allyl)]_2$ and AuCl(tht) led to the decomposition of compound **4.2d**. Inconclusive data were obtained from reactions of **4.2d** with a range of main-group compounds (i.e. I_2, Se, MeI) and Lewis acids (see experimental for details).

4.3.3 In-pursuit of Trifluoromethylphosphaalkynes

Phosphaalkynes are typically synthesised *via* 1,2-elimination reactions, one of the most common examples being base induced desilylation from silylated phosphaalkenes, losing $O(SiMe_3)_2$ as a by-product. With that in mind **4.2d** should be ideally suited to afford the corresponding trifluoromethylphosphaalkyne (**4.1**) upon treatment with base (**Scheme 31**).

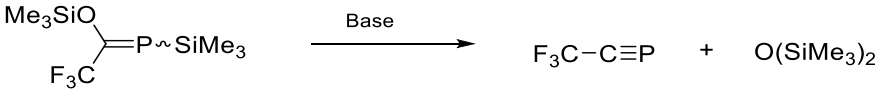

***Scheme 31**. Proposed synthetic route to prepare trifluoromethylphosphaalkyne.*

Reacting **4.2d** with a stoichiometric amount of $LiN(SiMe_3)_2$ at ambient temperature results in a broad triplet in the ^{31}P NMR spectrum at δ_F 4 (**Figure 89**), which resolves into a doublet of doublets at 213 K (J_{PF} = 8, 15 Hz; **Figure 90**), consistent with coupling to two inequivalent fluorine centres. The associated fluorine centres are observed in the corresponding ^{19}F NMR spectrum (−90.2, −109.9), **Figure 91**), in a region consistent with precedent alkenic CF_2 groups (e.g. $F_2C=CH_2$).[220] The observation of two signals in the ^{19}F NMR spectrum each exhibiting doublet multiplicity and integrating 1:1, indicates the loss of a fluorine atom from the CF_3 moiety, which is supported by the observation of trimethylsilylflouride (δ_F 158).[221*] The higher frequency signal exhibits additional coupling reminiscent of long range P-methyl coupling as observed due to from the CH_3 groups on Si ($SiMe_3$ or $OSiMe_3$) (*cf.* TMSF), which could suggest retention of the TMS-substituent and might be consistent with the formation of a phosphaallene **4.10a** (**Scheme 32**).

[*] TMSF integrates 4:1 relative to the proposed product, suggesting multiple things could be occurring in solution.

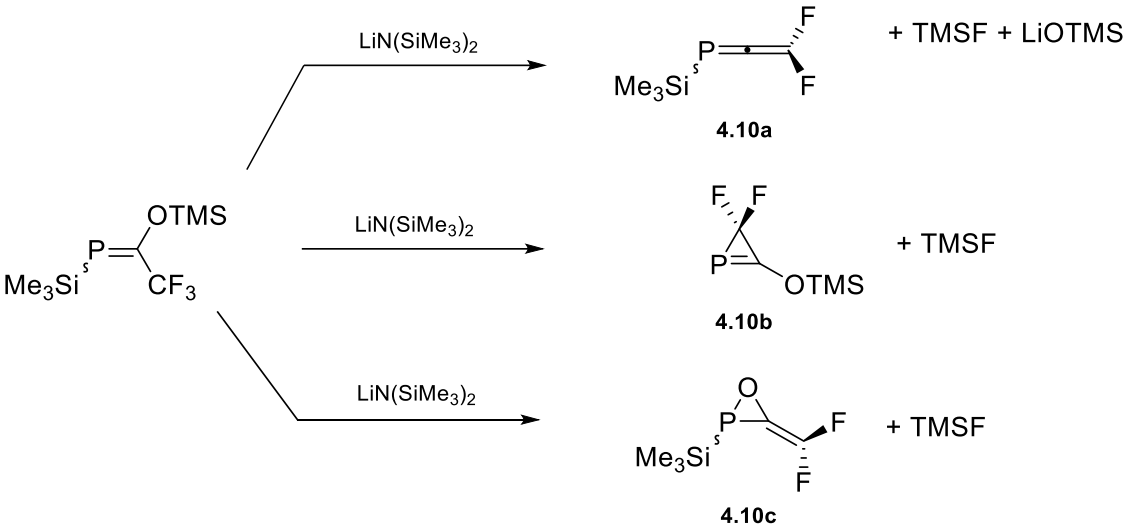

Scheme 32. *Proposed products from reacting* ***4.2d*** *with* $LiN(SiMe_3)_2$

However, no ^{29}Si satellites were visible in the ^{19}F NMR spectrum, similarly, no Si-F coupling was seen by $^{29}Si\{^1H\}$ NMR, though the spectrum was poorly resolved. Alternatively, a intramolecular cyclisation could have occurred, which would explain the loss of trimethylsilylfluoride, one possible product being phosphirene (**4.10b**), though the two fluorine atoms would presumably be equivalent, as seen for $RP{=}CH\text{-}CF_2$[222] and therefore inconsistent with the coupling observed in the ^{19}F NMR spectrum. Another possibility is oxaphosphirane formation (**4.10c**), the unsaturated $-C{=}CF_2$ would render the two fluorine atoms inequivalent and account for the loss of trimethylsilylfluoride, though it would not account for the coupling observed on the higher frequency fluorine resonance and thus further evidence would be required to unequivocally confirm specifics of this product. For the reactivity studies this unidentified species will be described as compound **4.10**.

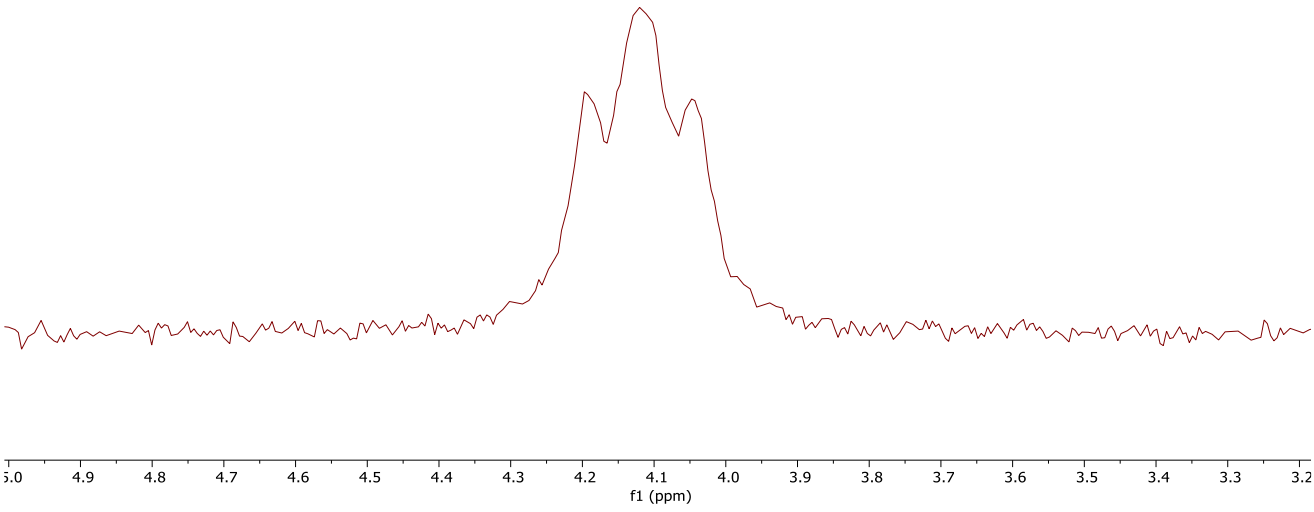

Figure 89. *$^{31}P\{^1H\}$ NMR (C_6D_6, 303 K, 161.72 MHz) spectrum from reacting* ***4.2d*** *with* $LiN(SiMe_3)_2$.

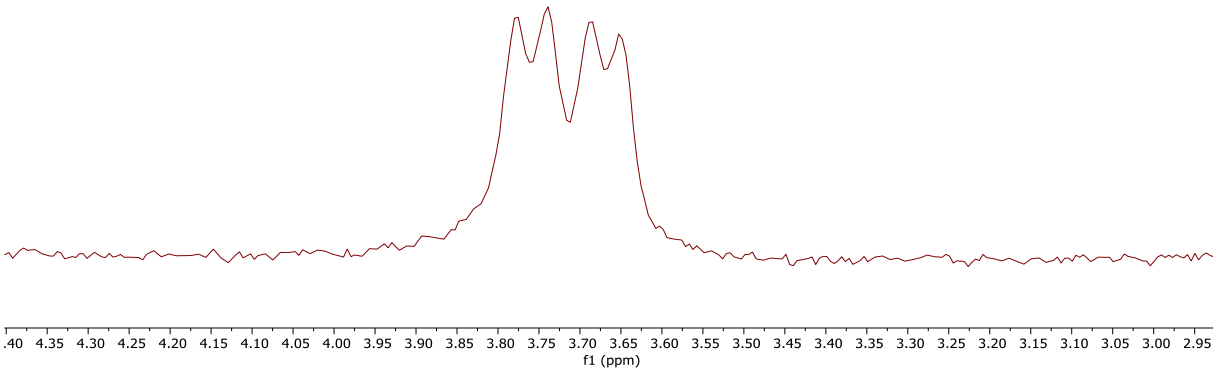

Figure 90. *$^{31}P\{^{1}H\}$ NMR (C_6D_6, 213 K, 161.72 MHz) spectrum from reacting* ***4.2d*** *with $LiN(SiMe_3)_2$.*

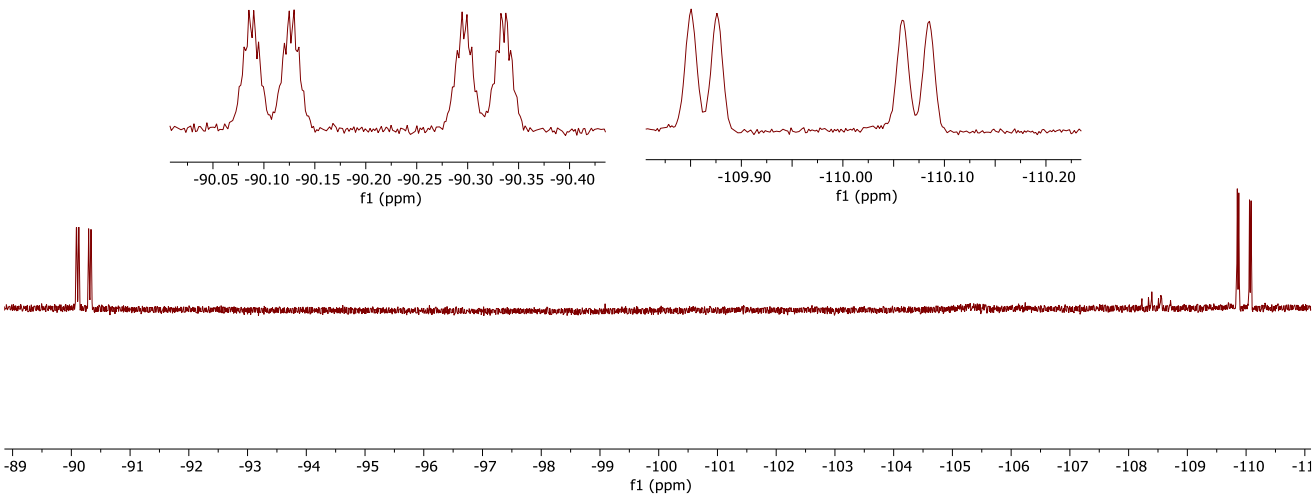

Figure 91. *^{19}F NMR (C_6D_6, 303 K, 375.87 MHz) spectrum from reacting* ***4.2d*** *with $LiN(SiMe_3)_2$..*

To confirm the identity of **4.10** more conclusive data such as structural evidence is required, therefore, attempts were made to coordinate this product to a metal centre. Firstly, reactions were performed with $W(CO)_5(THF)$ resulting in the observation of a doublet at 12.5 ppm in the $^{31}P\{^{1}H\}$ NMR spectrum, exhibiting tungsten satellites (J_{PW} = 272 Hz). Notably, in the proton-coupled spectrum, this appears as a doublet of doublets, the magnitude of coupling (J_{PH} = 359 Hz) being consistent with a direct P-H bond.[223] Unfortunately, attempts to grow crystals of this species were not successful. Similar reactions with $Fe_2(CO)_9$ or $Pt(COD)Cl_2$ led to its decomposition and reactions with $[(Ph_3P)_2Pt\text{-}(\eta^2\text{-}C_2H_4)]$ resulted only in the observation of the platinum starting material.

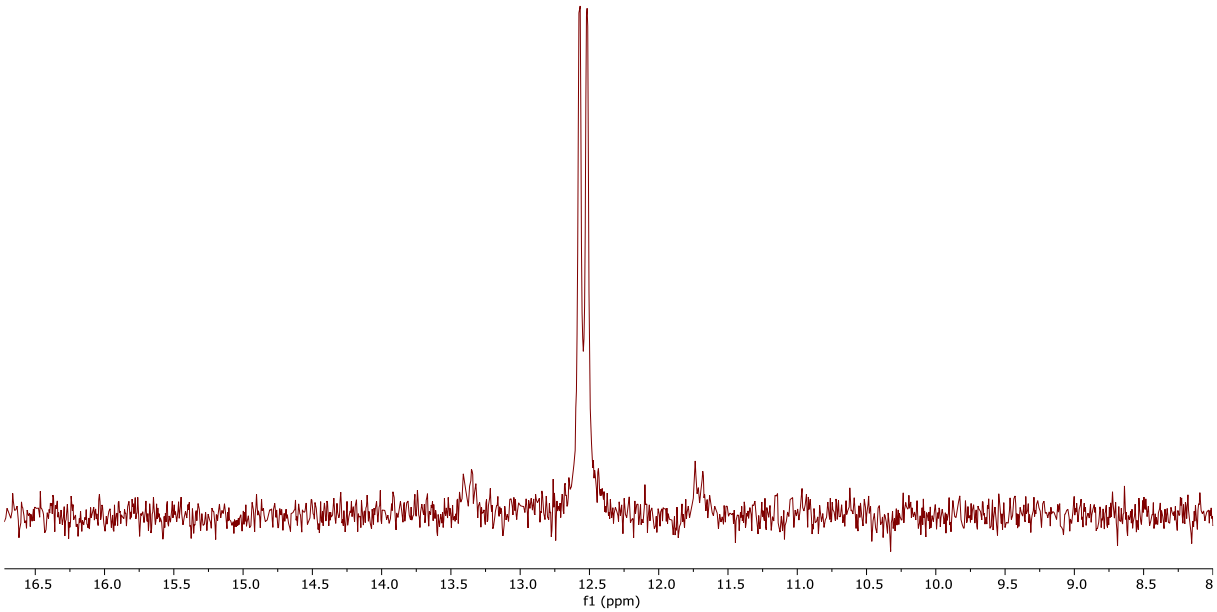

Figure 92. *$^{31}P\{^{1}H\}$ NMR (C_6D_6, 161.72 MHz) spectrum of **4.10** + $W(CO)_5$(thf) reaction product.*

Though the identity of **4.10** remains to be definitively established, the formation of **4.10a** and **4.10b** may imply the transient formation of the desired trifluoromethylphosphaalkyne (**4.1**), which constitutes a viable intermediate en route to such compounds. Kinetically unstabilised phosphaalkynes are known to exhibit limited lifetimes under ambient conditions.[205] Therefore **4.2d** was reacted with $LiN(SiMe_3)_2$ at −78 °C (**Scheme 33**); the NMR-probe was pre-cooled and initial analyses were performed at 193 K. The probe was then actively warmed to ambient temperature, with the NMR spectra recorded at regular temperature intervals (every 10 °C). At 193 K unreacted **4.2d** is the predominant species observed, alongside the formation of compound **4.10**. Additionally, a resonance at δ_P 6 (q, *J* = 37 Hz; **Figure 93**) is also observed with an associated doublet in the ^{19}F NMR spectrum at δ_F −72 (37 Hz; **Figure 94**), the mutual coupling being in the range of precedent $^{3}J_{PF}$ couplings (21-56 Hz),[215,224] including unsaturated species such as phosphorane, $CF_3C(F)=C(F)PBu_3$ (23 Hz),[225] while smaller than the $^{2}J_{PF}$ coupling seen for FC≡P (82 Hz);[207] these data could be consistent with the formation of **4.1**, though this species is only observed at temperatures below 253 K and thus this cannot be confirmed.

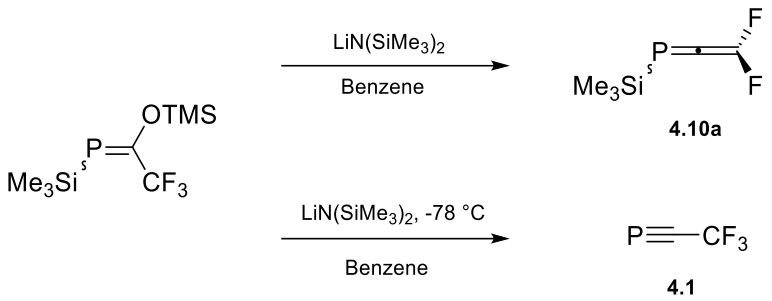

Scheme 33. *Reacting* ***4.2d*** *with $LiN(SiMe_3)_2$ at room temperature or –78 °C. At room temperature could also be* ***4.10b*** *or* ***4.10c****.*

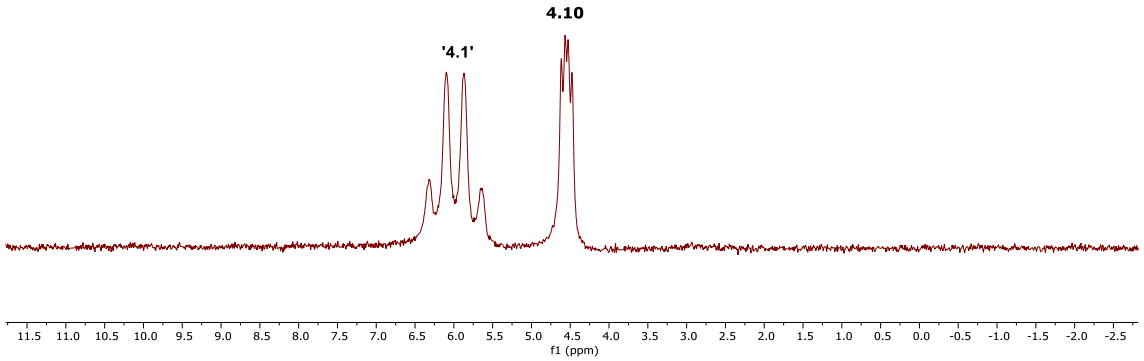

Figure 93. *$^{31}P\{^1H\}$ NMR (C_6D_6, 193K, 161.72 MHz) for Compound* ***4.2d*** *+ $LiN(SiMe_3)_2$.at –78 °C.*

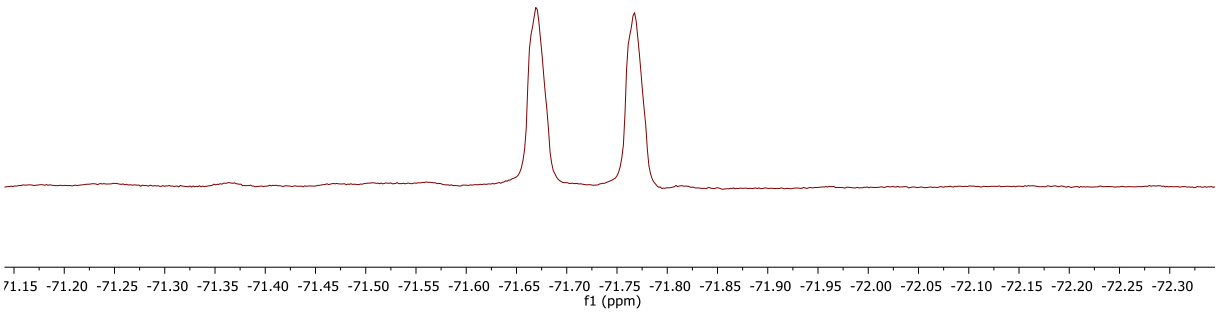

Figure 94*. ^{19}F NMR (C_6D_6, 193K, 375.87 MHz) associated fluorine resonance for the proposed compound '****4.1****', obtained from reacting* ***4.2d*** *and $LiN(SiMe_3)_2$.at –78 °C..*

The ^{31}P NMR resonances of precedent phosphaalkynes have been observed across a wide range of frequencies (98.7 to –69.2 ppm; **Table 21**),[202,226,227,228,229] making their chemical shifts difficult to predict. However, a DFT protocol has recently been documented, predicting ^{31}P NMR shifts with relative accuracy, typically within a few ppm.[230] In this method the ^{31}P NMR shifts are computationally derived from **Equation 1**, where δ is the chemical shift and σ is the isotropic magnetic shielding constant. Therefore, to predict the ^{31}P resonance for compound **4.1**, calculations were performed at

the PBE0/6-311+g (3d, 3p) level of theory, including a CPCM (C_6H_6 or CH_2Cl_2) solvent model; for comparison H-C≡P, ^{t}Bu-C≡P, TMS-C≡P, Me-C≡P, Ph-C≡P and PH_3 were calculated using the same model. These calculations were performed using a PMe_3 secondary reference (δ_P −62.5), relative to 85% phosphoric acid in H_2O. The results from these calculations are tabulated below (**Table 21**).

$$\delta_X = \sigma_{ref} - \sigma_X + \delta_{ref} \quad (1)$$

***Table 21**. Experimental and Calculated ^{31}P Chemical Shift (ppm), relative to phosphoric acid of selected phosphaalkynes, phosphanes and compound **4.1**.*[*]*

Compound	δ_{Exp}[a]	δ_{Calc}[b]	δ_{Calc}[c]
H-C≡P	*-32*	*-10*	*-9.0*
^{t}Bu-C≡P	*-69.2*	*-40.5*	*-40.5*
TMS-C≡P	*98.7*	*144.3*	*-144.6*
Me-C≡P	*-61*	*-38.1*	*-41.0*
Ar-C≡P	*37.2-32.1*	*9.4*	*7.7*
4.1	*6*	*-6.3*	*-2.0*
PH_3	*-238*	*-266.4*	*-266.3*
PMe_3	*-62.5*	*-62.5 (Reference)*	*-62.5 (Reference)*

a. in C_6D_6. b. with a benzene solvent model. c. with a DCM solvent model.

Although there is significant deviation from the experimental values, the general region of the computationally observed resonances are not unreasonable and thus the calculated chemical shift of **4.1**, δ_P = −6 or −2, could support the experimentally observed species (δ_P = 6) to indeed be trifluoromethylphosphaalkyne (**4.1**), though further evidence would be required to unequivocally confirm this.

Alternative bases were also explored in the pursuit of compound **4.1** (**Scheme 34**), for example reacting **4.2d** with NaOPh at ambient temperature resulted in a doublet of multiplets in the $^{31}P\{^1H\}$ NMR spectrum at 131 ppm, as well as a broad resonance at −52 ppm and a resonance at −58 ppm exhibiting a higher order splitting pattern (**Figure 95**). Attempts to remove the volatiles resulted in a viscous oil, which was sparingly soluble in acetone but defied further characterisation. In contrast, repeating the reaction with NaOH resulted in two species in the ^{31}P NMR spectrum, a quartet (δ_P −7.4

[*] The values presented are adjusted relative to 85% H_3PO_4 in H_2O (δ_P 0)

(7.3 Hz)) and a singlet (δ_P −25), though after a couple of hours only the singlet remained, with trimethylsilyl fluoride, a doublet at δ_F −128 (J = 54 Hz) and multiple broad signals observed in the associated ^{19}F NMR spectrum.

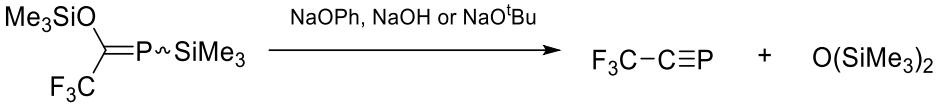

Scheme 34. *Alternative bases explored and desired reaction products.*

Similar reactions with NaO^{t}Bu resulted in a doublet of doublets at δ_P 62.0 (J = 59, 2 Hz; **Figure 96**), a significantly higher frequency than observed from the reactions with LiN(SiMe$_3$)$_2$ (**4.10**). The corresponding ^{19}F NMR spectrum exhibits a doublet (−90.6 ppm) and a doublet of doublets (−106.6 ppm) (**Figure 97**), the latter exhibiting J_{FF} and J_{PF} coupling of 56 and 59 Hz respectively, as well as a resonance consistent with the loss of trimethylsilyl fluoride (δ_F 158).[221] These data could indicate a series of different products, much like for compound **4.10**, however, in this instance the higher frequency fluorine is presumably not fully resolved. Notably, relative to **4.10** the phosphorus resonance is at a higher frequency, which could indicate the substituent at phosphorus is different. The observation of a resonance at 1.1 ppm in the ^1H NMR spectrum could support this notion, though further investigation would be required to identify this product. Upon exposure to vacuum, the species observed in the reaction mixture decomposed, resulting in the loss of all phosphorus resonances.

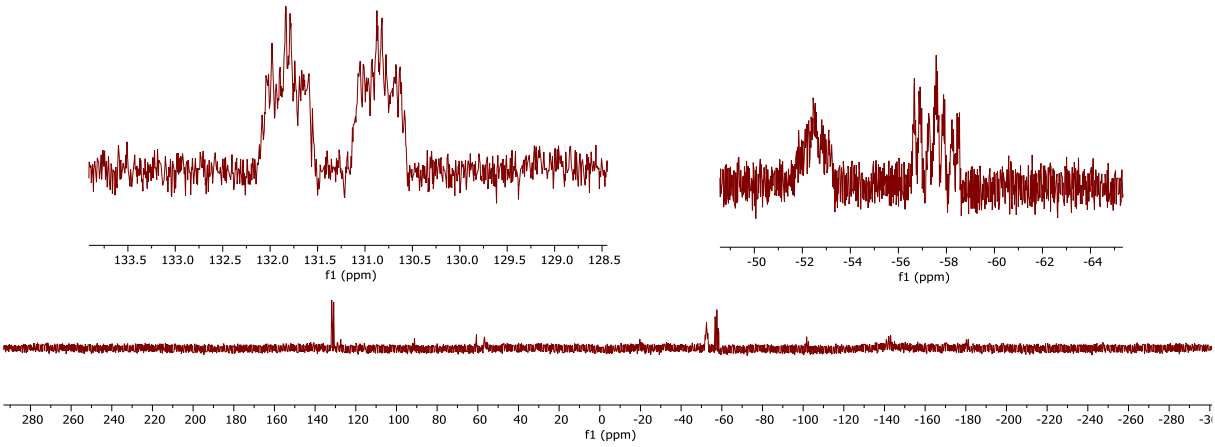

Figure 95. *$^{31}P\{^1H\}$ NMR (C_6D_6, 161.72 MHz) for reaction mixture of **4.2d** + NaOPh.*

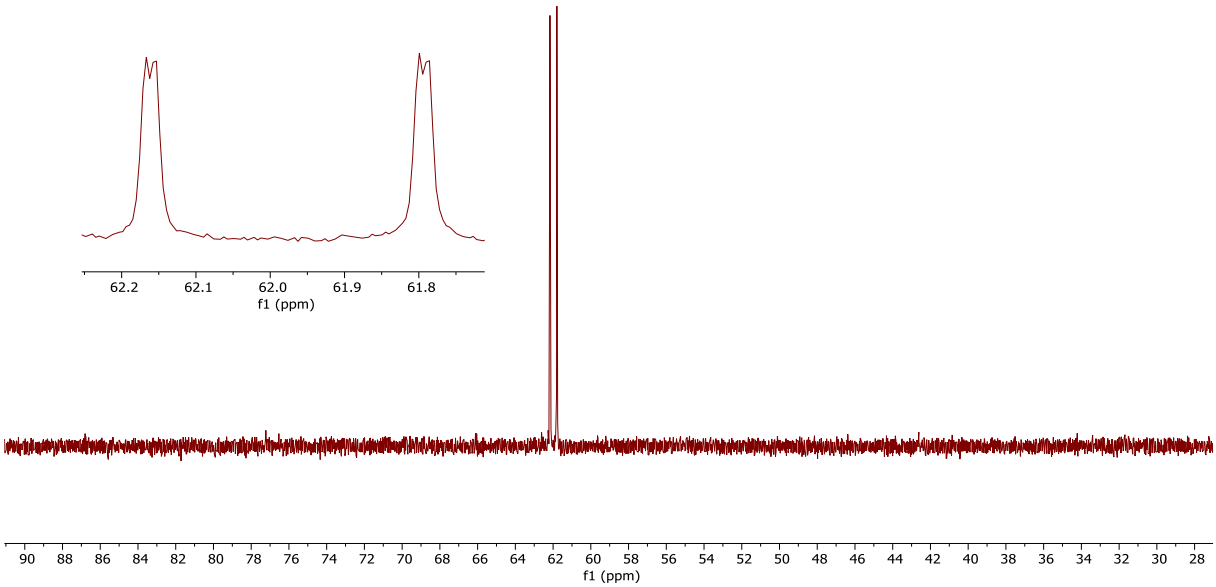

Figure 96. *$^{31}P\{^{1}H\}$ NMR (C_6D_6, 161.72 MHz) for reaction mixture of* ***4.2d*** *+ NaO^tBu.*

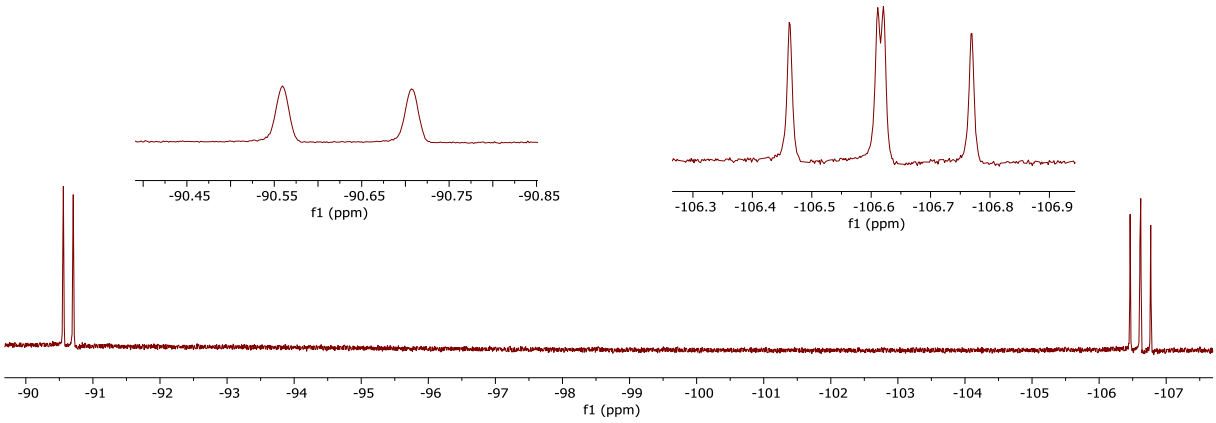

Figure 97. *^{19}F NMR (C_6D_6, 375.87 MHz) for reaction mixture of* ***4.2d*** *+ NaO^tBu.*

In an attempt to trap the transient phosphaalkyne (**4.1**), the reaction was repeated in the presence of [RuHCl(CO)(PPh_3)$_3$], which has previously been demonstrated to insert phosphaalkynes into the Ru-H bond.[231] This was initially attempted by reacting **4.2d** with LiHMDS at −78 °C and subsequently adding [RuHCl(CO)(PPh_3)$_3$], which resulted in a brown precipitate. After filtration the precipitate was analysed by ^{31}P NMR, which exhibited only resonances for **4.10**, suggesting this was the predominant product. In contrast, upon analysing the filtrate by NMR spectroscopy, four sets of doublets and a broad singlet were observed in the $^{31}P\{^{1}H\}$ NMR spectrum (**Figure 98**), with the associated ^{19}F NMR spectrum exhibiting a singlet resonance at −54.0 ppm, suggesting only one fluorine environment is present. A comparable outcome was achieved by transferring the transient trifluoromethylphosphaalkyne (**4.1**)

into a solution of [RuHCl(CO)(PPh_3)$_3$] *via* static-vacuum distillation. This species remained after exposure to vacuum, however, efforts to grow crystals resulted in the formation of (PPh_3)$_2$Ru(X)μ_2Cl$_3$Ru(CO)(PPh_3)$_2$ (**Figure 99**) by X-Ray diffraction, the source of which remains unclear.

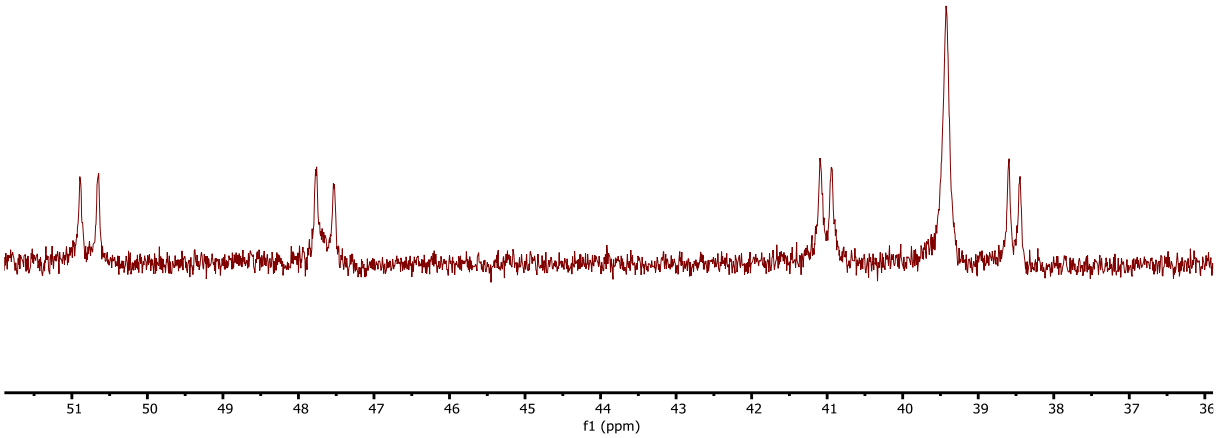

Figure 98. *$^{31}P\{^1H\}$ NMR (C_6D_6, 161.72 MHz) for* ***4.2d*** *+ [RuHCl(CO)(PPh_3)$_3$].*

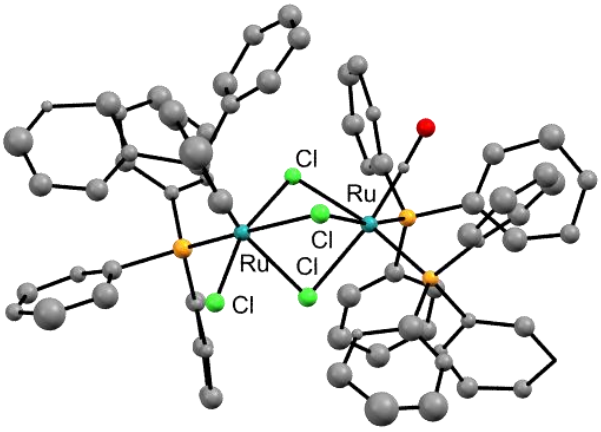

Figure 99. *Molecular structure of (PPh_3)$_2$Ru(X)μ_2Cl$_3$Ru(CO)(PPh_3)$_2$ with thermal ellipsoids at the 50 % probability level.*

4.4 Summary

A series of trifluoromethylphosphaalkenes, $RPC(OSiMe_3)CF_3$, have been successfully synthesised and characterised by NMR spectroscopy. Among these, the trimethylsilyl-analogue, **4.d** demonstrated the highest chemical stability, allowing purification *via* static-vacuum distillation, while **4.2a** and **4.2b** appear unstable to removal of volatiles and **4.2c** slowly converts to a new unidentified species. Compound **4.2d** was therefore used in reactivity studies, including being reacted with a range of bases in an attempt to form trifluoromethylphosphaalkyne (F_3C-C≡P; **4.1**); at ambient temperature the reaction with $LiN(SiMe_3)_2$ afforded resonances which indicate a product reminiscent of phosphaallene, phosphirene or indeed oxaphosphirane formation (**4.10**). Alternatively, analysing the reaction mixture at −80 °C led to the observation of resonances in the ^{31}P and ^{19}F NMR spectra which could be consistent with the formation of **4.1**; this is supported by DFT studies, the computed phosphorus shift of **4.1** being in the same region as the experimental data.

Attempts to coordinate the trifluoromethylphosphaalkenes and **4.10** to metal centres led to the observation of tungsten-pentacarbonyl complexes *in situ*. In the case of the trifluoromethylphosphaalkenes an apparent kinetic product was observed, which is consistent with $[(CO)_5WP(TMS)=(OTMS)CF_3]$; this is seen to convert to a thermodynamic product which is tentatively assigned as the η^2-analogue, though the coordination mode has yet to be confirmed. Similar attempts with other metal complexes typically resulted in decomposition of the phosphaalkenes, noting the sensitivity of the compounds.

Chapter 5 – The First Dianionic Diphosphaboracycles

"Not all those who wander are lost."

--The Lord of the Rings: The Fellowship of the Ring (2001)

5.1 Introduction

Since the discovery of ferrocene in 1951,[232] the cyclopentadienyl ligand (Cp; **5.1a**) has played a pivotal role in developing the field of organometallic chemistry.[233] Metal cyclopentadienyl complexes are widely used within the fields of catalysis[234,235] and molecular magnetism,[236] as well as in coordination and organometallic chemistry more generally.[237] This inspired the development of the dianionic systems pentalenide (**5.1b**) and cyclooctatetranide (**5.1c**),[238,239] which can be used to stabilise both mono- and bi-metallic complexes with coordination modes ranging from η^8 to η^3, thus featuring heavily in organometallic chemistry.[240] Although mono-anionic heterocyclic derivatives have been developed, their use in organometallic chemistry is sparsely reported in comparison to compounds **5.1a**-**5.1c**.[241] These heterocycles are limited to pyrrolide, imidazolide, 1,2,3-triazolide, along with their benzo-fused analogues (**Figure 101**).

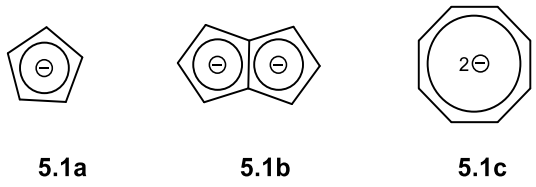

Figure 100. *Carbocyclic anionic ligands.*

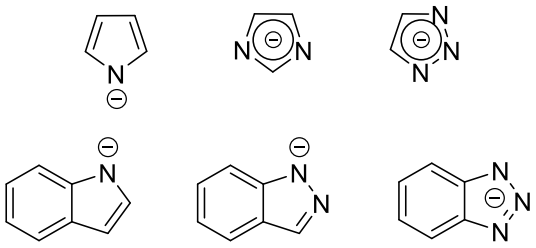

Figure 101. *Pyrrolide, imidazolide, 1,2,3-triazolide and benzo-fused analogues.*[241]

Much like nitrogenous systems, anionic phosphorus heterocycles are rare in comparison to carbon congeners, the first 1,2-diphospholide only being discovered in 1995 (**5.2a**),[242] with reports of triphospholide (**5.2b**),[243] tetraphospholide (**5.2c**) and pentaphospholide (**5.2d**) following shortly afterwards.[244,245] More recently, benzo-fused systems have been explored, with examples limited to those illustrated in **Figure 102**. Compounds **5.3a**-**5.3e** have been reported between 2015 and 2018 and Wright or Hey-Hawkins,[246,247,248] and the P_3 and P_2As derivatives (**5.4a-5.b**) by Russell and co-workers.[249] Whereas Schulz synthesised a chlorinated aza-diphospha-indane-1,3-diyl (**5.5a**), which can be reduced to access the resonance-stabilized biradical, **5.5b**.[250]

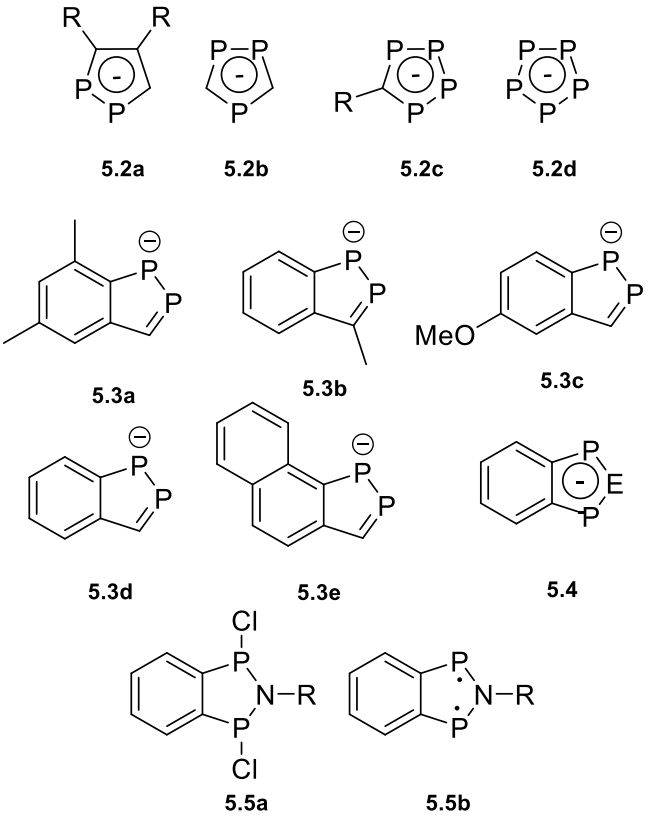

Figure 102. *Examples of heterocyclic monoanions with their respective counterions not included.* ***5.2a****: R = Ph, Et,* ***5.2b****: R = Mes*;* ***5.4****: E = P (****5.4a****), As (****5.4b****);* ***5.5a****,* ***5.5b****: R = tert-Butyl hydroperoxide (*^{tBu}*Bhp).*

Notably absent from the aforementioned benzo-fused examples are dianionic ligands, as surprisingly no such species are known; moreover, while a range of pnictogen linkages have been accessed including P-P, P-N-P and P-P-P, no group 13-group 15 have been reported. Nonetheless, the *in silico* study of the $BP_2C_2H_3$ and $BC_2P_2H_3^{2-}$ found that these heterocycles possess significant aromatic character,[251] similar to that of the Cp^- and P_5^- ions. The isoelectronic relationship between boroles and the cyclopentadienyl cation and the exploitation of the former within catalysis[252,253] renders the benzo-fused $C_2P_2B^{2-}$ heterocycles a desirable proposition for organometallic and coordination chemistry in general. Herein the development of novel dianionic diphosphaboracycles is reported and their reactivity is explored with both main-group compounds and transition-metal complexes.

5.2 Synthesis and Characterisation of $[C_6H_4P_2BC_6H_5]^{2-}$ 2[Li(solv.)]$^{2+}$ (solv. = THF, TMEDA)

The precedent benzofused-1,2-diphospholide **5.4a** was accessed *via* a one pot reaction with 1,2-bis(phosphino)benzene and ^{n}BuLi (4 equiv.), followed by the addition of PCl_3 (**Scheme 35**).[249] Unlike **5.4a**, it was previously found that attempts to tetralithiate 1,2-bis(phosphino)benzene and then add $PhBCl_2$ did not afford the desired dianionic diphosphaboracycle.[254] However, the double

deprotonation of 1,2-bis(phosphino)benzene with ^{n}BuLi, addition of dichlorophenyl borane and then subsequent treatment with a further two equivalents of ^{n}BuLi affords compound **[5.6].2[Li(THF)$_{1.5}$]** as an intense yellow solid in moderate yield (**Scheme 36**).*

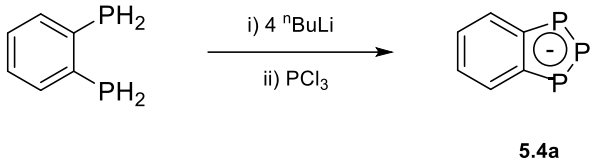

5.4a

Scheme 35. *Synthesis of* ***5.4a****.*[249]

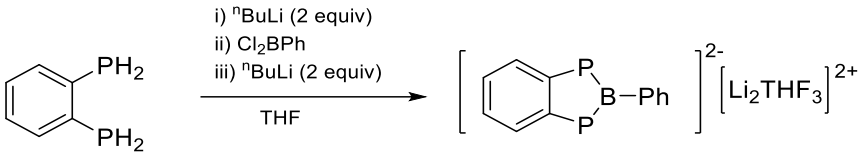

[5.6].2[Li(THF)$_{1.5}$]

Scheme 36. *Synthesis of compound* ***[5.6].2[Li(THF)$_{1.5}$]****.*

The ^{31}P NMR spectrum of **[5.6].2[Li(THF)$_{1.5}$]** displays a single resonance at δ_P 50.5 (d_8-THF), the lack of P-H coupling being consistent with the loss of all P-H bonds. In the ^{1}H NMR spectrum, resonances were observed for coordinated THF (δ_H 3.62, 1.77) as well as five aromatic environments, the latter integrating consistently for the benzo-backbone and phenyl group, with consistent resonances observed in the ^{13}C{^{1}H} NMR spectrum. These data suggest the benzo-fused C_2P_2B heterocycle has formed, which is supported by the corresponding ^{11}B NMR spectrum exhibiting a resonance at δ_B 69.4, consistent with a three-coordinate boron centre.[255]

The structure of **[5.6].2[Li(THF)$_{1.5}$]** was ultimately confirmed by X-Ray diffraction, identifying **[5.6].2[Li(THF)$_{1.5}$]** as a polymeric network in the solid state, in which the planar-C_2P_2B rings are bridged by η^1-coordination to Li, with alternate units also having an η^5-interaction to another lithium ion (**Figure 103**). This η^5 coordination results in the boron-bound phenyl group being slightly offset from planarity (ϕ = 26.49 °), which contrast those that lack this interaction, wherein the phenyl group is completely planar with respect to the C_2P_2B ring.

* Initial synthesis of **[5.6].2[Li(THF)$_{1.5}$]** was performed alongside summer student Elinor Canham.

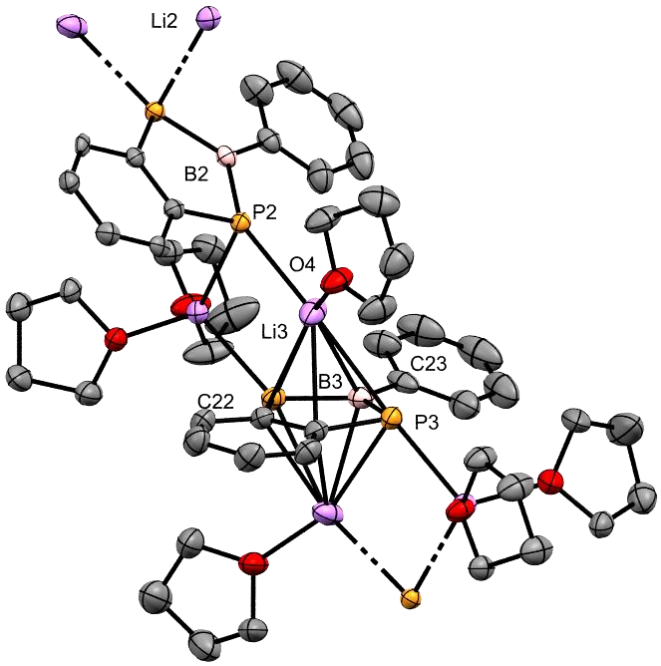

Figure 103. *Molecular Structure of* ***[5.6].2[Li(THF)$_{1.5}$]*** *with hydrogen atoms and disorder omitted for clarity; displacement ellipsoids at the 50% probability level. Selected bond lengths (Å) and angles (°): P2-B2 1.874(3), B2-C30 1.574(7), P2-C31 1.797(4), P2-Li2 2.582(12), Li2-O3 1.925(13), C31-C31' 1.420(6), P3-B3 1.866(2), B3-C23 1.582(5), P3-C22 1.813 (2), P3-Li3 2.661(5), B3-Li3 2.667(5), C22-Li3 2.517(6), Li3-O4 1.946(5), C22-C22' 1.418(5). P2-B2-P2' 111.2(3), C30-B2-P2 124.42(13), B2-P2-C31 96.70(18), P2-C31-C31' 117.71(12), Li2-P2-B2 98.6(3), P2-Li3-P3 96.12(15), P3-Li3-P3' 68.97(11), O4-Li3-P3 154.8(3), P3-Li3-B3 121.7(2), C23-B3-P3 123.59(10), B3-P3-C22 95.73(13), B3-Li3-C22 63.44(14), P3-C22-C22' 117.68(8), Li2-P3-C22 108.4(3).*

In seeking disaggregation of **[5.6].2[Li(THF)$_{1.5}$]**, the synthesis was repeated in the presence of TMEDA, which afforded the monomeric **[5.6].2[Li(TMEDA)]** (**Scheme 37**). The hydrocarbon backbone of **[5.6].2[Li(TMEDA)]** exhibit comparable spectroscopic features to those of **[5.6].2[Li(THF)$_{1.5}$]**, with the addition of resonances associated with TMEDA integrating consistently for the formation of **[5.6].2[Li(TMEDA)]**. Notably, the ^{31}P NMR resonance (δ_P 52.1 (d_8-THF)) is at a higher chemical shift relative to **[5.6].2[Li(THF)$_{1.5}$]**, while the boron centre resonates at lower frequency (δ_B 66.4).

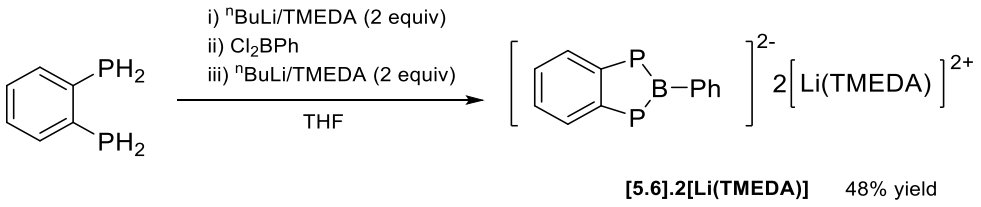

Scheme 37*. Synthesis of Compound* ***[5.6].2[Li(TMEDA)]****.*

The structure of **[5.6].2[Li(TMEDA)]** was confirmed by X-Ray diffraction, these data showing the monomeric diphosphaboracycle unit coordinating a lithium atom to each face of the C_2P_2B ring in an η^5 arrangement (**Figure 104**) with the boron-bound phenyl group slightly offset from planarity (ϕ = 8.78 °). The internal geometry of the heterocycle is largely comparably to **[5.6].2[Li(THF)$_{1.5}$]**, the P-B linkage (1.877(2) Å) being consistent with a single bond,[256] while, the P-C distances (1.812(2) Å) are consistent with precedent singly bonded species, including the neutral cyclic P/B system, Mes*P(CH_2CH_2)$_2$BC_6F_5 (1.818(3)),[257,258] and the C-C lengths are consistent with aromatic C-C bonds (*ca* 1.4-1.5 Å).[259,260]

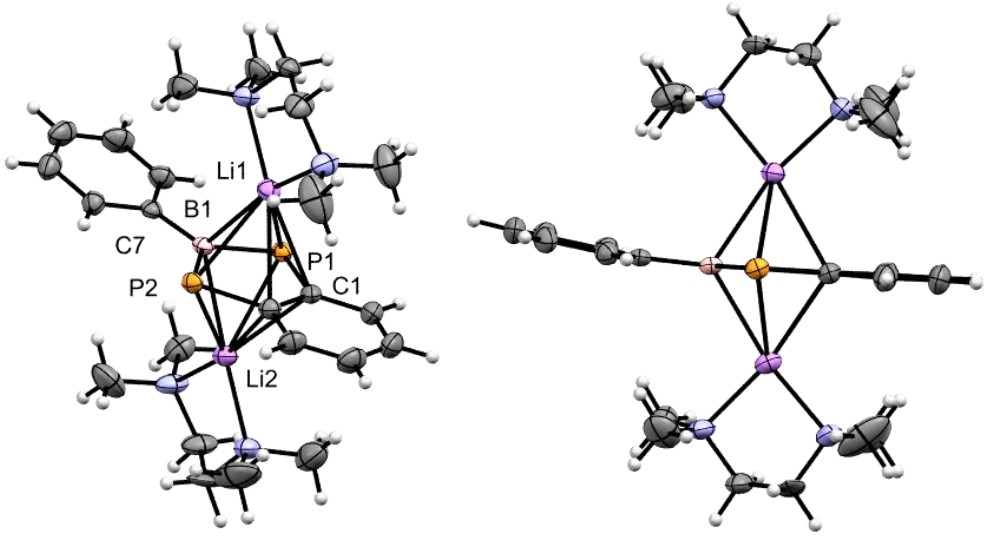

Figure 104. *Molecular Structure of **[5.6].2[Li(TMEDA)]** with the TMEDA disorder omitted for clarity; displacement ellipsoids at the 50% probability level. Selected bond lengths (Å) and angles (°): P1-B1 1.877(2), P2-B1 1.883(2), P1-C1 1.812(2), P2-C2 1.811(2), C1-C2 1.441(3), B1-C7 1.580(3), Li1-P1 2.636(3), Li1-P2 2.664(3), Li1-B1 2.458(4), Li1-C1 2.610(4), Li1-C2 2.638(4), Li2-P1 2.636(3), Li2-P2 2.607(3), Li2-B1 2.490(4), Li2-C1 2.528(4), Li2-C2 2.490(4). P1-B1-P2 114.35(11), P1-C1-C2 118.34(14), P2-C2-C1 118.31(15), P1-Li1-B1 43.07(7), P1-Li1-P2 73.20(8), C1-P1-B1 94.53(9), C2-P2-B1 94.45(9), C1-Li1-C2 31.87(7), P1-Li2-B1 42.63(7), P1-Li2-P2 43.28(7), C1-Li2-C2 33.35(8), C7-B1-P1 122.80(14), C7-B1-P2 112.80(14).*

The sodium salt of **[5.6]$^{2-}$** was also pursued, employing ^{n}BuNa in place of ^{n}BuLi. Though the initial metalation appeared to proceed, affording a characteristic yellow solution, the addition of $PhBCl_2$ resulted in a loss of colouration and formation of a precipitate. The precipitate was presumably NaCl, as only the regeneration of 1,2-bis(phosphino)benzene was confirmed spectroscopically. Similar results were obtained while pursuing potassium analogues.

In an effort to incorporate a softer metal centre, $MgCl_2$ was added to **[5.6].2[Li(THF)$_{1.5}$]**, the product from which exhibited a broad $^{31}P\{^1H\}$ resonance at 46 ppm (**Figure 105**); the broad nature of this species could indicate a dynamic equilibrium, albeit VT NMR studies failed to reach the low or high

temperature limiting regimes, however, similar behaviour has been observed, for example with $Mg[P(C_6H_5)_2]_2$,[261,262] as a result of the Schlenk equilibrium.[263] The solvent dependence of the Schlenk equilibrium has been well documented,[264] with the addition of dioxane often employed to drive the equilibrium to one side (typically forming R_2Mg, RMg in this instance),[265] however in this case only decomposition was observed. Attempts to elucidate the 'R_2Mg' structure through the growth of single crystals only resulted in the observation of **[5.6].2[Li(THF)$_{1.5}$],** which could suggest not simply just Schlenk equilibrium is taking place. Attempts to sequester the cation with 12-crown-4 were unsuccessful.

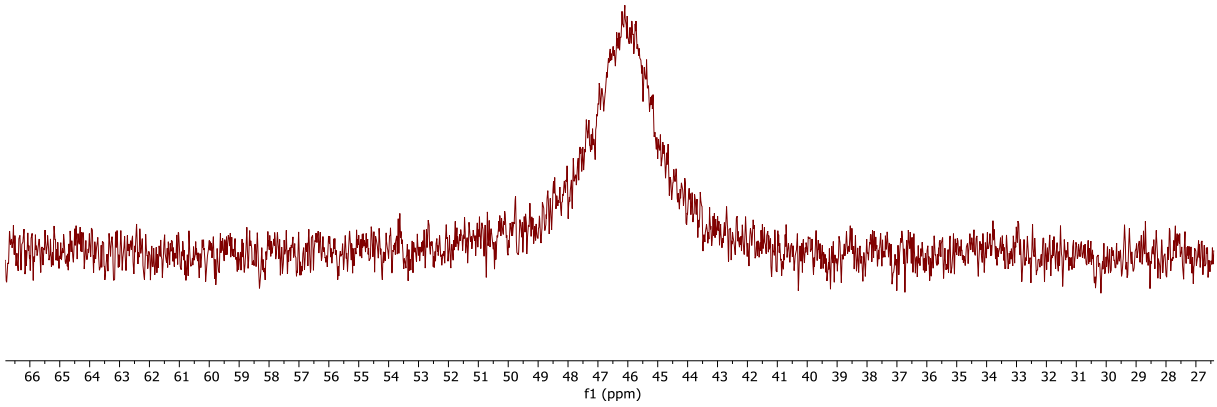

Figure 105. *$^{31}P\{^1H\}$ NMR (C_6D_6, 161.72 MHz) spectrum for the product from reaction* ***[5.6].2[Li(THF)$_{1.5}$]*** *with $MgCl_2$.*

To gain further insight into the electronic structure of **[5.6]$^{2-}$**, DFT analyses were performed (PBE0/6-311++G(3d, 3p)); the bond metrics from the optimised structure are in good agreement with the solid-state. The HOMO is composed of an antisymmetric π_{PC}-orbital which is nodal at boron, while the low-lying HOMO-1 is comprised of π_{cc} and π_{BP} components; the phosphorus lone pairs are not observed until HOMO-2 (**[5.6$_{DFT}$]$^{2-}$**; **Figure 106**). These data can be compared with those for $BC_2P_2H_3^{2-}$,[251] for which the HOMO was determined to be predominantly associated with boron, with slightly contributions from π_{BP} and π_{PC} orbitals, while the HOMO-1 is a π_{CC}-orbital and the HOMO-2 delocalised round the whole molecule. These differences presumably arise from the benzo-fused substituent, which $BC_2P_2H_3^{2-}$ does not possess.

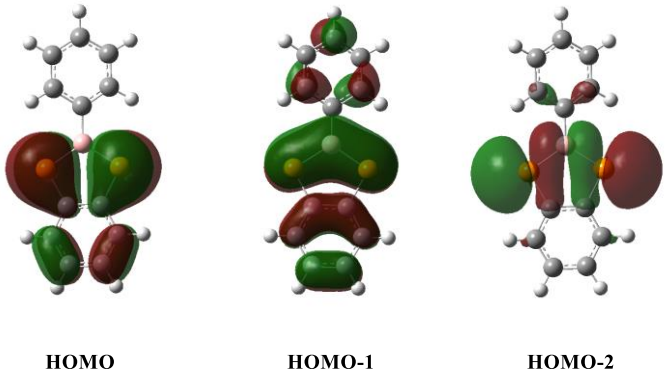

Figure 106. *Frontier molecular orbitals of* ***5.6$_{DFT}$*** *at the PBE0/6-311++G(3d,3p) level.*

Nucleus-independent chemical shift (NICS) calculations were explored to ascertain the degree of aromaticity for **[5.6]$^{2-}$**; these were performed at the centres of the benzo and diphosphaborole rings (NICS(0)) and 1 Å above / below each ring (NICS(1)). The data were compared against a benzene reference computed at the same level of theory. The reference data (–8.3, –10.4)* compare well against precedent literature,[266] affording confidence in the chosen model. Values for the C_2P_2B ring (–5.3, –7.4) and benzo-backbone (–4.1, –6.7) for NICS(0) and NICS(1) respectively, suggest **[5.6$_{DFT}$]^2** to be aromatic in nature, though notably less so than benzene and indeed the proposed $BC_2P_2H_3^{2-}$ species (−10.5 and −9.2).[251] The difference in frontier molecular orbitals and NICS values between **5.6$_{DFT}$** and $BC_2P_2H_3^{2-}$ suggests that the benzo-fused backbone and/or the boron substituent significantly influence their aromatic character, presumably with **[5.6$_{DFT}$]$^{2-}$** experiencing poor orbital overlap for the boron-bound phenyl group as illustrated by the off-set from planarity observed in both the solid state and gas phase (*in silico*).

5.3 The Attempted Synthesis of $[\{C_6H_4P_2B\}_2C_6H_4]^{4-}$ 4[Li(solv.)]$^{4+}$ (solv. = THF or TMEDA)

If the phenyl group of **[5.6$_{DFT}$]$^{2-}$** could be fixed in a planar arrangement, the delocalisation may be enhanced, thus affording an extended π-conjugated analogue of **[5.6]$^{2-}$**. Therefore, attempts were made to bridge two $C_6H_4P_2B$ units *via* a phenyl group. With this in mind, 1,2-bis(phosphino)benzene was deprotonated with ^{n}BuLi (2 equiv.), treated with 1,4-Bis(boryldichloride)benzene (0.5 equiv.), which was prepared following modified literature procedures (**Scheme 38**), and then subsequently a further two equivalents of ^{n}BuLi, affording a yellow solid after workup. The product exhibited an AA'BB' spin system in the $^{31}P\{^1H\}$ NMR spectrum, with resonances centred at δ_P –1.0 and δ_P –44.5, the

* (NICS(0), NICS(1))

associated proton-coupled spectrum clearly displaying P-H coupling. The product was ultimately identified to be the previously reported compound $[C_6H_4P_2H]_2$ by single crystal diffraction (**5.7**; **Figure 107**), with which the spectroscopic data agree.[267] Compound **5.7** has previously been prepared catalytically using $CpTi(C_4H_8)N=P^tBu_3$ and $[Cp^*_2ZrH_3]$[-267,268] at elevated temperatures (75 and 90 °C for 72 h and 30 min, respectively), however, this would seem to be the first preparation under ambient conditions.

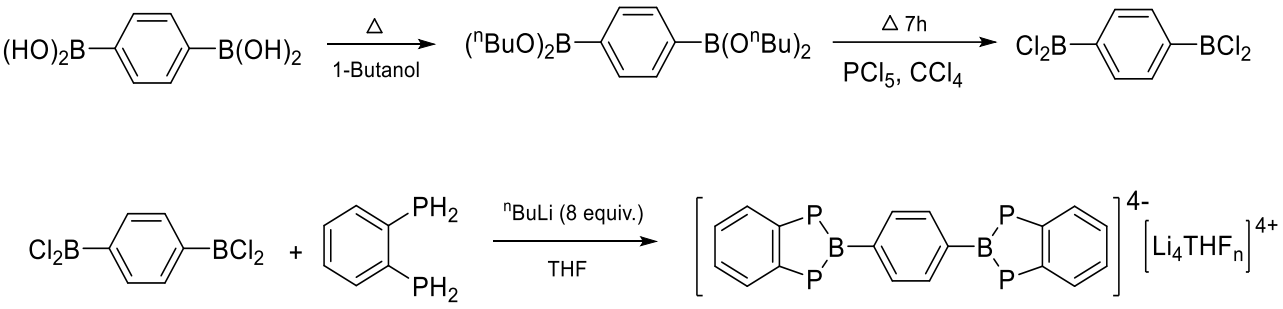

Scheme 38. *Synthesis of 1,4-bis(boryldichloro)benzene and proposed scheme for the preparation of* ***[{C6H4P2B}2C6H4]4- 4[Li(THF)n]4+****.*

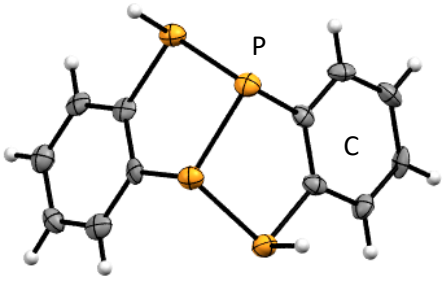

Figure 107. *Molecular Structure of* ***5.7****; displacement ellipsoids at the 50% probability level.*

This reaction was repeated in the presence of TMEDA, the product exhibiting a singlet resonance in the $^{31}P\{^1H\}$ NMR spectrum at −127 ppm, which resolved as a doublet of doublets in the proton-coupled spectrum; in addition, resonances associated with TMEDA were observed in the ^1H NMR and a singlet at δ_{Li} 0.66 in the ^7Li NMR spectrum, all of which match the literature for $[C_6H_4\{P(H)\}_2][Li_2TMEDA_2]$ (**5.8**; **Figure 108**).[267]

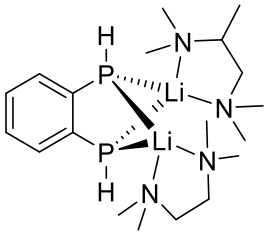

5.8

***Figure 108**. Structure of [C_6H_4{P(H)}$_2$][Li_2TMEDA_2] (**5.8**).*

5.4 The Attempted Synthesis of $[C_6H_4P_2EC_6H_5]^{2-}$ $2[Li(THF)_{1.5}]^{2+}$ (E = Al, Si).

Lappert and co-workers previously investigated neutral 1,3-diphospha-2-metallapentanes (**Figure 109**),[255] incorporating ML_n fragments (ML_n = $ZrCp_2$, $SnMe_2$, SnR_2 or BAr; R = $CH(SiMe_3)_2$, Ar = $C_6H_2{}^tBu_3$-2,4,5). Similarly, Wright and Russell have incorporated P, As or Sb into a benzo-fused phosphacycle (**Scheme 35**, *vide supra*), the products from which show some analogy to **[5.6].2[Li(THF)$_{1.5}$]**, based on these similarities, the development of analogues of **[5.6].2[Li(THF)$_{1.5}$]** incorporating main group elements seemed a logical target.

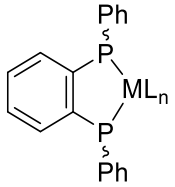

***Figure 109.** Lappert and co-workers 1,3-diphospha-2-metallapentanes.[255]*

The aluminium analogue of **[5.6].2[Li(THF)$_{1.5}$]** (**Scheme 39**) was pursued by reacting 1,2-bis(phosphino)benzene with ^{n}BuLi (2 equiv.), followed by the addition of $MeAlCl_2$ and subsequently another two equivalents of ^{n}BuLi. The product exhibited a very broad ^{31}P NMR resonance, δ_P −132, at significantly lower frequency than that of **[5.6].2[Li(THF)$_{1.5}$]** (δ_P 50.5), exhibiting a $^1J_{PH}$ coupling in the ^{31}P spectrum (J_{PH} = 204 Hz), inconsistent with the desired product. In contrast, employing Cl_2SiPh_2 in place of $MeAlCl_2$, resulted in a doublet at δ_P −110 (J_{PP} = 18 Hz), which resolved into a doublet of multiplets in the proton-coupled spectrum (J_{PH} = 191 Hz), indicative of a P-H containing species. There

was also a broad singlet at δ_P –130 in the $^{31}P\{^1H\}$ NMR spectrum. None of the observed resonances appear to display J_{PSi} coupling, suggesting a P-Si bond was not formed.

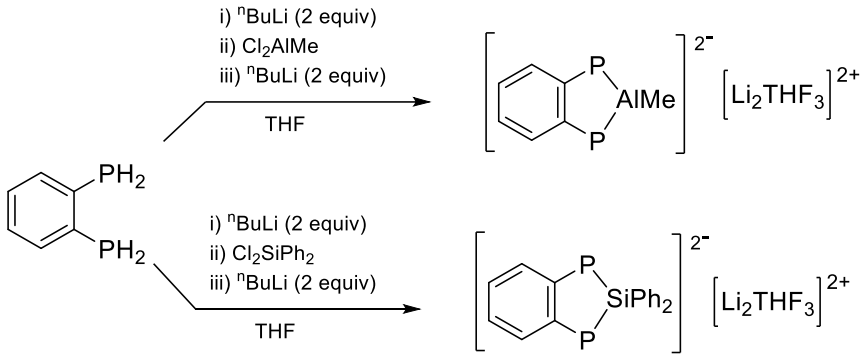

Scheme 39. *Attempted synthetic route to access the aluminium and silicon Analogues of* ***5.6.2[Li(THF)$_{1.5}$]****.*

5.5 Electrochemical investigation of $[5.6]^{2-}$

As noted (*vide supra*) a common feature from efforts to prepare analogues of **[5.6].2[Li(THF)$_{1.5}$]** has been the reformation of 1,2-bis(phosphino)benzene; this is also encountered during efforts to coordinate **$[5.6]^{2-}$** to transition metals (*vide infra*; Section **5.6.2**). This raises the possibility that **$[5.6]^{2-}$** may be particularly reducing in nature, and thus not readily stabilised by anything more oxidising than Li^+ (–3.04 V).[269] In order to explore this possibility and probe the electronics of the system more generally, cyclic voltammetry studies were conducted on **[5.6].2[Li(TMEDA)]** in THF solutions at a platinum disk working electrode (1 mm) with $[^nBu_4N][PF_6]$ supporting electrolyte.

Compound **[5.6].2[Li(TMEDA)]** exhibits a distinctive irreversible oxidative event at E_{pc} = –0.755 V relative to the Fc/Fc^+ couple (–0.131 V vs SHE)[2*270] (**Figure 110**), this event becoming more resolved at higher scan rates (**Figure 111**). While this is consistent with **[5.6].2[Li(TMEDA)]** exhibiting an appreciably reducing character, this should not be prohibit coordination. Thus, while complexes based on Zn^{2+}, Fe^{3+}, and Sn^{2+} (–0.76, –0.77, –0.14 V)[◊],[271] may indeed be unstable, less oxidising species (e.g. Pt^{2+}, Ru^{+3}, U^{4+} (+0.73, +0.25, +0.52 V)[◊] should still be viable targets.

[*] *Common redox potentials are typically reported relative to the standard hydrogen electrode (SHE), therefore a conversion factor (+624 mV) was implemented for the oxidative event.*

[◊] Standard electrode potentials for selected metals as aqueous solutions (25 °C).

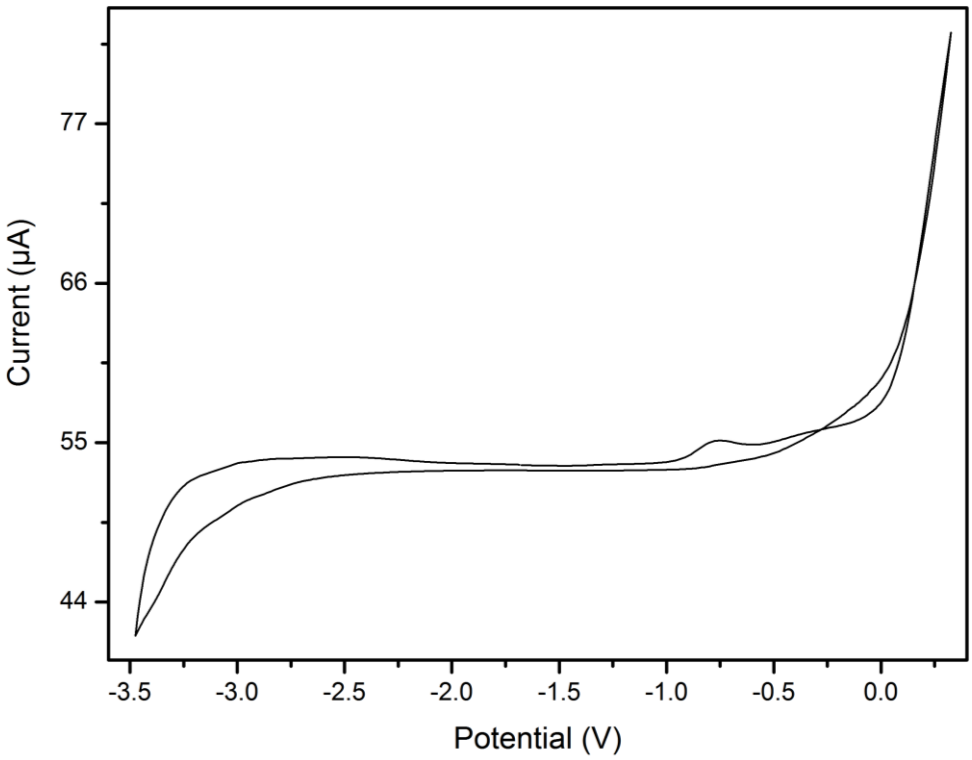

Figure 110. *Cyclic Voltammagram for* ***[5.6].2[Li(TMEDA)]*** *as solution in THF (5 mM) with* $^{n}Bu_4NPF_6$ *(0.1 M) supporting electrolyte; recorded at 100 mV* S^{-1}.

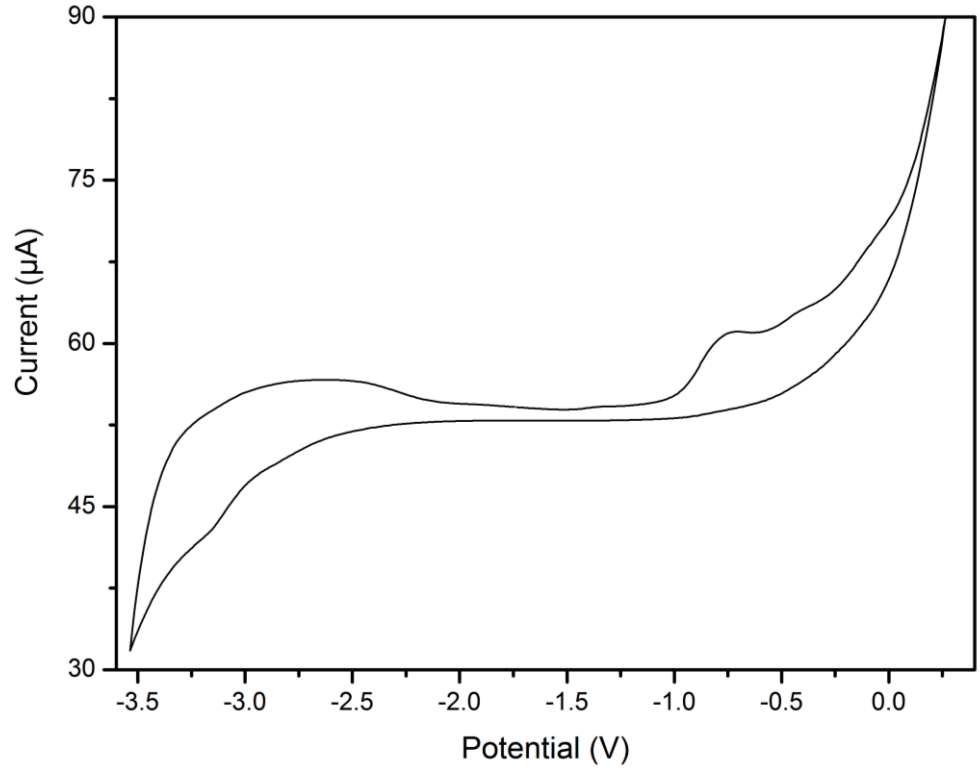

Figure 111. *Cyclic Voltammagram for* ***[5.6].2[Li(TMEDA)]*** *as solution in THF (5 mM) with* $^{n}Bu_4NPF_6$ *(0.1 M) supporting electrolyte; recorded at 300 mV* S^{-1}.

5.6 Reactivity Studies of $[C_6H_4P_2BC_6H_5]^{2-}$ $[Li_2(solv.)]^{2+}$ (solv. = THF, TMEDA)

5.6.1 In Pursuit of Phosphorus Functionalisation.

The solid-state structures for compounds **[5.6].2[Li(THF)$_{1.5}$]** and **[5.6].2[Li(TMEDA)]** suggest there are two possible sites for reactivity, viz. the π-system or phosphorus centre. In order to explore the latter, compounds **[5.6].2[Li(THF)$_{1.5}$]** and **[5.6].2[Li(TMEDA)]** were reacted with electrophiles based on main group elements, including Si, Sn, Pb and I in pursuit of neutral diphosphaboracyclic ligands.

In an effort to prepare compound **5.9** (**Figure 112**), **[5.6].2[Li(THF)$_{1.5}$]** was reacted with two equivalents of TMSCl, NMR analysis of which noted the the formation of a new broad singlet in the ^{31}P NMR spectrum, δ_P –40, appreciably shifted from that of **[5.6].2[Li(THF)$_{1.5}$]** (δ_P 50.5). Notably, this species is only observed *in situ*, attempts to remove volatiles *via* static-vacuum distillation leading to the observation of only 1,2-bis(phosphino)benzene (δ_P –126),[272] which could potentially be a facet of a weak P-B bond and the basic nature of phosphorus in this compound, presumably abstracting protons from the solvent.

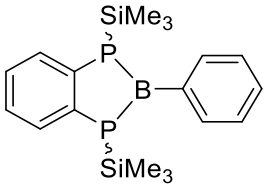

5.9

Figure 112*. The proposed silylated diphosphaborole, $C_6H_4P_2(SiMe_3)_2BPh$ (**5.9**).*

Attempts to methylate at phosphorus proceeded by reacting **[5.6].2[Li(THF)$_{1.5}$]** with two equivalents of MeI, however, in this instance a mixture of P-H containing species was observed around δ_P –124, these species being unisolable and short-lived; repeating this reaction with **[5.6].2[Li(TMEDA)]** resulted in the loss of all phosphorus resonances. Alternatively, the preparation of alkylphosphanes from silylated phosphane precursors have been reported to afford higher yields as a consequence of reduced side product formation.[273] Therefore, the proposed compound **5.9** was generated *in situ* and reacted with two equivalents of methyl iodide. However, again only the formation of 1,2-bis(phosphino)benzene was observed.

Moving to slightly longer alkanes than methyl, reactions with two equivalents of isopropyl bromide and **[5.6].2[Li(THF)$_{1.5}$]** were performed, initially resulting in two new broad resonances in the ^{31}P NMR spectrum at δ_P 95.6 and 6.7 respectively (**Figure 113**), which were no longer observed after exposure

to vacuum. Attempts to isolate this species by static-vacuum distillation led to the observation of two new doublets instead (**Figure 114**), both exhibiting a mutual coupling constant of 66 Hz. A singlet was observed at δ_{Li} 0.4 in the ^{7}Li NMR spectrum, consistent with LiBr formation.[274] Nevertheless, this species is unlikely to be compound **5.10** (**Scheme 40**), as if this product had formed the two phosphorus centres would presumably exhibit very similar chemical shifts or indeed be equivalent. This product was found to decompose over time and no molecular ion peak consistent with **5.10** was observed by mass spectrometry.

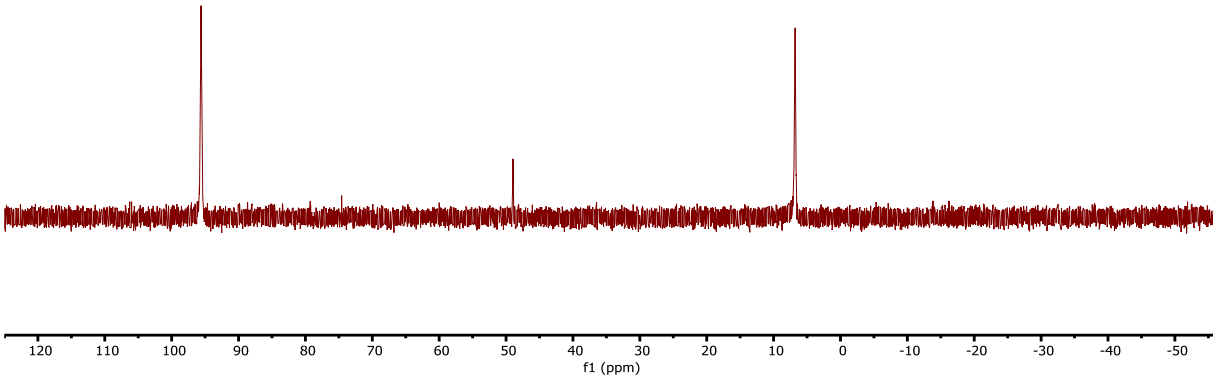

Figure 113. *$^{31}P\{^{1}H\}$ NMR (C_6D_6, 161.72 MHz) spectrum for the reaction of* ***[5.6].2[Li(THF)$_{1.5}$]*** *with ^{i}PrBr.*

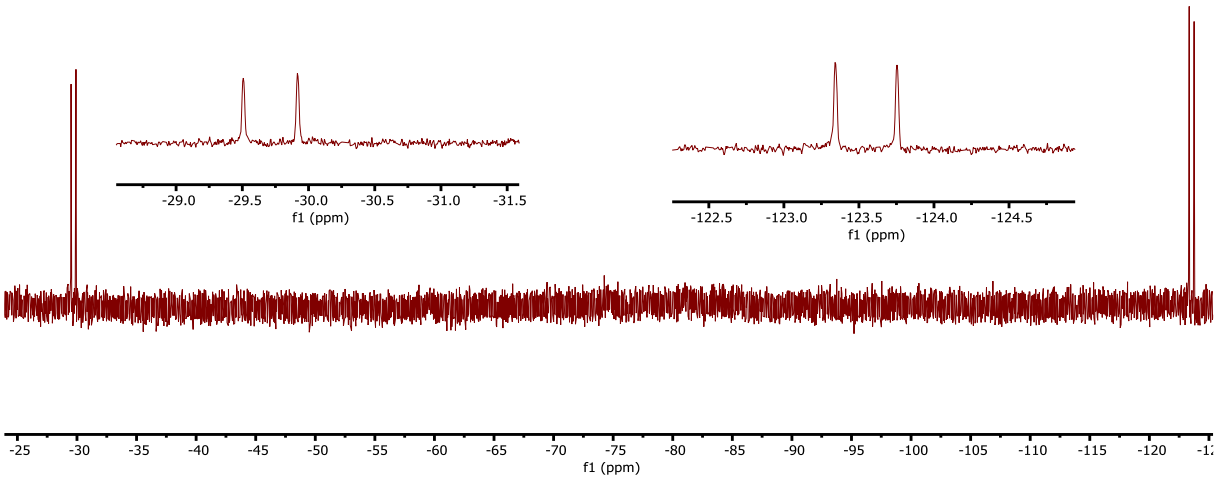

Figure 114. *$^{31}P\{^{1}H\}$ NMR (C_6D_6, 161.72 MHz) spectrum for the reaction of* ***[5.6].2[Li(THF)$_{1.5}$]*** *with ^{i}PrBr, after exposure to vacuum.*

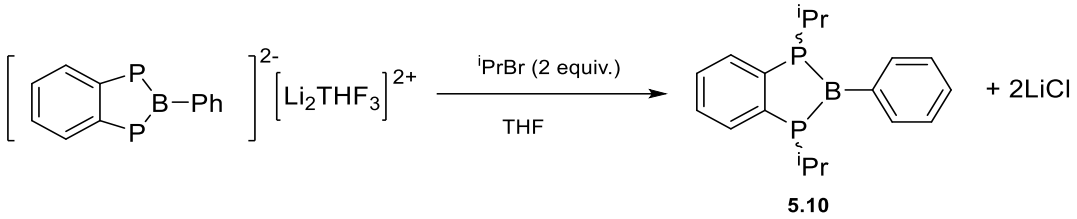

5.10

Scheme 40. *Reaction scheme and desired product from the reaction of* ***[5.6].2[Li(THF)$_{1.5}$]*** *and* ^{i}*PrBr.*

Repeating this reaction with **[5.6].2[Li(TMEDA)]** in place of **[5.6].2[Li(THF)$_{1.5}$]**, resulted in the observation of a multitude of resonances below −10 ppm in the $^{31}P\{^{1}H\}$ NMR spectrum, though higher order coupling was observed for the resonances at δ_P 53 and −0.7 (**Figure 115**). Efforts to isolate this species led to loss of all phosphorus resonances. Reactions were also performed with benzyl chloride which afforded two doublet resonances at δ_P −22 and −40 respectively, exhibiting a mutual coupling (J_{PP} = 120 Hz), though there were also multiple other signals present and attempts to purify this species led to the loss of all phosphorus resonances.

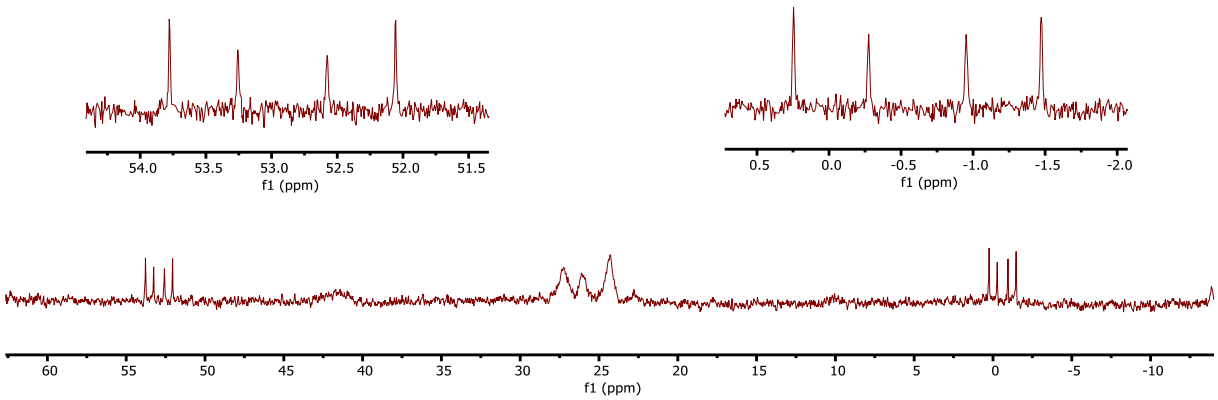

Figure 115. *$^{31}P\{^{1}H\}$ NMR (C_6D_6, 161.72 MHz) spectrum for the reaction of* ***[5.6].2[Li(TMEDA)]*** *with* ^{i}*PrBr.*

In an attempt to halogenate the phosphorus centres, compound **[5.6].2[Li(THF)$_{1.5}$]** was reacted with I_2 (**Scheme 41**), initially resulting in a higher order splitting pattern (**Figure 116**) reminiscent of that seen in **Figure 115**, though at a different chemical shift. The respective ^{11}B resonance has shifted to significantly lower frequency δ_B 27.8, relative to **[5.6].2[Li(THF)$_{1.5}$]** (δ_P 69.4) and the ^{7}Li NMR spectrum exhibits a single resonance at δ_{Li} −0.27, consistent with the formation of LiI.[275] Interestingly, leaving the reaction mixture for longer led to the loss of the higher order $^{31}P\{^{1}H\}$ resonances, which are

replaced by multiple new species, the major resonances being at δ_P 74.9 and δ_P −78.42, exhibiting a similar higher order splitting pattern (**Figure 117**).

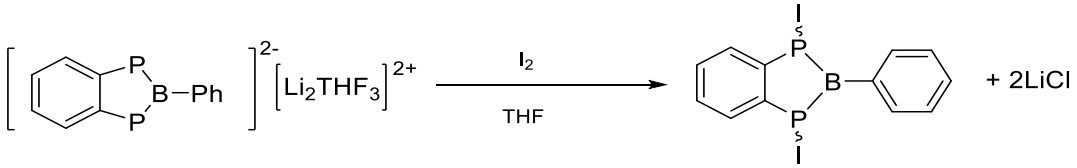

***Scheme 41**. Reaction between **[5.6].2[Li(THF)$_{1.5}$]** and I_2 and the desired product.*

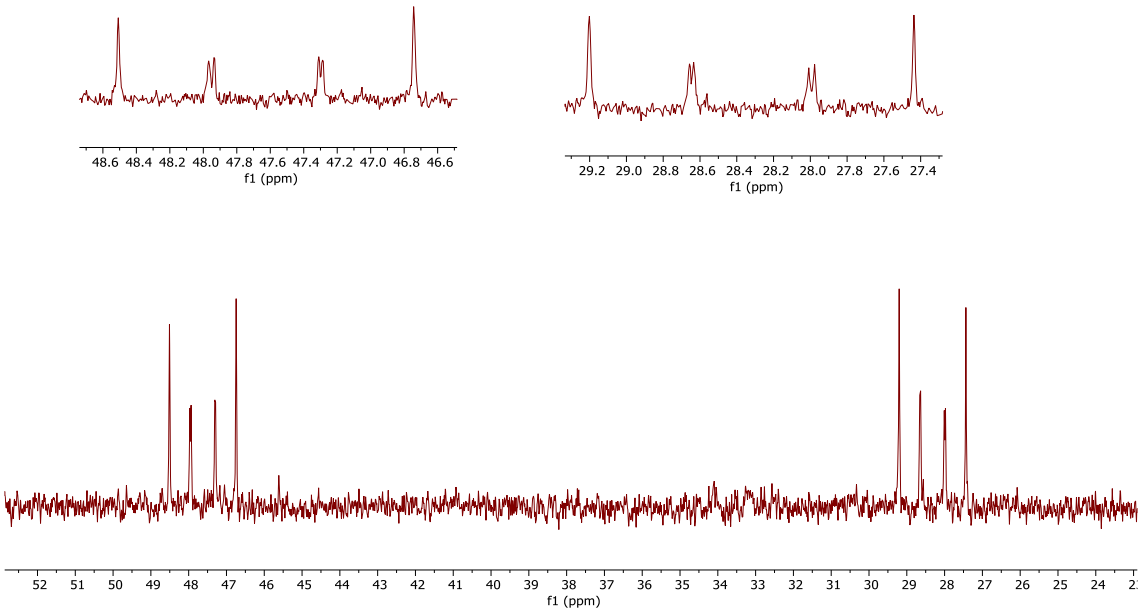

***Figure 116** .$^{31}P\{^1H\}$ NMR (C_6D_6, 161.72 MHz) spectrum for the reaction of **[5.6].2[Li(THF)$_{1.5}$]** with I_2.*

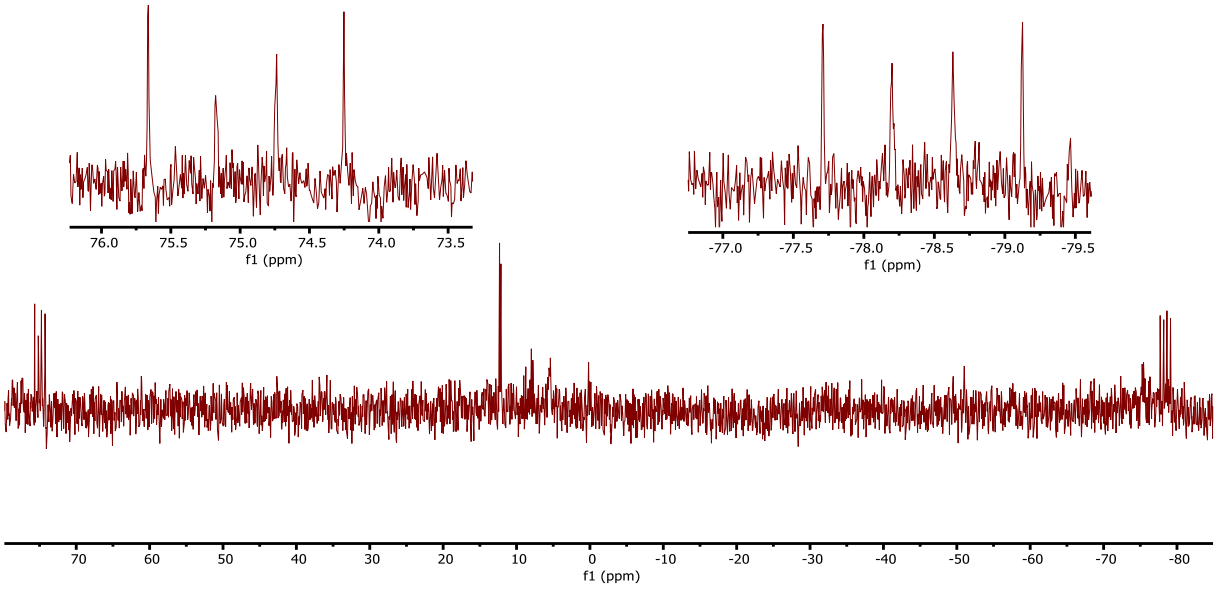

Figure 117. *$^{31}P\{^{1}H\}$ NMR (C_6D_6, 161.72 MHz) spectrum for the reaction of* ***[5.6].2[Li(THF)$_{1.5}$]*** *with I_2, longer reaction time.*

In efforts to bridge the two phosphorus centres, **[5.6].2[Li(THF)$_{1.5}$]** was reacted with $PhPCl_2$, however, only intractable mixtures were observed. Similar reactions with **[5.6].2[Li(TMEDA)]** and two equivalents of Ph_2PCl resulted in apparent decomposition as only the halophosphane starting material was observed in the ^{31}P NMR spectrum (δ_P 82).[276] Alternatively, reacting **[5.6].2[Li(THF)$_{1.5}$]** with Ph_2SnCl_2 resulted in a sharp singlet resonance in the ^{31}P NMR spectrum at δ_P −156 (**5.11**), exhibiting ^{119}Sn and ^{117}Sn satellites (I = ½, 8.59 %; I = ½, 7.68 % respectively; **Figure 118**) at significantly lower frequency relative to precedent triaryl and trialkyl stannyl phosphanes ([Me_3SnPPh_2]; δ_P −56.2, [Ph_3SnPPh_2]; δ_P −56.6).[277,278] Tin-phosphorus couplings of 705 Hz were observed, these being consistent with precedent $^{1}J_{SnP}$ coupling,[279,280] though a small trace component is observed as a doublet of doublets which is almost coincident with these satelites, the identify of which has not been established. The associated ^{119}Sn NMR spectrum, exhibits a corresponding signal to that of δ_P −156, supporting the formation of a P-Sn bond. The ^{1}H NMR spectrum of **5.11** exhibits eight broad features in the aromatic region, the smaller resonances integrating consistently for the benzo-fused and boron-bound phenyl group, a broad resonance is observed in the boron NMR spectrum at δ_B 77. The $^{13}C\{^{1}H\}$ NMR spectrum exhibits nine aromatic resonances, though the ipso carbon was unresolved. Compound **5.11** was isolated as a pale-yellow oil and attempts to crystallise this material were unsuccessful, similarly, mass spectrometric analyses were inconclusive. A small trace component is observed as a doublet of doublets which is almost coincident with these satellites, the identity of which has not been established.

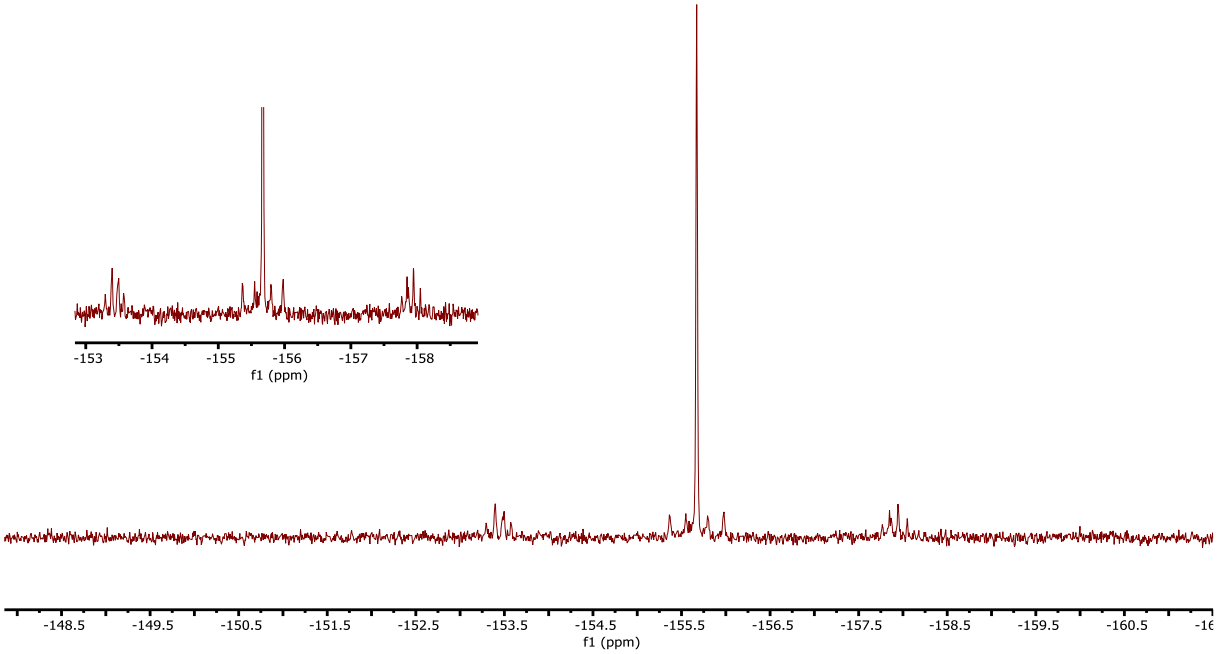

Figure 118. *$^{31}P\{^{1}H\}$ NMR (C_6D_6, 161.72 MHz) spectrum for the product from reaction* ***6.2[Li(THF)$_{1.5}$]*** *with Ph_2SnCl_2 (**5.11**).*

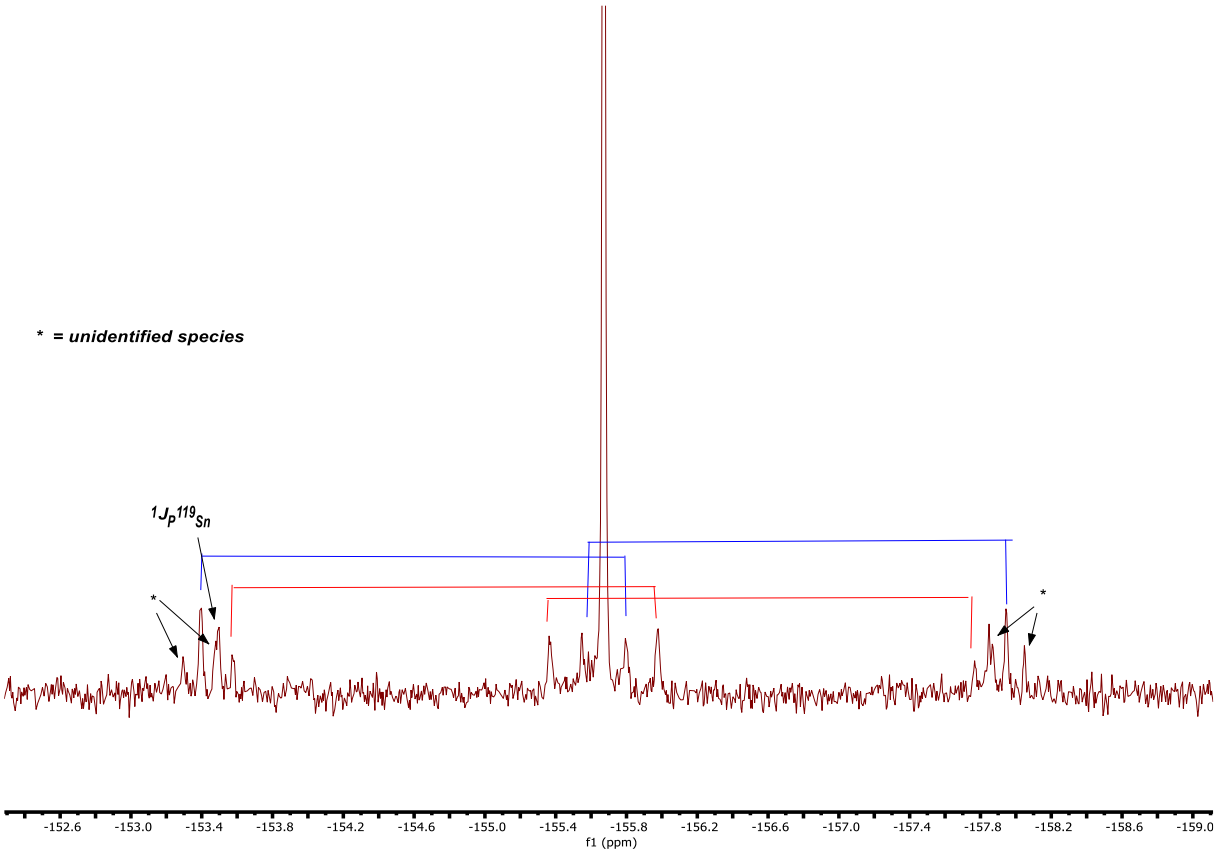

Figure 119*.$^{31}P\{^{1}H\}$ NMR (C_6D_6, 161.72 MHz) spectrum for the product from reaction* ***[5.6].2[Li(THF)$_{1.5}$]*** *with Ph_2SnCl_2 (**5.11**), satellites are overlapping with a trace impurity, exhibiting a doublet of doublets.*

In seeking similar systems to **5.11** and to try and prepare a solid, rather than an oil, comparable reactions were undertaken using $^{t}Bu_2SnCl_2$. However, in this instance the reaction was not as clean, the product exhibiting a multitude of P-H species; nevertheless, a resonance is observed at δ_P −118 which appears to display Sn satellites, the magnitude of which (J = 1004, 962 Hz) is much larger than observed for **5.11**. There is , however, some precedent for such large $^{1}J_{PSn}$ coupling, for example β-diketiminatotin(II) dicyclohexylphosphanide ($^{1}J_{PSn}$ = 949 Hz), diphenylphosphanide ($^{1}J_{PSn}$ = 978 Hz;)[281] [Ph*SnP(H)Trip] (Ph* = 2,6-(Trip)$_2C_6H_3$, Trip = 2,4,6-$^{i}Pr_3C_6H_2$; $^{1}J_{PSn}$ = 934 Hz) and [Trip$_2$Sn(F)P(H)Ar] (Ar = (2,4,6-$^{t}Bu_3C_6H_2$; $^{1}J_{PSn}$ = 995 Hz).[282,283] Similar reactions with two equivalents of $^{n}Bu_3SnCl$ show multiple species by $^{31}P\{^{1}H\}$ NMR, though notably there are doublets at δ_P −140 and −160, both exhibiting a coupling of 184 Hz, consistent with P-P interaction.[284] The aforementioned analyses were performed with the reaction mixture and removal of volatiles under reduced pressure resulted in the loss of some impurities (**Figure 120**), however, the desired species at δ_P −118 decomposed over time. In contrast, reacting **[5.6].2[Li(TMEDA)]** with Ph_2SnCl_2 resulted in resonances displaying a similar splitting pattern to those seen in reactions with I_2 and $^{i}PrBr$ (*vide supra*); reactions with $^{n}Bu_3SnCl$ and $SnCl_4$ resulted in the loss of all phosphorus resonances.

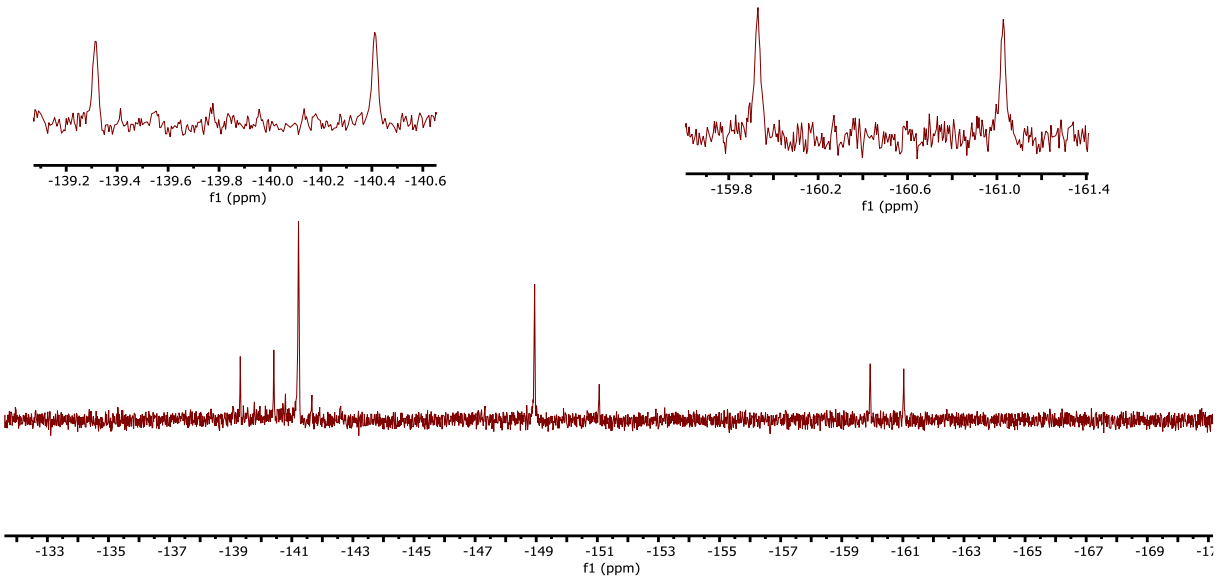

Figure 120. *$^{31}P\{^{1}H\}$ NMR (C_6D_6, 161.72 MHz) spectrum for the product from the reaction of **[5.6].2[Li(THF)$_{1.5}$]** with $^{n}Bu_3SnCl$ after removal of volatiles.*

Looking to heavier group 14 elements, **[5.6].2[Li(THF)$_{1.5}$]** was reacted with $PbCl_2$, resulting in the observation of a broad resonance at δ_P 82 ($w_{1/2}$ = 11 Hz; **Figure 121**), with no apparent ^{209}Pb satellites ($^{1}J_{PPb}$ (212-470 Hz),[285] $^{2}J_{PPb}$ (69 Hz)).[286] The aromatic region of the ^{1}H NMR spectrum only displayed extremely broad resonances (7.8-6.6 ppm) and attempts to isolate this species only led to

decomposition. Repeating the reaction with **[5.6].2[LiTMEDA]** resulted in the loss of all phosphorus resonances.

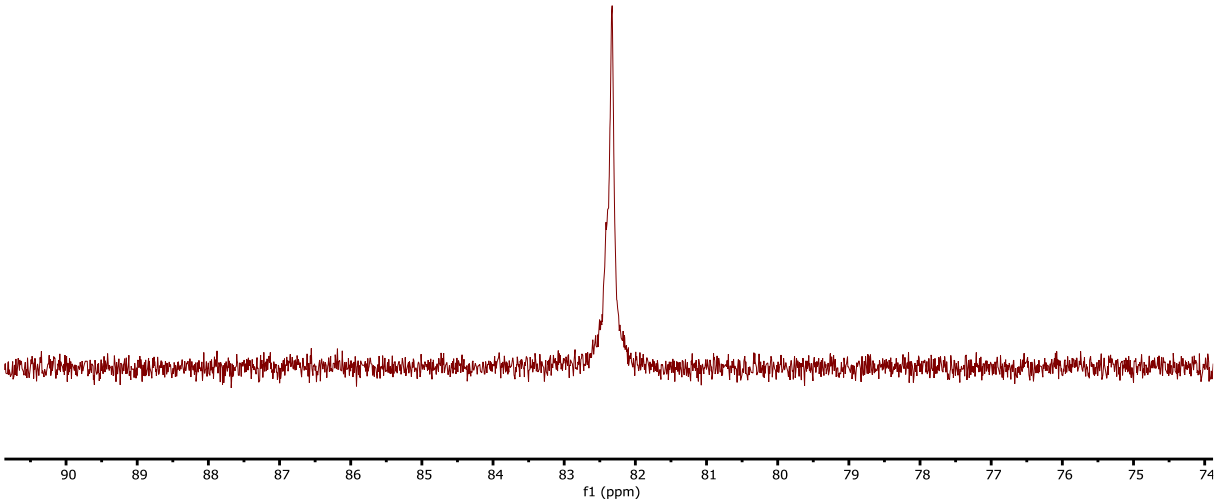

Figure 121. *$^{31}P\{^{1}H\}$ NMR (C_6D_6, 161.72 MHz) spectrum for the product from the reaction of* ***[5.6].2[Li(THF)$_{1.5}$]*** *with $PbCl_2$.*

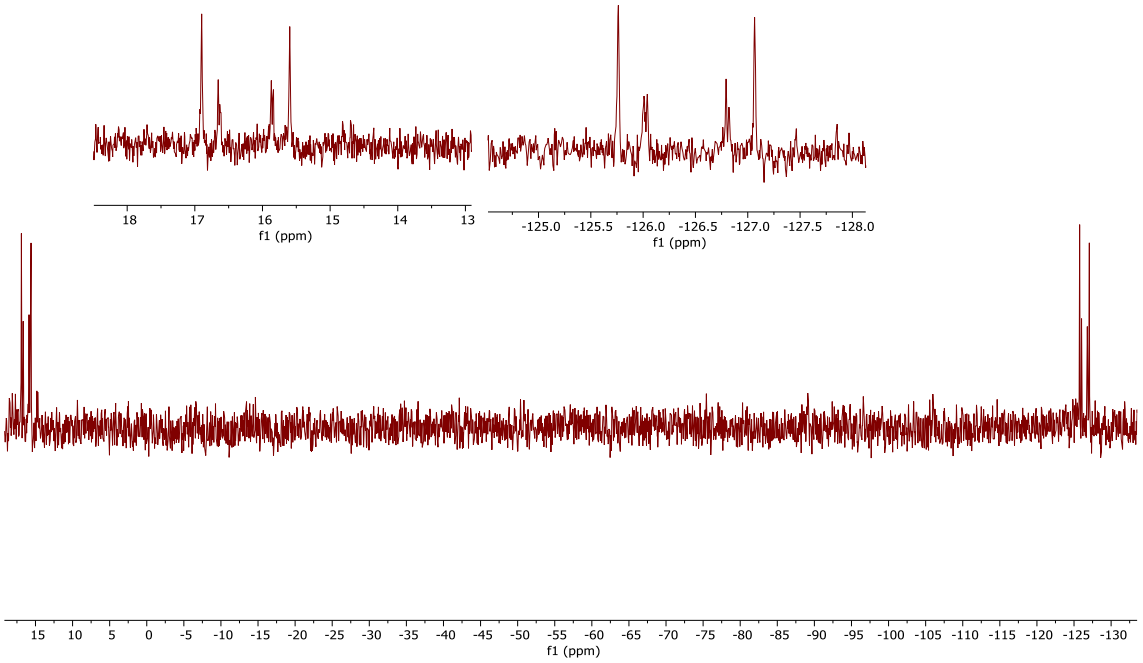

Figure 122. *$^{31}P\{^{1}H\}$ NMR (C_6D_6, 161.72 MHz) spectrum for the product from reaction of* ***[5.6].2[Li(TMEDA)]*** *with Ph_2SnCl_2.*

5.6.2 π-Coordination of $[C_6H_4P_2BC_6H_5]^{2-}$

To investigate **[5.6]$^{2-}$** as a potential π-ligand, reactions were performed with a series of different metal complexes. Reactions with either **[5.6].2[Li(THF)$_{1.5}$]** or **[5.6].2[Li(TMEDA)]** with Cp_2ZrCl_2, resulted in a

blue colouration and a new ^{31}P resonance (δ_P 81.6, **Figure 123**), to higher frequency than the starting materials and which could be consistent with metal coordination; the blue colouration could also suggest reduction of the metal as Zr(III) species are known to be blue, though they are also paramagnetic.[287] Attempts to remove solvent from this product resulted in an oily film, which exhibited a phosphorus resonance consistent with 1,2-bis(phosphino)benzene, with no evidence for the apparent metal complex.

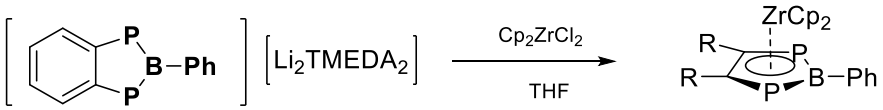

***Scheme 42**.Reaction between **[5.6].2[Li(THF)$_{1.5}$]** or **[5.6].2[Li(TMEDA)]** and Cp_2ZrCl_2.*

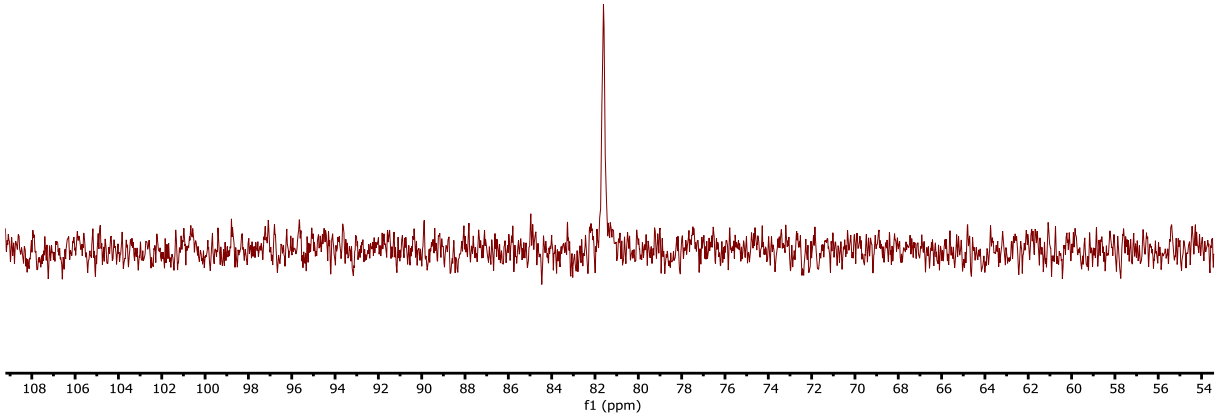

***Figure 123.** $^{31}P\{^1H\}$ NMR (C_6D_6, 161.72 MHz) spectrum for the product from the reaction of **[5.6].2[Li(THF)$_{1.5}$]** with Cp_2ZrCl_2.*

Similar reactions were performed with [Cp(Ph_2N)ZrCl], with no reaction initially observed with **[5.6].2[Li(THF)$_{1.5}$]**, while after a few days only intractable mixtures were visible by ^{31}P NMR spectroscopy. Alternatively, reacting **[5.6].2[Li(TMEDA)]** with two equivalents of [Cp(Ph_2N)ZrCl] (**Scheme 43**) resulted in a single resonance at δ_P 97.3 (**Figure 124**), reminiscent of Lappert's complex, [Cp''$_2$Zr{P(Ph)C_6H_4PPh}] (Cp'' = $C_5H_3(SiMe_3)_2$; δ_P 105).[255] In the associated ^{11}B NMR spectrum only a singlet resonance was observed (δ −17), which correlates with an impurity occasionally encountered in samples of **[5.6].2[Li(TMEDA)]**, which would seem to suggest the loss of boron from the ring. Attempts to elucidate the identity of this species via mass-spectrometry or indeed by the growth of single crystals were both unsuccessful. Similarly, reacting **[5.6].2[Li(THF)$_{1.5}$]** or **[5.6].2[Li(TMEDA)]** with ZrI_4 or $ZrCl_4$ resulted in the loss of all phosphorus resonances and the observation of 1,2-bis(phosphino)benzene.

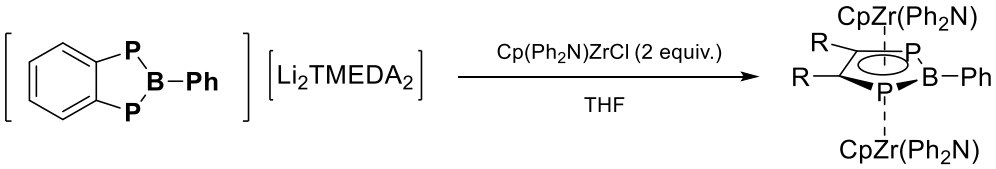

***Scheme 43**. Reaction between **5.6].2[Li(TMEDA)]** and Cp(Ph$_2$N)ZrCl and the desired product.*

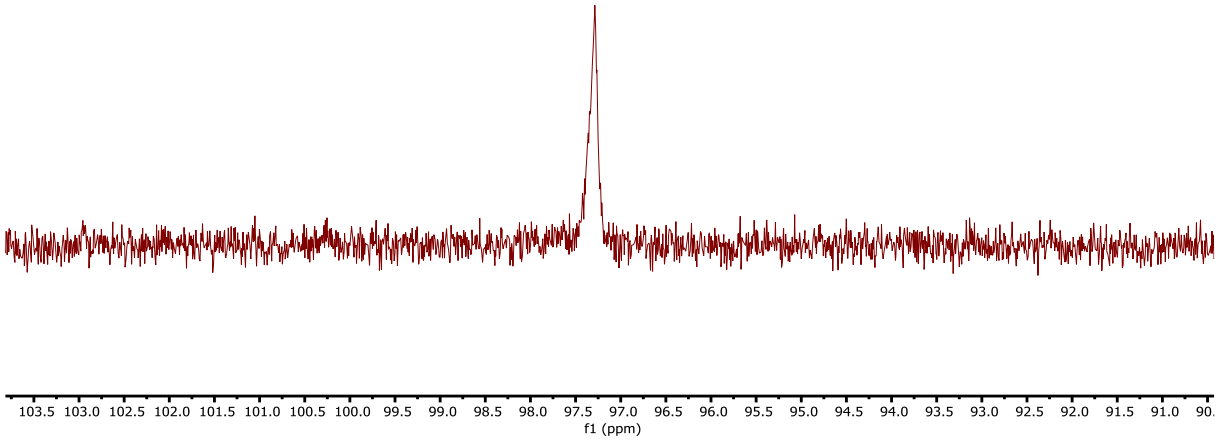

***Figure 124.** $^{31}P\{^1H\}$ NMR (C_6D_6, 161.72 MHz) spectrum for the product from the reaction of **[5.6].2[Li(TMEDA)]** with Cp(Ph$_2$N)ZrCl.*

Cyclopentadienyl iron complexes have previously been used to coordinate monoanionic diphospholides in an η^5 arrangement ([(η^5-$P_2C_3H_3$)Fe(η^5-C_5H_5)]),[288,289] therefore, reacting **[5.6].2[Li(THF)$_{1.5}$]** or **[5.6].2[Li(TMEDA)]** with two equivalents of [(CpFe(benzene)][PF_6] to sandwich the diphosphaboracycle between two iron centres seemed a logical target. In both cases a new resonance was observed at δ_P −35.7 as well as the characteristic PF_6^- resonance at δ_P −144 (**Figure 125**).[290] The associated $^{11}B\{^1H\}$ NMR spectrum exhibits two broad resonances at δ_B 29.5 and 23.7 (**Figure 126**), suggesting multiple products have formed, the resonances being observed in the lower region of 3 coordinate boron species.[291] Solvent removal results in a pale brown solid, however, the compound instantly starts to decompose to a black solid. Similarly, attempts to purify this product by growing crystals, extraction, washing or trituration resulted only in the observation of $LiPF_6$ by X-Ray diffraction or ^{31}P NMR (**Figure 127**).

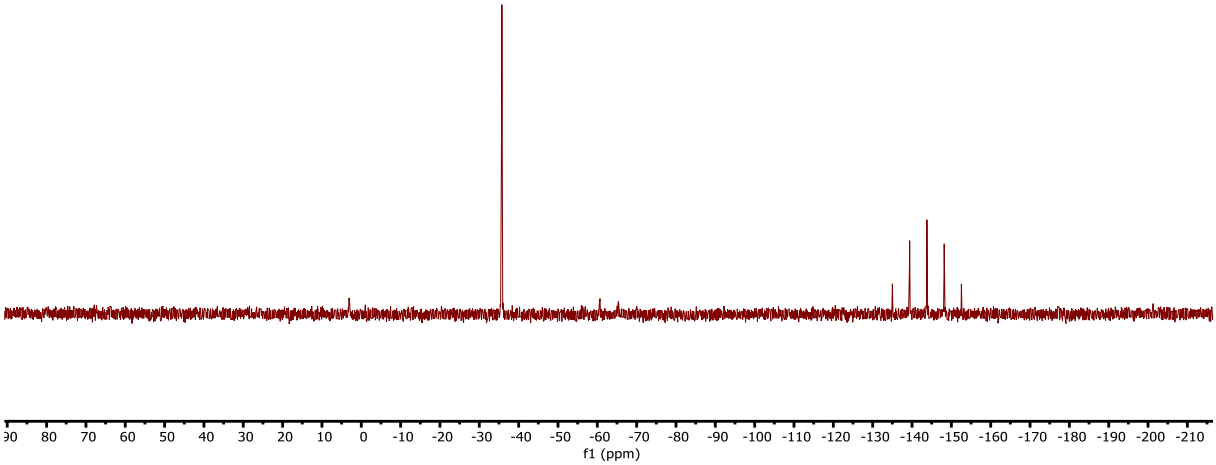

Figure 125. *$^{31}P\{^{1}H\}$ NMR (C_6D_6, 161.72 MHz) spectrum for the product from the reaction of compound* ***[5.6].2[Li(THF)$_{1.5}$]*** *with [CpFe(benzene)][PF_6].*

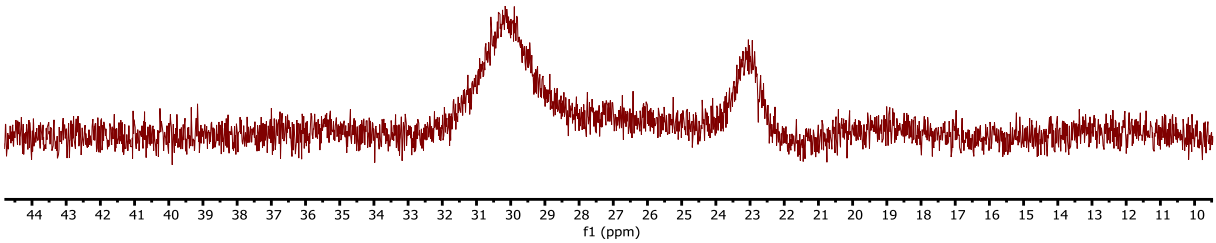

Figure 126. *$^{11}B\{^{1}H\}$ NMR (C_6D_6, 160.4 MHz) spectrum for the product from the reaction of compound* ***[5.6].2[Li(THF)$_{1.5}$]*** *with [CpFe(benzene)][PF_6].*

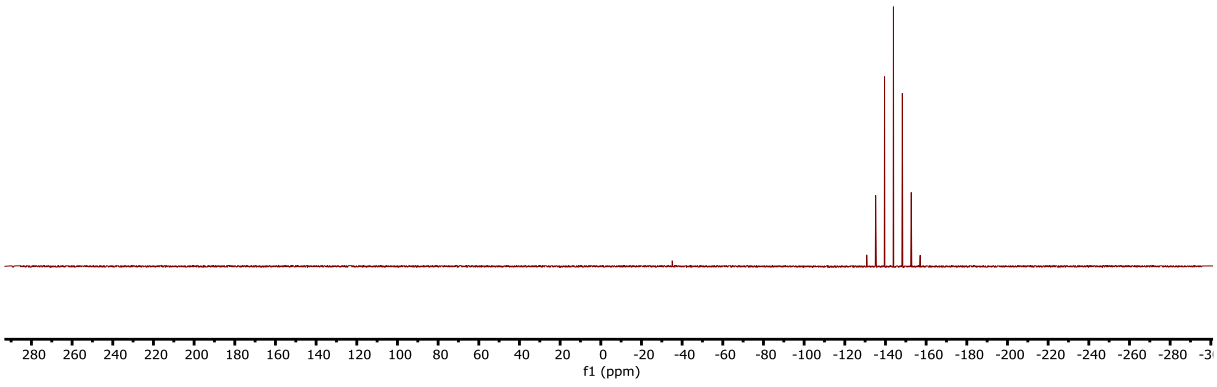

Figure 127. *$^{31}P\{^{1}H\}$ NMR (C_6D_6, 161.72 MHz) spectrum from the attempted purification of the reaction of the product from reacting* ***[5.6].2[Li(THF)$_{1.5}$]*** *with [CpFe(benzene)][PF_6].*

A range of ruthenium complexes were reacted with **[5.6].2[Li(THF)$_{1.5}$]** or **[5.6].2[Li(TMEDA)]**, including $CpRu(PPh_3)_2Cl$, CpRu(dppe)Cl or $Ru(CO)(PCy_3)_2Cl$. However, these reactions all resulted in the recovery

of the ruthenium starting material. In contrast, reactions with $[Rh(COD)Cl]_2$, AuCl(tht), $AuCl(PPh_3)$, CuI or $(PPh_3)_2PtCl_2$ resulted in intractable mixtures suggesting complete decomposition of both species. Similarly, reactions between $Rh(Ph)Cl_2(PPh_3)_2$[292] and **[5.6].2[Li(THF)$_{1.5}$]** or **[5.6].2[Li(TMEDA)]**, resulted in the observation of multiple doublets in the $^{31}P\{^1H\}$ NMR spectrum alongside that for free PPh_3 (δ_P −5; **Figure 128**).[293] In the associated ^7Li NMR spectrum, a singlet resonance is observed at δ_{Li} 0.6 and notably no boron resonance was observed in the ^{11}B NMR spectrum. After five hours only the doublet at δ_P 31.7 and δ_P 21, alongside free PPh_3 were present (**Figure 129**). The removal of volatiles resulted only in the observation of the doublet at δ_P 31.7 and free PPh_3, attempts to purify this species and elucidate the structure through crystal growth were unsuccessful.

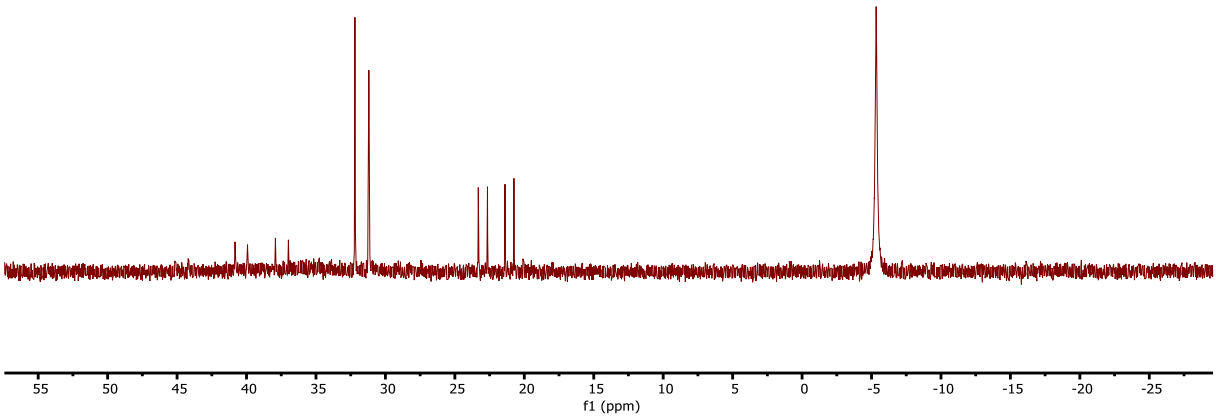

Figure 128. *$^{31}P\{^1H\}$ NMR (C_6D_6, 161.72 MHz) spectrum from the reaction of* ***[5.6].2[Li(THF)$_{1.5}$]*** *with $Rh(Ph)Cl_2(PPh_3)_2$.*

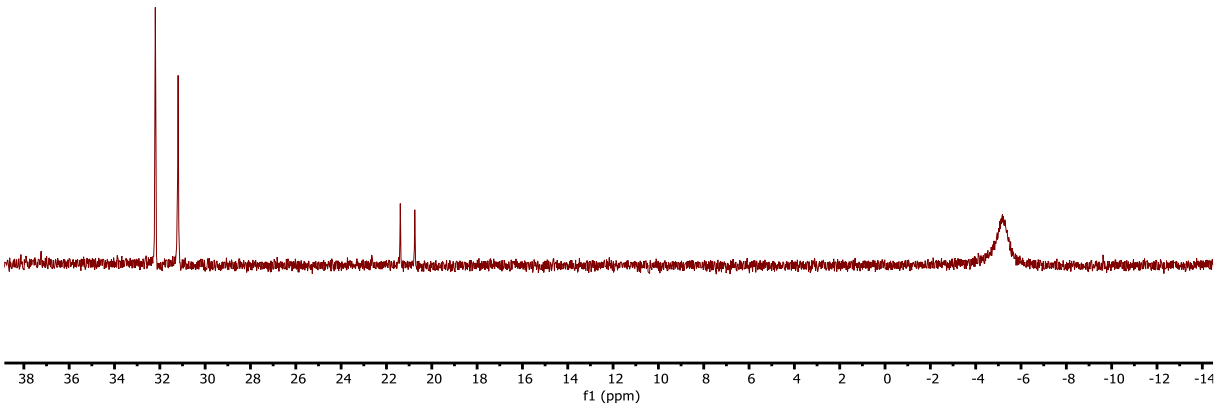

Figure 129. *$^{31}P\{^1H\}$ NMR (C_6D_6, 161.72 MHz) spectrum from the reaction of* ***[5.6].2[Li(THF)$_{1.5}$]*** *with $Rh(Ph)Cl_2(PPh_3)_2$ after a few hours.*

Reactions with two equivalents of Vaska's complex, [IrCl(CO)[PPh_3)$_2$], and **[5.6].2[Li(THF)$_{1.5}$]**, resulted in a new species, the ^{31}P NMR spectrum of which exhibiting six resonances (**Figure 131**); the same resonances are observed from the reaction with **[5.6].2[Li(TMEDA)]**. The ^{11}B NMR spectrum displays a single broad resonance at δ_B 25.3, at significantly lower frequency relative to **[5.6].2[Li(THF)$_{1.5}$]**, though still suggestive of a three-coordinate boron centre and only one boron containing species in solution.[291]

Attempts to elucidate the number of species present in the ^{31}P NMR spectrum by ^{1}H-^{13}C HMBC, HSQC and ^{1}H-^{31}P COSY were inconclusive due to the significant overlap in the aromatic regions of both the ^{1}H and ^{13}C{^{1}H} NMR spectra. However, the six phosphorus resonances observed in the ^{31}P NMR spectrum (**Figure 131**) integrate consistently for six different environments (1:1:1:1:1:1), thus reasonably excluding the formation of product **5.12** or **5.13** (**Figure 130**), as they would presumably exhibit two phosphorus environments if P-Ir-P were aligned perfectly or three environments if they aligned in the plane; this would also result in significantly larger coupling due to *trans*-$^{2}J_{PP}$ interaction.[294] In comparison, there would presumably be six phosphorus environments for **5.14**, though this would depend on the orientation.

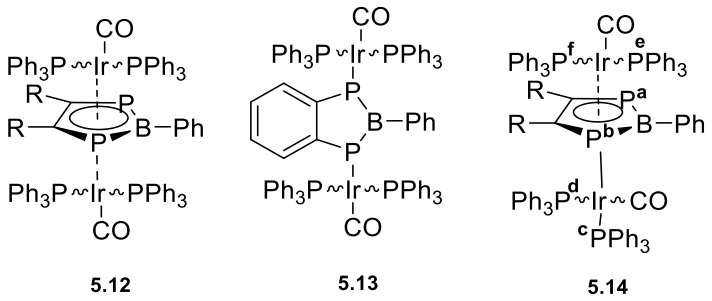

Figure 130. *Potential products from the reaction of* ***[5.6].2[Li(THF)$_{1.5}$]*** *with Vaska's complex.*

The highest frequency resonance, δ_P 23, appears to be coupling to three phosphorus centres resulting in a triplet of doublets, the 1:2:1 ratio of the triplet base is reminiscent of an overlapping doublet of doublet of doublets suggesting that two of the coupled centres are similar, whilst one is slightly different (J = 27Hz, 8 Hz), the magnitude of coupling is consistent with $^{2}J_{pp}$ coupling.[294,295] If **5.14** has formed, this resonance is presumably associated with **P^{a}**, the only centre able to experience three $^{2}J_{pp}$ couplings, two being similar (**P^{e}** and **P^{f}**) and one different (**P^{b}**). The resonance at δ_P 16 exhibits a doublet of doublets multiplicity, exhibiting $^{2}J_{PP}$ (200 Hz and 28 Hz) consistent with coupling both *cis*- and *trans*- across the metal, therefore if **5.14** is the product this signal would be associarted with **P^{c}**, exhibiting a

trans-$^2J_{PP}$ coupling with $\mathbf{P^b}$ and *cis*-$^2J_{PP}$ coupling with $\mathbf{P^d}$. Although the resonances at δ_P 9 and −80.6 are significantly broad ($w_{1/2}$ = 53 Hz, 72 Hz respectively) mutual coupling is observed, the magnitude of which is consistent with *trans*-$^2J_{PP}$ coupling (170 Hz), therefore these resonances would be associated with $\mathbf{P^e}$ and $\mathbf{P^f}$, if **5.14** has formed. At δ_P 6 a broad multiplet is observed ($w_{1/2}$ = 47 Hz), though no coupling can be resolved, this resonance could feasibly be $\mathbf{P^b}$ as mutual coupling with $\mathbf{P^c}$ (*trans*-$^2J_{PP}$ = 200 Hz) has not been observed and the poor resolution of the $\mathbf{P^b}$ resonance could be a reasonable explanation, if **5.14** is the product. Finally, the resonance at δ_P −66 exhibits a doublet of doublets multiplicity (28 Hz, 11 Hz), consistent with coupling to two phosphorus centres, the coupling of which suggests they are in notably different environments and therefore could be $\mathbf{P^d}$, experiencing cis-coupling with both $\mathbf{P^c}$ (28 Hz) and $\mathbf{P^b}$. Based on the spectroscopic data it is reasonable to propose that compound **5.14** or a similar structure could have formed, resonances being generally consistent for $\mathbf{P^a}$-$\mathbf{P^f}$. Attempts to elucidate this structure through mass spectrometry and X-Ray diffraction were unsuccessful.

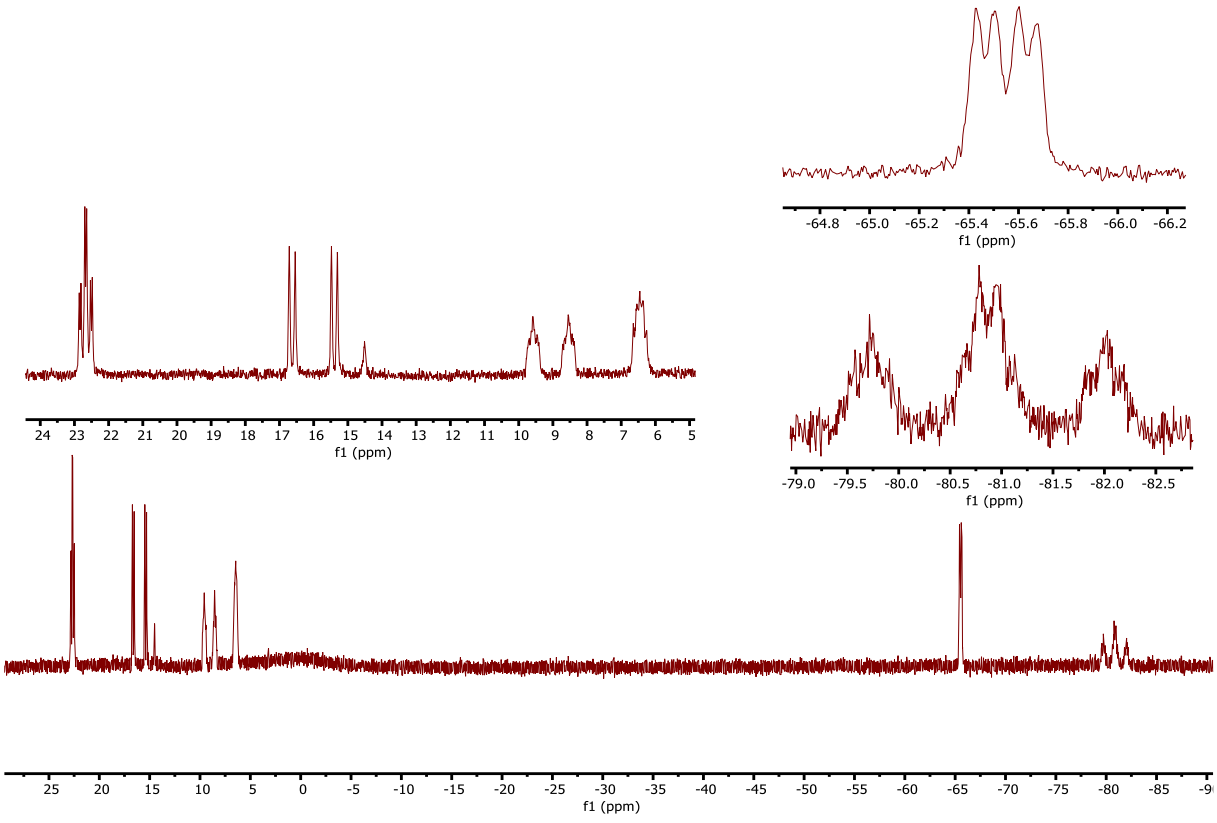

Figure 131. *$^{31}P\{^1H\}$ NMR (C_6D_6, 161.72 MHz) spectrum from the reaction of* ***[5.6].2[Li(THF)$_{1.5}$]*** *with Vaska's complex.*

5.6.3 Reactivity of $[C_6H_4P_2BC_6H_5]^{2-}$ $2[LiTHF_{1.5}]^{2+}$ and $[Mo(NCEt)_3(CO)_3]$

Molybdenum tricarbonyl complexes, $[Mo(L)_3(CO)_3]$ (L = labile organic fragment), are often used as precursors to π-arene complexes under mild conditions.[296] Moreover, reactions between $[Mo(NCEt)_3(CO)_3]$ and 2,4,6-tritertiarybutyl-1,3,5-triphosphabenzene result in the η^6-coordination of $Mo(CO)_3$.[297] Inspired by this, reactions were performed with compound **[5.6].2[Li(TMEDA)]** and $[Mo(NCEt)_3(CO)_3]$ (**Scheme 44**), resulting in a shift in the ^{31}P NMR resonance to δ_P 8.1 ($\Delta\delta_P$ = –44), which is consistent with Mo-coordination. The ^7Li NMR spectrum exhibits a resonance at δ_{Li} 0.31 and resonances associated with TMEDA and the aromatic fragments were observed, suggesting the phosphaboracyclic core is intact and both lithium and TMEDA are associated with the complex. Upon exposure to vacuum this species decomposes. However, layering the reaction mixture (C_6D_6/THF) with hexanes resulted in the growth of yellow crystals, the X-Ray diffraction study of which confirmed η^5-coordination of Mo to the diphosphaboracyclic core, with further coordination of Mo fragments to each phosphorus lone pair (**5.15**; **Figure 133**; **Table 22**).

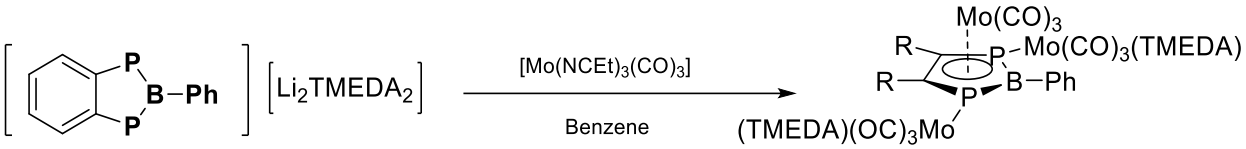

***Scheme 44**. Reaction performed to prepare compound **5.15**, from **[5.6].2[Li(TMEDA)]** and $[Mo(NCEt)_3(CO)_3]$.*

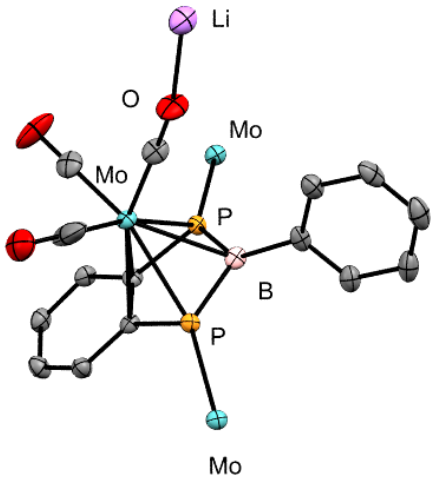

***Figure 132**. Molecular structure of the diphosphaboracycle core of compound **5.15**; displacement ellipsoids at the 50% probability level. Hydrogen atoms and extended ligation omitted for clarity. The molybdenum atoms coordinated in an η^1-arrangement, also have ligated three carbonyl functionalities and a TMEDA unit.*

Table 22. *Selected bond lengths (Å) and angles (°) for compound* ***5.15****, with estimated standard parentheses.*

			Bond Length (Å)				
P1-B1	*1.874(7)*	*Mo1-B1*	*2.578(7)*	*B1-C7*	*1.584(9)*	*C13-O1*	*1.225(14)*
P2-B1	*1.859(7)*	*Mo1-C1*	*2.535(6)*	*Mo3-P1*	*2.6108(16)*	*C14-O3*	*1.188(9)*
P1-C1	*1.802(6)*	*Mo1-C2*	*2.494(6)*	*Mo2-P2*	*2.6203(15)*	*O3-Li1*	*1.912(15)*
P2-C2	*1.807(6)*	*Mo1-C13*	*1.954(9)*	*Mo1-P1*	*2.6397(16)*	*Li1-O4*	*1.937(14)*
C1-C2	*1.433(8)*	*Mo1-C14*	*1.894(7)*	*Mo1-P2*	*2.6211(15)*	*Mo2-N1*	*2.355(6)*
			Bond Angle (°)				
P1-B1-P2	*42.08(16)*	*Mo3-P1-Mo1*	*145.59(6)*	*C1-P1-B1*	*97.0(3)*	*C14-O3-Li1*	*154.6(7)*
P1-C1-C2	*116.8(4)*	*Mo3-P1-B1*	*135.15(7)*	*C2-P2-B1*	*96.8(3)*	*O3-Li1-O4*	*118.9(7)*
P2-C2-C1	*117.7(4)*	*C13-Mo1-C14*	*86.2(4)*	*C1-Mo1-C2*	*33.11(19)*	*O3-Li1-O5*	*112.3(7)*
P1-Mo1-B1	*42.08(16)*	*Mo1-C13-O1*	*160.7(12)*	*C7-B1-P1*	*121.7(5)*	*O3-Li1-O6*	*110.9(8)*
P1-Mo1-P2	*71.88(5)*	*Mo1-C14-O3*	*177.6(6)*	*C7-B1-P2*	*126.5(5)*	*N1-Mo2-N2*	*77.8(2)*

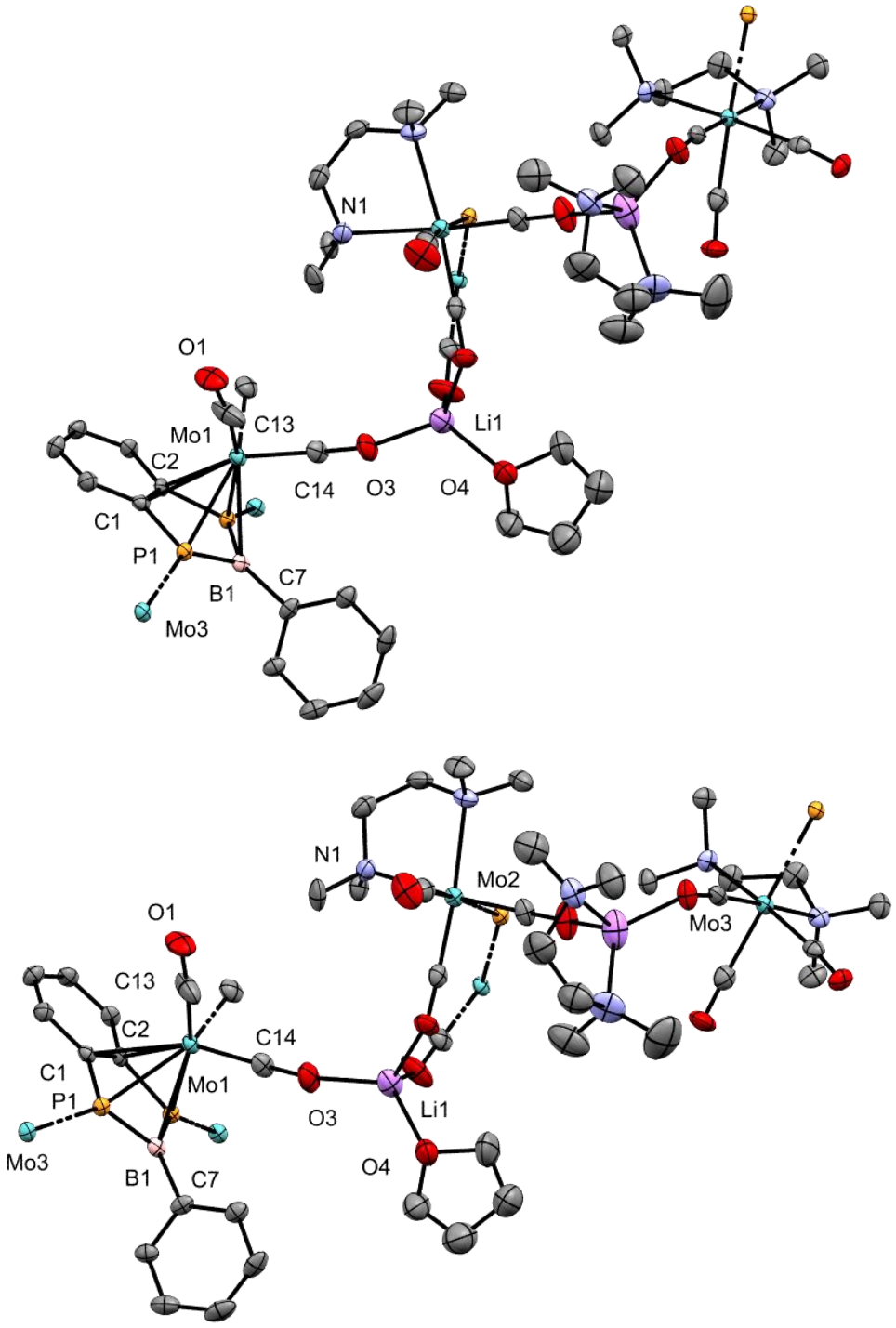

Figure 133. *Molecular structure of compound* ***5.15****; displacement ellipsoids at the 50% probability level. Hydrogen atoms omitted for clarity, the third carbonyl oxygen is present but not included in the asymmetric unit.*

Compound **5.15** adopts a polymeric structure in the solid state, where one Mo is bound η^5 to the P_2BC_2 ring, with each phosphorus centre also being coordinated to an additional Mo centre, stabilised by a TMEDA molecule which has transferred from lithium; the lithium atom is associated with the carbonyl moieties and a THF molecule, bridging the molybdenum units. The bond lengths about the

diphosphacyclic core are comparable to compound **[5.6].2[Li(TMEDA)]**, similarly both of the P-Mo bond distances are consistent with a dative bond, comparable with that observed for 2,4,6-tritertiarybutyl-1,3,5-triphosphabenzene (2.5772(9) Å)[297]. This structure confirms that the diphosphaboracycle can act as a π-ligand with metals other than lithium.

5.6.4 Reactivity Studies with Actinides and Lanthanides

The f-block elements are known to exhibit notably different reactivity to transition metals, bearing a preference for more electronegative elements,[298] therefore, to explore the potential of **5.6** as a ligand for the f-block, **[5.6].2[Li(THF)$_{1.5}$]** and **[5.6].2[Li(TMEDA)]** were initially reacted with Cp^{ttt}Y(BH$_4$)$_2$(THF), yttrium being commonly used as a diamagnetic analogue of the lanthanides. These reactions resulted in broad singlet resonances at δ_P 44.8 and 50.5, respectively, with a broad resonance also observed in the ^{11}B NMR spectra at δ_B –26, at somewhat lower frequency relative to the starting material (δ_B –22); interestingly from the reaction with **[5.6].2[Li(TMEDA)]** there is also a boron resonance consistent with [Li][BH$_4$] (δ_B –40).[299] Only very broad resonances are observed in the ^{1}H NMR spectrum, impeding analysis, though coordination could have occurred. The removal of solvent resulted in the loss of all phosphorus resonances.

Reactions were then performed with Cp*SmBPh$_4$, generated from Cp*$_2$Sm,[300] the product from which exhibits only three resonances in the ^{1}H NMR alongside signals associated with TMEDA; the former resonances integrate consistently for the Cp* and BPh$_4$ groups. The ^{31}P{^{1}H} NMR spectrum exhibits a singlet resonance at δ_P 48.9 (**Figure 134**), however, much-like many of the transition metal complexes formed, this species was only observed *in-situ* and attempts to isolate it resulted in the loss of the phosphorus resonance. Similarly, only [Li(THF)$_4$][BPh$_4$] was observed by X-Ray diffraction, though this does suggest a reaction occurred between Cp*SmBPh$_4$ and **[5.6].2[Li(THF)$_{1.5}$]**, albeit the other products could not be definitely identified.

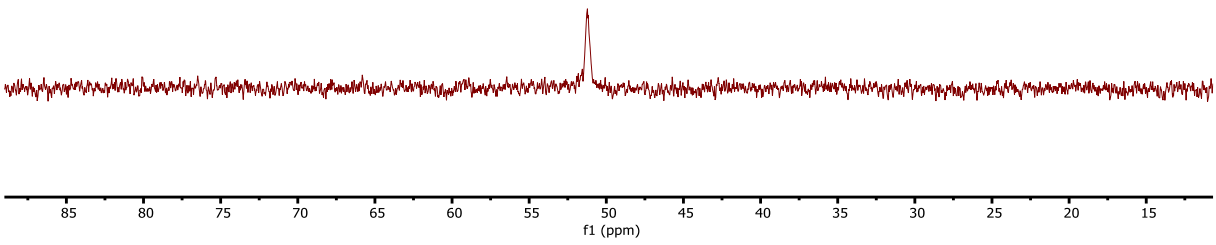

Figure 134. *^{31}P{^{1}H} NMR (C$_6$D$_6$, 161.72 MHz) spectrum from the reaction of* ***[5.6].2[Li(THF)$_3$]*** *with Cp*SmBPh$_4$.*

Finally, given the range of oxidation states observed for uranium,[301] complexes with **[5.6]$^{2-}$** seemed a logical target. Reacting compounds **[5.6].2[Li(THF)$_{1.5}$]** or **[5.6].2[Li(TMEDA)]** with UCl_4 (e.g. **Scheme 45**), initially resulted in a light brown coloured solution; the ^{1}H NMR spectrum for the reaction with **[5.6].2[Li(THF)$_{1.5}$]** displays a broad resonance across the aromatic region (δ_H 9.7-8.2). Alternatively, the reaction with **[5.6].2[Li(TMEDA)]** resulted in three aromatic signals as well as resonances associated with TMEDA, though a phosphorus resonance was not found. Shortly after mixing the two reagents together a green precipitate formed which was no longer soluble in common solvents and has defied further analysis and appears to be a common decomposition pathway associated with uranium systems.[302]

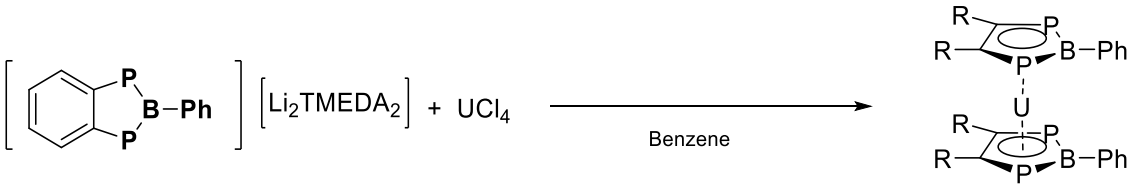

***Scheme 45**. Reaction between **[5.6]. 2[Li(TMEDA)]** and UCl_4, along with the desired product.*

5.7 Summary

The first dianionic diphosphaboracycles, **[5.6].2[Li(THF)$_{1.5}$]** and **[5.6].2[Li(TMEDA)]** have been synthesised and characterised by heteronuclear NMR spectroscopy and unequivocally confirmed by X-Ray diffraction, the latter confirming their polymeric and monomeric structures, respectively. NICS calculations suggest the diphosphaboracycles exhibit aromatic character, though are somewhat less aromatic than benzene and the hypothetical $BP_2C_2H_3$ and $BC_2P_2H_3^{2-}$ species.[251]

The reactivity of the diphosphaboracycles with main-group, transition-metal and f-block elements was explored, leading to the *in situ* observation of multiple new species. Attempts to isolate these species, generally resulted in the reformation of 1,2-bis(phosphino)benzene or decomposition, therefore, the redox chemistry of **[5.6].[Li(TMEDA)]$_2$** was investigated, exhibiting a distinctive irreversible oxidative event at E_{pc} = –0.755 V relative to the Fc/Fc^+ couple, which suggests **[5.6].2[Li(TMEDA)]** is appreciably reducing, though this should not prohibit coordination to all metal centres.

Reacting **[5.6].2[Li(TMEDA)]** with $[Mo(NCEt)_3(CO)_3]$ afforded complex **5.15,** in which the dianionic charge of the diphosphaboracyclic ring is stabilised by the incorporation of lithium in the structure, bridging the respective Mo-CO units and resulting in a polymeric network; this structure unequivocally proves the diphosphaboracycle can act as a π-ligand.

Chapter 6 – Experimental

“Po-tay-toes! Boil ‘em, mash ‘em, stick ‘em in a stew.”

--The Lord of the Rings: The Two Towers (2002)

General Considerations

Unless otherwise stated all materials were prepared and handled under an inert Ar atmosphere on a dual manifold Schlenk line or under catalytically purified dry-nitrogen or dry-argon in an MBraun glovebox. Solvents were distilled under dinitrogen from potassium (THF, toluene, benzene, 1,4-dioxane, DME), sodium-potassium alloy (pentane, hexane, Et_2O) or CaH_2 (DCM), degassed and stored under argon over molecular sieves (diethyl ether, THF, 1,4-dioxane, benzene and DCM) or potassium mirrors (pentane, hexane and toluene). Deuterated solvent for NMR spectroscopy were purchased from Goss Scientific (Cambridge) or Sigma Aldrich, degassed using the freeze-pump-thaw method and heated under reflux over calcium hydride ($CDCl_3$, CD_2Cl_2) or potassium (d_8-THF, C_6D_6) for 3 days, then transferred to Youngs' ampoules *via* static vacuum distillation and stored under a nitrogen or argon atmosphere in the glovebox.

Unless otherwise stated, starting materials were used as supplied by Sigma Aldrich, Fluorochem, Fisher Scientific, Alfa Aesar or Acros Organics. 2,6-Pyridinedicarbonyl dichloride was recrystallised from hot toluene prior to use. Glutaryl chloride, adipoyl chloride, succinyl chloride, and dichlorophenylborane were distilled prior to use. Wilkinson's catalyst ($RhCl(PPh_3)_3$) was prepared *via* the inorganic synthesis procedure.[303] ^{n}BuNa and ^{n}BuK were prepared by literature methods.[304] $[PtCl_2(PhCN)_2]$, $[PtCl_2(PEt_3)]_2$, $M(\eta^4\text{-}C_8H_{12})Cl]_2$ (M=Rh, Ir) were available within the laboratory from previous workers.

Characterisation Details

All NMR spectra were recorded on a Varian VNMRS 400 MHz (^{1}H 399.5 MHz, ^{13}C 100.46 MHz, 150.81 MHz, ^{31}P 161.71 MHz, ^{11}B 160.4 MHz,^{19}F 375.87 MHz, ^{195}Pt 85.53 MHz, ^{29}Si 79.37 MHz, ^{119}Sn 148.97 MHz, ^{7}Li 38.86 MHz) or 600 MHz (^{1}H 599.68 MHz, ^{13}C 150.81 MHz) spectrometer. The spectra were referenced to external Me_4Si, 85% H_3PO_4, $KPtCl_6$, $SnMe_4$, $CFCl_3$ or LiCl as appropriate. Carbon spectra were assigned with reference to 2D (HSQC, HMBC) spectra, and all heteronuclear NMR spectra were recorded at 303 K unless otherwise stated.

UV-Vis spectra were recorded on either a Thermo Spectronic UV300 or a Perkin Elmer Lambda 265 instrument. IR spectra were recorded on a Perkin Elmer Spectrum One instrument in the solid state or as solution cells.

Mass spectrometric data were recorded by Dr A. Abdul-Sada of the departmental service. Single crystal X-Ray diffraction experiments were performed on an Agilent Xcalibur EoS Gemini Ultra diffractometer with CCD plate detector using Cu-Kα (λ = 1.514184 Å) radiation and solved using SHELXT[305] and SHELXL[306] running under Olex2.[307] Elemental analyses were performed by Mr Stephen Boyer at the London Metropolitan University Service, or by Mikroanalytisches Labor Pascher.

Cyclic voltammetry studies were conducted under argon or dinitrogen atmosphere in the glovebox using an EmStat3+ Blue potentiostat under computer control at 298 K. Sample concentrations of 10^{-5} M (2 cm^3 DCM or THF) were used throughout, alongside either 0.1 M [$^nBu_4$][PF_6] or 0.1M [$^nBu_4$][BAr^F] supporting electrolyte concentrations. All experiments were conducted using a standard three-electrode setup comprising of a platinum disc (1 mm) working electrode, platinum wire counter electrode, and a silver wire pseudoreference electrode. Potentials are reported relative to the [$FeCp_2$] 0/+ redox couple determined by doping samples with ferrocene.

DFT Calculations were preformed using Gaussian 09, Revision D.01,[308] running on the Sussex High Performance Cluster. Results were visualised using Gaussview 5.0; orbital contributions and UV/Vis spectra were obtained using Gaussum.[309]

Synthesis Hazard Information.

Caution! Silyl-phosphanes are intrinsically pyrophoric and require handling under stringently anaerobic and moisture-free conditions. Any glassware which has been in contact with a phosphane should be bleached after use to quench residues and prevent stench. The washings from which should be collected in a designated waste container to be appropriately disposed of. If a cannula (especially filter cannulae) has been used with phosphanes and still smells after cleaning, it should be left in the fumehood to vent. Teflon cannulae can be submerged in bleach unlike metal cannulae (corrosion).

Experimental Details for Chapter 2

Preparation of $P(SiMe_3)_3$

A suspension of red phosphorus (6.18 g, 200 mmol) and naphthalene (1.25 g, 9.75 mmol) in DME (250 cm^3) was stirred with an overhead stirrer fitted with a PTFE stirrer paddle, the mixture was heated to 40 °C and sodium chunks (5 x 5 x 5 mm^3, 13.8 g, 600 mmol) were slowly added, 3 pieces at a time, over 2 hours. After all the sodium was added the mixture was heated to reflux and the black suspension was left to stir overnight. The reaction mixture was allowed to cool to ambient temperature and Me_3SiCl (78.7 cm^3, 620 mmol) in DME (75 cm^3) was added *via* pressure-equalising dropping funnel over a period of 3 hours. The solution was heated to reflux and left to stir overnight. The reaction was allowed to cool to ambient temperature and filtered through a bed of Celite® (2 cm) and a porosity 3 frit. The solvent was removed *in* vacuo and the yellow oil was transferred to a distillation rig. Distillation was performed at 9.2 x 10^{-1} mbar, 50 °C affording $P(SiMe_3)_3$ as a colourless liquid. Spectroscopic data conform with literature values.[310] Yield: 14.7 g, 30%.

^1H NMR (C_6D_6): δ = 0.31 (d, CH_3, *J* = 4.47 Hz).

$^{31}P\{^1H\}$ NMR (C_6D_6): δ = −252 (s).

Synthesis of $HP(SiMe_3)_2$

Adapted from literature procedures.[310] Neat $P(SiMe_3)_3$ (7.83 g, 31.3 mmol) was treated with MeOH (1.26 cm^3, 31.3 mmol) and the mixture stirred for 10 h. Purification by bulb-to-bulb distillation afforded $HP(SiMe_3)_2$ as a colourless liquid, the identity of which was confirmed by comparison to literature data. Yield: 3.88 g, 70%. ^{1}H NMR (C_6D_6): δ_H 0.68 (d, PH, $^1J_{HP}$ = 187 Hz, 1H); 0.24 (d, $SiMe_3$, J_{HP} = 4.2 Hz, 18H). ^{31}P NMR (C_6D_6): δ_P –236.8 (dm, J_{HP} 187 Hz, 4 Hz).

Synthesis of $MeP(SiMe_3)_2$

To a cooled (–78 °C) solution of $HP(SiMe_3)_2$ (0.727 g, 4.08 mmol) in THF (10 cm^3) was added ^{n}BuLi (2.07 M, 2.0 cm^3, 4.08 mmol) dropwise over 5 min. The mixture was stirred at –78 °C for 10 min. then allowed to warm slowly to ambient temperature over 45 min with continued stirring. The mixture was cooled to –78 °C prior to dropwise addition of MeI (0.26 cm^3, 4.2 mmol) over 10 min, before allowing to warm to ambient temperature, resulting in formation of a white precipitate; the suspension was stirred for a further 4 h. The mixture was filtered and the THF removed from the filtrate under reduced pressure; the residue was extracted with pentane (2 x 10 cm^3), filtered and the solvent removed under reduced pressure. The crude product was distilled to purity (2.12 mbar, 32 °C), affording $MeP(SiMe_3)_2$ as a colourless liquid, as confirmed by comparison of spectroscopic data with the literature.[311] Yield 0.633 g, 81%. ^{1}H NMR (C_6D_6): δ_H 0.95 (d, PCH_3, $^2J_{HP}$ = 1.2 Hz, 3H); 0.19 (d, $SiMe_3$, J_{HP} = 4.3 Hz, 18H). ^{31}P{^{1}H} NMR (C_6D_6): δ_P –196 (s).

Synthesis of ^{n}BuP(SiMe$_3$)$_2$

To a cooled (–78 °C) solution of $HP(SiMe_3)_2$ (3.992 g, 22.4 mmol) in Et_2O (40 cm^3) was added ^{n}BuLi (2.5 M, 9.0 cm^3, 22.5 mmol) dropwise over 5 min. The mixture was stirred at –78°C for 10 min. then allowed to warm slowly to ambient temperature and stir for a further 30 min. The mixture was cooled to –78 °C prior to dropwise addition of 1-chlorobutane (2.34 cm^3, 22.4 mmol) over 5 min, before allowing to warm to ambient temperature; the suspension was left to stir overnight. The mixture was filtered and the residue washed with Et_2O (2 x 5 cm^3); the filtrates were, combined, concentrated and then triply distilled (40 °C, 2 x 10^{-2} mbar) to afford ^{n}BuP(SiMe$_3$)$_2$ as a colourless liquid Yield 2.71 g, 52 %. ^{1}H NMR (C_6D_6): δ_H 1.57 (br, m, CH_2CH_2Et 4H); 1.40 (dt, CH_2CH_2Me, J_{HH} *ca* 6 Hz, 2H); 0.88 (t, CH_3, J_{HH} = 6Hz); 0.24 (*d*, $SiMe_3$, J_{HP} =4.2 Hz, 18H). ^{31}P{^{1}H} NMR (C_6D_6): δ_P –176.1 (s).

Synthesis of ^{t}BuPH$_2$

A diethyl ether solution of ^{t}BuPCl$_2$ (5 g, 31.45 mmol) was slowly added dropwise to a cooled (–5 °C) ethereal suspension (50 cm^3) of $LiAlH_4$ (1.4 g, 36.7 mmol) over 15 minutes. The reaction mixture was

then allowed to warm to ambient temperature and stir for 2 hours. The reaction flask was cooled to 0 °C and water was added until effervescence halted, resulting in two distinct layers. The ether layer was decanted onto $MgSO_4$, after washing the water layer with Et_2O (2 x 10 cm^3) the ether extracts were also decanted onto the $MgSO_4$. The solution was filtered and purified *via* distillation. Diethyl ether was removed under argon at 40 °C and $^tBuPH_2$ was collected under 5.2 x 10^{-2} mbar of pressure at ambient temperature. 1.82 g of colourless liquid was isolated in 64% yield. The NMR spectroscopic data agree with the literature.[312]

^1H NMR (C_6D_6): δ = 2.88 (d, $^1J_{HP}$ = 187 Hz, $^tBuP\underline{H}_2$, 2H), 1.10 (d, $C(C\underline{H}_3)_3$, 7.21 Hz, 9H).

^{31}P NMR (C_6D_6): δ = –80.35 (t of octets, $^1J_{PH}$ = 187 Hz, J_{PH} = 12 Hz)).

Synthesis of $^tBuP(SiMe_3)_2$

To a cooled (–78 °C) ethereal solution of $^tBuPH_2$ (0.159 M, 82 cm^3, 13.04 mmol) was added ^nBuLi (2.5 M, 11.06 cm^3, 27.64 mmol) dropwise over 5 min. The mixture was stirred at –78°C for 10 min. then allowed to warm slowly to ambient temperature and stir for a further 2 h. The mixture was cooled to –78 °C prior to the addition of Me_3SiCl (3.7 cm^3, 29.0 mmol) over 5 min and stirred for a further 10 minutes before allowing to warm to ambient temperature; the suspension was left to stir overnight. The mixture was filtered and the residue washed with Et_2O (2 x 5 cm^3); the filtrates were, combined, concentrated and distilled (50-55 °C, 2.7 x 10^{-2} mbar) to afford $^tBuP(SiMe_3)_2$ as a colourless liquid, as confirmed by comparison of spectroscopic data with the literature.[313] Yield 2.637 g, 86%.

^1H NMR (C_6D_6): δ_H 1.31 (d, $C(CH_3)_3$, J_{HP} 12 Hz, 9H); 0.31 (*d*, $SiMe_3$, J_{HP} =4 Hz, 18H).

$^{31}P\{^1H\}$ NMR (C_6D_6): δ_P –108.8 (s).

Synthesis of $PhPH_2$

$PhPCl_2$ (3.1 cm^3, 22.53 mmol) in diethyl ether (15 cm^3) was slowly added dropwise to a cooled (–5 °C) ethereal solution (25 cm^3) of $LiAlH_4$ (1 g, 26.3 mmol) over 15 minutes. The reaction mixture was then allowed to warm to ambient temperature and stir for 2 hours. The reaction flask was cooled to 0 °C and water was added until effervescence halted, resulting in two distinct layers. The ether layer was decanted onto $MgSO_4$, after washing the water layer with Et_2O (2 x 10 cm^3) the ether extracts were also decanted onto the $MgSO_4$. The solution was filtered and purified *via* distillation. Diethyl ether was removed under Argon at 64 °C and phenyl phosphane was collected under 4.0 x 10^{-1} mbar of pressure at ambient temperature. 1.705 g of colourless liquid was isolated in 69% yield. The NMR data agree with the literature.[314]

^{1}H NMR (C_6D_6): δ = 7.27 (m, aromatic C-H, 2H), 6.99 (m, aromatic C-H, 3H), 3.83 (d, $^{1}J_{HP}$ = 198.5 Hz, PhP$\underline{H}_2$, 2H).

^{31}P NMR (C_6D_6): δ = −124 (t, $^{1}J_{PH}$ = 199 Hz).

Synthesis of PhP(SiMe$_3$)$_2$

To a cooled (–78 °C) solution of $PhPH_2$ (6 g, 32.6 mmol) in THF (25 cm^3) was added ^{n}BuLi (2.5 M, 27.6 cm^3, 69 mmol) dropwise over 10 min, resulting in formation of a yellow solution. After 10 min. the solution was allowed to warm to ambient temperature stir for a further 2 h. The mixture was then cooled to –78 °C prior to the addition of Me_3SiCl (9.2 cm^3, 72.4 mmol) over 10 min. and stirred for a further 10 minutes before allowing to return to ambient temperature; the suspension was left to stir overnight. The resulting suspension was filtered, concentrated and then purified via bulb-to-bulb distillation to afford $PhP(SiMe_3)_2$ as a colourless liquid. as confirmed by comparison of spectroscopic data with the literature.[315] Yield 6.401 g, 77%.

^{1}H NMR (C_6D_6): δ_H 7.59 (t, 7 Hz, 2H), 7.10 -7.01 (m, 3H), 0.25 (*d*, $SiMe_3$, J_{HP} = 5 Hz, 18H).

^{31}P{^{1}H} NMR (C_6D_6): δ_P –137.0 (s).

Synthesis of MesP(SiMe$_3$)$_2$

To a cooled (–78 °C) solution of $MesPH_2$ (4.05 g, 26.6 mmol) in Et_2O (80 cm^3) was added ^{n}BuLi (2.07 M, 27.3 cm^3, 56.42 mmol) dropwise over 10 min, resulting in formation of a yellow solution. After 10 min. the solution was allowed to warm to ambient temperature stir for a further 2 h. The mixture was then cooled to –78 °C prior to the addition of Me_3SiCl (7.5 cm^3, 59.1 mmol) over 5 min., resulting in formation of a yellow precipitate. The mixture was stirred for a further 10 minutes before allowing to return to ambient temperature and stir overnight. The resulting suspension was filtered and volatile components removed from the filtrate under reduced pressure; the product was triply distilled to purity, affording $MesP(SiMe_3)_2$ as a colourless liquid, as confirmed by comparison of spectroscopic data with the literature.[316] Yield 3.24 g, 41%.

^{1}H NMR (C_6D_6): δ_H 6.87 – 6.84 (m, 2H), 2.63 (s, CH_3, 6H), 2.09 (s, CH_3, 3H), 0.28 (*d*, $SiMe_3$, J_{HP} = 5.8 Hz, 18H).

^{31}P{^{1}H} NMR (C_6D_6): δ_P –162.6 (s).

Crystal data for $C_{15}H_{29}PSi_2$ (M_w = 296.53 g/mol): monoclinic, $P2_1/c$ (no. 14), a = 12.2774(2) Å, b = 24.2123(3) Å, c = 13.4741(2) Å, β = 113.140(2) °, V = 3683.12(11) Å^3, Z = 4, T = 100(2) K, μ(CuKα) = 2.430 mm^{-1}, D_c = 1.069 Mg m^{-3}, 7100 independent reflections, full matrix F^2 refinement, R_1 = 0.0331

on 6594 independent absorption corrected reflections [I > 2σ(I); $2\theta_{max}$ = 143.2 °), 343 parameters, wR_2 = 0.0895 (all data).

Synthesis of 5-Iodo isophthalic acid dimethyl ester

Dimethyl 5-aminoisophthalate (5 g, 24 mmol) was introduced to a cold (0 °C) solution of 6M HCl (56.25 cm^3), then $NaNO_2$ (1.71 g, 25 mmol) in H_2O (14.58 cm^3) was slowly added resulting a golden solution. This golden solution was added to a pre-cooled (0 °C) H_2O solution (50 cm^3) of KI (5.25 g, 31 mmol), followed by DCM (100 cm^3) to facilitate stirring. The resulting black solution was left to stir at ambient temperature overnight (16 hours). The product was extracted and the aqueous layer washed with DCM (2 x 90 cm^3). The organic layers were combined and washed with sodium thiosulphate (3 x 50 cm^3), then the resulting organic layer was dried over $MgSO_4$ and concentrated to afford a crude gum-like red solid. Recrystallisation from hot methanol afforded 3.43 g of pale-yellow/orange solid, 45% yield. NMR data agree with the literature.[317]

^{1}H NMR ($CDCl_3$): δ = 8.62 (t, aromatic-^{i}CH, $^2J_{HH}$ = 1.51 Hz, 1H), 8.53 (d, aromatic-^{o}CH, $^2J_{HH}$ = 1.51 Hz, 2H), 3.95 (s, CH_3, 6H).

Synthesis of 5-Iodoisophthalic acid

5-Iodo isophthalic acid dimethyl ester (4.8 g, 15 mmol) was dissolved in methanol (200 cm^3) and 1M NaOH in H_2O was added (1.8 g, 45 mmol, 45 cm^3 H_2O); the resulting mixture was heated to 40 °C for 12 hours. The solution was allowed to cool to ambient temperature, diluted with H_2O (10 cm^3) and acidified to pH 2-3. The product was extracted into EtOAc (3 x 20 cm^3), washed with brine (20 cm^3), dried over Na_2SO_4 and concentrated *in vacuo*, affording 4.13 g of the product as a pale orange solid in 94% yield. NMR data agree with the literature.[318]

^{1}H NMR ($(D_3C)_2SO$): δ = 8.59 (br, s, aromatic, 3H), 13.23 (br, OH, 2H).

Synthesis of 5-Iodoisophthaloyl chloride

Thionyl chloride (10 cm^3) was added to a Schlenk flask containing 5-iodoisophthalic acid (0.172 g, 0.59 mmol), the flask was fitted with a condenser and brought to reflux for 4 hours before removing the volatile components *in vacuo*, affording 0.165 g of an orange/red oil, 85% yield. NMR data agree with the literature.[319]

^{1}H NMR ($CDCl_3$): δ = 8.79 (br t, aromatic-^{i}CH, 1H), 8.69 (d, aromatic-^{o}CH, $^2J_{HH}$ = 1.6 Hz, 2H).

Synthesis of 5-Tertbutylsophthaloyl chloride

Thionyl chloride (10 cm^3) was added to a Schlenk flask containing 5-tertbutyl isophthalic acid (5 g, 22.5 mmol), the flask was fitted with a condenser and brought to reflux for 4 hours before removing the volatile components *in vacuo*, affording 5.097 g of colourless solid, 87.4% yield. The NMR spectral data agree with the literature.[320]

^{1}H NMR ($CDCl_3$): δ = 8.71 (t, ^{i}aromatic CH, $^2J_{HH}$ = 1.6 Hz, 1H), 8.41 (d, ^{p}aromatic CH, $^2J_{HH}$ = 1.6 Hz, 2H), 1.42 (s, C($C\underline{H}_3$)$_3$, 9H).

Synthesis of 5-Methylisophthaloyl dichloride

5-Methylisophthalic acid (2 g, 11.1 mmol) in thionyl chloride (10 cm^3) was brought to reflux for 6 hours. After cooling, the volatile components were removed under reduced pressure to afford a pale-yellow solid. Yield: 2.3 g, 95%.

^{1}H NMR ($CDCl_3$, 399.5 MHz): δ = 8.67 (br t, aromatic, 1H), 8.21 (br q, aromatic, J_{HH} = 0.78 Hz, 2H), 2.55 (s, CH_3, 3H). ^{1}H NMR ($CDCl_3$, 599.68 MHz): δ = 8.67 (m, aromatic, 1H), 8.21 (m, aromatic, 2H), 2.55 (m, CH_3, 3H).

^{13}C{^{1}H} NMR ($CDCl_3$, 150.81 MHz): δ = 167.6 (s, C=O), 140.6 (s, aromatic-C^p) 137.7 (s, aromatic-C^m), 134.4 ((s, aromatic-C^o), 131.4 (s, aromatic-C^i), 21.2 (2, CH_3).

Synthesis of 1,3-Dimethyl 5-phenylbenzene-1,3-dicarboxylate (Suzuki)

5-Iodo isophthalic acid dimethyl ester (1.22 g, 3.81 mmol), phenyl boronic acid (0.51 g, 4.19 mmol), $Pd(PPh_3)_4$ (0.22 g, 0.19 mmol) and cesium carbonate (1.36 g, 4.19 mmol) were introduced to a 100 cm^3 round-bottom flask and dissolved in a mixed solvent system of H_2O (2 cm^3), C_7H_8 (21 cm^3) and Et_2O (4 cm^3). The reaction flask was fitted with a condenser, flushed with N_2, and heated to reflux for 6 hours. The reaction was allowed to cool to ambient temperature before being filtered through celite® and concentrated *in vacuo*, affording a red solid. The crude red solid was eluted through a 30 g column in a 0-10 % EtOAc/Hexane solvent system over 14 column volumes obtaining 0.54 g of the desired product as a colourless fluffy solid in 52% yield.

The reaction was monitored by TLC. The NMR spectral data agree with the literature.[321]

^{1}H NMR ($CDCl_3$): δ = 8.66 (t, aromatic-^{i}CH, $^2J_{HH}$ = 1.62 Hz, 1H), 8.47 (d, aromatic-^{o}CH, $^2J_{HH}$ = 1.62 Hz, 2H), 7.66 (dd, aromatic-^{m}CH, $^1J_{HH}$ = 7.52 Hz, 2H), 7.49 (t, aromatic-^{o}CH, $^1J_{HH}$ = 7.52 Hz, 2H), 7.41 (t, aromatic-^{p}CH, $^1J_{HH}$ = 7.52 Hz, 1H), 3.98 (s, CH_3, 6H).

Synthesis of 1,1'biphenyl-3,5-dicarboxylic acid

Methanol (20 cm^3) was added to 1,3-dimethyl 5-phenylbenzene-1,3-dicarboxylate (0.54 g, 2 mmol) followed by 1M NaOH in H_2O (0.24 g, 6 mmol). The solution was heated at 40 °C for 5 hours, acidified to pH 2-3 resulting in a colourless precipitate which was collected *via* filtration, washed with H_2O (5 cm^3) and dried in a desiccator overnight. 0.383 g of the colourless solid was isolated in 79% yield. The NMR data agree with the literature.[322]

^{1}H NMR ($(D_3C)_2SO$): δ = 13.36 (s, O<u>H</u>, 2H), 8.46 (s, ^{i}CH, 1H), 8.37 s, ^{o}CH, 2H), 7.74 (d, ^{m}CH, $^1J_{HH}$ = 7.40 Hz, 2H), 7.53 (t, ^{o}CH, $^1J_{HH}$ = 7.40 Hz, 2H), 7.45 (t, ^{P}CH, $^1J_{HH}$ = 7.40 Hz).

Synthesis of 5-Phenylisophthaloyl chloride

5-Phenylisophthalic acid (2 g, 11.1 mmol) in thionyl chloride (10 cm^3) was brought to reflux for 6 hours. After cooling, the volatile components were removed under reduced pressure to afford a colourless solid. Yield: 0.321 g, 77%.

^{1}H NMR ($CDCl_3$, 399.5 MHz): δ = 8.82 (br t, aromatic-C^i, 1H), 8.6 (d, aromatic-C^m, $^1J_{HH}$ = 1.5 Hz, 2H), 7.65 (d, aromatic-C^o, $^1J_{HH}$ = 7.32 Hz, 2H), 7.56-7.42 (m, aromatic-$C^{m,p}$, 3H).

^{1}H NMR ($CDCl_3$, 599.68 MHz): δ = 8.82 (br t, aromatic-C^i, 1H), 8.6 (dd, aromatic-C^m, $^1J_{HH}$ = 1.6 Hz, 2H), 7.65 (d, aromatic-C^o, $^1J_{HH}$ = 7.31 Hz, 2H), 7.54 (t, aromatic-C^m, $^1J_{HH}$ = 7.31 Hz, 2H), 7.49 (t, aromatic-C^p,7.31 Hz, 1H).

$^{13}C\{^1H\}$ NMR ($CDCl_3$, 150.81 MHz): δ = 167.6 (s, C=O), 143.8 (s, aromatic-C^p), 137.6 (s, aromatic-C^i), 135.5 (s, aromatic-C^m), 135.1 (s, aromatic-C^p), 132.4 (s, aromatic-C^o), 129.6 (s, aromatic-C^o), 129.4 (s, aromatic-C^i), 127.4 (s, aromatic-C^m).

Synthesis of Dimethyl 4-Cyanobiphenyl-3,5-dicarboxylate

5-Iodo isophthalic acid dimethyl ester (2.83 g, 8.85 mmol), 4-cyanophenylboronic acid (1.37 g, 9.29 mmol), sodium carbonate (3.7 g, 35.49 mmol) and Pd/C (10%, 0.48 g) were combined in a round-bottom flask flushed with argon and fitted with a condenser. MeOH (60 cm^3) was added and the mixture was heated at 60 °C for 3 hours. After cooling to ambient temperature the mixture was filtered through a porosity 3 frit, the residue on the frit was washed with DCM and EtOH until the filtrate ran through clear and then volatile components were removed under reduced pressure. The product was extracted into DCM and washed with water (3 x 20 cm^3), dried over $MgSO_4$ and concentrated to afford a fluffy yellow solid. Yield: 1.31 g, 50%. Confirmed by comparison with literature data.[323]

^{1}H NMR ($CDCl_3$): δ = 8.73 (br t, aromatic. 1H), 8.46 (d, aromatic, $^2J_{HH}$ = 1.45 Hz), 2H), 7.78 (s, aromatic, 4H), 3.99 (s, CH_3, 6H).

Synthesis of 5-(4-Cyanophenyl)benzene-1,3-dicarboxylic acid

Dimethyl 4-cyanobiphenyl-3,5-dicarboxylate (1.19 g, 4.01 mmol) was dissolved in MeOH (30 cm^3), NaOH (0.48 g, 12.09 mml) in water (10 cm^3) was added and the mixture was heated to 40 °C for 4 hours. After cooling to ambient temperature, the reaction mixture was neutralised by addition of acid to afford an off-white precipitate which was dried in a desiccator overnight. Yield: 0.93 g, 86%.

^{1}H NMR ($(D_3C)_2SO$, 599.68 MHz): δ = 13.50 (br, OH, 2H), 8.51 (t, aromatic, $^2J_{HH}$ = 1.45 Hz, 1H), 8.43 (d, aromatic, $^2J_{HH}$ = 1.45 Hz, 2H), 7.98 (aromatic, 4H).

$^{13}C\{^1H\}$ NMR ($CDCl_3$, 150.81 MHz): δ = 166.3 (s, C=O), 142.9 (s, aromatic-C^p), 139.42 (s, CN), 133.1 (s, aromatic-C^o), 132.3 (s, aromatic-C^m), 131.7 (s, aromatic-C^i), 129.9 (s, aromatic-C^o), 128.1 (s, aromatic-C^m), 118.7 (s, aromatic C^i), 110.1 (s, aromatic-C^p).

Synthesis of Cyanobiphenyl diacyl chloride

5-Cyanophenylisophthalic acid (0.6 g, 2.2 mmol) in thionyl chloride (20 cm^3) was brought to reflux for 6 hours. After cooling, the volatile components were removed under reduced pressure to afford a pale-orange solid. Yield: 0.43 g, 64%.

^{1}H NMR ($CDCl_3$): δ = 8.90 (t, aromatic-C^i,$^2J_{HH}$ = 1.5 Hz, 1H), 8.59 (d, aromatic-C^m, $^2J_{HH}$ = 1.5 Hz, 2H), 7.85 (d, aromatic-C^o, $^1J_{HH}$ = 8.32 Hz, 2H), 7.77 (d, aromatic-C^m, $^1J_{HH}$ = 8.32 Hz, 2H).

$^{13}C\{^1H\}$ NMR ($CDCl_3$): δ = 167.1 (s, C=O), 141.9 (s, aromatic-C^p),141.7 (s, CN), 135.6 (s, aromatic-C^o), 135.3 (s, aromatic-C^m), 133.4 (s, aromatic-C^i), 133.3 (s, aromatic-C^o), 128.1 (s, aromatic-C^m), 118.2 (s, aromatic C^i), 113.4 (s, aromatic-C^p).

Synthesis of Dimethyl 5-(trimethylsilylethynyl)benzene-1,3-dicarboxylate

5-Iodo isophthalic acid dimethyl ester (2.3 g, 7.17 mmol), $PdCl_2(PPh_3)_2$ (0.253 g, 0.36 mmol) and CuI (0.07 g, 0.36 mmol) were introduced to a round-bottom Schlenk and placed under vacuum, next THF (39 cm^3), trimethylsilylacetylene (1.53 cm^3, 10.76 mmol) and triethylamine (1.5 cm^3, 10.76 mmol) were added and the reaction mixture was stirred for 20 hours. The reaction mixture was concentrated and extracted into DCM, the DCM extracts were washed with brine (3 x 25 cm^3), dried over $MgSO_4$ and voltailes removed under reduced pressure to give 2.594 g of crude material. The crude product was purified *via* column chromatography using a hexane/ethyl acetate solvent system (30:1), affording 1.68 g of yellow solid, 81% yield. The reaction was monitored by TLC, NMR data agree with the literature.[324]

^{1}H NMR ($CDCl_3$): δ = 8.60 (t, aromatic-^{i}CH, $^2J_{HH}$ = 1.85 Hz, 1H), 8.29 (d, aromatic-^{o}CH, $^2J_{HH}$ = 1.85 Hz, 2H), 3.95 (s, CH_3, 6H), 0.26 (s, $SiMe_3$, 9H).

Synthesis of 1,3-Dimethyl 5-ethynylisophthalate

Dimethyl 5-(trimethylsilylethynyl)benzene-1,3-dicarboxylate (1.68 g, 5.79 mmol) and K_2CO_3 (0.16 g, 1.2 mmol) were dissolved in THF/MeOH (12.8/32 cm^3) and stirred for 24 hours, resulting in a dark suspension, which was concentrated *in vacuo*. The solid was extracted into DCM (50 cm^3) and washed with water (50 cm^3). The aqueous layer was washed with DCM (3 x 25 cm^3), the organic extracts were combined, washed with brine (3 x 25 cm^3) and dried over $MgSO_4$. After the removal of volatile components a crude light brown solid was collected and purified *via* sublimation (100 °C, 1 mbar) to afford a colourless solid. 0.4 g, 31% yield. NMR data agree with the literature.[325]

^{1}H NMR ($CDCl_3$): δ = 8.64 (t, aromatic-^{i}CH, $^2J_{HH}$ = 1.53 Hz, 1H), 8.32 (d, aromatic-^{o}CH, $^2J_{HH}$ = 1.53 Hz, 2H), 3.96 (s, CH_3, 6H), 3.17 (s, CCH, 1H).

Synthesis of 5-Ethynylisophthalic acid chloride

Thionyl chloride (10 cm^3) was added to a round-bottom flask containing 5-ethynyl isophthalic acid (0.18 g, 0.1 mmol), the flask was fitted with a condenser and brought to reflux for 4 hours before removing the volatile components *in vacuo*, affording 0.14 g of beige solid, 64% yield.

^{1}H NMR (CD_2Cl_2): δ = 8.76 (br t, aromatic-^{i}CH, 1H), 8.50 (d, aromatic-^{o}CH, $^2J_{HH}$ = 1.6 Hz, 2H), 3.39 (s, CC<u>H</u>, 1H).

Synthesis of 5-Cyanoisophthaloyl chloride

Thionyl chloride (10 cm^3) was added to a round-bottom flask containing 5-cyanoisophthalic acid (1.28 g, 6.68 mmol), the flask was fitted with a condenser and brought to reflux for 4 hours before filtering and removing the volatile components *in vacuo*, affording 0.576 g of colourless solid, 38 % yield. The NMR data agree with the literature.[326]

^{1}H NMR ($CDCl_3$): δ = 9.00 (br s, aromatic-^{i}CH, 1H), 8.66 (br s, aromatic-^{o}CH, 2H).

Synthesis of *m*-{-C(O)-C_6H_4-(C(O)PMe)}$_2$ (2.1)

A diethyl ether solution of isophthaloyl chloride (0.251 g, 1.23 mmol) was added, slowly, to a pre-cooled (−78 °C) ethereal solution of $MeP(SiMe_3)_2$ (0.237 g, 1.23 mmol). During addition the solution assumes a yellow colouration. After stirring at −78 °C for 30 min. the mixture was allowed to warm to RT and stirred for a further 12 h, whereupon the precipitate was collected by filtration, washed with diethyl ether and dried *in vacuo*, resulting in 0.124 g of a yellow solid in 57% yield. Product identity was confirmed by comparison of spectroscopic data with the literature.[111]

^{1}H NMR (C_6D_6): δ = 1.58 (d, 6H, *J* = 14.799 Hz) 6.45 (br, 2H), 7.17 (br, 4H), 9.28 (br, 2H). ^{31}P{^{1}H} NMR (C_6D_6): δ = 32.7 (s).

Synthesis of *m*-{-C(O)-$C_5N_1H_4$(C(O)PMe)}$_2$ (2.5)

A diethyl ether solution of 2,6-pyridinedicarbonyl dichloride (0.312 g, 1.5 mmol) was added, slowly, to a pre-cooled (−78 °C) ethereal solution of $MeP(SiMe_3)_2$ (0.294 g, 1.5 mmol). During addition the solution assumes a green-yellow colouration. After stirring at −78 °C for 30 min. the mixture was allowed to warm to ambient temperature and stirred for a further 16 h, whereupon the precipitate was collected by filtration, washed with diethyl ether and dried *in vacuo*, resulting in 0.161 g of a green-yellow solid in 60% yield.

^{1}H NMR (C6D6): δ = 7.2 (d, aromatic ^{o}CH, $^{2}J_{HH}$ = 7.8 Hz, 4H), 6.58 (t, aromatic – ^{p}CH, $^{2}J_{HH}$ = 7.8 Hz, 2H), 1.63 (d, CH_3, $^{2}J_{PH}$ = 6.2 Hz, 6H).

^{13}C{^{1}H} NMR (C_6D_6): δ = 209.1 (d, C(O), $^{1}J_{CP}$ = 51 Hz), 152.9 (d, aromatic – C^{m}, $^{2}J_{CP}$ = 33 Hz), 138.4 (s, aromatic –C^{p}), 124.7 (br t, aromatic –C^{o}, $^{3}J_{CP}$ = 2 Hz), 3.65 (d, CH_3, $^{1}J_{CP}$ = 8 Hz).

^{31}P{^{1}H} NMR (C_6D_6): δ = 30.1 (s).

IR ν_{CO} 1656, 1640 cm^{-1}.

Anal. Calc. for $C_{16}H_{12}N_2O_4P_2$: C, 53.63; H, 3.38; N, 7.82. Found: C, 52.89; H, 3.34; N, 7.80.

X-Ray quality crystals were grown at -29 °C from THF. **Crystal Data** for $C_{16}H_{12}N_2O_4P_2$ (M_w = 358.22 g/mol): orthorhombic, space group Pmmn (no. 59), *a* = 13.4667(13) Å, *b* = 12.5171(13) Å, *c* = 4.7670(6) Å, *V* = 803.54(15) Å^3, *Z* = 2, *T* = 100 K, μ(Cu Kα) = 2.680 mm^{-1}, D_{calc} = 1.481 g/cm^3, 2552 reflections measured (9.646° ≤ 2Θ ≤ 134.122°), 778 unique (R_{int} = 0.0427, R_{sigma} = 0.0363), which were used in all calculations. The final R_1 value was 0.0428 (I > 2σ(I)) and wR_2 was 0.1215 (all data).

Synthesis of *m*-{-C(O)-C_6H_4(C(O)PPh)}$_2$ (2.4)

Isophthaloyl chloride (0.5 g, 2.46 mmol) was dissolved in diethyl ether (6 cm^3) and slowly added dropwise to a pre-cooled (−78 °C) ethereal solution (10 cm^3) of $PhP(SiMe_3)_2$ (0.627 g, 2.46 mmol) over 5 minutes yielding a yellow colour change. The yellow solution was stirred for 30 minutes at -78 °C, then allowed to warm to ambient temperature and stir for 16 hours leading to a yellow precipitate which was filtered, washed with diethyl ether (3 x 5 cm^3) and dried *in vacuo*, initially yielding 0.181 g of yellow powder. The solid was dissolved in the minimum amount of DCM and layered with pentane resulting in 0.102 g of matt yellow solid isolated in 17% yield.

^{1}H NMR (CD_2Cl_2): δ = Conformation 1: 8.50 (br, aromatic, 1H), 8.03 (br, aromatic, 2H), 7.33 (br, aromatic, 5H). Conformation 2: 8.63 (br, aromatic, 1H), 8.21 (br, aromatic, 2H), 7.47 (br, aromatic, should be 5H but overlapped by base of other conformer).

^{13}C{^{1}H} NMR (CD_2Cl_2): δ = 208.5 (d, C(O), $^{1}J_{CP}$ = 35 Hz), 140.3 – 127.8 (aromatic region).

^{31}P{^{1}H} NMR (C_6D_6): δ = 30.5 (s). ^{31}P{^{1}H} NMR (CD_2Cl_2): δ = 32.2 (s).

IR ν_{CO} 1639 (w) cm^{-1}.

HRMS (*m/z*): Calc. for $C_{28}H_{18}O_4P_2$ 480.0680 ([M]+). Found 480.0699 ([M]+).

X-Ray quality crystals were grown at − 29 °C from DCM/Hexane. **Crystal Data** for $C_{30}H_{22}Cl_4O_4P_2$ (M_w = 650.21 g/mol): monoclinic, space group $P2_1/c$ (no. 14), a = 15.182(3) Å, b = 14.3566(16) Å, c = 15.409(3) Å, β = 116.03(2)°, V = 3018.1(9) Å^3, Z = 4, T = 293(2) K, μ(Cu Kα) = 4.857 mm^{-1}, *Dcalc* = 1.431 g/cm^3, 9294 reflections measured (8.872° ≤ 2Θ ≤ 142.474°), 5148 unique (R_{int} = 0.1032, R_{sigma} = 0.1162) which were used in all calculations. The final R_1 value was 0.0674 (I > 2σ(I)) and wR_2 was 0.2178 (all data).

Synthesis of *m*-{-C(O)-C$_7$H$_6$-(C(O)PMe)}$_2$ (2.7)

A diethyl ether solution of 5-methylisophthaloyl chloride (0.487 g, 2.25 mmol) was added, slowly, to a pre-cooled (−78 °C) ethereal solution of $MeP(SiMe_3)_2$ (0.432 g, 2.25 mmol). During addition the solution assumes a yellow colouration. After stirring at −78 °C for 30 min. the mixture was allowed to warm to ambient temperature and stir for a further 16 h, whereupon the precipitate was collected by filtration, washed with diethyl ether (3 x 5 cm^3), hexanes (3 x 5 cm^3), Et_2O again (3 x 5 cm^3) and dried *in vacuo*, resulting in a yellow solid. Yield: 94 mg, 22%.

^{1}H NMR (CD_2Cl_2): δ = 9.34 (br, aromatic-^{i}CH, 2H), 7.33 (br, aromatic-^{o}CH, 4H), 2.23 (s, Ar-C$\underline{H}_3$, 6H), 1.58 (d, P-C$\underline{H}_3$, $^{2}J_{HP}$ = 2.7 Hz).

^{13}C{^{1}H} NMR (CD_2Cl_2): δ = 207.3 (d, C(O), $^{1}J_{CP}$ = 46 Hz), 141.5 (br t, aromatic-C^{i}) 138.0 (d, aromatic-C^{m}, $^{2}J_{CP}$ = 37 Hz), 131.97 (d, aromatic-C^{o}, $^{3}J_{CP}$ = 14 Hz), 131.8 (d, aromatic-C^{P}, $^{4}J_{CP}$ = 2 Hz), 21.3 (s, Ar-$\underline{C}H_3$), 1.9 (d, P-$\underline{C}H_3$, $^{1}J_{CP}$ = 4 Hz).

^{31}P{^{1}H} NMR (CD_2Cl_2): 34.2 (s).

^{31}P{^{1}H} NMR (C_6D_6): 32.3 (s).

IR ν_{CO} 1653 cm^{-1}, 1640 cm^{-1}.

HRMS (m/z): Calc. for $C_{20}H_{18}O_4P_2$ 384.0680 ([M]+). Found 384.0691 ([M]+).

X-Ray quality crystals were grown at − 29 °C from DCM/Pentane. **Crystal Data** for $C_{20}H_{18}O_4P_2$ (M_w = 382.27 g/mol): orthorhombic, space group Pmmn (no. 59), a = 13.9090(11) Å, b = 13.0284(10) Å, c = 4.7978(4) Å, V = 869.42(12) Å^3, Z = 2, T = 100.00(10) K, μ(Cu Kα) = 2.481 mm^{-1}, D_{calc} = 1.460 g/cm^3, 2495 reflections measured (9.3° ≤ 2Θ ≤ 142.768°), 911 unique (R_{int} = 0.0587, R_{sigma} = 0.0611) which were used in all calculations. The final R_1 value was 0.0682 (I > 2σ(I)) and wR_2 was 0.1903 (all data).

Synthesis of *m*-{-C(O)-$C_{10}H_{12}$(C(O)PMe)}$_2$ (2.6)

To a precooled (−78 °C) ethereal solution (5 cm^3) of $MeP(SiMe_3)_2$ (0.254 g, 1.32 mmol) was added 5-tertbutyl isophthaloyl chloride dropwise over 5 minutes in ether (5 cm^3), resulting in yellow colouration. After stirring for 30 minutes at −78 °C the mixture was allowed to warm to ambient temperature and stir for a further 16 hours, whereupon the precipitate was collected by filtration, washed with diethyl ether (2 x 5 cm^3) and dried *in vacuo*, affording 65 mg of an intense yellow solid in 21% yield.

^{1}H NMR ($CDCl_3$): δ = 9.27 (br, t – can't resolve coupling, aromatic-^{i}CH, 2H), 7.50 (d, aromatic-^{o}CH, J_{HH} = 1.4 Hz, 4H), 1.65 (d, CH_3, $^2J_{PH}$ = 2.7 Hz, 6H), 1.1 (s, ^{t}Bu $(CH_3)_3$, 18H).

^{13}C{^{1}H} NMR ($CDCl_3$): δ = 207.2 (d, C(O), $^1J_{CP}$ = 46 Hz), 154.1 (br t, 2 Hz), 137.5 (d, aromatic-C^m, $^2J_{CP}$ = 38 Hz), 131.2 (t, aromatic-C^i, $^3J_{CP}$ = 14 Hz), 127.5 (dd, aromatic-C^o, $^3J_{CP}$ = 2 Hz), 35.2 (s, $\underline{C}(CH_3)_3$), 30.9 (s, $C(\underline{C}H_3)_3$), 1.6 (d, CH_3, $^1J_{CP}$ = 4 Hz).

^{31}P{^{1}H} NMR ($CDCl_3$): δ = 36.1 (s).

^{31}P{^{1}H} NMR (C_6D_6): δ = 34.5 (s).

IR ν_{CO} 1657, 1641 cm^{-1}.

Anal. Calc. for $C_{26}H_{30}O_4P_2$: C, 66.64; H, 6.46. Found: C, 66.54; H, 6.52.

X-Ray quality crystals were grown at − 29 °C from DCM/Pentane. **Crystal Data** for $C_{26.5}H_{31}ClO_4P_2$ (M_w = 510.90 g/mol): monoclinic, space group C2/c (no. 15), a = 17.3966(3) Å, b = 12.4858(2) Å, c = 24.2953(4) Å, β = 93.924(2)°, V = 5264.82(15) Å^3, Z = 8, T = 293(2) K, μ(Cu Kα) = 2.677 mm^{-1}, D_{calc} = 1.289 g/cm^3, 9137 reflections measured (7.294° ≤ 2Θ ≤ 143.39°), 5028 unique (R_{int} = 0.0202, R_{sigma} = 0.0256) which were used in all calculations. The final R_1 value was 0.0393 (I > 2σ(I)) and wR_2 was 0.1010 (all data).

Synthesis of *m*-{-C(O)-C_6H_3I -(C(O)PMe)}$_2$ (2.8)

A diethyl ether solution of 5-Iodoisophthaloyl chloride (1 g, 3 mmol) was cooled to (−78 °C) and $MeP(SiMe_3)_2$ (0.7 cm^3, 3 mmol) was added. During addition the solution assumes a purple colouration,

after stirring at −78 °C for 30 min. the mixture was allowed to warm to ambient temperature and stirred for a further 16 h, whereupon the precipitate was collected by filtration, washed with diethyl ether and concentrated *in vacuo*. The product was extracted into toluene and dried *in vacuo*, resulting in 0.169 g of an orange-yellow solid in 18.5% yield.

^{1}H NMR (CD_2Cl_2): δ = 9.43 (br t, aromatic-^{i}CH, 2H), 7.87 (d, aromatic-^{o}CH, $^{2}J_{HH}$ = 1.41 Hz, 4H), 1.61 (d, P-C$\underline{H}_3$, $^{2}J_{HP}$ = 3 Hz, 6H).

^{13}C{^{1}H} NMR (CD_2Cl_2): δ = 205.4 (d, C(O), $^{1}J_{CP}$ = 47 Hz), 139.9 (dd, overlapping aromatic-C^{o,p}, $^{2}J_{CP}$ = *ca*2 Hz), 139.1 (d, aromatic-C^{m}, $^{2}J_{CP}$ = 38 Hz), 132.8 (t, aromatic-C^{i}, $^{3}J_{CP}$ = 14 Hz), 1.88 (d, CH_3, $^{1}J_{CP}$ = 5 Hz). ^{31}P{^{1}H} NMR (CD_2Cl_2): δ = 36.3 (s).

^{31}P{^{1}H} NMR (C_6D_6): δ = 36.1 (s).

IR ν_{CO} 1640 (br) cm^{-1}.

HRMS (m/z): Calc. for $C_{18}H_{12}O_4P_2I_2$ 607.8300 ([M]+). Found 607.8306 ([M]+).

X-Ray quality crystals were grown from the slow evaporation of a saturated benzene solution. **Crystal Data** for $C_{18}H_{12}I_2O_4P_2$ (M_w = 608.02 g/mol): triclinic, space group P-1 (no. 2), a = 8.9974(5) Å, b = 10.3834(5) Å, c = 11.7875(5) Å, α = 71.137(4)°, β = 79.100(4)°, γ = 72.531(4)°, V = 988.85(9) Å^3, Z = 2, T = 100.00(10) K, μ(Cu Kα) = 26.698 mm^{-1}, D_{calc} = 2.042 g/cm^3, 6114 reflections measured (7.968° ≤ 2Θ ≤ 143.478°), 3745 unique (R_{int} = 0.0304, R_{sigma} = 0.0384), which were used in all calculations. The final R_1 value was 0.0337 (I > 2σ(I)) and wR_2 was 0.0927 (all data).

Synthesis of *m*-{-C(O)-$C_{12}H_8$-(C(O)PMe)}$_2$ (2.9)

A diethyl ether solution of 5-phenylisophthaloyl chloride (0.32 g, 1.1 mmol) was added, slowly, to a pre-cooled (−78 °C) ethereal solution of $MeP(SiMe_3)_2$ (0.22 g, 1.1 mmol). During addition the solution assumes a yellow colouration. After stirring at −78 °C for 30 min. the mixture was allowed to warm to RT and stirred for a further 12 h, whereupon the precipitate was collected by filtration, washed with diethyl ether and dried *in vacuo*, resulting in 77 mg of a yellow solid in 26% yield.

^{1}H NMR (CD_2Cl_2): δ = 9.46 (s, aromatic-^{i}CH, 2H), 7.71 (s, aromatic-^{o}CH, 4H), 7.34 (t, aromatic-^{p,o,m}CH, 10H), 1.66 (d, P-CH_3, $^{2}J_{HP}$ = 2.3 Hz, 6H). ^{1}H NMR (C_6D_6): δ = 9.21 (br, aromatic-^{i}CH, 1H), 7.57 (d, aromatic-^{m}CH, $^{2}J_{HH}$ = 1.1 Hz, 2H), 6.94 (t, aromatic-^{p}CH, $^{1}J_{HH}$ = 7.5 Hz, 1H), 6.87 (t, aromatic-^{m}CH, $^{1}J_{HH}$ = 7.5 Hz, 2H), 6.72 (d, aromatic-^{o}CH, $^{1}J_{HH}$ = 7.53 Hz).

^{13}C{^{1}H} NMR (CD_2Cl_2): δ = 207.4 (d, C(O), $^{1}J_{CP}$ = 46 Hz), 144.3 (s, aromatic-C^{p}, 138.83 (d, aromatic-C^{m}, $^{2}J_{CP}$ = 37 Hz), 138.8 (s, aromatic-C^{i}), 132.6 (t, aromatic-C^{i}, $^{3}J_{CP}$ = 13 Hz), 129.5 (2 s overlapping, aromatic-C^{m,o}), 129.1 (s, aromatic-C^{o}), 127.6 (s, aromatic-C^{p}), 1.9 (d, P-$\underline{C}H_3$, $^{1}J_{CP}$ = 5 Hz).

$^{31}P\{^{1}H\}$ NMR (CD_2Cl_2): δ = 36.16 (s).

$^{31}P\{^{1}H\}$ NMR (C_6D_6): δ = 35.7 (s).

IR v_{CO} 1658, 1639 cm^{-1}.

HRMS (m/z): Calc. for $C_{30}H_{22}O_4P_2$ 508.0993 ([M]+). Found 508.0996 ([M]+).

X-Ray quality crystals were grown from the slow evaporation of a saturated benzene solution. **Crystal Data** for $C_{30.75}H_{22.75}O_4P_2$ (M_w = 518.18 g/mol): monoclinic, space group $P2_1/c$ (no. 14), a = 12.63370(10) Å, b = 18.1737(2) Å, c = 11.41730(10) Å, β = 97.7110(10)°, V = 2597.72(4) $Å^3$, Z = 4, T = 100.00(10) K, μ(CuKα) = 1.810 mm^{-1}, D_{calc} = 1.325 g/cm^3, 24517 reflections measured (8.576° ≤ 2Θ ≤ 143.576°), 5038 unique (R_{int} = 0.0217, R_{sigma} = 0.0152) which were used in all calculations. The final R_1 value was 0.0481 (I > 2σ(I)) and wR_2 was 0.1220 (all data).

Synthesis of *m*-{-C(O)-$C_{13}H_7N_1$-(C(O)PMe)}$_2$ (2.10)

To a cooled (−78 °C) solution of 5-(4-cyanophenyl)isophthaloyl chloride (0.316 g, 1.04 mmol) in Et_2O (5 cm^3) was added $MeP(SiMe_3)_2$ (1.04 g, 1.04 mmol) resulting in an orange colouration. After stirring for 30 minutes at this temperature, the mixture was allowed to warm to ambient temperature and stirred for a further 16 hours. At this point the reaction had only proceeded halfway warranting the addition of another equivalent of $MeP(SiMe_3)_2$ (1.04 g, 1.04 mmol) and stirring for a further 16 hours, whereupon the orange precipitate was collected by filtration, washed with Et_2O (3 x 10 cm^3) and dried *in vacuo*. Yield: 69 mg, 24%.

^{1}H NMR (C_6D_6): δ = 9.29 (br, aromatic, 1H), 7.43 (d, aromatic, $^{2}J_{HH}$ = 1.5 Hz, 2H), 6.82 (d, aromatic, $^{1}J_{HH}$ = 8.5 Hz, 2H), 6.33 (d, aromatic, $^{1}J_{HH}$ = 8.5 Hz, 2H), 1.66 (d, CH_3, $^{2}J_{HP}$ = 3.1 Hz, 3H).

$^{13}C\{^{1}H\}$ NMR (C_6D_6): δ = 205.9 (d, C(O), $^{1}J_{CP}$ = 46 Hz), 141.8 (s, C≡N), 141.4 (s, aromatic-C^i), 138.5 (d, aromatic-C^o, $^{2}J_{CP}$ = 38 Hz), 133.4 (t, aromatic-C^i, $^{3}J_{CP}$ = 13 Hz), 132.5 (s, aromatic-C^o), 129.1 (dd, aromatic-C^m, $^{3}J_{CP}$ = 2 Hz), 127.3 (s, aromatic-C^m), 118.2 (s, aromatic-C^p), 112.9 (s, aromatic-C^p), 1.8 (d, CH_3, $^{1}J_{CP}$ = 5 Hz).

$^{31}P\{^{1}H\}$ NMR (C_6D_6): δ = 35.2 (s).

IR v_{CO} 1648 (br) cm^{-1} v_{CN} 2227 cm^{-1}.

HRMS (m/z): Calc. for $C_{30}H_{22}O_4P_2$ 558.0898 ([M]+). Found 558.0906 ([M]+).

X-Ray quality crystals were grown from layering THF/hexane at ambient temperature. **Crystal Data** for $C_{32.75}H_{21.75}N_2O_4P_2$ (M_w = 569.21 g/mol): monoclinic, space group I2/a (no. 15), a = 16.7950(6) Å, b = 19.1020(5) Å, c = 19.2856(5) Å, β = 98.907(3)°, V = 6112.6(3) $Å^3$, Z = 8, T = 99.97(13) K, μ(Cu Kα) =

1.607 mm^{-1}, D_{calc} = 1.237 g/cm^3, 9548 reflections measured (7.056° ≤ 2Θ ≤ 142.842°), 5753 unique (R_{int} = 0.0539, R_{sigma} = 0.0857) which were used in all calculations. The final R_1 value was 0.0786 (I > 2σ(I)) and wR_2 was 0.2401 (all data).

Attempted synthesis of 5-Ethynyl and 5-Nitrile derivatives

Alkynyl isophthaloyl chloride (5-ethynyl or 5-Nitrile) was reacted with an equivalent of $MeP(SiMe_3)_2$ in ether *via* the typical protocol, unfortunately $MePH_2$ and $MeP((H)SiMe_3$ formation was observed.

Attempted Oxidations

Chalocogens

Compound **2.1** was reacted with an excess of chalcogen (S, Se, Te) and brought to reflux in toluene for 16 hours, the solution was filtered from the black/yellow precipitate and volatile components removed under reduced pressure affording a yellow solid, recovering **2.1** in all cases.

H_2O_2:

Compound **2.1** (50 mg, 0.14 mmol) was dissolved in DCM (5 cm^3) and cooled to 0 °C, degassed H_2O (*ca* 3 cm^3) and H_2O_2 (10 drops) were added and left to stir for 2 hours. Only **2.1** and decomposition products were observed.

***m*-CPBA:**

Compound **2.1** (8 mg, 0.02 mmol) and *m*-CPBA (7.76 mg, 0.045 mmol) were introduced to a Schlenk flask containing DCM (5 cm^3) and wrapped in aluminium foil to exclude light, the mixture was stirred for 40 minutes, resulting in a cloudy solution. Et_2O (5 cm^3) was added, resulting in precipitate formation. The solution was filtered from the solid, which was dried *in vacuo*. No phosphorus signals were observed by NMR spectroscopy.

Exposure to air:

A sample of **2.1** in a J Young's NMR tube was intentionally exposed to air, resulting in a colourless precipitate, the precipitate is almost insoluble even after sonication, though the following data were obtained after sonication.

^{31}P NMR (CD_2Cl_2): δ = 37 (d q, J_{PH} = 554 Hz, $^1J_{PH}$ = 15 Hz).

^1H NMR (CD_2Cl_2): δ = 8.86 (s, aromatic, 1H), 8.38 (dd, aromatic, *J* = 31 Hz, *J* = 7.5 Hz, 2H), 7.95 (s, aromatic, 1H), 6.57 (m, aromatic, 1H), 1.5 (dd, CH_3, $^1J_{HP}$ = 15 Hz, 6H), 1.67 (d, *J* = 554 Hz, 1 H).

Coordination Chemistry

Synthesis of [Rh(η^4-C_8H_{12})Cl{3-C(O)-C_6H_4-(C(O)PMe)}$_2$]

[Rh(η^4-C_8H_{12})Cl]$_2$ (0.088 g, 0.18 mmol) was dissolved in DCM (5 cm^3) and added to *m*-{-C(O)-C_6H_4-(C(O)PMe)}$_2$ (0.064 g, 0.18 mmol) in DCM (5 cm^3), resulting in a red solution, next hexane was added resulting in a fine precipitate which was filtered, washed and dried in vacuo. 28.5 mg, 26% (crude yield) was obtained. This solid was dissolved in the minimum amount of DCM and layered with hexane (1:3) yielding red crystals suitable for diffraction.

^{1}H NMR (CD_2Cl_2): δ = 10.59 (br, aromatic, 2H), 7.59 (br, aromatic, 4H), 7.32 (t, aromatic, 7.18 Hz, 2H), 5.78 (br, COD, 2H), 3.74 (br, COD, 2H), 2.50 (br, COD, 4H), 2.16 (br, COD, 4H), 1.91 (d, CH_3PRh, *J* = 6.05 Hz, 3H), 1.69 (br, CH_3P, 3H).

^{31}P NMR (CD_2Cl_2): δ = 50.3 (d, CH_3PRH, $^1J_{P\text{-}RH}$ = 135 Hz), 32.3 (s, CH_3P).

Crystal Data for $C_{26}H_{26}ClO_4P_2Rh$ (M_w = 602.77 g/mol): monoclinic, space group $P2_1/n$ (no. 14), a = 9.2257(5) Å, b = 20.1926(11) Å, c = 13.9484(7) Å, β = 106.546(6)°, V = 2490.9(2) Å3, Z = 4, T = 293(2) K, μ(CuKα) = 8.009 mm-1, D_{calc} = 1.607 g/cm3, 9255 reflections measured (7.93° ≤ 2Θ ≤ 143.15°), 4735 unique (R_{int} = 0.0413, R_{sigma} = 0.0521) which were used in all calculations. The final R_1 value was 0.0681 (I > 2σ(I)) and wR_2 was 0.2002 (all data).

Synthesis of [Ir(η^4-C_8H_{12})Cl{3-C(O)-C_6H_4-(C(O)PMe)}$_2$]

[Ir(η^4-C_8H_{12})Cl]$_2$ (0.094 g, 0.14 mmol) was dissolved in DCM (5 cm^3) and added to *m*-{-C(O)-C_6H_4-(C(O)PMe)}$_2$ (0.1 g, 0.28 mmol) resulting in a red solution, next hexane (5 cm^3) was added resulting in a fine precipitate which was filtered, washed and dried in vacuo. 0.04 g of impure product was isolated. This solid was dissolved in the minimum amount of DCM and layered with hexane (1:3) yielding 0.011 g of red crystals suitable for diffraction, 8% yield.

^{1}H NMR (CD_2Cl_2): δ = 10.55 (s, aromatic CC<u>H</u>C, 2H), 7.58 (t, aromatic CC<u>H</u>CHC<u>H</u>C, $^1J_{HH}$ = 9.92 Hz, 4H), 7.33 (t, aromatic CCHC<u>H</u>CHC, $^1J_{HH}$ = 7.62 Hz, 2H), 5.53 (s, COD, 2H), 3.26 (s, COD, 2H), 2.47 (br, m, COD, 2H), 2.29 (br, m, COD, 2H), 4.57 (br, m, COD, 2H), 1.92 (d, Ir-PC<u>H</u>$_3$, J = 6.64 Hz, 3H), 1.83 (quin, COD, *J* = , 2H), 1.66 (s, PC<u>H</u>$_3$,3H).

^{31}P{^{1}H} NMR (CD_2Cl_2): δ = 43.2 (s, (M-<u>P</u>(Me)R_2) and 32.97 (s, Me<u>P</u>R_2).

Crystal Data for $C_{26}H_{26}ClIrO_4P_2$ (M =692.06 g/mol): monoclinic, space group $P2_1/n$ (no. 14), a = 9.2079(4) Å, b = 20.2526(8) Å, c = 13.8415(6) Å, β = 106.501(5)°, V = 2474.91(19) Å3, Z = 4, T = 293(2) K, μ(CuKα) = 12.925 mm-1, D_{calc} = 1.857 g/cm3, 9121 reflections measured (7.964° ≤ 2Θ ≤ 143.508°),

4717 unique (R_{int} = 0.0283, R_{sigma} = 0.0334) which were used in all calculations. The final R_1 value was 0.0262 (I > 2σ(I)) and wR_2 was 0.0745 (all data).

Synthesis of [{Pt(PEt$_3$)Cl$_2$}$_2${3-C(O)-C$_6$H$_4$-(C(O)PPh)}$_2$]

[Pt(PEt$_3$)Cl$_2$]$_2$ (31 mg, 0.04 mmol) were dissolved in the minimum amount of THF and added dropwise to solid (*m*-{-C(O)-C$_6$H$_4$(C(O)PPh)}$_2$) (19 mg, 0.04 mmol), resulting in a straw coloured solution which was concentrated in vacuo. 25.2 mg (50% crude yield) of crystals resulted from the slow evaporation of DCM, however, they were only microcrystalline.

^{1}H NMR (CD_2Cl_2): δ = 1.15 (br, PCH$_2$C<u>H</u>$_3$), 1.94 br, PC<u>H</u>$_2$CH$_3$), (9-7.45 br,m aromatic CH's). ^{31}P NMR (CD_2Cl_2): δ = 40.8 (d, $^2J_{P\text{-}P}$ 425 Hz, $^1J_{P\text{-}Pt}$ 1406 Hz, <u>P</u>Ph), 16.5 (d, $^2J_{P\text{-}P}$ 425 Hz, $^1J_{P\text{-}Pt}$ 1406 Hz, <u>P</u>Et$_3$). 10.7 [Pt(PEt$_3$)Cl$_2$]$_2$ (5%).

Phosphaalkenes

Synthesis of {RPC(OSiMe$_3$)}$_2$C$_6$H$_4$ (R= ^{t}Bu, Mes)

RP(SiMe$_3$)$_2$ (R = ^{t}Bu, Mes) was reacted with half an equivalent of isophthaloyl chloride in ether, resulting in a yellow colouration. Reaction aliquots were analysed *via* NMR spectroscopy, indicating phosphaalkene formation, *ca* 16 hours were required for complete conversion. Attempts to isolate *via* vac-transfer, distillation and trituration all led to decomposition or unidentified species which could be dimeric formation, commonly observed for phosphaalkenes.

^{31}P{^{1}H} NMR (d_6-DMSO capillary): δ = 197 (^{t}Bu).

^{31}P{^{1}H} NMR (C_6D_6 capillary): δ = 153 (Mes).

Synthesis of [(CO)$_5$WP(Mes)C(OSiMe$_3$)}$_2$C$_6$H$_4$]

In situ generated {MesPC(OSiMe$_3$)}$_2$C$_6$H$_4$ was reacted with W(CO)$_5$(THF) generated *via* literature procedure, retaining its yellow colour, NMR analysis suggests tungsten coordination, though attempt to isolate the complex led to decomposition.

^{31}P{^{1}H} NMR (C_6D_6 capillary): δ = 110 (s, J_{PW} = 255 Hz)

Nitrogenous Analogues of the Diphosphametacyclophanes

Synthesis of N,N-Diphenylisophthalamide

Aniline (0.91 cm^3, 10 mmol) was added dropwise to isopthaloyl chloride (1.012 g, 5 mmol) dissolved in pyridine (5 cm^3), resulting in a light-pink coloured solution. After 30 minutes DCM (15 cm^3) was added to facilitate stirring, after a further 90 minutes more DCM (15 cm^3) was added and the resultant

precipitate was filtered *via* Buchner funnel resulting in 1.318 g of colourless solid in 83% yield. NMR spectral data agrees with the literature.[327]

^{1}H NMR ($(D_3C)_2SO$): δ = 7.69 (t, $^1J_{HH}$ = 8.10 Hz, 1H), 8.14 (dd, $^1J_{HH}$ = 7.84 Hz, 2H), 8.55 (s, 1H), 10.43 (s, 2H), 7.81 (d, $^1J_{HH}$ = 7.53 Hz, 4H), 7.37 (t, $^1J_{HH}$ = 8.32 Hz, 4H), 7.12 (t, $^1J_{HH}$ = 7.72 Hz, 2H).

Synthesis of N,N'-Diphenylpyridine-2,6-dicarboxyamide

Aniline (0.91 cm^3, 10 mmol) was added dropwise to pyridine-dicarbonyl-dichloride (1.02 g, 5 mmol) dissolved in pyridine (5 cm^3), resulting in a slight exotherm, the solution also turned more viscous and obtained a brown colouration. After 20 minutes DCM (15 cm^3) was added to facilitate stirring, after a further 90 minutes more DCM (15 cm^3) was added and the resultant precipitate was filtered *via* Buchner funnel resulting in 1.168 g of colourless solid in 74% yield.

NMR data agrees with the literature.[327]

^{1}H NMR ($(D_3C)_2SO$): δ = 11.02 (S, 2H), 8.41 (d, $^1J_{HH}$ = 7.93 Hz, 2H), 8.31 (t, $^1J_{HH}$ = 8.27 Hz, 1H), 7.93 (d, $^1J_{HH}$ = 8.27, 4H), 7.45 (t, $^1J_{HH}$ = 8.27 Hz, 4H), 7.20 (t, $^1J_{HH}$ = 7.93 Hz, 2H).

Synthesis of $\{C_6H_4C(O)NC(O)C_6H_5\}_2$ (2.21)

N,N-Diphenylisopthalamide (0.198 g, 0.625 mmol) was suspended in THF (*ca* 20 cm^3), ^{n}BuLi (2.5M in hexanes, 0.5 cm^3, 1.25 mmol) was added and stirred for 1 hour at RT resulting in a cloudy orange solution. The reaction mixture was heated to reflux and benzoyl chloride (0.18 cm^3, 1.25 mmol) was added and brought to reflux for 4 hours.

Water (150 cm^3) was added, followed by MeOH (20 cm^3) resulting in a yellow precipitate which was filtered. The yellow solid was washed with MeOH (30 cm^3) and dried under vacuum resulting in 0.257 g, 78% yield.

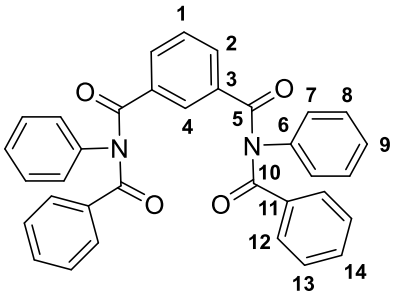

^{1}H NMR (CD_2Cl_2): δ = 8.02 (s, aromatic **4**, 1H), 7.80 (dd, aromatic **2**, $^1J_{HH}$ = 1.69 Hz, $^1J_{HH}$ = 7.83 Hz, 2H), 7.66 (d, aromatic **7**, $^1J_{HH}$ = 7.32 Hz, 4H), 7.5 (t, aromatic **1**, $^1J_{HH}$ = 7.4Hz, 1H), 7.35 (m, aromatic **13**, **8**, **14** and **9**, 12H), 7.12 (d, aromatic **12** , $^1J_{HH}$ = 7.49 Hz, 4H). $^{13}C\{^1H\}$ NMR (CD_2Cl_2): δ = 173.8 (**5** C=O), 172.5 (**10** C=O), 148.5 (**6** NC(CH)$_5$), 135.6 (3), 135.2 (**11**), 133.3 (**2**), 133.1 (**1**), 130.5 (**4**), 130.2 (**13**), 129.7 (**7**), 129.5(**8**), 129.2 (**4**), 128.5 (**9**), 128.4 (**12**) Assigned using HSQC for assistance. LRMS-EI *m/z*: 524 $[M]^+$.

X-Ray quality crystals were grown at ambient temperature from the slow evaporation of DMF. Crystal Data: $C_{34}H_{24}N_2O_4$ (M_w = 524.55 g/mol): monoclinic, space group $P2_1/c$ (no. 14), a = 9.1759(4) Å, b =

23.9133(8) Å, c = 13.1029(5) Å, β = 107.400(4)°, V = 2743.55(19) Å^3, Z = 4, T = 293(2) K, μ(CuKα) = 0.676 mm^{-1}, D_{calc} = 1.270 g/cm^3, 14012 reflections measured (7.394° ≤ 2Θ ≤ 122.272°), 4203 unique (R_{int} = 0.0441, R_{sigma} = 0.0380) which were used in all calculations. The final R_1 value was 0.0504 (I > 2σ(I)) and wR_2 was 0.1477 (all data).

Attempted synthesis of *m*-{-C(O)-C$_6$H$_4$-(C(O)NPh)}$_2$

Triethylamine (0.305 cm^3, 2.190 mmol) was added dropwise to a pre-cooled ethereal solution of isopthaloyl chloride (0.222 g, 1.095 mmol), aniline (0.1 cm^3, 1.095 mmol) was added after a few minutes and left to stir for 30 minutes before warming to RT. The product produced diphenylisophthalamide (**36**), the $[Cl]^-[HNEt_3]^+$ salt and some very small impurities in the aromatic region.

Attempted synthesis of *m*-{-C(O)-C$_6$H$_4$-(C(O)NPh)}$_2$

N,N-Diphenylisophthalamide was reacted with another equivalent of isophthaloyl chloride using both triethylamine and ^{n}BuLi over a range of temperatures to try to make a nitrogen macrocycle, unfortunately in all cases only starting material was recovered.

Attempted synthesis of *m*-C(O)-C$_6$H$_4$-(C(O)NPhC(O)CH$_2$CH$_2$CH$_2$C(O)NPh

N,N-Diphenylisopthalamide (0.198 g, 0.625 mmol) was suspended in THF (*ca* 20 cm^3), ^{n}BuLi (2.5M in hexanes, 0.5 cm^3, 1.25 mmol) was added and stirred for 1 hour at RT resulting in a cloudy orange solution. The reaction mixture was heated to reflux and Glutaryl chloride (0.08 cm^3, 0.625 mmol) was added and brought to reflux for 4 hours. Water (150 cm^3) was then added, followed by MeOH (20 cm^3) resulting in brown solid which was isolated *via* filtration.

LRMS (m/z): 316.

Experimental Details for Chapter 3

Synthesis of [Pt(PEt$_3$)Cl$_2$]$_2$

$PtCl_2$ (1.19 g, 4.48 mmol) and PEt_3 (0.6 cm^3, 4.07 mmol) was brought to reflux for 3 hours in 4-chlorotoluene (15 cm^3). The solvent was removed under reduced pressure to afford a brown solid. Product was dissolved in DCM and filtered through Celite®, the solid was washed till the filtrate ran clear. Solvent was removed under reduced pressure and the product was recrystallised from DCM to afford bright yellow crystals. Crystals were washed with DCM (5 cm^3) and dried under vacuum. Yield: 0.635 g, 41%. Product was confirmed by comparison of spectroscopic data with the literature.[219]

^{1}H NMR ($CDCl_3$): δ_H = 1.82 (m, CH_2, 2H), 1.23 (dt, CH_3, $^{1}J_{HH}$ = 7.6 Hz, $^{2}J_{HP}$ = 18.1 Hz, 3H).

^{31}P{^{1}H} NMR ($CDCl_3$): δ_P = 10.2 (s, $^{1}J_{PtP}$ 3845 Hz).

Synthesis of 1-Methylphosphinane-2,6-dione (3.2a)

To a cooled (–78°C) solution of $MeP(SiMe_3)_2$ (1.01 g, 5.25 mmol) in Et_2O (5 cm^3) was added glutaryl chloride (0.7 cm^3, 5.25 mmol). After stirring for 30 minutes at this temperature, the mixture was allowed to warm to ambient temperature and stir for a further 16 hours. The mixture was filtered and the Et_2O removed from the filtrate under reduced pressure. The product was purified by distillation (60 °C, 5 x 10^{-3} mbar) affording **3.2a** a colourless liquid. Yield: 0.337 g, 45%.

NMR ($CDCl_3$, 303 K):

^{1}H NMR: δ_H = 2.75 (br, CH_2, 4H, unresolved), 2.36 (br, CH*H*, 1 H, unresolved), 1.92 (br, C*H*H, 1 H, unresolved), 1.44 (s, CH_3, 3H).

^{13}C{^{1}H} NMR: δ_C = 220.6 (d, C(O), $^{1}J_{CP}$ = 43 Hz), 44.5 (d, CH_2, $^{2}J_{CP}$ = 29 Hz), 18.1 (d, CH_2, $^{3}J_{CP}$ = 3 Hz), 1.0 (d, CH_3, $^{1}J_{CP}$ = 9 Hz).

^{31}P NMR: δ_P = 39.5 (qnt, J_{PH} = 7.3 Hz).

^{31}P{^{1}H} NMR (C_6D_6; 303 K): δ_P = 36.9 (s).

NMR (C_7D_8):

^{1}H NMR (303 K): δ_H = 2.06 (br, CH_2, 4H, unresolved), 1.54 (br, CH*H*, 1 H, unresolved), 1.26 (s, CH_3, 3H), 1.00 (br, C*H*H, 1 H, unresolved).

^{1}H NMR (238 K): δ_H = 1.99 (m, CH_2, 2H), 1.86 (m, CH_2, 2H) , 1.38 (br, CH*H*, 1 H), 1.29 (s, CH_3, 3H), 0.80 (br, C*H*H, 1 H).

^{13}C{^{1}H} NMR (303 K): δ = 218.5 (d, C(O), $^{1}J_{CP}$ = 42 Hz), 44.0 (d, CH_2, J_{CH} = 29 Hz), 17.8 (d, CH_2, $^{3}J_{CP}$ = 3 Hz), 0.67 (d, CH_3, $^{1}J_{CP}$ = 9 Hz).

^{31}P{^{1}H} NMR (303 K): δ_P = 36.6 (s).

IR (THF): ν_{CO} 1739 (w), 1668 (s) cm^{-1}.

EI HRMS (m/z): Calc. for $C_6H_9O_2P$ 144.0340 ([M]+). Found 144.0337 ([M]+).

Synthesis of 1-^{n}Butylphosphinane-2,6-dione (3.2b)

As for **3.2a** using ^{n}BuP$(SiMe_3)_2$ (0.25 g, 1.08 mmol) and 0.14 cm^3 (1.08 mmol) glutaryl chloride. Purified by distillation (85-90 °C, 1.3 x 10^{-2} mbar). Yield: 0.089 g, 44%. ^{1}H NMR (C_6D_6): δ_H = 2.08 (m, C*H*$_2$ Butyl

2H, overlapping CH_2 (ring) 4H), 1.57 (m, CH_2 (ring) 1H), 1.51 (m, CH_2 butyl, 2H), 1.31 (br. Unres, CH_2 (ring) 1H), 1.28 (sextet CH_2 (butyl), $^1J_{HH}$ = 7.40 Hz, 2H), 0.81 (t, CH_3, $^1J_{HH}$ = 7.40 Hz, 3H). $^{13}C\{^1H\}$ NMR (C_6D_6): δ_C = 219.3 (d, C(O), $^1J_{CP}$ = 42 Hz), 44.4 (d, CH_2 (ring), $^2J_{CP}$ = 29 Hz), 29.2 (d, CH_2 (butyl), $^1J_{CP}$ = 13 Hz), 24.3 (d, CH_2 (butyl), $^2J_{CP}$ = 12 Hz), 18.9 (d, CH_2 (butyl), $^3J_{CP}$ = 8 Hz), 17.8 (d, CH_2 ring, $^3J_{CP}$ = 3 Hz), 13.7 (s, CH_3).

$^{31}P\{^1H\}$ NMR (C_6D_6): δ_P = 47.7 (s).

IR (THF): ν_{CO} 1768 (w), 1660 (s) cm^{-1}.

EI HRMS (m/z): Calc. for $C_9H_{15}O_2P$ 186.0810 ([M]+). Found 186.0818 ([M]+).

Synthesis of 1-^{t}Butylphosphinane-2,6-dione (3.2c)

As for **3.2a** using ^{t}BuP($SiMe_3$)$_2$ (0.295 g, 1.26 mmol) and 0.16 cm^3 (1.26 mmol) glutaryl chloride. After removal of volatile components from the filtrate, the residue was washed with cold hexane (5 cm^3, 0 °C) and dried in vacuo, yielding **3.2c** as a wax-like white solid. Yield: 0.092 g, 40%.

^1H NMR ($CDCl_3$): δ = 2.67 (q, CH_2, *J* = 6.2 Hz, 4H), 2.09 (br, CH_2, 2H), 1.34 (d, *J* = 13.6 Hz, 9H).

$^{13}C\{^1H\}$ NMR (C_6D_6): δ_C = 218.8 (d, C(O) $^1J_{CP}$ = 48 Hz), 45.8 (d, CH_2, $^2J_{CP}$ = 27 Hz), 34.5 (d, $\underline{C}(CH_3)_3$, $^1J_{CP}$ = 12 Hz), 28.1 (d, CH_3, $^2J_{CP}$ = 8 Hz), 17.7 (d, CH_2, $^3J_{CP}$ = 3 Hz).

$^{31}P\{^1H\}$ NMR (C_6D_6): δ_P = 68.2 (s).

IR (THF): ν_{CO} 1736 (w), 1655 (s) cm^{-1}.

EI HRMS (m/z): Calc. for $C_9H_{15}O_2P$ 186.0810 ([M]+). Found 186.0795 ([M]+).

Synthesis of 1-Phenylphosphinane-2,6-dione (3.2d)

As for **3.2a** using PhP($SiMe_3$)$_2$ (1.039 g, 4.1 mmol) and 0.52 cm^3 (4.1 mmol) glutaryl chloride. The solvent was removed under reduced pressure, affording a white solid, which was dried *in vacuo*. Yield: 0.750 g, 91%.

^1H NMR (CD_2Cl_2): δ_H = 7.40-7.55 (m, aromatic, 5H), 2.86 (br, CH_2, 4H), 2.22 (br, CH_2, 2H).

$^{13}C\{^1H\}$ NMR (CD_2Cl_2): δ_C = 218.5 (d, CO, $^1J_{CP}$ = 44 Hz), 137.1 (d, C^o, $^2J_{CP}$ = 18 Hz), 131.7 (d, C^p, $^4J_{CP}$ = 3 Hz), 129.5 (d, C^m, $^3J_{CP}$ = 9 Hz), 126.9 (s, C^i), 45.6 (d, CH_2, $^2J_{CP}$ = 31 Hz), 18.4 (d, CH_2, $^3J_{CP}$ = 3 Hz).

$^{31}P\{^1H\}$ NMR: δ_P(CD_2Cl_2) = 52.5 (s); δ_P(C_6D_6) = 49.2 (s).

IR (THF): ν_{CO} 1737 (w), 1667 (s) cm^{-1}.

EI HRMS (m/z): Calc. for $C_{11}H_{11}O_2P$ 206.0497 ([M]+). Found 206.0486 ([M]+).

Crystal data for $C_{11}H_{11}O_2P$ (M_w = 206.17 g/mol): orthorhombic, $Pna2_1$ (no. 33), a = 14.2522(3) Å, b = 5.97643(12) Å, c = 12.0658(2) Å, V = 1027.73(3) Å^3, Z = 4, T = 173(2) K, μ(CuKα) = 2.134 mm^{-1}, D_{calc} = 1.332 Mg m^{-3}, 1817 independent reflections, full matrix F^2 refinement, R_1 = 0.0588 on 1736 independent absorption corrected reflections [I > 2σ(I); 2θ_{max} = 134.0 °), 127 parameters, wR_2 = 0.1635 (all data).

Synthesis of 1-Mesitylphosphinane-2,6-dione (3.2e)

As for **3.2a** using $MesP(SiMe_3)_2$ (0.05 g, 0.169 mmol) and 0.021 cm^3 (0.169 mmol) glutaryl chloride. After removal of volatile components from the filtrate, the residue was extracted into pentane (3 x 10 cm^3), the extracts combined and the solvent removed under reduced pressure, affording **2e** as a colourless solid, dried in vacuo. Yield: 0.014 g, 33%.

^{1}H NMR (C_6D_6): δ_H = 6.71 (br s, aromatic C-H, 2H), 2.27 (q, C$\underline{H}_2$CH$_2$C$\underline{H}_2$, $^1J_{HH}$ = 6.8 Hz, 4H), 2.22 (s, CH$_3$, 6H), 2.01 (s, CH$_3$, 3H), 1.41 (br m, CH$_2$C$\underline{H}_2$CH$_2$, 2H).

^{13}C{^{1}H} NMR (C_6D_6): δ_C = 217.0 (d, C(O), $^1J_{CP}$ = 41 Hz), 145.8 (s, aromatic), 142.0 (d, aromatic, J_{CP} 2 Hz), 129.8 (d, aromatic, 7 Hz), 121.0 (aromatic, from HMBC), 45.2 (d, $\underline{C}$H$_2$CH$_2$$\underline{C}H_2$, $^2J_{CP}$ = 34 Hz), 23.9 (d, CH$_3$, $^3J_{CP}$ = 13 Hz), 21.2 (s, CH$_3$), 18.1 (CH$_2$$\underline{C}H_2CH_2$, $^3J_{CP}$ = 2 Hz).

^{31}P{^{1}H} NMR (C_6D_6): δ_P = 31.3 (s).

IR (THF): ν_{CO} 1738 (w), 1659 (s) cm^{-1}.

EI HRMS (m/z): Calc. for $C_{14}H_{17}O_2P_1$ 248.0966 ([M]+). Found 248.0960 ([M]+).

Crystal data for $C_{14}H_{17}O_2P$ (M_w = 248.24 g/mol): monoclinic, $P2_1/c$ (no. 14), a = 10.8705(3) Å, b = 9.7423(2) Å, c = 11.9167(2) Å, β = 93.452(2), V = 1259.83(5) Å^3, Z = 4, T = 100(2) K, μ(CuKα) = 1.828 mm^{-1}, D_{calc} = 1.309 Mg m^{-3}, 2407 independent reflections, full matrix F^2 refinement, R_1 = 0.0344 on 2237 independent absorption corrected reflections [I > 2σ(I); 2θ_{max} = 143.4 °), 157 parameters, wR_2 = 0.0915 (all data).

Synthesis of 1-Methylphosphepane-2,7-dione (3.3a)

To a cooled (–78 °C) solution of $MeP(SiMe_3)_2$ (0.199 g, 1.03 mmol) in Et_2O (5 cm^3) was added adipoyl chloride (0.15 cm^3, 1.03 mmol). After stirring for 30 minutes at this temperature, the mixture was allowed to warm to ambient temperature and stir for a further 16 hours. The mixture was filtered through an alumina plug, washing with Et_2O (5 x 5 cm^3), then concentrated under reduced pressure to afford **3a** as a colourless oil. Yield: 0.02 g, 12%.

^{1}H NMR ($CDCl_3$): δ_H = 2.81 (br, CH_2, 4H), 1.61 (br, CH_2, 4H), 1.53 (d, CH_3, $^{2}J_{HP}$ = 2.0 Hz, 3H). ^{1}H NMR (C_6D_6): δ_H = 2.26 (br, CH_2, 4H), 1.50 (br, CH_2, 2H), 1.36 (d, CH_3, $^{2}J_{HP}$ = 1.95 Hz, 3H), 1.30 (br, CH_2, 2H).

$^{13}C\{^{1}H\}$ NMR (C_6D_6): δ_C = 217.3 (d, C(O), $^{1}J_{CP}$ = 48 Hz), 48.0 (d, 2 x CH_2, $^{2}J_{CP}$ = 35 Hz), 22.5 (d, 2 x CH_2, $^{3}J_{CP}$ = 3 Hz), 1.8 (d, CH_3, $^{1}J_{CP}$ = 6 Hz).

$^{31}P\{^{1}H\}$ NMR (C_6D_6): δ_P = 39.7 (s).

IR (THF): ν_{CO} 1659 (s) cm^{-1} (symm not observed).

EI HRMS (m/z): Calc. for $C_7H_{11}O_2P$ 158.0497 ([M]+). Found 158.0495 ([M]+).

Synthesis of 1-^{n}Butylphosphepane-2,7-dione (3.3b)

As for **3.3a**, using ^{n}BuP($SiMe_3$)$_2$ (0.38 g, 1.4 mmol) and 0.2 cm^3 (1.4 mmol) adipoyl chloride. Yield: 0.09 g, 31%.

^{1}H NMR (C_6D_6): δ_H = 2.27 (br, CH_2 (ring), 4H), 2.16 (m, C$\underline{H}_2$ (butyl), 2H), 1.51 (m, CH_2 (butyl), 2H), 1.40 (br. Unresolved, CH_2 (ring), 4H), 1.33 (sextet, CH_2 (butyl), J = 7.2 Hz, 2H), 0.83 (t, CH_3, $^{1}J_{HH}$ 7.2 Hz, 3H).

$^{13}C\{^{1}H\}$ NMR (C_6D_6): δ_C = 218. 5 (d, C(O), $^{1}J_{CP}$ = 48 Hz), 47.7 (d,CH_2 ring, $^{2}J_{CP}$ = 32 Hz), 28.7 (d, CH_2, $^{1}J_{CP}$ = 15 Hz), 24.4 (d, CH_2, $^{2}J_{CP}$ = 13 Hz), 22.4 (d, CH_2 ring, $^{3}J_{CP}$ = 3 Hz), 19.3 (d, CH_2, $^{3}J_{CP}$ = 7 Hz), 13.9 (s, CH_3).

^{31}P NMR (C_6D_6): δ_P = 48.9 (apparent nonet, J_{PH} = 6 Hz).

IR (THF): ν_{CO} 1736 (w), 1657 (s) cm^{-1}.

EI HRMS (m/z): Calc. for $C_{10}H_{17}O_2P$ 200.0966 ([M]+). Found 200.0980 ([M]+).

Synthesis of 1-^{t}Butylphosphepane-2,7-dione (3.3c).

As for **3.3a**, using ^{t}BuP($SiMe_3$)$_2$ (0.330 g, 1.4 mmol) and 0.2 cm^3 (1.40 mmol) adipoyl chloride. After stirring overnight, the mixture was filtered and the solvent removed under reduced pressure. The crude product was extracted into cold hexane (10 cm^3) and the extracts stripped of volatile components then dried in vacuo, affording **3.3c** as a colourless solid. Yield: 0.114 g, 40%.

^{1}H NMR ($CDCl_3$): δ_H = 2.74 (br, CH_2, 4H), 2.08 (br, CH_2, 4H), 1.29 (d, $^{2}J_{HP}$ = 13.24 Hz, 9H).

$^{13}C\{^{1}H\}$ NMR ($CDCl_3$): δ_C = 221.7 (d, C(O), $^{1}J_{CP}$ = 50 Hz), 48.0 (d, CH_2, $^{2}J_{CP}$ = 27 Hz), 34.5 (d, $\underline{C}(CH_3)_3$, $^{1}J_{CP}$ = 13 Hz), 27.8 (d, C($\underline{C}H_3$)$_3$, $^{2}J_{CP}$ = 9 Hz), 22.6 (d, CH_2 $^{3}J_{CP}$ = 4 Hz).

$^{31}P\{^{1}H\}$ NMR: δ_P($CDCl_3$) = 62.3 (s). δ_P(C_6D_6) = 60.9.

IR (THF): ν_{CO} 1736 (w), 1652 (s) cm^{-1}.

HRMS (m/z): Calc. for $C_{10}H_{17}O_2P$ 200.0966 ([M]+). Found 200.0863 ([M]+).

Synthesis of 1-Phenylphosphepane-2,7-dione (3.3d)

As for **3.3c**, using $PhP(SiMe_3)_2$ (0.27 g, 1.1 mmol) and 0.15 cm^3 (1.1 mmol) adipoyl chloride. Yield: 0.025 g, 11%.

^1H NMR ($CDCl_3$): δ = 7.57-7.35 (m, aromatic, 5H), 2.93 (br, CH_2, 4H), 2.20 (br, CH_2, 4H).

$^{13}C\{^1H\}$ NMR ($CDCl_3$): δ_C = 218.3 (d, C(O), $^1J_{CP}$ = 47 Hz), 137.0 (d, C^i, $^1J_{CP}$ = 19 Hz), 131.1 (d, C^m, $^3J_{CP}$ = 3 Hz), 128.9 (d, C^o, $^2J_{CP}$ = 9 Hz), 127.5 (s, C^p), 47.6 (d, CH_2, $^2J_{CP}$ = 34 Hz), 22.8 (d, CH_2, $^3J_{CP}$ = 4 Hz).

$^{31}P\{^1H\}$ NMR ($CDCl_3$): δ_P = 52.2 (s); $\delta_P(C_6D_6)$ = 49.0.

IR (THF): ν_{CO} 1735 (w), 1665 (s) cm^{-1}.

HRMS (m/z): Calc. for $C_{12}H_{13}O_2P$ 220.0653 ([M]+). Found 220.0650 ([M]+).

Synthesis of *cis*-[$PtCl_2$(Ph)P{C(O)$(CH_2)_3$C(O)}] (3.4)

Dichloromethane solutions (5 cm^3) of **3.2d** (20 mg, 0.049 mmol) and $[Pt(PEt_3)Cl_2]_2$ (37 mg, 0.049 mol) were combined and stirred for 16 h. The resulting yellow solution was concentrated under reduced pressure, affording a yellow solid that was recrystallised from DCM/pentane. Yield: 24 mg, 83% yield.

^1H NMR (CD_2Cl_2): δ_H = 7.72 (m, aromatic, 2H), 7.64 (m, aromatic, 1H), 7.54 (dt, aromatic, J_{HH} = 7.40 Hz, 2H), 3.47 (m, CH_2 (ring) 2H), 2.80 (m, CH_2 (ring) + CH*H*, 3H), 1.90 (m, C*H*H, 1 H), 1.81 (dq, CH_2 (PEt_3), J_{PH} 10.2 Hz, J_{HH} 7.7 Hz, 6H), (dt, CH_3 (PEt_3), J_{PH} 18.1 Hz, $^1J_{HH}$ = 7.7 Hz, 9H).

$^{13}C\{^1H\}$ NMR (CD_2Cl_2): δ_C = 208.8 (dd, C(O), $^1J_{CP}$ = 6 Hz, 1 Hz), 136.1 (d, C^m, $^3J_{CP}$ = 10 Hz, J_{PtC} 33 Hz), 133.9 (d, C^p, $^4J_{CP}$ = 3 Hz), 129.6 (d, C^o, $^2J_{CP}$ = 11 Hz), 121.0 (d, C^i, $^1J_{CP}$ = 55 Hz), 45.7 (d, CH_2, $^2J_{CP}$ = 38 Hz), 18.1 (d, J_{CP} = 1.6 Hz, CHH), 16.1 (d, CH_2 (PEt_3), $^1J_{CP}$ = 40 Hz, J_{PtC} 35 Hz), 8.5 (d, CH_3 (PEt_3), $^2J_{CP}$ = 3 Hz, J_{PtC} 25 Hz).

$^{31}P\{^1H\}$ NMR (CD_2Cl_2): δ = 26.8 (d, R_2PhPPt, $^2J_{PP}$ = 15 Hz, J_{PtP} = 3413 Hz), 9.0 (d, $PtPEt_3$, $^2J_{PP}$ = 15 Hz, $J_{(PtP)}$ = 3166 Hz).

^{195}Pt NMR (CD_2Cl_2): δ_P = –4432 (dd, $^1J_{PtP}$ = 3410, 3164 Hz).

IR (THF): ν_{CO} 1717, 1694 cm^{-1}.

Anal. Calc. for $C_{17}H_{26}Cl_2O_2P_2Pt$: C, 34.59; H, 4.44. Found: C, 34.62; H, 4.49.

Crystal data for $C_{17}H_{26}Cl_2O_2P_2Pt$ (M_w = 590.31 g/mol): orthorhombic, $P2_12_12_1$ (no. 19), a = 7.4569(9) Å, b = 10.591(2) Å, c = 26.251(4) Å, V = 2073.2(6) $Å^3$, Z = 4, T = 173(2) K, μ(CuKα) = 16.553 mm^{-1}, D_{calc} =

1.891 Mg m^{-3}, 3724 independent reflections, full matrix F^2 refinement, R_1 = 0.1055 on 1793 independent absorption corrected reflections [I > 2σ(I); 2θ_{max} = 136.4 °), 172 parameters, wR_2 = 0.3003 (all data).

Synthesis of [(η^4-C_8H_{12})RhCl(Ph)P{C(O)$(CH_2)_3$C(O)}] (3.5).

3.2d (30 mg, 0.14 mmol) and [Rh(η^4-C_8H_{12})Cl]$_2$ (35 mg, 0.07 mmol) were combined in DCM (*ca* 5 cm^3), instantly assuming a red colouration. Concentrated under reduced pressure and red crystals were grown from DCM/pentane. Yield: 24 mg, 38%.

NMR (CD_2Cl_2, 303 K):

^{1}H NMR: δ_H = 7.76 (m, aromatic-^{o}CH, 2H), 7.57 (m, aromatic-^{p}CH, 1H), 7.51 (m, aromatic-^{m}CH, 2H), 4.49 (unresolved, COD, 3H), 3.25 (unresolved, CH_2, 2H), 2.75 (br s, no coupling resolved, COD, CH_2, 3H), 2.43 (unresolved, COD, CH_2, 5H), 2.09 (unresolved, COD, CH_2, 5H).

^{31}P{^{1}H} NMR: δ_P = 49.2 (s, $w_{1/2}$ = 4 Hz).

^{13}C{^{1}H} NMR: δ_C = 214.4 (d, C(O), $^1J_{CP}$ = 6 Hz), 136.4 (d, C^o, $^2J_{CP}$ = 11 Hz), 132.3 (d, C^p, $^4J_{CP}$ = 2 Hz), 129.2 (d, C^m, $^3J_{CP}$ = 11 Hz), 129.0 (s, Rh-C=C), 123.2 (d, C^i, $^1J_{CP}$ = 40 Hz), 45.5 (d, ($\underline{C}H_2)_2$, $^2J_{CP}$ = 33 Hz), 31.3 (br s, COD-saturated backbone, $w_{1/2}$ = 28 Hz), 28.4 (s, COD-saturated backbone),17.9 (s, CH_2).

NMR (CD_2Cl_2, 193 K):

^{1}H NMR: δ_H = 7.74 (m, aromatic-^{o}CH, 2H), 7.61 (m, aromatic-^{p}CH, 1H), 7.53 (m, aromatic-^{m}CH, 2H), 5.59 (br s, COD, 2H), 3.36 (s, COD, 2H), 3.14 (m, CH_2, 2H), 2.90 (m, CH_2, 1H), 2.69 (m, CH_2, 2H), 2.4 (br t, COD, 4H), 2.12 (br d, COD, 2H), 2.03 (m, COD, CH_2, 2H, 1H).

^{31}P{^{1}H} NMR: δ_P = 55.7 (d, $^1J_{PRh}$ = 137 Hz).

Crystal Data for $C_{19}H_{23}O_2PClRh$ (M_w = 452.70 g/mol): monoclinic, space group $P2_1/c$ (no. 14), a = 10.0696(2) Å, b = 14.1423(3) Å, c = 13.0777(2) Å, β = 104.991(2)°, V = 1798.98(6) Å^3, Z = 4, T = 293(2) K, μ(CuKα) = 9.950 mm^{-1}, D_{calc} = 1.671 g/cm^3, 6400 reflections measured (9.092° ≤ 2Θ ≤ 143.36°), 3436 unique (R_{int} = 0.0246, R_{sigma} = 0.0356) which were used in all calculations. The final R_1 value was 0.0509 (I > 2σ(I)) and wR_2 was 0.1426 (all data).

Synthesis of [$W(CO)_5$(L)]

In a typical procedure, a THF solution (2 cm^3) of **3.2a** (20 mg, 0.14 mmol) was combined with excess of [$W(CO)_5$(THF)] (*ca* 0.1 M, 2.8 cm^3, *ca* 0.28 mmol) and the mixture stirred for 16 h. The volatile components were removed under reduced pressure and the crude product extracted first into Et_2O (5

cm^3) then, following concentration of the extract, into cold pentane (5 cm^3, 0 °C). Removal of the solvent afforded **3.6a** as a pale-yellow solid. Yield: 23 mg, 35%.

^{1}H NMR (C_6D_6): δ_H = 2.40 (ddd, CH_2, $^2J_{CP}$ = 16.2 Hz, 12.2, 4.8 Hz, 2H), 1.97 (tdd, CH_2, $^2J_{CP}$ = 15,3, 5.7, 3.4 Hz, 2H), 1.40 (d, CH_3, $^1J_{CP}$ = 8 Hz, 3H), 1.18 (m, CH_2, 1H), 0.62 (m, CH_2, 1H).

$^{13}C\{^1H\}$ NMR (C_6D_6): δ_C = 214.8 (d, C(O), $^1J_{CP}$ = 3 Hz), 197.9 (d, $W(CO)_{trans}$,$^2J_{CP}$ = 22 Hz, $^1J_{CW}$ = 149 Hz), 195.4 (d, $W(CO)_{cis}$, $^2J_{CP}$ = 6 Hz, $^1J_{WC}$ = 125 Hz), 42.3 (d, CH_2, $^2J_{CP}$ = 36 Hz), 17.8 (d, CH_2, $^3J_{CP}$ = 3 Hz), 9.0 (d, CH_3, $^1J_{CP}$ = 29 Hz).

$^{31}P\{^1H\}$ NMR (C_6D_6): δ_P = 20.7 (s, $^1J_{WP}$ = 202 Hz).

IR(THF) ν/cm^{-1}: 2076, 1946, 1933 [WCO], 1702, 1685 [CO].

Anal. Calc. for $C_{11}H_9O_7PW$: C, 28.23; H, 1.94. Found: C, 28.55; H, 2.17.

Crystal data for $C_{11}H_9O_7PW$ (M_w = 460.00 g/mol): monoclinic, $P2_1/n$ (no. 14), a = 6.89715(9) Å, b = 12.94011(18) Å, c = 15.8307(2) Å, β = 101.0523(13) °, V = 1386.69(3) $Å^3$, Z = 4, T = 173(2) K, μ(CuKα) = 16.818 mm^{-1}, D_c = 2.242 Mg m^{-3}, 2671 independent reflections, full matrix F^2 refinement, R_1 = 0.0204 on 2620 independent absorption corrected reflections [I > 2σ(I); 2θ_{max} = 143.2 °), 182 parameters, wR_2 = 0.0508 (all data).

Synthesis of 3.6b.

From **3.2b** (13 mg, 0.07 mmol). Obtained as a yellow oil. Yield: 18 mg, 50%.

^{1}H NMR (C_6D_6): δ_H = 2.34 (ddd, CH_2(ring), J = 16.3, 12.09, 4.2 Hz, 2H), 2.06 – 1.96 (m x 2, CH_2 (butyl) + CH_2 (ring), 4H), 1.25 (m, CH_2 (butyl), 2H), 1,22 (m, CH*H*, 1H), 1.01 (sextet, CH_2, $^2J_{HH}$ = 7.47 Hz, 2H), 0.79 (m, CH*H*, 1H), 0.67 (t, CH_3, $^2J_{HH}$ = 7.36 Hz, 3H).

$^{13}C\{^1H\}$ NMR (C_6D_6): δ_C = 214.8 (d, C(O), $^1J_{CP}$ = 4 Hz), 197.9 (d, WCO_{trans}, $^1J_{CP}$ = 21 Hz, J_{WP} = 148 Hz), 195.4 (d, WCO_{cis}, $^2J_{CP}$ = 6 Hz, $^1J_{WC}$ = 125 Hz), 43.1 (d, CH_2 (ring), $^2J_{CP}$ = 33 Hz), 28.9 (d, CH_2 (butyl), $^3J_{CP}$ = 7 Hz), 26.3 (d, CH_2 (butyl), $^1J_{CP}$ = 23 Hz), 24.2 (d, CH_2 (butyl), $^2J_{CP}$ = 13 Hz), 17.6 (d, CH_2 (ring), $^3J_{CP}$ = 3 Hz), 13.4 (s, CH_3).

$^{31}P\{^1H\}$ NMR (C_6D_6): δ_P = 33.1 (s, $^1J_{WP}$ = 202 Hz).

IR(THF) ν/cm^{-1}: 2075, 1953, 1950, 1942 [WCO], 1683, 1660 [CO].

Anal. Calc. for $C_{14}H_{15}O_7PW$: C, 32.97; H, 2.96. Found: C, 33.15; H, 3.17.

Synthesis of 3.6c.

From **3.2c** (35 mg, 0.19 mmol). Yield: 60 mg, 62%.

^{1}H NMR (C_6D_6): δ_H = 2.29 (ddd, CH_2 *J* = 16.5, 11.5, 4.3 Hz, 2H), 1.95 (dddd, CH_2, *J* = 16.6, 9.9, 6.7. 3.4 Hz, 2H), 1.15 (m, CH_2, 1H), 1.14 (d, $C(C\underline{H}_3)_3$, *J* = 15.3 Hz, 9H), 0.90 (m, CH_2, 1H).

^{13}C{^{1}H} NMR (C_6D_6): δ_C = 215.8 (d, C(O), $^{1}J_{CP}$ = 8 Hz), 197.2 (d, WCO_{trans}, $^{2}J_{CP}$ = 22 Hz, J_{PW} 146 Hz), 196.0 (d, WCO_{cis}, $^{2}J_{CP}$ = 6 Hz, $^{1}J_{WC}$ = 125 Hz), 44.1 (d, CH_2, $^{2}J_{CP}$ = 30 Hz), 37.9 (d, $\underline{C}(CH_3)_3$, $^{1}J_{CP}$ = 14 Hz), 27.6 (d, $C(\underline{C}H_3)_3$, $^{2}J_{CP}$ = 2 Hz)), 16.9 (d, CH_2, $^{3}J_{CP}$ = 3 Hz).

^{31}P{^{1}H} NMR (C_6D_6): δ_P = 51.3 (s, $^{1}J_{WP}$ = 207 Hz).

IR(THF) *v*/cm^{-1}: 2075, 1942, 1934 [WCO], 1676, 1655 [CO].

Anal. Calc. for $C_{14}H_{15}O_7PW$: C, 32.97; H, 2.96. Found: C, 32.84; H, 3.15.

Crystal data for $C_{14}H_{15}O_7PW$ (M_w = 510.08 g/mol): orthorhombic, Pbca (no. 61), a = 12.3442(2) Å, b = 12.5495(2) Å, c = 21.9424(4) Å, *V* = 3399.18(10) Å^3, *Z* = 8, *T* = 173(2) K, μ(CuKα) = 13.786 mm^{-1}, D_{calc} = 1.993 Mg m^{-3}, 3219 independent reflections, full matrix F^2 refinement, R_1 = 0.0301 on 2866 independent absorption corrected reflections [I > 2σ(I); 2θ_{max} = 143.4 °), 211 parameters, wR_2 = 0.0852 (all data).

Sythesis of 3.6d.

From **3.2d** (31 mg, 0.15 mmol). Yield: 20 mg, 25%.

^{1}H NMR (C_6D_6): δ_H = 7.58 (m, Ph, 2H), 6.97 (m, Ph, 3H), 2.35 (ddd, CH_2, *J* = 16.5, 11, 4 Hz, 2H), 2.03 (dddd, CH_2, *J* = 16.5, 11, 7, 3.5 Hz, 2H), 1.19 (m, C*H*, 1H), 0.87 (dtt, C*H*, *J* = 14, 11, 3.5 Hz, 1H).

^{13}C{^{1}H} NMR (C_6D_6): δ_C = 213.2 (d, C(O), $^{1}J_{CP}$ = 5 Hz), 197.8 (d, $W\underline{C}(O)_{trans}$, $^{1}J_{CP}$ = 23 Hz, , $^{1}J_{WC}$ = 148 Hz), 195.7 (d, $W\underline{C}O_{cis}$, $^{1}J_{CP}$ = 6 Hz, $^{1}J_{WC}$ = 125 Hz), 133.1 (d, C^{o}, $^{2}J_{CP}$ = 10 Hz), Hz), 131.5 (d, C^{p}, $^{4}J_{CP}$ = 3 Hz), 129.3 (d, C^{m}, $^{3}J_{CP}$ = 10 Hz), 127.2 (d, C^{i}, $^{1}J_{CP}$ = 40 Hz), 43.2 (d, CH_2, $^{2}J_{CP}$ = 34 Hz), 17.1 (d, CH_2, $^{3}J_{CP}$ = 3 Hz).

^{31}P{^{1}H} NMR (C_6D_6): δ_P = 28.9 ($^{1}J_{PW}$ = 214 Hz).

IR(THF) *v*/cm^{-1}: 2076, 1949 (br) [WCO], 1688 (br) [CO] cm^{-1}.

Anal. Calc. for $C_{16}H_{11}O_7PW$: C, 36.25; H, 2.09. Found: C, 36.02; H, 1.87.

Crystal data for $C_{16}H_{11}O_7PW$ (M_w = 530.06 g/mol): monoclinic, $P2_1/n$ (no. 14), a = 11.0044(3) Å, b = 9.7434(3) Å, c = 32.7494(10) Å, β = 91.882(3) °, *V* = 3509.51(18) Å^3, *Z* = 4, *T* = 100(2) K, μ(CuKα) = 13.364 mm^{-1}, D_{calc} = 2.004 Mg m^{-3}, 6635 independent reflections, full matrix F^2 refinement, R_1 = 0.0672

on 5673 independent absorption corrected reflections [I > 2σ(I); $2\theta_{max}$ = 143.6 °), 463 parameters, wR_2 = 0.1678 (all data).

Synthesis of [W(CO)$_5$(3.3b)] (3.6)

A THF solution (2 cm^3) of **3.3b** (15 mg, 0.075 mmol) was combined with excess of [W(CO)$_5$(THF)] (*ca* 0.1 M, 3.0 cm^3, *ca* 0.30 mmol) and the mixture stirred for 16 h. The volatile components were removed under reduced pressure and the crude product extracted into Et$_2$O (5 cm^3); the extract was passed sequentially through four plugs of Celite®, then the solvent removed under reduced pressure to afford **3.7** as a pale-yellow solid. Yield: 3 mg, 13%.

^{1}H NMR (C$_6$D$_6$): δ_H = 2.54 (br m, CH$_2$ (ring), 2H), 2.09 (br m, CH$_2$ (ring), 2H), 2.01 (m, PC̲H$_2$, 2H), 1.32 (m, CH$_2$ (ring), 2H), 1.30 (m, CH$_2$ (butyl), 2H), 1.14 (br m, CH$_2$ (ring), 2H), 1.06 (Sextet, -CH$_2$C̲H$_2$CH$_3$, $^1J_{HH}$ = 7.40 Hz, 2H), 0.70 (t, CH$_3$, $^1J_{HH}$ = 7.40 Hz).

^{13}C{^{1}H} NMR (C$_6$D$_6$): δ_C = 215.7 (d, C(O), $^1J_{CP}$ = 3 Hz), 198.0 (d, WC̲(O), $^1J_{CP}$ = 23 Hz, $^1J_{CW}$ 147 Hz), 195.8 (d, WC̲O, $^1J_{CP}$ = 6Hz, $^1J_{WC}$ = 125 Hz), 44.2 (d, CH$_2$ $^2J_{CP}$ = 37 Hz), 27.8 (d, CH$_2$, $^3J_{CP}$ = 3 Hz), 27.6 (d, CH$_2$, $^1J_{CP}$ = 22 Hz), 24.2 (d, CH$_2$, $^2J_{CP}$ = 13 Hz), 24.0 (s, CH$_2$), 13.4 (s, CH$_3$).

^{31}P{^{1}H} NMR (C$_6$D$_6$): δ_P = 39.2 (s, $^1J_{WP}$ = 216 Hz).

IR(THF) ν/cm^{-1}: 2075, 1951, 1946, 1938 [WCO], 1691, 1678 [CO].

EI MS [M]$^+$ Calc. for C$_{15}$H$_{17}$O$_7$PW 522 (77), 523 (55), 524 (100), 525 (17), 526 (85), 527 (15); Found 522 (70), 523 (47), 524 (100), 525 (21), 526 (83), 527 (15).

Experimental Details for Chapter 4

Synthesis of ^{t}BuP=C(OSiMe$_3$)CF$_3$ (4.2a)

To a cooled (–78 °C) solution of ^{t}BuP(SiMe$_3$)$_2$ (0.185 g, 0.79 mmol) in Et$_2$O (5 cm^3) was added TFAA (0.11 cm^3, 0.79 mmol). After stirring for 30 minutes at this temperature, the mixture was allowed to warm to ambient temperature and stirred for a further 16 hours. A reaction aliquot was taken to ensure no starting material remained. Attempts to purify product *via* static vacuum distillation led to decomposition.

^{31}P{^{1}H} NMR (C$_6$D$_6$): δ_P = 211.5 (q, $^3J_{PF}$ = 47 Hz).

^{19}F NMR (C$_6$D$_6$): δ_P = –68.3 (d, $^3J_{FP}$ = 47 Hz).

Synthesis of MesP=C(OSiMe$_3$)CF$_3$ (4.2b)

As for **4.2a** using Mes(SiMe$_3$)$_2$ (0.102 g, 0.084 mmol) and 0.012 cm^3 (0.084 mmol) TFAA.

^{31}P{^{1}H} NMR (C_6D_6): δ_P = 228.4 (q, $^3J_{PF}$ = 38 Hz).

^{19}F NMR (C_6D_6): δ_P = −69.4 (d, $^3J_{FP}$ = 38 Hz).

Synthesis of PhP=C(OSiMe$_3$)CF$_3$ (4.2c)

As for **4.2a** using Ph(SiMe$_3$)$_2$ (0.102 g, 0.084 mmol) and 0.012 cm^3 (0.084 mmol) TFAA. Static vacuum distillation removed solvent and by-products. A dimeric species starts to form from initial synthesis.

Phosphaalkene:

^{31}P{^{1}H} NMR (C_6D_6): δ_P = 168.2 (q, $^3J_{PF}$ = 46 Hz).

^{19}F NMR (C_6D_6): δ_P = −70.6 (d, $^3J_{FP}$ = 46 Hz).

Dimer:

^{31}P{^{1}H} NMR (C_6D_6): δ_P = 31.0 (septet, $^3J_{PF}$ = 13 Hz).

^{19}F NMR (C_6D_6): δ_P = −75.4 (d, $^3J_{FP}$ = 13 Hz).

Synthesis of Me$_3$SiP=C(OSiMe$_3$)CF$_3$ (4.2d)

As for **4.2a** using P(SiMe$_3$)$_3$ (2 cm^3, 6.89 mmol) and 0.96 cm^3 (6.89 mmol) TFAA. Static vacuum distillation led to purification, by the removal of solvent and by-products, affording a yellow liquid, **4.2d**. Stored in the glovebox freezer. Yield: 1.538 g, 81%.

^{1}H NMR (C_6D_6): δ_H = E-isomer: 0.2 (d, (C$\underline{H}_3$)$_3$Si-P-, J = 4Hz), 0.16 (poorly resolved q, P=C(OSi(C$\underline{H}_3$)$_3$), 0.91 Hz).

^{13}C{^{1}H} NMR (C_6D_6): δ_C = E-isomer: 189.2 (qd, P=C), 120.9 (q, $^1J_{CF}$ = 280 Hz, CF_3), 0.6 (q, OSi($\underline{C}$H$_3$)$_3$, 2 Hz), -0.03 (d, ($\underline{C}$H$_3$)$_3$Si-P-, 8.43 Hz).

^{31}P{^{1}H} NMR (C_6D_6): δ_P = 161.3 (q, E-isomer, $^3J_{PF}$ = 39 Hz), 153.6 (br, Z-isomer, poorly resolved coupling)

^{19}F NMR (C_6D_6): δ_P = −67.1 (d, E-isomer, $^3J_{FP}$ = 39 Hz), −66.9 (br s, Z-isomer).

^{29}Si NMR (C_6D_6): δ_{Si} = 26.4 (d, J_{SiP} = 4 Hz), 24.0 (s), 6.99 (s), -0.54 (dq, J_{SiP} = 43 Hz, J_{SiF} = 3 Hz) .

$Me_3SiP=C(OSiMe_3)CF_3$ (4.2d) + $LiN(SiMe_3)_2$ at ambient conditions (4.10)

An ethereal solution of $LiN(SiMe_3)_2$ (0.065 g, 0.386 mmol) was added to compound **3d** (0.106 g, 0.386 mmol) in diethyl ether (5 cm^3) at −78 °C, resulting in an orange colouration. After 10 minutes, the solution was allowed to warm to ambient temperature and concentrated resulting in a brown solid.

NMR (C_6D_6, 303 K):

^1H NMR: δ_H = 0.18 (br d, TMS-P), 0.02 (br s, OTMS).

$^{13}C\{^1H\}$ NMR: δ_C = 154 (ddd, P=C, 25 Hz, 278 Hz), 116.5 (ddd, CF_2, *J* = 44 Hz, 43Hz, 3Hz), 33.7 (s), 30.4 (s), 27.4 (s), 14.8 (s), 3.37 (d, *J* = 7 Hz), 2.2 (s), 0.36 (dd, *J* = 19 Hz, 1 Hz), 0.56 (dd, *J* = 4 Hz, 1 Hz).

$^{31}P\{^1H\}$ NMR: δ_P = 4.12 (broad triplet).

^{19}F NMR: δ_P = −90.2 (dd, $^3J_{PF}$ = 15 Hz, $^1J_{FF}$ = 79 Hz), −109.9 (dd, 8, 79 Hz)

NMR (C_6D_6, 213 K):

$^{31}P\{^1H\}$ NMR: δ_P = 3.71 (dd, J_{PF} = 8, 15 Hz).

Potential Synthesis of 4.1, F_3C-C≡P (4.1)

Compound **4.2d** was added to a J Young's NMR tube (63 mg, 0.23 mmol) and dissolved in a few drops of d_8-THF and cooled to −78 °C. Next an ethereal solution (0.6 cm^3) of $LiN(SiMe_3)_2$ (38.4 mg, 0.23 mmol) was added. The cooled Young's NMR tube was placed into a pre-cooled NMR probe (−80 °C) and analysed, from −80 °C to ambient temperature, observing decomposition above −20 °C.

$^{31}P\{^1H\}$ NMR: δ_P = 6.0 (q, $^3J_{PF}$ = 37 Hz).

^{19}F NMR: δ_P = −71.7 (d, $^3J_{FP}$ = 37 Hz).

Compound **4.10** and **4.2d** were also present.

$Me_3SiP=C(OSiMe_3)CF_3$ (4.2d) + NaOPh

Compound **4.2d** (0.1 g, 0.36 mmol) was dissolved in C_6D_6 (0.6 cm^3) and NaOPh (42.3 mg, 0.36 mmol) was added, resulting in an intense-red colouration, which consequently turned dark red.

$^{31}P\{^1H\}$ NMR: δ_P = 131 (dm), −52 (br s), −58 (br s).

$Me_3SiP=C(OSiMe_3)CF_3$ (4.2d) + NaO^tBu

Compound **4.2d** (20 mg, 0.073 mmol) was dissolved in C_6D_6 (0.6 cm^3) and NaOtBu (7 mg, 0.073 mmol) was added, resulting in an orange colouration.

$^{31}P\{^{1}H\}$ NMR: δ_P = 62.0 (dd, J = 1.54 Hz, J_{PF} = 59 Hz).

^{19}F NMR: δ_P = −90.6 (d, J_{FF} = 56 Hz), −106.6 (dd, J_{FF} = 56 Hz, J_{FP} = 59 Hz).

$Me_3SiP=C(OSiMe_3)CF_3$ (4.2d) + Butadiene

Compound **4.2d** (21 mg, 0.077 mmol) was introduced to a J. Young's NMR tube and dissolved in C_6D_6 (0.6 cm^3) and a freeze-pump-thaw cycle was performed. Next the NMR tube was connected to a cooled (−5 °C) cannister of butadiene *via* a piece of T-junction tubing. The butadiene was allowed to fill the tubing apparatus (*ca* 1 bar) and then allowed to diffuse into the NMR tube. After 5 days, 20% of **4.2d** still remained, static-vacuum distillation was performed.

Reaction Ampoule (remains after vacuum applied):

$^{31}P\{^{1}H\}$ NMR: δ_P = 161.3 (q, **4.2d** - E-isomer, $^{3}J_{PF}$ = 39 Hz), 153.6 (br s, **4.2d** - Z-isomer, poorly resolved coupling), −62.8 (q, $^{3}J_{PF}$ = 18 Hz), -66.9 (q, $^{3}J_{PF}$ = 19 Hz), −76.1 (q, $^{3}J_{PF}$ = 13 Hz), −77.5 (q, $^{3}J_{PF}$ = 10 Hz).

^{19}F NMR: δ_P = −66.9 (br s, **4.2d** - Z-isomer), −67.1 (d, **4.2d** - E-isomer, $^{3}J_{FP}$ = 39 Hz), −76.1 (br m), −77.7 (dm, $^{3}J_{FP}$ = 19 Hz), −78.6 (d, $^{3}J_{FP}$ = 13 Hz).

Destination Ampoule (where the volatile components were collected):

$^{31}P\{^{1}H\}$ NMR: δ_P = 161.3 (q, **4.2d** - E-isomer, $^{3}J_{PF}$ = 39 Hz), 153.6 (br s, **4.2d** - Z-isomer, poorly resolved coupling), −62.8 (q, $^{3}J_{PF}$ = 18 Hz), −76.1 (q, $^{3}J_{PF}$ = 13 Hz).

EI-MS *m/z*: 328 $[M]^+$.

$Me_3SiP=C(OSiMe_3)CF_3$ (4.2d) + 1,4-Diphenyl-1,3-Butadiene

Compound **4.2d** (30 mg, 0.11 mmol) was introduced to a J. Young's NMR tube and dissolved in C_6D_6 (0.6 cm^3) and 1,4-diphenyl-1,3-butadiene (23 mg, 0.11 mmol) was added, after 1 week and almost no reaction the sample was irradiated by a high-pressure Hg lamp for 16 hours. Then transferred to an ampoule and volatile components removed under reduced pressure, resulting in a beige oil.

$^{31}P\{^{1}H\}$ NMR: δ_P = 46.3 (m), 44.75 (m), 44.9 (br s), 43.7 (br s), −79.5 (dq, J_{PP} = 130 Hz, J_{PF} 16 Hz).

^{19}F NMR: δ_F = −70.6 (d, 25 Hz), −71.5 (d, 22 Hz), −73.9 (d, 23 Hz), −74.5 (d, 22 Hz), −75.2 (d, 21 Hz), −75.9 (dd, J_{PF} = 16 Hz, J_{FF} = 2 Hz).

EI-MS *m/z*: 548 $[M]^+$ (2+2/dimerisation product). 480$[M]^+$ (4+2 product).

$Me_3SiP=C(OSiMe_3)CF_3$ (4.2d) + PhNCO

Compound **4.2d** (25 mg, 0.09 mmol) was introduced to a J. Young's NMR tube and dissolved in C_6D_6 (0.6 cm^3) and phenylisocyanate (9.98 µl, 0.09 mmol) was added, after essentially no reaction for a couple of days, the sample was irradiated by a high-pressure Hg lamp. Volatile components were removed under reduced pressure, resulting in an orange oil.

$^{31}P\{^1H\}$ NMR: δ_P = 46.3 (m), 44.7 (m), 44.9 (br s), 43.7 (br s).

^{19}F NMR: δ_F = −70.6 (d, 25 Hz), −71.5 (d, 22 Hz), −73.9 (d, 23 Hz), −74.5 (d, 22 Hz), −75.2 (d, 21 Hz), −76.2 (s).

EI-MS *m/z*: 393 $[M]^+$.

$Me_3SiP=C(OSiMe_3)CF_3$ (4.2d) + Furan

Compound **4.2d** (30 mg, 0.11 mmol) was introduced to a J. Young's NMR tube and dissolved in C_6D_6 (0.6 cm^3) and Furan (7.95 µl, 0.11 mmol) was added. No reaction occurred, even after a week only **4.2d** observed.

$Me_3SiP=C(OSiMe_3)CF_3$ (4.2d) + 1-Hexyne

Compound **4.2d** (20 mg, 0.07 mmol) was introduced to a J. Young's NMR tube and dissolved in C_6D_6 (0.6 cm^3) and 1-Hexyne (8.4 µl, 0.07 mmol) was added, resulting in a dark yellow colouration.

$^{31}P\{^1H\}$ NMR: δ_P = Intractable mixture of peaks.

$Me_3SiP=C(OSiMe_3)CF_3$ (4.2d) + CO

Compound **4.2d** (20 mg, 0.07 mmol) was introduced to a J. Young's NMR tube and dissolved in C_6D_6 (0.6 cm^3) and a freeze-pump-thaw cycle was performed. The NMR tube was connected to a cannister of CO *via* T junction tubing and the gas filled the tubing apparatus (*ca* 1 bar) and was then allowed to diffuse into the NMR tube. No reaction occurred.

$Me_3SiP=C(OSiMe_3)CF_3$ (4.2d) + $[RuHCl(CO)(PPh_3)_3]$

$LiN(SiMe_3)_2$ (62.2 mg, 0.37 mmol) was added to a pre-cooled (−78 °C) ethereal solution of **4.2d** (0.102 g, 0.37 mmol) and stirred for 30 minutes at this temperature. Next the reaction mixture was transferred cold into a DCM solution of $[RuHCl(CO)(PPh_3)_3]$ (0.354 g, 0.37 mmol) and stirred cold for 1 h then allowed to warm to ambient temperature and volatile components were removed under reduced pressure. The resulting crude product was washed with hexane (20 cm^3) and vigorously

stirred before filtration, resulting in a pale brown solid and an orange-brown filtrate which were dried and concentrated under reduced pressure. The filtrate was identified as **4.10** and PPh_3 (−5 ppm).

Solid:

$^{31}P\{^1H\}$ NMR: δ_P = 50.8 (d, J_{PP} = 40 Hz), 47.6 (d, J_{PP} = 40 Hz), 41.0 (d, J_{PP} = 25 Hz), 39.4 (br s), 38.5 (d, J_{PP} = 25 Hz).

^{19}F NMR: δ_P = −54.0 (s).

The same result was observed when transferring the contents of the initial reaction into a solution of $[RuHCl(CO)(PPh_3)_3]$ *via* vac-transfer.

$Me_3SiP=C(OSiMe_3)(CF_3)\{CH_2CH\}_2$ + $W(CO)_5(THF)$

An NMR sample of $Me_3SiPC(OSiMe_3)(CF_3)\{CH_2CH\}_2$ (0.077mmol; in 0.6 cm^3 C_6D_6) was added to a THF solution of $W(CO)_5(THF)$ (0.1 M, 4 cm^3) and concentrated under reduced pressure.

$^{31}P\{^1H\}$ NMR: δ_P = −40.7 (q, $^3J_{PF}$ = 7 Hz, $^1J_{PW}$ 238 Hz).

^{19}F NMR: δ_P = −74.2 (br s), −75.2 (br, s).

$Me_3SiP=C(OSiMe_3)CF_3$ (4.2d) + $W(CO)_5(THF)$

An NMR sample of **4.2d** (8 mg, 0.029 mmol) in C_6D_6, was added to $W(CO)_5(THF)$ (0.1 M, 4 cm^3) resulting in an orange colouration. If analysed at this stage, only **4.9a** was observed (η^1 coordination). After this point **4.9b** starts to form (η^2 coordination), and after 16 hours is the only species present. Alternatively, if solvent is instantly removed after addition, compound **4.9c** is afforded.

Initial – **4.9a**:

$^{31}P\{^1H\}$ NMR: δ_P = 172 (q, $^3J_{PF}$ = 15 Hz, $^1J_{PW}$ 272 Hz).

^{19}F NMR: δ_P = −61.0 (d, $^3J_{FP}$ = 15 Hz).

After 16 hours – **4.9b**:

$^{31}P\{^1H\}$ NMR: δ_P = 162 (q, $^3J_{PF}$ = 29 Hz, $^1J_{PW}$ 260 Hz).

^{19}F NMR: δ_P = −74.2 (br s), −75.2 (br, s).

If solvent is instantly removed – **4.9c**:

$^{31}P\{^1H\}$ NMR: δ_P = 136 (q, $^3J_{PF}$ = 25 Hz, $^1J_{PW}$ 214 Hz).

^{19}F NMR: δ_P = −74.2 (br s), −75.2 (br, s).

$Me_3SiP=C(OSiMe_3)CF_3$ (4.2d) + $Fe(CO)_5$

$Fe(CO)_5$ (0.05 cm^3, 0.34 mmol) was added dropwise to a THF solution of **4.2d** (47 mg, 0.17 mmol).

η^2-$[(CO)_5WP(TMS)=(OTMS)CF_3]$ + $LiN(SiMe_3)_2$

To a solution of **4.9b** (generated *in-situ* , 0.1 mmol) in THF, was added $LiN(SiMe_3)_2$ (16.7 mg, 0.1 mmol), resulting in an orange colouration. **4.9b** still initially present so left to stir for 48 hours. Viscous polymeric film formed after the removal of solvent.

$^{31}P\{^1H\}$ NMR: δ_P = 205 (br s), 102 (t, J = 5 Hz, J_{PW} = 287 Hz), 9.7 (q, J_{PF} = 11 Hz) .

Dimer of $PhPC(OSiMe_3)CF_3$ (4.2c) + $W(CO)_5$(THF)

Only the proposed 'dimer' of **4.2c** reacts with $W(CO)_5$(THF).

After full conversion to the proposed 'dimer' of **4.2c** (δ_P 31), which begins to form immediately after the formation of **3c**, $W(CO)_5$(THF) (0.1 M, 4 cm^3) was added. After stirring for 16 hours, volatile components were removed under reduced pressure, resulting in a dark brown solid.

$^{31}P\{^1H\}$ NMR: δ_P = 47.8 (septet, J_{PF} = 4 Hz, $^1J_{PW}$ 242 Hz).

^{19}F NMR: δ_P = −71.4 (d, J_{FP} = 4 Hz).

$Me_3SiP=C(OSiMe_3)CF_3$ (4.2d) + $(Ph_3P)_2Pt$-C_2H_4

$(PPh_3)_2Pt$-C_2H_4 (69 mg, 0.08 mmol) was added to an ethereal solution of **4.2d** (0.08 mmol) and left to stir for 16 hours. Only starting material peaks were observed.

$Me_3SiP=C(OSiMe_3)CF_3$ (4.2d) + (η^4-C_8H_{12})PtMeCl

Compound **4.2d** (32 mg, 0.12 mmol) and (η^4-C_8H_{12})PtMeCl (21 mg, 0.06 mmol) were dissolved in THF, resulting in an intense red colouration.

$^{31}P\{^1H\}$ NMR: δ_P = −25 (s).

$Me_3SiP=C(OSiMe_3)CF_3$ (4.2d) + $Pt(dppe)_2$

$Pt(dppe)_2$ (94 mg, 0.1 mmol) was added to a d_8-THF NMR sample of **4.2d** (26 mg, 0.1 mmol), only $Pt(dppe)_2$ was observed in the ^{31}P NMR.

$^{31}P\{^1H\}$ NMR: δ_P = 32 ($^1J_{PtP}$ = 3732 Hz).[218]

$Me_3SiP=C(OSiMe_3)CF_3$ (4.2d) + $[Pt(PEt_3)Cl_2]_2$

$[Pt(PEt_3)Cl_2]_2$ (31 mg, 0.04 mmol) was added to a d_2-DCM sample of **4.2d** (22 mg, 0.08 mmol), only the resonance for $[Pt(PEt_3)Cl_2]_2$ was observed.

$^{31}P\{^1H\}$ NMR: δ_P = 11 (s, $^1J_{PPt}$ = 3840 Hz).[219]

$Me_3SiP=C(OSiMe_3)CF_3$ (4.2d) + $[PdCl(allyl)]_2$

Compound **4.2d** (20 mg, 0.07 mmol) and $[PdCl(allyl)]_2$ (13.3 mg, 0.04 mmol) were introduced to a J. Youngs' NMR tube and dissolved in C_6D_6, no ^{31}P NMR resonances were observed.

$Me_3SiP=C(OSiMe_3)CF_3$ (4.2d) + Se

Compound **4.2d** (15 mg, 0.06 mmol) and Se (43 mg, 0.06 mmol) were introduced to a J. Young's NMR tube and dissolved in d_2-DCM then heated to 90 °C, however, **4.2d** decomposes with heat (previously observed by variable temperature NMR). Repeating the reaction without heating still resulted in the loss of **4.2d** resonances and no observation of new species.

$Me_3SiP=C(OSiMe_3)CF_3$ (4.2d) + Se in the presence of NEt_3

Compound **4.2d** (15 mg, 0.055 mmol) and Se (43 mg, 0.055 mmol) were introduced to a J. Young's NMR tube and dissolved in d_2-DCM, next a couple of drops of NEt_3 were added.

$^{31}P\{^1H\}$ NMR: δ_P = −24.6 (s), −112.8 (s), −113.2 (s).

$Me_3SiP=C(OSiMe_3)CF_3$ (4.2d) + I_2

Compound **4.2d** (10 mg, 0.036 mmol) and I_2 (9.3 mg, 0.036 mmol) were introduced to a J. Young's NMR tube and dissolved in C_6D_6, resulting in a yellow colouration, the unidentified species were only present *in-situ* and were not stable after exposure to vacuum.

$^{31}P\{^1H\}$ NMR: δ_P = 228.6 (s), 176.4 (q, $^3J_{PF}$ = 51 Hz), 173.2 (s), 101.8 (s), 81.2 (m), 64.1 (dd, *J* = 7 Hz, 106 Hz), 62.1 (d, *J* = 11 Hz), -7.8 (d, *J* = 7 Hz).

$Me_3SiP=C(OSiMe_3)CF_3$ (4.2d) + F_3B-OEt_2

F_3B-OEt_2 (0.03 cm^3, 0.28 mmol) was added to an ethereal solution of compound **4.2d** (76 mg, 0.28 mmol).

After exposure to vacuum no species remained.

$^{31}P\{^1H\}$ NMR: δ_P = 62.5 (t, *J* = 16 Hz), 57.0 (q, $^1J_{PF}$ = 20 Hz), 29.9 (q, *J* = 19 Hz) , 20 (s), 12.4 (s)

$Me_3SiP=C(OSiMe_3)CF_3$ (4.2d) + BPh_3

Compound **4.2d** (0.187 g, 0.68 mmol) and BPh_3 (0.165 g, 0.68 mmol) were introduced to an ampoule, dissolved in Et_2O (*ca* 10 cm^3) and left to stir overnight. The sample was then concentrated under reduced pressure.

$^{31}P\{^1H\}$ NMR: δ_P = 46.2 (m), −7.8 (q, *J* = 7 Hz), −26 (s), −111 (m), −148.9 (quartet of multiplets).

After vacuum:

$^{31}P\{^1H\}$ NMR: δ_P = −26 (s).

$SiMe_3P=C(OSiMe_3)CF_3$ (4.2d) + $AlPh_3$

$AlPh_3$ (9.4 mg, 0.036 mmol) was added to a C_6D_6 solution of compound **4.2d** (10 mg, 0.036 mmol).

$^{31}P\{^1H\}$ NMR: δ_P = 161.3 (q, **4.2d** - E-isomer, $^3J_{PF}$ = 39 Hz), 153.6 (br s, **4.2d** - Z-isomer, poorly resolved coupling), 74.6 (s), −30.0 (s), −69.7 (d, *J* = 42.6 Hz).

After Vacuum:

$^{31}P\{^1H\}$ NMR: δ_P = −30.0 (s), −59.3 (dd, *J* = 39.6, 3 Hz), −70.0 (d, *J* = 43 Hz).

Phosphaallene, phosphirene or oxaphosphirane (4.10) + $W(CO)_5(THF)$

Compound **4.10** (25 mg, 0.15 mmol) was added to a solution of $W(CO)_5(THF)$ (0.1 M, 4 cm^3), resulting in a dark red colouration.

Aliquot:

$^{31}P\{^1H\}$ NMR: δ_P = 11.0 (m), 4.1 (m).

Concentrated:

$^{31}P\{^1H\}$ NMR: δ_P = 12.6 (d, *J* = 7, 261 Hz)

Compound 4.10 + $(Ph_3P)_2Pt\text{-}C_2H_4$

Compound **4.10** (20 mg, 0.12 mmol) and $(PPh_3)_2Pt\text{-}C_2H_4$ (90 mg, 0.12 mmol) were combined in a Schlenk flask and THF (*ca*5 cm^3) was added.

Compound 4.10 + $(\eta^4\text{-}C_8H_{12})PtCl_2$

Compound **4.10** (14 mg, 0.08 mmol) and $Pt(\eta^4\text{-}C_8H_{12})Cl_2$ (32 mg, 0.08 mmol) were combined in a Schlenk flask and dissolved in Et_2O/THF solvent mixture and stirred for 2 hours.

No species were observed in the NMR spectra.

Compound 4.10 + AuCl(tht)

Compound **4.10** (0.23 mmol) and AuCl(tht) (38.5 mg, 0.23 mmol) were combined in a J. Young's NMR tube, C_6D_6 was added. Intractable mixture was observed by NMR spectroscopy.

Experimental Details for Chapter 5

Synthesis of 1,2-Bis(phosphino)benzene

To a pre-cooled (−78 °C) THF solution of $LiAlH_4$ (5.4 g, 143.5 mmol) and Me_3SiCl (18.2 cm^3, 143.5 mmol), a THF solution of 1,2-Bis(dimethoxyphosphoryl)benzene (7 g, 23.79 mmol) was slowly added dropwise resulting in exotherm, the reaction mixture was allowed to warm to ambient temperature after addition and stir for a further 16 hours. The reaction mixture was cooled to 0 °C and de-gassed water was slowly added dropwise until effervescence stopped, next a NaOH solution (1 M in H_2O; 40 cm^3) was added facilitating separation of the two sovent layers. The organic layer was extracted and dried over $MgSO_4$, the product solution was then filtered into a distillation rig and fractional distillation was performed to remove the solvent and then subsequently purify the product (55 °C, 3 x 10^{-1} mbar) as a colourless liquid. Yield: 1.48 g, 44%.

^{1}H NMR (C_6D_6): δ = 7.2 (quintet, *J* = 4 Hz, 2H), 6.8 (dd, *J* = 4 Hz, 5.5 Hz, 2H), 4.0 (higher order pattern, PH_2, 2H), 3.5 (Higher order pattern, PH_2, 2H).

$^{31}P\{^1H\}$ NMR (C_6D_6): δ = −125.9 (s).

In agreement with the literature.[272]

Synthesis of $[C_6P_2BC_6H_5]^{2-}$ 2[Li(THF)$_{1.5}$] ([5.6].2[Li(THF)$_{1.5}$])

To a THF solution (*ca* 10 cm^3) of 1,2-bis(phosphino)benzene (0.35 cm^3, 2.71 mmol) was added ^{n}BuLi (2.5 M, 2.17 cm^3, 5.43 mmol) effecting yellow colouration. After stirring for 2 hours, the yellow solution was slowly added to neat dichlorophenylborane (0.35 cm^3, 2.71 mmol), resulting in an exothermic reaction. After a further 2 hours ^{n}BuLi (2.5 M, 2.17 cm^3, 5.43 mmol) was added dropwise and the resultant mixture left to stir for 3 hours. Volatile components were removed under reduced pressure, product extracted into diethyl ether (20 cm^3) and washed with hexane (3 x 40 cm^3), to afford an intense yellow solid. Yield: 0.53 g, 48%.

^{1}H NMR (C_4D_8O): δ = 7.96 (d, *J* = 7.27 Hz, 2H), 7.89 (sextet, *J* = 2.79 Hz, 2H), 6.96 (t, *J* = 7.28 Hz, 2H), 6.83 (t, B-Ar^{p}, *J* = 7.28 Hz, 1H), 6.46 (unresolved, 2H), THF signals (don't integrate correctly but clearly different to solvent peaks).

^{13}C{^{1}H} NMR (C_4D_8O) δ = 163.8 (dd, P-C, $^{1}J_{PC}$ = 26 Hz), 152.3 (B-Ar^{i}, identified from HMBC), 134.2 (t, B-Ar^{m}, $^{4}J_{PC}$ = 12 Hz), 131.7 (t, P-CC $^{2}J_{PC}$ = 14 Hz), 127.1 (s, B-Ar^{o}), 125.0 (s, B-Ar^{p}), 117.3 (br t, P-CCC, $^{3}J_{PC}$ = 5 Hz), 67.9 (m, O(CH_2CH_2)$_2$), 25.8 (m, O(CH_2CH_2)$_2$).

^{31}P{^{1}H} NMR (C_4D_8O): δ = 50.5 (s).

^{11}B NMR (C_4D_8O): δ = 69.4 (br s).

^{7}Li NMR (C_4D_8O): δ = −0.48 (br s).

Crystal Data for $C_{24}H_{32}BLi_2O_3P_2$ (M_w = 455.12 g/mol): monoclinic, space group P2/c (no. 13), a = 11.8623(2) Å, b = 13.6299(3) Å, c = 15.4811(3) Å, β = 101.215(2)°, V = 2455.22(8) Å^3, Z = 4, T = 100.00(10) K, μ(CuKα) = 1.776 mm-1, D_{calc} = 1.231 g/cm^3, 9110 reflections measured (7.598° ≤ 2*Θ* ≤ 143.47°), 4707 unique (R_{int} = 0.0171, R_{sigma} = 0.0232) which were used in all calculations. The final R_1 value was 0.0614 (I > 2σ(I)) and wR_2 was 0.1703 (all data).

Synthesis of $[C_6P_2BC_6H_5]^{2-}$ 2[Li(TMEDA)]$^{2+}$ ([5.6].2[Li(TMEDA)])

TMEDA (0.25 cm^3, 3.26 mmol) and 1,2-bis(phosphino)benzene (0.21 cm^3, 1.63 mmol) were dissolved in THF (*ca* 5 cm^3) and ^{n}BuLi (2.5 M, 1.3 cm^3, 3.26 mmol) was added dropwise resulting in a yellow colouration. Stirred for 2 hours then dichlorophenylborane (0.21 cm^3, 1.63 mmol) was added dropwise, red colouration observed before reverting back to yellow. After 3 hours TMEDA/^{n}BuLi (0.25 cm^3, 3.26 mmol/2.5 M, 1.3 cm^3, 3.26 mmol) were added, reaction mixture exhibiting a red colouration. After 2 hours volatile components were removed under reduced pressure, extracted into ether, extracted into THF (leaving behind Li powder) and washed twice with hexane (3 x 30 cm^3). Affording a pale-yellow solid. Yield: 0.303 g, 39%.

^{1}H NMR (C_4D_8O): δ = 8.02 (d, B-Ar^{m}, $^{1}J_{HH}$ = 7.35 Hz, 2H), 7.95 (br s, P-CCH, 2H), 7.00 (t, B-ArH^{o}, $^{1}J_{HH}$ = 7.35 Hz, 2H), 6.87 (t, B-ArH^{p}, $^{1}J_{HH}$ = 7.40 Hz, 1H), 6.51 (br s, P-CCCH, 2H), 2.28 (s, $(CH_2)_4$, 8H), 2.11 (s, $(CH_3)_8$, 24H).

^{13}C{^{1}H} NMR (C_4D_8O) δ = 163.4 (dd, P-C, $^{1}J_{PC}$ = 26 Hz), 134.2 (t, B-Ar^{m}, $^{4}J_{PC}$ = 12 Hz), 132.1 (t, P-CC $^{2}J_{PC}$ = 14 Hz), 127.2 (s, B-Ar^{o}), 125.2 (s, B-Ar^{p}), 117.6 (br t, P-CCC, $^{3}J_{PC}$ = 5 Hz), 58.8 (s, $(CH_2)_4$), 46.2 (s, $(CH_3)_8$).

^{31}P{^{1}H} NMR (C_4D_8O): δ = 52.1 (s).

^{11}B NMR (C_4D_8O): δ = 66.4 (br s).

^{7}Li NMR (C_4D_8O): δ = −0.17 (s).

Anal. Calc. for $C_{24}H_{41}B_1Li_2N_4P_2$: C, 61.04; H, 8.75; N, 11.86. Found: C, 60.02; H, 8.66; N, 11.3.

Crystal Data for $C_{24}H_{41}BLi_2N_4P_2$ (M_w = 472.24 g/mol): triclinic, space group P-1 (no. 2), a = 9.1053(4) Å, b = 11.0882(5) Å, c = 14.6123(6) Å, α = 80.603(3)°, β = 88.369(4)°, γ = 74.447(4)°, V = 1402.00(11) Å^3, Z = 2, T = 99.9(4) K, μ(Cu Kα) = 1.525 mm-1, D_{calc} = 1.119 g/cm^3, 9226 reflections measured (8.388° ≤ 2Θ ≤ 143.582°), 5325 unique (R_{int} = 0.0182, R_{sigma} = 0.0270) which were used in all calculations. The final R_1 value was 0.0489 (I > 2σ(I)) and wR_2 was 0.1235 (all data).

Attempted Synthesis of $[C_6P_2BC_6H_5]^{2-}$ 2[Na(THF)$_{1.5}$]

^{n}BuNa (0.248 g, 3.1 mmol) was introduced to a Schlenk flask and dissolved in THF. Next, 1,2-bis(phosphino)benzene (0.1 cm^3, 0.77 mmol) was slowly added dropwise resulting in an intense yellow colouration. After 2 hours the reaction mixture was slowly added to Cl_2BPh (0.1 cm^3, 0.77 mmol), resulting in a white suspension. After a further 2 hours another 2 equivalents of ^{n}BuNa was added. After stirring for a further 4 hours the volatile components were removed under reduced pressure and the product was extracted into ether. 1,2-bis(phosphino)benzene was observed by ^{31}P NMR. Similar attempts using NaH, potassium equivalents and attempts to perform ion exchange reactions also only resulted in recovery of 1,2-bis(phosphino)benzene.

Attempted synthesis of $C_6H_4P_2(H)_2BPh$

To a THF solution (*ca* 10 cm^3) of 1,2-bis(phosphino)benzene (0.35 cm^3, 2.71 mmol) was added ^{n}BuLi (2.5 M, 2.17 cm^3, 5.43 mmol) resulting in a yellow colouration. After stirring for 2 hours, the yellow solution was slowly added to neat dichlorophenylborane (0.35 cm^3, 2.71 mmol), resulting in exotherm.

Synthesis of 1,4-bis(di-^{n}butoxy)boryl-phenylene

Benzene-1,4-diboronic acid (5.2 g, 31.48 mmol) was introduced into a distillation rig along with 1-butanol (35 cm^3) and heated to 90-92 °C for 2 hours, after which time the temperature was increased to 140 °C and the reaction was placed under vacuum (1.58x10^{-2} mbar) removing the volatile components from the light-brown viscous oil. Yield: 9.65 g, 79%.

^{1}H NMR (C_6D_6): δ = 8.1 (s, aromatic, 1H), 7.8 (s, aromatic, 2H), 7.7 (s, aromatic, 1H), 4.0 (s, O-C$\underline{H}_2$CH$_2$CH$_2$CH$_3$, 8H), 1.54 (d, O-CH$_2$C$\underline{H}_2$CH$_2$CH$_3$, J_{HH} = 5 Hz, 8H), 1.36 (t, O-CH$_2$CH$_2$C$\underline{H}_2$CH$_3$, J_{HH} = 6 Hz, 8H), 0.85 (m, O-CH$_2$CH$_2$CH$_2$C$\underline{H}_3$, 12 H). Consistent with the literature.[328]

^{11}B NMR (C_6D_6): δ = 28.2 (s).

Synthesis of 1,4-Bis(boryldichloride)benzene

PCl_5 (3.28 g, 15.76 mmol) was added to a CCl_4 (20 cm^3) solution of 1,4-bis(di-^{n}butoxy)boryl-phenylene (1.545 g, 3.96 mmol) and brought to reflux for 16 hours. A precipitate formed which was collected by filtration and dried *in vacuo*, affording a colourless solid which was purified by sublimation. Yield: 0.458 g, 48%.

^{1}H NMR (C_6D_6): δ = 7.9 (s).

^{11}B NMR (C_6D_6): δ = 55.2 (s).

In agreement with the literature.[329]

1,2-Bis(phosphino)benzene + 1,4-Bis(boryldichloride)benzene (5.7)

^{n}Butyllithium (2.5 M, 0.17 cm^3, 0.42 mmol) was added dropwise to a THF (5 cm^3) solution of 1,2-Bis(phosphino)benzene (0.03 cm^3, 0.2 mmol) and stirred for 2 hours. Next 1,4-bis(boryldichloride)benzene (25 mg, 0.1 mmol) was dissolved in THF (5 cm^3) and the yellow reaction mixture was slowly added dropwise resulting in an orange colouration. After a further 2 hours, another 2 equivalents of ^{n}butyllithium (2.5 M, 0.17 cm^3, 0.42 mmol) was added and stirred for 4 hours. The reaction mixture was concentrated and extracted into diethyl ether. Resulting in a yellow solid.

Initially the ^{31}P NMR spectrum displayed a multitude of species, however, after drying under reduced pressure for 8 hours, the dominant resonances were consistent with the formation of **5.7**.

^{31}P{^{1}H} NMR (C_6D_6): δ = −1.05 (higher order coupling, **5.7**), −44.5 (higher order coupling, **5.7**), −55.9 (m), −125.8 (s).

1,2-Bis(phosphino)benzene + 1,4-Bis(boryldichloride)benzene + TMEDA (5.8)

TMEDA (0.13 cm^3, 0.835 mmol) and ^{n}Butyllithium (2.5 M, 0.34 cm^3, 0.835 mmol) were added dropwise to a THF (15 cm^3) solution of 1,2-Bis(phosphino)benzene (0.05 cm^3, 0.418 mmol) and stirred for 2 hours. Next 1,4-bis(boryldichloride)benzene (25 mg, 0.1 mmol) was dissolved in THF (5 cm^3) and the yellow reaction mixture was slowly added dropwise resulting in a red colouration. After a further 2 hours, another two equivalents of TMEDA (0.125 cm^3, 0.835 mmol) and ^{n}butyllithium (2.5 M, 0.17 cm^3, 0.415 mmol) was added and stirred for 4 hours. The reaction mixture was concentrated to a crude orange oily solid, which was then extracted into diethyl ether. The crude product was then washed with hexanes (3 x 10 cm^3) and dried in vacuo affording an orange-yellow solid. Multiple species present in the ^{31}P NMR spectrum, though **9** was identified and later confirmed by X-Ray diffraction.

$^{31}P\{^{1}H\}$ NMR (C_6D_6): δ = 256 (dd, *J* = 11, 501 Hz), 6.0 (dd, *J* = 84, 265 Hz), −20.2 (d, *J* = 319 Hz), −33.7 (d, *J* = 214 Hz), −52 (dd, *J* = 89, 269 Hz), −67.5 (dd, *J* = 210, 318 Hz), −105 (d, *J* = 79 Hz), −127 (s (**5.8**, P-H species) −128 (d, *J* = 69 Hz).

Attempted Synthesis of $[C_6P_2AlCH_3]^{2-}$ 2[Li(THF)$_{1.5}$]

^{n}Butyllithium (2.5 M, 0.62 cm^3, 1.55 mmol) was added dropwise to a THF (10 cm^3) solution of 1,2-Bis(phosphino)benzene (0.05 cm^3, 0.42 mmol), resulting in a yellow colouration, the mixture was then stirred for 2 hours. Next $MeAlCl_2$ (1 M, 0.78 cm^3, 0.8 mmol) was dissolved in THF (5 cm^3) and the yellow reaction mixture was slowly added dropwise resulting in a grey/pale-black colouration. After a further 2 hours, another 2 equivalents of ^{n}butyllithium (2.5 M, 0.17 cm^3, 0.42 mmol) was added and stirred for 4 hours before the reaction mixture was concentrated and extracted into ether.

^{31}P NMR (C_6D_6): δ = −131 (dm, $J_{P\text{-}H}$ = 212 Hz), −133 (dm, J_{PH} = 208 Hz).

$^{7}Li\{^{1}H\}$ NMR (C_6D_6): δ = 1.3 (s).

Attempted Synthesis of $[C_6P_2Si(C_6H_5)_2]^{2-}$ 2[Li(THF)$_{1.5}$]

^{n}Butyllithium (2.5 M, 0.62 cm^3, 1.6 mmol) was added dropwise to a THF (10 cm^3) solution of 1,2-Bis(phosphino)benzene (0.05 cm^3, 0.42 mmol), resulting in a yellow colouration, the mixture was then stirred for 2 hours. Next Ph_2SiCl_2 (0.16 cm^3, 0.8 mmol) was dissolved in THF (5 cm^3) and the yellow reaction mixture was slowly added dropwise resulting in a red colouration, which slowly turned pale-yellow. After a further 2 hours, another two equivalents of ^{n}butyllithium (2.5 M, 0.17 cm^3, 0.42 mmol) was added and stirred for 4 hours before the reaction mixture was concentrated and extracted into ether.

^{1}H NMR (C_6D_6): δ = 8.0 (br d, *J* = 29 Hz, 4H), 7.8 (br d, *J* = 33 Hz, 3H), 6.9 (br s, 2H), 6.8 (br s, 2H), 4.4 (d, P-H, *J* = 187 Hz).

$^{31}P\{^{1}H\}$ NMR (C_6D_6): δ = −110.7 (d, *J* = 18 Hz), −126 (s), −130.4 (br s).

^{31}P NMR (C_6D_6): δ = −110.7 (dm, J_{PH} = 187 Hz), −126 (higher order pattern, consistent with 1,2-bis(phosphino)benzene), −130.4 (br s).

Attempted Synthesis of $[C_6P_2B\text{-}F]^{2-}$ 2[Li(THF)$_{1.5}$]

^{n}Butyllithium (2.5 M, 0.62 cm^3, 1.55 mmol) was added dropwise to a THF (10 cm^3) solution of 1,2-Bis(phosphino)benzene (0.05 cm^3, 0.42 mmol), resulting in a yellow colouration, the mixture was then stirred for 2 hours. Next $BF_3.OEt_2$ (0.1 cm^3, 0.8 mmol) was slowly added dropwise resulting in a colourless solution. After a further 2 hours, another two equivalents of ^{n}butyllithium (2.5 M, 0.17 cm^3,

0.42 mmol) was added, resulting in a red colouration and the solution was stirred for another 4 hours before the reaction mixture was concentrated.

Only 1,2-bis(phosphino)benzene was observed by ^{31}P NMR.

$[C_6P_2BC_6H_5]^{2-}$ $2[Li(THF)_{1.5}]^{2+}$ ([5.6].2[Li(THF)$_{1.5}$]) + TMSCl (5.9)

Compound **[5.6].2[Li(THF)$_{1.5}$]** (12 mg, 0.029 mmol) was dissolved in a mixed C_6D_6/protio-THF solvent system and Me_3SiCl (7.5 µl, 0.059 mmol) wad added resulting in a pale-yellow solution. Any attempts to purify this product led to only the observation of 1,2-bis(phosphino)benzene, including just from a freeze-degas-thaw cycle.

^1H NMR (C_6D_6): δ = 7.6 (s, 2H), 7.2 (s, 2H), 7.1 (s, 1H), 0.25 (s, 6H), 0.0 (s, 4H), −0.1 (s, 8H).

$^{31}P\{^1H\}$ NMR (C_6D_6): δ = −39.8 (s).

$[C_6P_2BC_6H_5]^{2-}$ $2[Li(THF)_{1.5}]^{2+}$ ([5.6].2[Li(THF)$_{1.5}$]) + TMSCl + MeI

Compound **5.10** was generated *in situ* (0.03 mmol) and MeI (3.7 µl, 0.059 mmol) was added. Observing only the regeneration of 1,2-bis(phosphino)benzene by ^{31}P NMR.

$[C_6P_2BC_6H_5]^{2-}$ $2[Li(THF)_{1.5}]^{2+}$ ([5.6].2[Li(THF)$_{1.5}$]) + MeI

Compound **[5.6].2[Li(THF)$_{1.5}$]** (12 mg, 0.03 mmol) was dissolved in a mixed C_6D_6/protio-THF solvent system and MeI (3.7 µl, 0.06 mmol) was added resulting in the formation of white precipitate. No phosphorus resonances were observed by NMR.

$[C_6P_2BC_6H_5]^{2-}$ $2[Li(TMEDA)]^{2+}$ ([5.6].2[Li(TMEDA)]) + MeI

Compound **[5.6].2[Li(TMEDA)]** (11 mg, 0.02 mmol) was dissolved in a mixed C_6D_6/protio-THF solvent system and MeI (2.93 µl, 0.05 mmol) was added resulting in the formation of a colourless precipitate. Only observed the observation of multiple P-H species and 1,2-bis(phosphino)benzene by ^{31}P NMR.

$[C_6P_2BC_6H_5]^{2-}$ $2[Li(THF)_{1.5}]^{2+}$ ([5.6].2[Li(THF)$_{1.5}$]]) + $PhPCl_2$

Compound **[5.6].2[Li(THF)$_{1.5}$]** (20 mg, 0.05 mmol) was dissolved in a mixed C_6D_6/protio-THF solvent system and an excess of $PhPCl_2$ was added, some colourless precipitate started to form. Observation of $PhPCl_2$ and an intractable mixture of resonances by ^{31}P NMR.

$[C_6P_2BC_6H_5]^{2-}$ $2[Li(TMEDA)]^{2+}$ ([5.6].2[Li(TMEDA)]) + Ph_2PCl

Compound **[5.6].2[Li(TMEDA)]** (30 mg, 0.06 mmol) was dissolved in a mixed C_6D_6/protio-THF solvent system and $PhPCl_2$ (0.02 cm^3, 0.13 mmol) was added resulting in a pale-yellow colouration.

^{1}H NMR (C_6D_6): δ = 7.4 (s), 2.2 (s, TMEDA, CH_2), 2.1 (s, TMEDA, CH_3).

^{31}P{^{1}H} NMR (C_6D_6): δ = 82.1 (s, $PhPCl_2$), −15.2 (s).

$[C_6P_2BC_6H_5]^{2-}$ $2[Li(THF)_{1.5}]^{2+}$ ([5.6].2[Li(THF)$_{1.5}$]) + H_2

Compound **[5.6].2[Li(THF)$_{1.5}$]** (10 mg, 0.03 mmol) was introduced into a J. Young's NMR tube and dissolved in a mixed C_6D_6/protio-THF solvent system, next a freeze-pump-thaw cycle was performed. The NMR tube was then connected to a H_2 gas cylinder *via* T-junction tubing and H_2 was allowed to fill the tubing apparatus (*ca* 1 bar) and diffuse into the NMR sample.

^{1}H NMR (C_6D_6): δ = Broad aromatic region, 2.15 (s, TMEDA-CH_2), 2.05 (s, TMEDA-CH_3).

^{31}P{^{1}H} NMR (C_6D_6): δ = −126 (s, 1,2-bis(phosphino)benzene).

^{11}B{^{1}H} NMR (C_6D_6): δ = −14.9 (s).

$[C_6P_2BC_6H_5]^{2-}$ $2[Li(TMEDA)]^{2+}$ ([5.6].2[Li(TMEDA)]) + H_2

Compound **[5.6].2[Li(TMEDA)]** (12 mg, 0.02 mmol) was introduced into a J. Young's NMR tube and dissolved in a mixed C_6D_6/protio-THF solvent system, next a freeze-pump-thaw cycle was performed. The NMR tube was then connected to a H_2 gas cylinder *via* T-junction tubing and after evacuating the tubing, H_2 was allowed to fill the tubing apparatus (*ca* 1 bar) and then the NMR cap was opened allowing the diffusion of H_2 into the NMR sample. No reaction occurred.

$[C_6P_2BC_6H_5]^{2-}$ $2[Li(THF)_{1.5}]^{2+}$ ([5.6].2[Li(THF)$_{1.5}$]) + CO

Compound **[5.6].2[Li(THF)$_{1.5}$]** (10 mg, 0.03 mmol) was introduced into a J. Young's NMR tube and dissolved in a mixed C_6D_6/protio-THF solvent system, next a freeze-pump-thaw cycle was performed. The NMR tube was then connected to a CO gas cylinder *via* T-junction tubing and after evacuating the tubing, CO was allowed to fill the tubing apparatus (*ca* 1 bar) and then the NMR cap was opened allowing the diffusion of CO into the NMR sample. The solution instantly turned colourless, and a precipitate formed.

^{1}H NMR (C_6D_6): δ = Broad aromatic region.

^{31}P{^{1}H} NMR (C_6D_6): δ = −126 (s, 1,2-bis(phosphino)benzene).

^{11}B{^{1}H} NMR (C_6D_6): δ = No visible resonances.

^{7}Li{^{1}H} NMR (C_6D_6): δ = 0.2 (s).

$[C_6P_2BC_6H_5]^{2-}$ $2[Li(THF)_{1.5}]^{2+}$ ([5.6].2[Li(THF)$_{1.5}$]) + ^{i}PrBr

Compound **[5.6].2[Li(THF)$_{1.5}$]** (12 mg, 0.03 mmol) was dissolved in a mixed C_6D_6/protio-THF solvent system and ^{i}PrBr (5.5 µl, 0.06 mmol) was added. A freeze-pump-thaw cycle was performed on the NMR sample followed by a static-vacuum-distillation.

Before vacuum-transfer:

^{1}H NMR (C_6D_6): δ = 8.24 (s, 1H), 7.91 (d, 5.3 Hz, 5H), 7.74 (br m, 3H), 7.66 (s, 3H), 7.01 (d, 24.5 Hz, 8H), 6.88 (s, 4H), 6.72 (s, 1H). 3.97 (br m, 8H), 2.43 (br m, 3H), 1.15 (br m, 15H).

^{31}P{^{1}H} NMR (C_6D_6): δ = 95 (s), 49.1 (s), 6.8 (s).

After vacuum-transfer:

^{1}H NMR (C_6D_6): δ = 7.91 (s, 1H), 7.76 (s, 2H), 7.66 (s, 3H), 7.30 (br m, 6H), 6.95 (s, 3H), 6.81 (s, 2H), intractable mixture in the alkyl region.

^{31}P{^{1}H} NMR (C_6D_6): δ = −29.7 (d, J_{PP} = 65 Hz), −123.6 (d, J_{PP} = 65 Hz).

^{11}B{^{1}H} NMR (C_6D_6): δ = −5.45 (s).

^{7}Li{^{1}H} NMR (C_6D_6): δ = 0.40 (br s).

$[C_6P_2BC_6H_5]^{2-}$ $2[Li(TMEDA)]^{2+}$ ([5.6].2[Li(TMEDA)]) + ^{i}PrBr

Compound **[5.6].2[Li(TMEDA)]** (12 mg, 0.02 mmol) was dissolved in a mixed C_6D_6/protio-THF solvent system and ^{i}PrBr (4.8 µl, 0.06 mmol) was added.

^{31}P{^{1}H} NMR (C_6D_6): δ = 52.9 (higher order pattern, J = 84 Hz, 110 Hz), −0.58 (higher order pattern, J = 84 Hz, 110 Hz).

$[C_6P_2BC_6H_5]^{2-}$ $2[Li(THF)_{1.5}]^{2+}$ ([5.6].2[Li(THF)$_{1.5}$]) + Benzyl Chloride

Compound **[5.6].2[Li(THF)$_{1.5}$]** (12 mg, 0.03 mmol) was dissolved in a mixed C_6D_6/protio-THF solvent system and benzyl chloride (6.8 µl, 0.06 mmol) was added. A freeze-pump-thaw cycle was performed on the NMR sample followed by a static-vacuum-distillation.

^{31}P{^{1}H} NMR (C_6D_6): δ = −21.6 (d, J_{PP} = 145 Hz), −39.7 (d, J_{PP} = 125 Hz), as well as multiple unidentified species.

$[C_6P_2BC_6H_5]^{2-}$ $2[Li(THF)_{1.5}]^{2+}$ ([5.6].2[Li(THF)$_{1.5}$]) + I_2

Compound **[5.6].2[Li(THF)$_{1.5}$]** (25 mg, 0.61 mmol) was introduced to a J. Young's NMR tube and dissolved in C_6D_6 along with a few drops of protio-THF. Next I_2 (39 mg, 0.15 mmol) was added resulting in a dark colouration. Observed only intractable mixtures by ^{31}P NMR.

$[C_6P_2BC_6H_5]^{2-}$ $2[Li(TMEDA)]^{2+}$ ([5.6].2[Li(TMEDA)]) + I_2

Compound **[5.6].2[Li(TMEDA)]** (40 mg, 0.09 mmol) was dissolved in d_8-THF (0.6 cm^3) and I_2 (53.9 mg, 0.21 mmol) was added, resulting in a dark colouration.

$^{31}P\{^1H\}$ NMR (C_4D_8O): δ = 17.8 (d, J_{PP} = 26 Hz), 4.9 (d, J_{PP} = 26 Hz).

$[C_6P_2BC_6H_5]^{2-}$ $2[Li(THF)_{1.5}]^{2+}$ ([5.6].2[Li(THF)$_{1.5}$]) + $GaCl_3$

Compound **[5.6].2[Li(THF)$_{1.5}$]** (10 mg, 0.03 mmol) was dissolved in a mixed C_6D_6/protio-THF solvent system and $GaCl_3$ (9 mg, 0.05 mmol) was added. No phosphorus resonances were observed.

$[C_6P_2BC_6H_5]^{2-}$ $2[Li(TMEDA)]^{2+}$ ([5.6].2[Li(TMEDA)]) + $GaCl_3$

Compound **[5.6].2[Li(THF)$_{1.5}$]** (12 mg, 0.03 mmol) was dissolved in a mixed C_6D_6/protio-THF solvent system and $GaCl_3$ (9 mg, 0.05 mmol) was added, resulting in a pale-yellow colouration. No phosphorus resonances were observed.

$[C_6P_2BC_6H_5]^{2-}$ $2[Li(TMEDA)]^{2+}$ ([5.6].2[Li(TMEDA)]) + Glutaryl Chloride

Compound **[5.6].2[Li(THF)$_{1.5}$]** (10 mg, 0.02 mmol) was dissolved in a mixed C_6D_6/protio-THF solvent system and glutaryl chloride (2.3 µl, 0.02 mmol) was added, resulting in a dark, viscous material, presumably polymerised. No phosphorus resonances were observed.

$[C_6P_2BC_6H_5]^{2-}$ $2[Li(TMEDA)]^{2+}$ ([5.6].2[Li(TMEDA)]) + Adipoyl Chloride

Compound **[5.6].2[Li(TMEDA)]** (10 mg, 0.02 mmol) was dissolved in a mixed C_6D_6/protio-THF solvent system and adipoyl chloride (2.7 µl, 0.02 mmol) was added, resulting in a green, viscous material, presumably polymerised. No phosphorus resonances were observed.

$[C_6P_2BC_6H_5]^{2-}$ $2[Li(THF)_{1.5}]^{2+}$ ([5.6].2[Li(THF)$_{1.5}$]) + $MgCl_2$

Compound **[5.6].2[Li(THF)$_{1.5}$]** (12 mg, 0.03 mmol) and $MgCl_2$ (2.8 mg, 0.03 mmol) were dissolved in a mixed C_6D_6/protio-THF solvent system.

^1H NMR (C_6D_6): δ = 8.08 (m, 4H), 7.03 (t, J_{HH} = 7.4 Hz, 2H), 6.80 (t, J_{HH} = 7.4 Hz, 1H), 6.62 (m, 2H)

$^{31}P\{^1H\}$ NMR (C_6D_6): δ = 46.1 (br s, $w_{1/2}$ = 23.3 Hz).

^{7}Li NMR (C_6D_6): δ = −1.1 (s).

^{11}B{^{1}H} NMR (C_6D_6): δ = 67.1 (s).

Attempts to remove solvent or drive the equilibrium by 1,4-dioxane addition led only to decomposition. Similarly, attempts to grow crystals of this species resulted only in the observation of **[5.6].2[Li(THF)$_{1.5}$]**.

[$C_6P_2BC_6H_5$]$^{2-}$ 2[Li(THF)$_{1.5}$]$^{2+}$ ([5.6].2[Li(THF)$_{1.5}$]) + Ph_2SnCl_2 (5.11)

Compound **[5.6].2[Li(THF)$_{1.5}$]** (12 mg, 0.03 mmol) and Ph_2SnCl_2 (10 mg, 0.03 mmol) were introduced to a J. Young's NMR tube and dissolved in C_6D_6 along with a few drops of protio-THF, colourless precipitate formed. The solution was filtered through a glass pipette and solvent removed under reduced pressure.

^{1}H NMR (C_6D_6): δ = 8.2 (s, 1H), 7.87 (s, 2H), 7.76 (s, 2H), 7.58 (s, 2H), 7.33 (s, 5H), 7.21 (s, 5H), 6.94 (s, 20H), 6.64 (s, 5H).

^{13}C{^{1}H} NMR (C_6D_6) δ = 137.9 (s), 137.6 (d, *J* = 34.1 Hz), 136.4 (s), 135.3 (s), 132.1 (s), 128.8 (s), 128.6 (s), 128.5 (s), 128.3 (s), 128.1 (s).

^{31}P{^{1}H} NMR (C_6D_6): δ = −155.7 (s, $^{1}J_{P}{}^{119}{}_{Sn}$ = 705 Hz).

^{7}Li NMR (C_6D_6): δ = No resonances observed.

^{11}B{^{1}H} NMR (C_6D_6): δ = 76.5 (s).

^{119}Sn{^{1}H} NMR (C_6D_6): δ = 719 (d, J_{SnP} = 705 Hz).

[$C_6P_2BC_6H_5$]$^{2-}$ 2[Li(TMEDA)]$^{2+}$ ([5.6].2[Li(TMEDA)]) + Ph_2SnCl_2

Compound **[5.6].2[Li(TMEDA)]** (12 mg, 0.03 mmol) and Ph_2SnCl_2 (8.8 mg, 0.03 mmol) were introduced into a J. Young's NMR tube and dissolved in C_6D_6 along with a few drops of protio-THF.

^{1}H NMR (C_6D_6): δ = 8.25 (m, 7H), 8.17 (d, *J* = 8.4 Hz, 8H), 8.07 (m, 2H), 7.97 (m, 4H), 7.71 (m, 1H), 7.49 (m, 4H), 7.09 (m, 27H), 6.88 (m, 5H), 6.51 (d, *J* = 7.2 Hz, 1H).

^{31}P{^{1}H} NMR (C_6D_6): δ = 15.7 (higher order pattern), −127.2 (higher order pattern), −155.7 (s, same species as seen in the reaction with **[5.6].2[Li(THF)$_{1.5}$]**.

[$C_6P_2BC_6H_5$]$^{2-}$ 2[Li(THF)$_{1.5}$]$^{2+}$ ([5.6].2[Li(THF)$_{1.5}$]) + $^{t}Bu_2SnCl_2$

Compound **[5.6].2[Li(THF)$_{1.5}$]** (10 mg, 0.03 mmol) and $^{t}Bu_2SnCl_2$ (7.4 mg, 0.03 mmol) were introduced to a J. Young's NMR tube and dissolved in C_6D_6 along with a few drops of protio-THF.

$^{31}P\{^{1}H\}$ NMR (C_6D_6): δ = −118 (s, $^{1}J_{P^{119}Sn}$ = 1004 Hz, $^{1}J_{P^{117}Sn}$ 962 Hz) as well as multiple P-H species.

$[C_6P_2BC_6H_5]^{2-}$ $2[Li(THF)_{1.5}]^{2+}$ ([5.6].2[Li(THF)$_{1.5}$]) + $^{n}Bu_3SnCl$

Compound **[5.6].2[Li(THF)$_{1.5}$]** (10 mg, 0.03 mmol) and $^{n}Bu_3SnCl$ (16 mg, 0.05 mmol) were introduced to a J. Young's NMR tube and dissolved in C_6D_6 along with a few drops of protio-THF, resulting in a colourless precipitate.

$^{31}P\{^{1}H\}$ NMR (C_6D_6): δ = −59 (s), −140 (d, J_{PP} = 184 Hz), −160 (d, J_{PP} = 184 Hz), along with multiple unidentified species between −139 to −161. The resonance at −59 is lost when exposed to vacuum, though the doublets remain.

$[C_6P_2BC_6H_5]^{2-}$ $2[Li(TMEDA)]^{2+}$ ([5.6].2[Li(TMEDA)]) + $^{n}Bu_3SnCl$

Compound **[5.6].2[Li(TMEDA)]** (10 mg, 0.02 mmol) and $^{n}Bu_3SnCl$ (16 mg, 0.04 mmol) were introduced to a J. Young's NMR tube and dissolved in C_6D_6 along with a few drops of protio-THF, resulting in a colourless precipitate. No resonances observed in the ^{31}P NMR.

$[C_6P_2BC_6H_5]^{2-}$ $2[Li(THF)_{1.5}]^{2+}$ ([5.6].2[Li(THF)$_{1.5}$]) + $SnCl_4$

Compound **[5.6].2[Li(THF)$_{1.5}$]** (12 mg, 0.03 mmol) was introduced to a J. Young's NMR tube and dissolved in C_6D_6 along with a few drops of protio-THF, $SnCl_4$ was added. All phosphorus resonances lost, however, TMEDA resonances now have ^{119}Sn satellites, consistent with the formation of [TMEDA.$SnCl_2$].[330]

^{1}H NMR (C_6D_6): δ = 3.02 (s, TMEDA-CH_2, $^{2}J_{SnH}$ = 47 Hz, 8H), 2.75 (s, TMEDA-CH_3, $^{2}J_{SnH}$ = 48 Hz, 24H).

$[C_6P_2BC_6H_5]^{2-}$ $2[Li(THF)_{1.5}]^{2+}$ ([5.6].2[Li(THF)$_{1.5}$]) + $PbCl_2$

Compound **[5.6].2[Li(THF)$_{1.5}$]** (10 mg, 0.03 mmol) and $PbCl_2$ (13.6 mg, 0.05 mmol) were introduced into a J. Young's NMR tube and dissolved in C_6D_6 along with a few drops of protio-THF, resulting in a red colouration.

$^{31}P\{^{1}H\}$ NMR (C_6D_6): δ = 82.3 (s).

$[C_6P_2BC_6H_5]^{2-}$ $2[Li(TMEDA)]^{2+}$ ([5.6].2[Li(TMEDA)]) + $PbCl_2$

Compound **[5.6].2[Li(TMEDA)]** (10 mg, 0.02 mmol) and $PbCl_2$ (11.8 mg, 0.04 mmol) were introduced into a J. Young's NMR tube and dissolved in C_6D_6 along with a few drops of protio-THF, resulting in a black colouration. No resonances were observed in the ^{31}P NMR spectrum.

$[C_6P_2BC_6H_5]^{2-}$ 2[Li(TMEDA)]$^{2+}$ ([5.6].2[Li(TMEDA)]) + Cp_2ZrCl_2

Cp_2ZrCl_2 (9.9 mg, 0.03 mmol) was added to Compound **[5.6].2[Li(TMEDA)]** (8 mg, 0.02 mmol) dissolved in C_6D_6 along with a few drops of THF, resulting in a blood-red colouration.

$^{31}P\{^1H\}$ NMR (C_6D_6): δ = 81.6 (s).

^7Li NMR (C_6D_6): δ = 0.6 (s).

$[C_6P_2BC_6H_5]^{2-}$ 2[Li(THF)$_{1.5}$]$^{2+}$ ([5.6].2[Li(THF)$_{1.5}$]) + $Cp(Ph_2N)ZrCl$

Compound **[5.6].2[Li(THF)$_{1.5}$]]** (12 mg, 0.03 mmol) and $Cp(Ph_2N)ZrCl$ (25 mg, 0.06 mmol) were introduced into a J. Young's NMR tube and dissolved in C_6D_6 along with a few drops of protio-THF, resulting in a red colouration. Only starting materials observed by NMR.

$[C_6P_2BC_6H_5]^{2-}$ 2[Li(TMEDA)]$^{2+}$ ([5.6].2[Li(TMEDA)]) + $Cp(Ph_2N)ZrCl$

Compound **[5.6].2[Li(TMEDA)]** (13.7 mg, 0.03 mmol) and $Cp(Ph_2N)ZrCl$ (25 mg, 0.06 mmol) were introduced into a J. Young's NMR tube and dissolved in C_6D_6 along with a few drops of protio-THF, resulting in a red colouration. After an hour the solution was light brown/orange in colour. Transferred to an ampoule and volatile components removed under reduced pressure.

$^{31}P\{^1H\}$ NMR (C_6D_6): δ = 97.2 (s).

^7Li NMR (C_6D_6): δ = 0.01 (br s), −1.1 (s).

^{11}B NMR (C_6D_6): δ = −17 (impurity sometimes seen in **[5.6].2[Li(TMEDA)]**.

$[C_6P_2BC_6H_5]^{2-}$ 2[Li(THF)$_{1.5}$]$^{2+}$ ([5.6].2[Li(THF)$_{1.5}$]) + $Cp^{ttt}Y(BH_4)_2(THF)$

Compound **[5.6].2[Li(THF)$_{1.5}$]** (10 mg, 0.03 mmol) and $Cp^{ttt}Y(BH_4)_2(THF)$ (10.4 mg, 0.03 mmol) were introduced into a J. Young's NMR tube and dissolved in C_6D_6 along with a few drops of protio-THF.

$^{31}P\{^1H\}$ NMR (C_6D_6): δ = 44.8 (s).

^7Li NMR (C_6D_6): δ = −1.1 (s).

$^{11}B\{^1H\}$ NMR (C_6D_6): δ = 68.9 (br), −26.3 (s).

All phosphorus resonances lost if exposed to vacuum.

$[C_6P_2BC_6H_5]^{2-}$ 2[Li(TMEDA)]$^{2+}$ ([5.6].2[Li(TMEDA)]) + $Cp^{ttt}Y(BH_4)_2(THF)$

Compound **[5.6].2[Li(TMEDA)]** (10 mg, 0.021 mmol) and $Cp^{ttt}Y(BH_4)_2(THF)$ (9.0 mg, 0.02 mmol) were introduced into a J. Young's NMR tube and dissolved in C_6D_6 along with a few drops of protio-THF.

$^{31}P\{^{1}H\}$ NMR (C_6D_6): δ = 50.4 (s).

$^{11}B\{^{1}H\}$ NMR (C_6D_6): δ = −26.4 (s), −39.0 (s)

All phosphorus resonances lost if exposed to vacuum.

$[C_6P_2BC_6H_5]^{2-}$ $2[Li(TMEDA)]^{2+}$ ([5.6].2[Li(TMEDA)]) + $TiCl_2$

Compound **[5.6].2[Li(TMEDA)]** (12 mg, 0.03 mmol) and $TiCl_2$ (3 mg, 0.03 mmol) were introduced into a J. Young's NMR tube and dissolved in C_6D_6 along with a few drops of protio-THF. No phosphorus resonances were observed by ^{31}P NMR spectroscopy.

Synthesis of [CpFe(benzene)][PF_6]

Ferrocene (2 g, 10.8 mmol) was dissolved in benzene (10 cm^3) in a 50 cm^3 round-bottom flask fitted with a condenser. Next, $AlCl_3$ (4 g, 30.0 mmol), Al powder (0.3 g, 11.12 mmol) and H_2O (0.2 cm^3) were added and the reaction mixture was brought to reflux for 45 minutes. The reaction mixture was allowed to cool to room-temperature and then further cooled in ice (0 °C), next ice-cold water (25 cm^3) was added and the aqueous layer was extracted and diluted to 50 cm^3. KPF_6 (2.5 g, 13.58 mmol) was added and left to stir for 10 minutes, the crude-product was then filtered and washed with ethanol, H_2O and diethyl ether, then dissolved in CH_3CN (10 cm^3) and CCl_4 (3 cm^3) was added, the acetonitrile was removed under reduced pressure and the product was collected by filtration as a green solid which was dried for 16 hours by blowing compressed air over the solid.

$[C_6P_2BC_6H_5]^{2-}$ $2[Li(THF)_{1.5}]^{2+}$ ([5.6].2[Li(THF)$_{1.5}$]) + CpFe(benzene)][PF_6]

Compound **[5.6].2[Li(THF)$_{1.5}$]** (10.4 mg, 0.16 mmol) and CpFe(benzene)][PF_6] (17.5 mg, 0.05 mmol) were introduced into a J. Young's NMR tube and dissolved in C_6D_6 along with a few drops of THF. Concentrated to a light brown solid.

$^{31}P\{^{1}H\}$ NMR (C_6D_6): δ = −35.7 (s), −143.9 (septet, J_{PF} = 705 Hz, PF6).

$^{11}B\{^{1}H\}$ NMR (C_6D_6): δ = 29.9 (s), 23.0 (s), −4.9 (s).

If exposed to vacuum the species observed slowly disappear

$[C_6P_2BC_6H_5]^{2-}$ $2[Li(TMEDA)]^{2+}$ ([5.6].2[Li(TMEDA)]) + CpFe(benzene)][PF_6]

Compound **[5.6].2[Li(TMEDA)]** (75 mg, 0.16 mmol) and CpFe(benzene)][PF_6] (110 mg, 0.32 mmol) were introduced into a Schlenk flask and dissolved in THF. Concentrated to a light brown solid.

$^{31}P\{^{1}H\}$ NMR (C_6D_6): δ = −35.3 (s), −60.8 (s), −143.9 (septet, J_{PF} = 705 Hz, PF_6).

$^{11}B\{^{1}H\}$ NMR (C_6D_6): δ = 22.5 (s).

^{7}Li NMR (C_6D_6): δ = –0.2 (s).

If exposed to vacuum the species observed slowly disappear.

$[C_6P_2BC_6H_5]^{2-}$ $2[Li(THF)_{1.5}]^{2+}$ ([5.6].2[Li(THF)$_{1.5}$]) + $CpRu(PPh_3)_2Cl$

Compound **[5.6].2[Li(THF)$_{1.5}$]** (10 mg, 0.03 mmol) and $CpRu(PPh_3)_2Cl$ (35.6 mg, 0.05 mmol) were introduced into a J. Young's NMR tube and dissolved in C_6D_6 along with a few drops of protio-THF. Only $CpRu(PPh_3)_2Cl$ was observed by NMR spectroscopy.

$[C_6P_2BC_6H_5]^{2-}$ $2[Li(TMEDA)]^{2+}$ ([5.6].2[Li(TMEDA)]) + $CpRu(PPh_3)_2Cl$

Compound **[5.6].2[Li(TMEDA)]** (10 mg, 0.03 mmol) and $CpRu(PPh_3)_2Cl$ (35 mg, 0.05 mmol) were introduced into a J. Young's NMR tube and dissolved in C_6D_6 along with a few drops of protio-THF. Only $CpRu(PPh_3)_2Cl$ was observed by NMR.

$[C_6P_2BC_6H_5]^{2-}$ $2[Li(THF)_{1.5}]^{2+}$ ([5.6].2[Li(THF)$_{1.5}$]) + CpRu(dppe)Cl

Compound **[5.6].2[Li(THF)$_{1.5}$]** (6.7 mg, 0.02 mmol) and CpRu(dppe)Cl (20 mg, 0.03 mmol) were introduced into a J. Young's NMR tube and dissolved in C_6D_6 along with a few drops of protio-THF, black colouration ($CpRu(PPh_3)_2Cl$ is black). No reaction occurred.

$[C_6P_2BC_6H_5]^{2-}$ $2[Li(TMEDA)]^{2+}$ ([5.6].2[Li(TMEDA)]) + CpRu(dppe)Cl

Compound **[5.6].2[Li(TMEDA)]** (5.2 mg, 0.01 mmol) and CpRu(dppe)Cl (3.3 mg, 0.01 mmol) were introduced into a J. Young's NMR tube and dissolved in C_6D_6 along with a few drops of protio-THF, pale-black colouration ($CpRu(PPh_3)_2Cl$ is black). No reaction occurred.

$[C_6P_2BC_6H_5]^{2-}$ $2[Li(THF)_{1.5}]^{2+}$ ([5.6].2[Li(THF)$_{1.5}$]) + $Rh(CO)(PCy_3)_2Cl$

Compound **[5.6].2[Li(THF)$_{1.5}$]** (10 mg, 0.03 mmol) and $CORh(PCy_3)_2Cl$ (35 mg, 0.05 mmol) were introduced into a J. Young's NMR tube and dissolved in C_6D_6 along with a few drops of protio-THF. No reaction occurred.

$[C_6P_2BC_6H_5]^{2-}$ $2[Li(TMEDA)]^{2+}$ ([5.6].2[Li(TMEDA)]) + $Rh(CO)(PCy_3)_2Cl$

Compound **[5.6].2[Li(TMEDA)]** (10 mg, 0.02 mmol) and $CoRh(PCy_3)_2Cl$ (30.5 mg, 0.04 mmol) were introduced into a J. Young's NMR tube and dissolved in C_6D_6 along with a few drops of protio-THF. No reaction occurred.

$[C_6P_2BC_6H_5]^{2-}$ $2[Li(THF)_{1.5}]^{2+}$ ([5.6].2[$Li(THF)_{1.5}$]) + AuCl(tht)

Compound **[5.6].2[$Li(THF)_{1.5}$]** (12 mg, 0.03 mmol) and AuCl(tht) (18.85 mg, 0.06 mmol) were introduced into a J. Young's NMR tube and dissolved in C_6D_6 along with a few drops of protio-THF. No phosphorus resonances observed in the ^{31}P NMR spectrum.

$[C_6P_2BC_6H_5]^{2-}$ $2[Li(TMEDA)]^{2+}$ ([5.6].2[Li(TMEDA)]) + AuCl(tht)

Compound **[5.6].2[Li(TMEDA)]** (20 mg, 0.04 mmol) and AuCl(tht) (27 mg, 0.09 mmol) were introduced into a J. Young's NMR tube and dissolved in C_6D_6 along with a few drops of protio-THF. No phosphorus resonances observed in the ^{31}P NMR spectrum.

$[C_6P_2BC_6H_5]^{2-}$ $2[Li(TMEDA)]^{2+}$ ([5.6].2[Li(TMEDA)]) + AuCl(PPh_3)

Compound **[5.6].2[Li(TMEDA)]** (10 mg, 0.02 mmol) and AuCl(PPh_3) (21 mg, 0.04 mmol) were introduced into a J. Young's NMR tube and dissolved in C_6D_6 along with a few drops of protio-THF. No phosphorus resonances observed in the ^{31}P NMR spectrum.

$[C_6P_2BC_6H_5]^{2-}$ $2[Li(TMEDA)]^{2+}$ ([5.6].2[Li(TMEDA)]) + CuI

Compound [**5.6].2[Li(TMEDA)]** (10 mg, 0.02 mmol) and CuI (8 mg, 0.04 mmol) were introduced into a J. Young's NMR tube and dissolved in C_6D_6 along with a few drops of protio-THF. No phosphorus resonances were observed by ^{31}P NMR spectroscopy.

$[C_6P_2BC_6H_5]^{2-}$ $2[Li(TMEDA)]^{2+}$ ([5.6].2[Li(TMEDA)]) + $(Ph_3P)_2PtCl_2$

Compound **[5.6].2[Li(TMEDA)]** (12 mg, 0.03 mmol) and $(PPh_3)_2PtCl_2$ (21 mg, 0.03 mmol) were introduced into a J. Young's NMR tube and dissolved in C_6D_6 along with a few drops of protio-THF. Only PPh_3 observed by ^{31}P NMR.

Synthesis of $PhRhCl_2(PPh_3)_2$

$RhCl(PPh_3)_3$ (1.23 g, 1.33 mmol) and PhHgCl (0.430 g, 1.37 mmol) were introduced into a round-bottom flask fitted with a condenser and charged with argon. Next the reagents were dissolved in THF (40 cm^3) and brought to reflux for 3 hours resulting in a red/orange colouration and the observation of mercury at the bottom of the reaction vessel. The solution was filtered through Celite® affording a red solution which was concentrated until orange solid started to form (*ca* 10 cm^3), then ethanol (60 cm^3) was added and the solution was removed by filtration and volatile components were removed under reduced pressure. The resulting solid was washed with Et2O (10 cm^3) and dried *in vacuo* resulting in a matt orange solid. In agreement with the literature.[292] Yield: 0.43 g, 38 %.

^{1}H NMR (CD_2Cl_2): δ = 7.5 (s, PPh_3, 15H), 7.3 (s, PPh_3, 15H), 6.8 (br s, aromatic (Rh-Ph^p, 1H) 6.65 (br s, aromatic (Rh-Ph), 2H), 6.5 (br s, aromatic (Rh-Ph), 2H).

^{31}P{^{1}H} NMR (CD_2Cl_2): δ = 20.8 (d, $^{2}J_{PP}$ = 102 Hz).

$[C_6P_2BC_6H_5]^{2-}$ $2[Li(THF)_{1.5}]^{2+}$ ([5.6].2[Li(THF)$_{1.5}$]) + $PhRhCl_2(PPh_3)_2$

Compound **[5.6].2[Li(THF)$_{1.5}$]** (12 mg, 0.03 mmol) and $PhRhCl_2(PPh_3)_2$ (22.8 mg, 0.03 mmol) were introduced into a J. Young's NMR tube and dissolved in C_6D_6 (0.6 cm^3) along with a few drops of protio-THF.

Initial NMR:

^{1}H NMR (C_6D_6): δ = 7.6 (br d, *J* = 29.6 Hz), 7.3 (s), 7.0 (s), 6.8 (br s), 6.8 (br s).

^{31}P{^{1}H} NMR (C_6D_6): δ = 40.4 (d, *J* = 146 Hz), 37.5 (d, *J* = 150 Hz), 31.8 (apparent doublet, *J* = 163 Hz), 23.0 (d, *J* = 106 Hz), 21.1 (d, *J* = 106 Hz), −5.3 (s, PPh_3).

^{7}Li NMR (C_6D_6): δ = 0.7 (s).

NMR after a few hours:

^{1}H NMR (C_6D_6): δ = 7.6 (br s), 7.3 (s), 7.1 (s), 6.8 (br s), 6.8 (br s).

^{31}P{^{1}H} NMR (C_6D_6): δ = 31.8 (apparent doublet, *J* = 163 Hz), 23.0 (d, *J* = 106 Hz), 21.0 (d, *J* = 104 Hz), −5.2 (s, PPh_3).

NMR after removal of solvent:

^{1}H NMR (C_6D_6): δ = 7.6 (br d, *J* = 29.6 Hz), 7.3 (s), 7.0 (br s).

^{31}P{^{1}H} NMR (C_6D_6): δ = 31.8 (apparent doublet, *J* = 163 Hz), −5.2 (s, PPh_3).

This reaction was also run on a larger scale, though the same result occurred.

$[C_6P_2BC_6H_5]^{2-}$ $2[Li(TMEDA)]^{2+}$ ([5.6].2[Li(TMEDA)]) + $PhRhCl_2(PPh_3)_2$

Compound **[5.6].2[Li(TMEDA)]** (12 mg, 0.03 mmol) and $PhRhCl_2(PPh_3)_2$ (19.7 mg, 0.03 mmol) were introduced into a J. Young's NMR tube and dissolved in C_6D_6 (0.6 cm^3) along with a few drops of protio-THF. The same result was observed as when **[5.6].2[Li(THF)$_{1.5}$]** and $PhRhCl_2(PPh_3)_2$ were reacted.

$[C_6P_2BC_6H_5]^{2-}$ $2[Li(THF)_{1.5}]^{2+}$ ([5.6].2[$Li(THF)_{1.5}$]) + PhHgCl

Compound **[5.6].2[$Li(THF)_{1.5}$]** (12 mg, 0.03 mmol) and PhHgCl (18.4 mg, 0.06 mmol) were introduced into a J. Young's NMR tube and dissolved in C_6D_6 (0.6 cm^3) along with a few drops of protio-THF. All phosphorus resonances were lost.

$[C_6P_2BC_6H_5]^{2-}$ $2[Li(TMEDA)]^{2+}$ ([5.6].2[Li(TMEDA)]) + PhHgCl

Compound **[5.6].2[Li(TMEDA)]** (12 mg, 0.03 mmol) and PhHgCl (15.9 mg, 0.05 mmol) were introduced into a J. Young's NMR tube and dissolved in C_6D_6 (0.6 cm^3) along with a few drops of protio-THF. All phosphorus resonances were lost.

$[C_6P_2BC_6H_5]^{2-}$ $2[Li(THF)_{1.5}]^{2+}$ ([5.6].2[$Li(THF)_{1.5}$]) + HgI_2

Compound **[5.6].2[$Li(THF)_{1.5}$]** (10 mg, 0.02 mmol) and HgI_2 (22.3 mg, 0.05 mmol) were introduced into a J. Young's NMR tube and dissolved in C_6D_6 (0.6 cm^3) along with a few drops of protio-THF. Resulted in a very pale-yellow colouration, essentially colourless and a green precipitate started to form which would not dissolve in any common solvents. No phosphorus resonances were observed.

$[C_6P_2BC_6H_5]^{2-}$ 2[Li(TMEDA)] ([5.6].2[Li(TMEDA)]) + HgI_2

Compound **[5.6].2[Li(TMEDA)]** (10 mg, 0.02 mmol) and HgI_2 (19.25 mg, 0.04 mmol) were introduced into a J. Young's NMR tube and dissolved in C_6D_6 (0.6 cm^3) along with a few drops of protio-THF. Resulted in a yellow precipitate which would not dissolve in any common solvents. No phosphorus resonances were observed.

$[C_6P_2BC_6H_5]^{2-}$ $2[Li(THF)_{1.5}]^{2+}$ ([5.6].2[$Li(THF)_{1.5}$]) + Vaska's complex [IrCl(CO)[PPh_3)$_2$]

IrCl(CO)[PPh_3)$_2$ (138.8 mg, 0.196 mmol) and compound **[5.6].2[$Li(THF)_{1.5}$]** (40 mg, 0.098 mmol) were introduced into a Schlenk flask and dissolved in a mixed solvent system of benzene/THF, upon the addition of THF a red colouration was observed. The mixture was stirred for 10 minutes and concentrated under reduced pressure; the product was then extracted into Et_2O.

^{1}H NMR (C_6D_6): δ = 7.6 (br s), 7.4 (br s), 7.3 (br s), 7.1 (s), 7.0 (s), 6.9 (br s), 6.9 (s), 6.7 (s), 6.2 (s), 5.8 (s).

$^{13}C\{^1H\}$ NMR (C_6D_6) δ = 139.7 (d, *J* = 33 Hz), 136.9 (s), 135.5 (s), 135.3 (d, *J* = 11 Hz), 135.0 (s), 134.8 (d, *J* = 12 Hz), 134.7 (d, *J* = 12 Hz), 134.2 (s), 133.8 (d, *J* = 19 Hz), 133.5 (d, *J* = 12.5 Hz), 131.9 (d, *J* = 52 Hz), 129.7 (d, *J* = 12 Hz), 129.0 (d, *J* = 15 Hz), 128.6 (s), 128.3 (d, *J* = 6.5 Hz), 127.0 (d, *J* = 10 Hz), 126.7 (s), 126.4 (d, *J* = 10 Hz), 124.1 (s), 123.6 (m), 122.0 (br d, *J* = 7 Hz)

$^{31}P\{^{1}H\}$ NMR (C_6D_6): δ = 22.7 (td, J_{PP} = 9 Hz, J_{PP} = 27 Hz), 16.1 (dd, J_{PP} = 28 Hz, J_{PP} = 200 Hz), 9.1 (br d, J_{PP} = 170 Hz), 6.5 (m), −65.6 (dd, J_{PP} = 11 Hz, J_{PP} = 28 Hz), −80.8 (br t, J_{PP} = 170 Hz).

^{11}B NMR (C_6D_6): δ = 25.3 (s).

^{7}Li NMR (C_6D_6): δ = 1.29 (shouldering peak), 0.62 (s).

$[C_6P_2BC_6H_5]^{2-}$ 2[Li(TMEDA)]$^{2+}$ ([5.6].2[Li(TMEDA)]) + [Mo(NCEt)$_3$(CO)$_3$] (15)

Compound **[5.6].2[Li(TMEDA)]** (22 mg, 0.05 mmol) and [Mo(NCEt)$_3$(CO)$_3$] (16.1 mg, 0.05 mmol) were combined in a J. Young's NMR tube and dissolved in C_6D_6 (0.6 cm^3) along with a few drops of protio-THF. Upon exposure to vacuum this species decomposes, however, yellow crystals were grown from laying the reaction mixture with hexane.

^{1}H NMR (C_6D_6): δ = 8.45 (s), 7.72 (d, *J* = 7.32 Hz), 7.47 (br m), 7.02 (t, *J* = 6.80 Hz), 6.67 (m), 2.20 (s, TMEDA-CH_2), 2.09 (s, TMEDA-CH_3), 1.90 (q, THF, *J* = 8.10 Hz), 0.85 (t, THF, *J* = 8.10 Hz).

$^{31}P\{^{1}H\}$ NMR (C_6D_6): δ = 8.1 (s).

^{7}Li NMR (C_6D_6): δ = 0.3 (s).

Crystal Data for $C_{43}H_{63}BLi_2N_6P_2$ (M_w = 1198.44 g/mol): triclinic, space group $P2_{1/c}$ (no. 14), a = 11.81600(10) Å, b = 31.3936(5) Å, c = 15.3079(2) Å, α = 90°, β = 108.5450(10)°, γ = 90°, V = 5383.56(12) Å^3, Z = 4, T = 99.9(4) K, μ(Cu Kα) = 1.525 mm-1, D_{calc} = 1.479 g/cm^3, 29708 reflections measured (7.892° ≤ 2Θ ≤ 143.4°), 9742 unique (R_{int} = 0.0699, R_{sigma} = 0.0526) which were used in all calculations. The final R_1 value was 0.0659 (I > 2σ(I)) and wR_2 was 0.1751 (all data).

$[C_6P_2BC_6H_5]^{2-}$ 2[Li(THF)$_{1.5}$]$^{2+}$ ([5.6].2[Li(THF)$_{1.5}$]) + YbI_2

Compound **[5.6].2[Li(THF)$_{1.5}$]]** (10 mg, 0.03 mmol) and YbI_2 (10.5 mg, 0.03 mg) were introduced into a J. Young's NMR tube and dissolved in C_6D_6 (0.6 cm^3), along with a few drops of protio-THF. No reaction occurred.

$[C_6P_2BC_6H_5]^{2-}$ 2[Li(TMEDA)]$^{2+}$ ([5.6].2[Li(TMEDA)]) + YbI_2

Compound **[5.6].2[Li(TMEDA)]** (10 mg, 0.02 mmol) and YbI_2 (9 mg, 0.02 mg) were introduced into a J. Young's NMR tube and dissolved in C_6D_6 (0.6 cm^3), along with a few drops of protio-THF. No reaction occurred.

Synthesis of Cp*SmBPh$_4$

Cp*$_2$Sm (100 mg, 0.24 mmol) was introduced into a J. Young's ampoule and dissolved in benzene (20 cm^3). To this solution [Et_3NH][BPH_4] (101 mg, 0.24 mmol) was slowly added and stirred for 30 minutes,

resulting in a dark blue/green solution. The solution was filtered, and volatile components were removed under reduced pressure, resulting in a dark blue solid, as per literature procedure.[300] Yield: 83.1 mg, 57 %.

^{1}H NMR (C_6D_6): δ = 0.23 (s), -2.93 (s).

^{11}B NMR (C_6D_6): δ = 27.1 (s).

$[C_6P_2BC_6H_5]^{2-}$ 2[Li(TMEDA)]$^{2+}$ ([5.6].2[Li(TMEDA)]) + Cp*SmBPh$_4$

Compound **[5.6].2[Li(TMEDA)]** (15 mg, 0.03 mmol) and Cp*SmBPh$_4$ (39.1 mg, 0.06 mmol) were combined in a J. Young's NMR tube and dissolved in C_6D_6 (0.6 cm^3) along with a few drops of protio-THF, resulting in a brown colouration and a colourless precipitate, the solid was removed by filtration.

^{1}H NMR (C_6D_6): δ = 7.4 (s, 14H), 6.9 (s, 15 H), 6.8 (s, 6H), 2.2 (s, TMEDA – CH_2, 8H), 2.02 (s, TMEDA – CH_3, 24H).

^{31}P{^{1}H} NMR (C_6D_6): δ = 48.9 (br s).

$[C_6P_2BC_6H_5]^{2-}$ 2[Li(THF)$_{1.5}$]$^{2+}$ ([5.6].2[Li(THF)$_{1.5}$]) + UCl$_4$

Compound **[5.6].2[Li(THF)$_{1.5}$]** (12 mg, 0.03 mmol) and UCl_4 (11.2 mg, 0.03 mmol) were introduced into a glass vial and placed in the glovebox freezer (–37 °C). Next pre-cooled THF (–37 °C) was added slowly to the reaction mixture resulting in a dark brown colouration. Attempts to grow crystals of the reaction product resulted only in a green insoluble precipitate.

$[C_6P_2BC_6H_5]^{2-}$ 2[Li(TMEDA)]$^{2+}$ ([5.6].2[Li(TMEDA)]) + UCl$_4$

Compound **[5.6].2[Li(TMEDA)]** (12 mg, 0.03 mmol) and UCl_4 (9.7 mg, 0.03 mmol) were introduced into a glass vial and placed in the glovebox freezer (–37 °C). Next pre-cooled THF (–37 °C) was added slowly to the reaction mixture resulting in a light brown colouration. Attempts to grow crystals of the reaction product resulted only in a green insoluble precipitate.

Miscellaneous Supplementary Data

“Certainty of death. Small chance of success. What are we waiting for?”

--The Lord of the Rings: Return of the King (2003)

The following structures were collected in the duration of this PhD, though not used within the thesis.

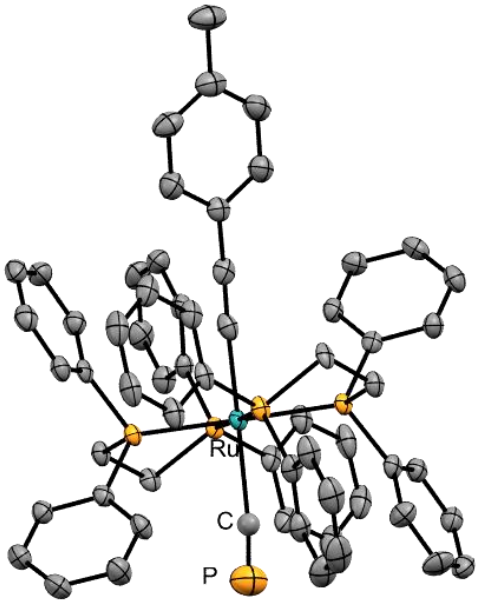

S 1. *Molecular structure of trans-[Ru(dppe)$_2$(C≡CC$_6$H$_4$Me)(C≡P)]; displacement ellipsoids at the 50% probability level. Hydrogen atoms and solvent of crystallisation omitted for clarity.*

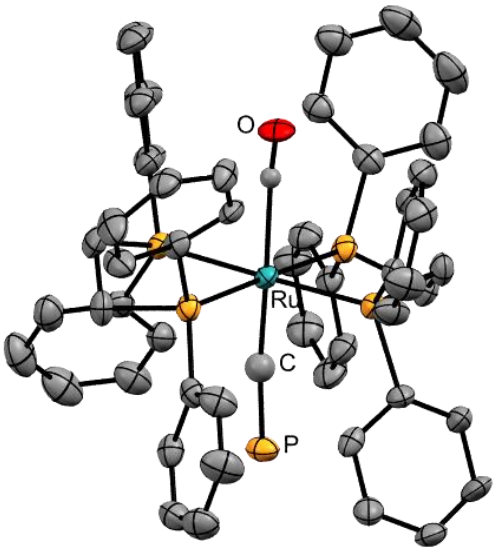

S 2. *Molecular structure of trans-[Ru(dppe)2(CO)(C≡P)]·OTf; displacement ellipsoids at the 50% probability level. Hydrogen atoms, counter-ion and solvent of crystallisation omitted for clarity.*

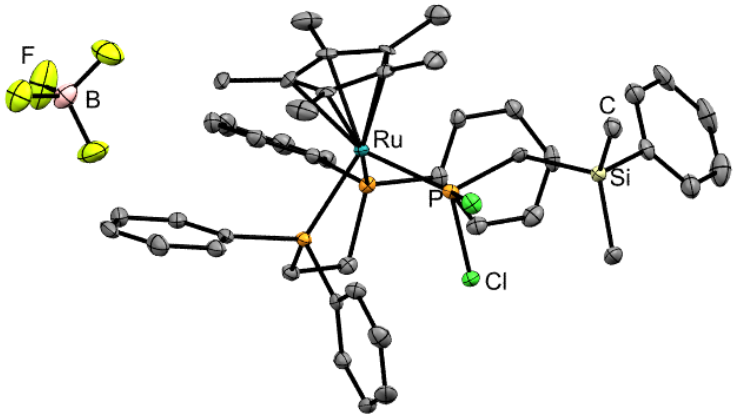

S 3. *Molecular structure of [Cp*Ru(dppe)P(Cl)$_2$CH$_2$Si(Ph)CH$_2$)]·BF$_4$; displacement ellipsoids at the 50% probability level. Hydrogen atoms omitted for clarity.*

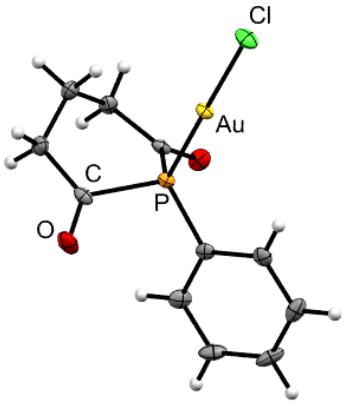

S 4. *Molecular structure of [AuCl(Ph)P{C(O)(CH$_2$)$_3$C(O)}]; displacement ellipsoids at the 50% probability level.*

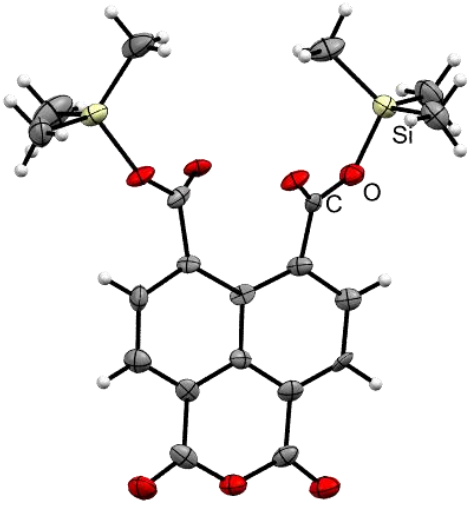

S 5. *Molecular structure of {(CH$_3$)$_3$SiOC(O)}$_2$C$_{12}$H$_4$(CH$_3$CO$_2$)O; displacement ellipsoids at the 50% probability level*

References

1. N. N. Greenwood and A. Earnshaw, Chemistry of the elements, Permagon Press, Oxford, 1984.

2. M. E. Weeks, *J. Chem. Ed.*, 1956, **41**, 39-109.

3. Shriver, Atkins. Inorganic Chemistry, Fifth Edition. W. H. Freeman and Company, New York; 2010; p. 379.

4. D. E. C. Corbridge, Applications of Phosphorus Compounds, CRC Press, Florida, 6th Ed., 2013.

5. E. Takeda, Y. Taketani, N. Sawada, T. Sato and H. Yamamoto, *Biofactors.*, 2004, **21**, 345-355.

6. P. F. Kelly, Phosphorus: Inorganic Chemistry, Encyclopedia of Inorganic and Bioinorganic Chemistry, 2006.

7. P. L. Floch, *Coord. Chem. Rev.*, 2006, **250**, 267.

8. C. E. Cleeton and N. H. Williams, *Phys. Rev.*, 1934, **45**, 234-237.

9. G. Becker, H. Schmidt, G. Uhl, and W. Uhl, *Inorganic Syntheses.*, 1990, **27**, 243–249.

10. E. I. Musina, A. V. Shamsieva, A. S. Balueva and A. A. Karasik, Organophosphorus Chemistry: Volume 49, Royal Society of Chemistry, London, 2020.

11. E. Sattler, E. Matern, A. Rothenberger, A. Okrut, P. Bombicz, I. Fernandez and I. Kovacs, *Eur. J. Inorg. Chem.*, 2014, 221-232.

12. H. A. Tallis, P. D. Newman, P. G. Edwards, L. Ooi and A. Stasch, *Dalton Trans.*, 2008, 47-53.

13. T. A. van der Knaap, T. C. Klebach, F. Visser, F. Bickelhaupt, P. Ros, E. J. Baerends, C. H. Stam, and M. Konun, *Tetrahedron*., 1984, **40**, 765-776.

14. B. M. Cossairt and C. C. Cummins, *New J. Chem.*, 2010, **34**, 1533-1536.

15. P. B. Arockriam, U. Lennert, C. Graf, R. Rothfelder, D. J. Scott, T. G. Fischer, K. Zeitler and R. Wolf*., Chem. Eur. J.*, 2020, **26**, 16374-16382.

16. Vogler, A. and H. Kunkely, *Coord. Chem. Rev.*, 2002, **230**, 243-251.

17. C. A. Tolman, *Chem. Rev.*, 1977, **77**, 313-348.

18. J. A. Bilbrey, A. H. Kazez, J. Locklin and W. D. Allen, *J. Comp. Chem.*, 2013, **34**, 1189-1197.

19. D. Benitez, E. Tkatchouk, A. Z Gonzalex, W. A. Goddard and F. D. Toste, *Org. Lett.*, 2009, **11**, 4798-4801.

20. D. Evans, J. A. Osborn and G. Wilkinson, *J. Chem. Soc. A.*, 1968, 3133-3142.

21. G. Erre, S. Enthaler, K. Junge, S. Gladiali and M. Beller, *J. Mole. Cat. A.*, 2008, **280**, 148-155.

22. J. F. Young, J. A. Osborn, F. A. Jardine and G. Wilkinson, *J. Chem. Soc., Chem. Commun*., 1965, 131-132.

23. C. O'Connor and G. Wilkinson, *Tetrahedron Lett*., 1969, **10**, 1375-1377.

24. J. Luo, A. G. Oliver and J. S. McIndoe, *Dalton Trans.*, 2013, **42**, 11312-11318.

25. L. Vaska and J. W. DiLuzio, *J. Am. Chem. Soc.*, 1961, **83**, 2784-2785.

26. P. Schwab, R. H. Grubbs and J. W. Ziller, *J. Am. Chem. Soc.*, 1996, **118**, 100-110.

27. M. S. Sanford, J. A. Love and R. H. Grubbs, *J. Am. Chem. Soc.*, 2001, **123**, 6543-6554.

28. R. F. Heck and J. P. Nolley, *J. Org. Chem.*, 1972, **37**, 2320-2322.

29. N. Miyaura and K. Yamada, *Tetrahedron Lett.*, 1979, **2**, 3437-3440.

30. B. J. K. Stille, *Angew. Chem. Int. Ed. Engl.*, 1986, **25**, 508-524.

31. K. Sonogashira, *J. Organomet. Chem.*, 2002, **653**, 46-49.

32. A. O. King, N. Okukado and E. Negishi, *J. Chem. Soc., Chem. Commun.*, 1977, 683-684.

33. P.C. J. Kamer and P. W. N. M. van Leeuwen, Phosphorus (III) ligands in homogeneous catalysis: design and synthesis, John Wiley & Sons Ltd, New Jersey, 2012.

34. R. Noyori, *Angew. Chem. Int. Ed.*, 2002, **41**, 2008-2022.

35. R. Noyori, H. Takaya, *Acc. Chem. Res.*, 1990, **23**, 345–350.

36. P. J. Pye, K. Rossen, R. A. Reamer, R. P. Volante and P. J. Reider, *Tetrahedron Lett.*, 1998, **39**, 4441-4444.

37. P. J. Pye, K. Rossen, R. A. Reamer, N. N. Tsou, R. P Volante and P. J. Reider, *J. Am. Chem. Soc.*, 1997, **119**, 6207-6208.

38. H. Staudinger and J. Meyer, *Helv. Chim. Acta.*, 1919, **2**, 635-646.

39. Y. G. Gololobov, I. N. Zhmurova and L. F. Kasukhin, *Tetrahedron.*, 1981, **37**, 437-472.

40. R. W. Hoffmann, *Angew. Chem*., 2001, **40**, 1411-1416.

41. S. Fletcher, *Org. Chem. Front.*, 2015, **2**, 739-752.

42. P. Steenwinkel, D. M. Grove, N. Veldman, A. L. Spek, and G. van Koten, *Organometallics*., 1998, **17**, 5647-5655.

43. D. R. Reddy and B. G. Maiya, *Chem. Commun.*, 2001, 117-118.

44. J. Crassous and R. Reau, *Dalton Trans.*, 2008, 6865-6876.

45. Y. Dienes, M. Eggenstein, T. Karpati, T. C. Sutherland, L. Nyulaszi and T. Baumgartner, *Chem. Eur. J.*, 2008, **14**, 9878-9889.

46. D. Joly, P. A. Bouit and M. Hissler, *J. Chem. Mater. Chem. C.*, 2016, **4**, 3686-3698.

47. Nalwa, H. S. Handbook of conductive materials and polymers; John Wiley and Sons: New York, 1997.

48. B. Werner, J. Posdorfer, B. Webling, H. Becker, S. Heun, H. Vestweber and T. Hassenkam, *SID 02 Digest.*, 2002, **33**, 603-605.

49. G. Fu, Y. He, W. Li, B. Wang, X. Lu, H. He and W. Wong, *J. Mater. Chem. C.*, 2019, **7**, 13743-13747.

50. F. M. A. Almuntaser, S. Majumder, P. K. Braviskar, J. V. Sali and B. R. Sankapal, *Applied Phys. A.*, 2017, **123**, 1-8.

51. T. Baumgartner and R. Reau, *Chem. Rev.*, 2006, **106**, 4681-4727.

52. U. Mitsche and P. Bauerle, *J. Mater. Chem.*, 2000, **10**, 1471-1507.

53. M. Tang, S. Zhu, Z. Liu, C. Jiang, Y. Wu, H. Li, B. Wang, E. Wang, J. Ma and C. Wang, *Inside Chem.*, 2018, **4**, 2600-2614.

54. F. Babudri, G. M. Farinola and F. Naso, *J. Mater. Chem.*, 2004, **14**, 11-34.

55. F. Babudri, G. M. Farinola, F. Naso and R. Ragni, *Chem. Commun.*, 2007, 1003-1022.

56. V. A. Wright, B. O. Patrick, C. Schneider and D. P. Gates, *J. Am. Chem. Soc.*, 2006, **128**, 8836-8844.

57. Mathey, F. Phosphorus-carbon Heterocyclic Chemistry: The Rise of a New Domain; Elsevier Science Ltd: Oxford, 2001.

58. D. E. Cabelli, A. H. Cowley and M. S. Dewar, *J. Am. Chem. Soc.*, 1981, **103**, 3286

59. Z. Zhang, Z. Zhang, R. Chen, J. Jia, C. Han, C. Zheng, H. Xu, D. Yu, Y. Zhao, P. Yan, S. Liu and W. Huang, *Chem. Eur. J.*, 2013, **19**, 9549-9561.

60. M. P. Duffy, W. Delaunay, P. A. Bouit and M. Hissler, *Chem. Soc. Rev.*, 2016, **45**, 5296-5310.

61. M. P. Washington, V. B. Gudimetla, F. L. Laughlin, N. Deligonul, S. He, J. L. Payton, M. C. Simpson and J. D. Protasiewicz, *J. Am. Chem. Soc.*, 2010, **132**, 4566-4567.

62. M. P. Washington, J. L. Payton, M. C. Simpson and J. D. Protasiewicz, *Organometallics.*, 2011, **30**, 1975-1983.

63. B. W. Rawe, M. R. Scott, C. M. Brown, H. K. MacKenzie and D. P. Gates, *Macromolecules.*, 2017, **50**, 8916-8927.

64. B. W. Rawe, C. M. Brown, M. R. MacKinnon, B. O. Patrick, G. J. Bodwell and D. P. Gates, *Organometallics.*, 2017, **36**, 2520-2526.

65. X. Chai, X. Cui, B. Wang, F. Yang, Y. Cai, Q. Wu and T. Wang, *Chem. Eur. J.,* 2015, **21**, 16754-16758.

66. T. Baumgartner, *Acc. Chem. Res.*, 2014, **47**, 1613-1622.

67. T. Leyssens and D. Peeters, *J. Org. Chem.*, 2008, **73**, 2725-2730.

68. Y. Ren and T. Baumgartner, *Dalton Trans.*, 2012, **41**, 7792-7800.

69. S. Yamaguchi, S. Akiyama and K. Tamao, *J. Organomet. Chem.*, 2002, **652**, 3-9.

70. T. L. Scott and M. O. Wolf, *J. Phys. Chem. B.*, 2004, **108**, 18815-18819.

71. E. Regulska, H. Ruppert, F. Rominger and C. Romero-Nieto, *J. Org. Chem.*, 2020, **85**, 1247-1252.

72. P. Hindenberg, F. Rominger and C. Romero-Nieto, *Angew. Chem. Int. Ed.*, 2021, **60**, 766-773.

73. H. Tsuji, K. Sato, Y. Sato and E. Nakamura, *J. Mater. Chem*, 2009, **19**, 3364-3366.

74. J. A. A. Qahouq, W. Al-Hoor, L. Yao and I. Batarseh, *IEEE Trans.*, 2009, **56**, 2277-2280.

75. Y. Xiang, Y. Zhao, N. Xu, S. Gong, F. Ni, K. Wu, J. Luo, G. Xie, Z. Lu and C. Yang, *J. Mater. Chem. C.*, 2017, **5**, 12204-12210.

76. D. Wu, L. Chen, N. Kwon and J. Yoon, *Inside Chem.*, 2016, **1**, 674-698.

77. H. Su, O. Fadhel, C. Yang, T. Cho, C. Fave, M. Hissler, C. Wu and R. Reau, *J. Am. Chem. Soc.*, 2006, **128**, 983-995.

78. F. Mathey, *Chem. Rev.*, 1988, **88**, 429-453.

79. K.Fourmy, S. Mallet-Ladeira, O. Dechy-Cabaret and M. Gouygou, *Organometallics.*, 2013, **32**, 1571-1574.

80. J. P. Green, D. M. Salazar, A. K. Gupta and A. Orthaber, *J. Org. Chem.*, 2020, **85**, 14619-14626.

81. Y. Dienes, M. Eggenstein, T. Neumann, U. Englert and T. Baumgartner, *Dalton Trans.*, 2006, 1424-1433.

82. Y. Li, J. Liu, Y. Zhao and Y. Cao, *Materials Today.*, 2017, **20**, 258-266.

83. X. He, J. Lin, W. H. Kan and T. Baumgartner, *Angew. Chem. Int. Ed.*, 2013, **52**, 8990-8994.

84. X. He, J. Borau-Garcia, A. Y. Y. Woo, S. Trudel and T. Baumgartner, *J. Am. Chem. Soc.*, 2013, **135**, 1137-1147.

85. H. J. Becher, D. Fenske, and E. Langer, Chem. Ber., 1974, **107**, 117-122.

86. R. A. Baber, M. L. Clarke, A. G. Orpen and D. A. Ratcliffe, *J. Organomet. Chem.*, 2003, **667**, 112-119.

87. A. J. Saunders, I. R. Crossley and S. M. Roe, *Eur. J. Inorg. Chem.*, 2016, 4076-4082.

88. P. Kumar, V. S. Kashid, Y. Reddi, J. T. Mague, R. B. Sunoj and M. S. Balakrishna, *Dalton Trans.*, 2015, **44**, 4167-4179.

89. A. C. Tsipis, *Organometallics.*, 2006, **25**, 2774-2781.

90. R. G. Kostyanovsky, V. V. Yakshin and S. L. Zimont, *Tetrahedron.*, 1968, **24**, 2995-3000.

91. L. Zhang, S. Su, H. Wu and S. Wang, *Tetrahedron.*, 2009, **65**, 10022-10024.

92. J. Brunet, A. Capperucci, R. Chauvin and B. Donnadieu, *J. Organomet. Chem.*, 1997, **553**, 79-81.

93. C.J. Brown and A. C. Farthing, *Nature.*, 1949, **164**, 915-916.

94. D. J. Cram and J. M. Cram, *Acc. Chem. Res.*, 1971, **4**, 204-213.

95. P. G. Ghasemabadi, T. Yao and G. J. Bodwell, *Chem. Soc. Rev.*, 2015, **44**, 6494-6518.

96. E. Elacque and L. R. MacGillivray, *Eur. J. Org. Chem.*, 2010, 6883-6894.

97. A. E. Mourad, *Spec. Act. Part A: Mol. Spec.*, 1987, **43**, 11-15.

98. G. C. Bazan, W. J. Oldham, Jr. R. J. Lachicotte, S. Tretiak, V. Chernyak and S. Mukamel, *J. Am. Chem. Soc.*, 1998, **120**, 9188-9204.

99. W. Baker, K. M. Buggle, J. F. W. McOmie and D. A. M. Watkins, *J. Chem. Soc.*, 1958, 3594-3603.

100. J. Bruhin and W. Jenny, *Chimia*, 1971, **25**, 308.

101. A. K. Wisor and L. Czuchajowski, *J. Phys. Chem.*, 1986, **90**, 1541-1547.

102. R. Gleiter, H. Hopf, Modern Cyclophane Chemistry, John Wiley & Sons, Weinheim, 2006, 150-160.

103. P. M. Keehn and S. M. Rosenfeld, Organic Chemistry: A Series of Monographs – Volume 45-II: Cyclophanes, Academic Press, New York, 1983, 359-436.

104. R. H. Mitchell and V. Boekelheide, *J. Am. Chem. Soc.*, 1974, **96**, 1547-1557.

105. H. E. Winberg, F. S. Fawcett, W. E. Mochel and C. W. Theobald, *J. Am. Chem. Soc.*, 1960, **82**, 1428-1435.

106. J. F. Haley Jr and P. M. Keehn, *Tetrahedron. Lett.*, 1975, **16**, 1675-1678.

107. F. Vogtle, Cyclophane Chemistry: Synthesis, Structures and Reactions, John Wiley & Sons, West Sussex – England, 1993, 169-185.

108. Y. I. Blokhin, K. N. Kornilov, Y. V. Osipova, A.M. Bagautdinov, M. V. Tabardak and I. A. Lubimov, *Phosphorus, Sulfur Silicon Relat. Elem.*, 2013, **188**, 1478-1496.

109. E. E. Nifant'ev, E. N. Rasadkina and Y. B. Evdokimenkova, *J. Gen. Chem. USSR.*, 2001, **71**, 366-372.

110. E. N. Rasadkina, P. V. Slitikov, M. S. Mel'nik, A. I. Stash, V. K. Bel'skii and E. E. Nifant'ev, *J. Gen. Chem. USSR.*, 2004, **74**, 1080-1086.

111. A. J. Saunders, I. R. Crossley, M. P. Coles and S. M. Roe, *Chem. Commun.*, 2012, **48**, 5766-5768.

112. M. Schmallegger, A. Eibel, J. P. Menzel, A. Kelterer, M. Zalibera, C. Berner-Kowollik, H. Grutzmacher and G. Gescheidt, *Eur. J. Chem.*, 2019.

113. K. Dietliker, T. Jung, J. Benkhoff, H. Kura, A. Matsumoto, H. Oka, D. Hristova, G. Gescheidt and G. Rist, *Macromol. Symp.*, 2004, **217**, 77-97.

114. V. S. Kashid, L. Radhakrishna and M. S. Balakrishna, *Dalton. Trans.*, 2017, **46**, 6510-6513.

115. K. Bourumeau, A. Gaumont and J. Denis, *J. Organomet. Chem.,* 1997, **529**, 205-213.

116. Y. Takeda, K. Hatanaka, T. Nishida, S. Minakata, *Chem. Eur. J.*, 2016, **22**, 10360-10364.

117. J. A. Iggo, NMR Spectroscopy in Inorganic Chemistry, Oxford University Press, Oxford, 1999.

118. C. A. Tolman, *J. Am. Chem. Soc.*, 1970, **92**, 2953-2956.

119. G. Glockler, *J. Phys. Chem.*, 1958, **62**, 1049.

120. Y. Takeda and S. Minakata, *Org. Biomol. Chem.*, 2019, **17**, 7807-7821.

121. R. Ruzziconi, S. Spizzichino, A. Mazzanti, L. Lunazzi and M. Schlosser, *Org. Biomol. Chem.*, 2010, **8**, 4463-4471.

122. J. Porter, M. Sola and F. M. Bickelhaupt, *Chem. Eur. J.*, 2006, **12**, 2889-2895.

123. T. Hanemann, W. Haase, I. Svoboda and H. Fuess, *Liquid Crystals.*, 1995, **19**, 699-702.

124. D. Ajami, O. Oeckler, A. Simon and R. Herges, *Nature*., 2003, **426**, 819-821.

125. L. Zhang, G. H. Peslherbe and H. M. Muchall, *Can. J. Chem.*, 2010, **88**, 1175-1185.

126. C. Hansch, A. Leo and R. W. Taft, *Chem. Rev.*, 1991, **91**, 165-195.

127. A. Eibel, M. Schmallegger, M. Zalibera, A. Huber, Y. Burkl, H. Grutzmacher and G. Gescheidt, *Eur. J. Inorg. Chem.*, 2017, 2469-2478.

128. C. Romero-Nieto, A. Lopez-Andrarias, C. Egler-Lucas, F. Gerbert, J. Neus and O. Pilgram, *Angew. Chem. Int. Ed.*, 2015, **54**, 15872-15875.

129. G. Hua and D. J. Woollins, *Angew. Chem. Int. Ed.*, 2009, **48**, 1368-1377.

130. T. Scherpf, I. Rodstein, M. Paaben and V. H. Gessner, *Inorg. Chem.*, 2019, **58**, 8151-8161.

131. Q. L. Horn, D. S. Jones, R. N. Evans, C. A. Ogle and T. C. Masterman, *Acta. Cryst. E*., 2002, **58**, 51-52.

132. S. N. Berry, N. Busschaert, C. L. Frankling, D. Salter and P. A. Gale, *Org. Biomol. Chem.,* 2015, **13**, 3136-3143.

133. J. F. Malone, C. M. Murray, G. M. Dolan, R. Docherty and A. J. Lavery, *Chem. Mater.*, 1997, **9**, 2983-2989.

134. E. Oberg, A. Orthaber, C. Lescop, R. Reau, M. Hissler and S. Ott, *Chem. Eur. J.*, 2014, **20**, 8421-8432.

135. J. I. Bates, B. O. Patrick and D. P. Gates, *New. J. Chem.*, 2010, **34**, 1660-1666.

136. V. Iaroshenko, Organophosphorus Chemistry: From Molecules to Applications, John Wiley & Sons, Germany, 2019.

137. H. Lesiecki, E. Lindner and G. Vordermaier, *Chem. Ber.*, 1979, **112**, 793-798

138. S. Gowrisankar, C. Federsel, H. Neumann, C. Ziebart, R. Jackstell, A. Spannenberg and M. Beller, *ChemSusChem.*, 2013, **6**, 85-91.

139. Y. Takeda, S. Minakata, *Org. Biomol. Chem.*, 2019, **17**, 7807.

140. G. Grüttner and M. Wiernik, *Chem. Ber.*, 1915, **48**, 1473.

141. R. A. Baber, M. F. Haddow, A. J. Middleton, A. G. Orpen, P. G. Pringle, A. Haynes, G. L. Williams and R. Papp, *Organometallics.*, 2007, **26**, 3, 713-725.

142. M. F. Haddow, A. J. Middleton, A. G. Orpen, P. G. Pringle and R. Papp, *Dalton Trans.*, 2009, 202-209.

143. M. Carreira, M. Charernsuk, M. Eberhard, N. Fey, R. V. Ginkel, A. Hamilton, W. P. Mul, A. G. Orpen, H. Phetmung and P.G. Pringle, *J. Am. Chem. Soc.*, 2009, **131**, 3078-3092.

144. R. Doherty, M. F. Haddow, Z. A. Harrison, A. G. Orpen, P. G. Pringle, A. Turner and R. L. Wingad, *Dalton Trans.*, 2006, 4310-4320.

145. G. A. Johnson and V. P. Wystrach, *J. Am. Chem. Soc.*, 1960, **82**, 4437-4438.

146. B. M. Butin, G. M. Isaeva, R. N. Ll'yasov and K. B. Erzhanov, *J. Gen. Chem. USSR.*, 1982, **52**, 1702.

147. J. D. Nobbs, C. H. Low, L. P. Stubbs, C. Wang, E. Drent, M. V. Meurs, *Organometallics*, 2017, **36**, 391-398.

148. T. Brenstrum, J. Clattenburg, J. Britten, S. Zavorine, J. Dyck, A. J. Robertson, J. McNulty, A. Capretta, *Org. Lett.*, 2006, **8**, 103-105.

149. S. O. Grim, W. Mcfarlane, *Nature.*, 1965, **208**, 995-996.

150. G. Becker, Z. Anorg. Allg. Chem., 1976, **423**, 121-133.

151. K. M. Szkop, M. B. Geeson, D. W. Stephan and C. C. Cummins, *Chem. Sci.*, 2019, **10**, 3627-3631.

152. Search of CCDC: C. R. Groom, I. Bruno, M. P. Lightfoot, S. C. Ward, *Acta Crystallogr., Sect. B: Struct. Sci, Cryst. Eng. Mater.*, 2016, **72**, 171-179.

153. T. W. G. Solomons and C. B. Fryhle, Solomons & Fryhle Organic Chemistry, John Wiley & Sons, Inc., United States of America, 8th Edition, 2003.

154. B. J. Dunne and A. G. Orpen, *Acta. Cryst.*, 1991, **47**, 345-347.

155. J. F. Blount, *Tetrahedron Lett.*, 1975, **16**, 909-912.

156. S. Sasaki, K. Sutoh, F. Murakami and M. Yoshifuji, *J. Am. Chem. Soc.*, 2002, **124**, 14830-14831.

157. R. T. Boere and M. Taghavikish, *Acta Crystallogr., Sect. C: Cryst. Struct. Commun.*, 2012, **68**, 381-382.

158. A. H. Cowley, M. Pakulski, N. C. Norman, *Polyhedron*, 1987, **6**, 915-919.

159. S. Roy, P. Stollberg, R. Herbst-Irmer, D. Stalke, D. M. Andrada, G. Frenking and H. W. Roesky, *J. Am. Chem. Soc.*, 2015, **137**, 150-153.

160. L. Wu, S. S. Chitnis, H. Jiao, V. T. Annibale, I. Manners, *J. Am. Chem. Soc.*, 2017, **139**, 16780-16790.

161. C. P. Rooney, J. L. Wade, A. C. Hinkle, R. M. Stolley, S. M. Miller, M. L. Helm, *Main Group Chem.*, 2008, **7**, 155-165.

162. J. C. Calabrese, R. T. Oakley, R. West, *Can. J. Chem.*, 1979, **57**, 1909-1914.

163. L.-C. Liang, J.-M. Lin, and W.-Y. Lee, *Chem. Commun.*, 2005, 2462.

164. P. G. Waddell, A. W. Slawin and J. D. Woollins, *Dalton Trans.*, 2010, **39**, 8620-8625.

165. C. J. Elsevier, B. Kowall and H. Kragten, *Inorg. Chem.*, 1995, **34**, 4836-4839.

166. J. Vincente, J. Gil-Rubio, D. Bautista, A. Sironi and N. Masciocchi, *Inorg. Chem.*, 2004, **43**, 5665-5675.

167. M. L. Wu, M. J. Desmond and R. S. Drago, *Inorg. Chem.*, 1979, **18**, 679-686.

168. B. R. James and D. Mahajan, *Can. J. Chem.*, 1979, **57**, 181-187.

169. J. A. Ibers and R. G. Snyder, *Acta. Cryst.*, 1962, **15**, 923-930.

170. B. J. Dunne, R. B. Morris and A. G. Orpen, *J. Chem. Soc. Dalton. Trans.*, 1991, 653-661.

171. S. O. Grim, P. R. McAllister and R. M. Singer, *J. Chem. Soc. D.*, 1969, 38-39.

172. M. Joost, W. J. Transue and C. C. Cummins, *Chem. Commun.*, 2017, **53**, 10731-10733.

173. G. G. Mather and A. Pidcock, *Chem.*and A. Pidcock, *J. Am. Chem. Soc.*, 1967, **89**, 1226-1229.

174. A. G. Orpen and N. G. Connelly, *Organometallics.*, 1990, **9**, 1206-1210.

175. S. T. Massey, B. Mansour and L. McElwee-White, *J. Organomet. Chem.*, 1995, **485**, 123-126.

176. R. G. Goel, W. O. Ogini and R. C. Srivastava, *J. Organomet. Chem.*, 1981, **214**, 405-417.

177. S. Holland and F. Mathey, *Organometallics.*, 1988, **7**, 1796-1801.

178. I. Inubushi, N. H. T. Huy, F. Mathey, *Chem. Commuun.*, 1996, 1903-1904.

179. V. Nesterov, L. Duan, G. Schnakenburg, R. Streubel, *Eur. J. Inorg. Chem.*, 2011, 567-572.

180. F. Nief, F. Mercier and F. Mathey, *J. Organomet. Chem.*, 1987, **328**, 349-355.

181. T. A. McCampbell, B. A. Kinkel, S. M. Mille and M. L. Helm, *J. Chem. Cryst.*, 2006, **36**, 271-275.

182. F. A. Cotton, D. J. Darensbourg and B. W. S. Kolthammer, *Inorg. Chem.*, 1981, **20**, 4440-4442.

183. M. J. Aroney, I. E. Buys, M. S. Davies and T. W. Hambley, *J. Chem. Soc. Dalton Trans.*, 1994, 2827-2834.

184. J. Pickardt, L. Rosch and H. Shumann, *Z. Anorg. Allg. Chem.*, 1976, **426**, 66-76.

185. J. F. Nixon and A. Pidcock, *Annual Reports on NMR Spectroscopy*., 1969, **2**, 345-422.

186. F. Heinemann and H. Schmidt, *Z. Kristallogr.*, 1992, **198**, 123-124.

187. W. Buchner and W. A. Schenk, *Inorg. Chem.*, 1984, **23**, 132-137.

188. H. K. Fun, S. Chantrapromma, Y. C. Liu, Z. F. Chen and H. Liang, *Acta Cryst. E.*, 2006, **62**, 1252-1254.

189. T. Barber, S. P. Argent and L. T. Ball, *ACS Catal.*, 2020, **10***,* 5454-5461.

190. P. J. Hay and W. R. Wadt, *J. Chem. Phys.*, 1985, **82**, 299–310.

191. K. B. Dillon, F. F. Mathey, J. F. Nixon, *Phosphorus: The Carbon Copy: From Organophosphorus to Phospha-organic Chemistry*, John Wiley and Sons, Chichester, 1998.

192. L. Pauling, *The Chemical Bond*, Cornell University Press, Ithaca, New York, 1967

193. A. L. Allred and A. L. Hensley Jr, *J. Inorg. Nucl. Chem.*, 1961, **17**, 43-54.

194. S. Lacombe, D. Gonbeau, J. L. Cabioch, B. Pellerin, J. M. Denis and G. Pfister-Guillouzo, *J. Am. Chem. Soc.*, 1988, **110**, 6964–6967.

195. A. Marinetti, S. Bauer, L. Ricard and F. Mathey, *Organometallics.*, 1990, **9**, 793-798.

196. J-F. Pilard, A-C. Gaumont, C. Friot and J-M. Denis, *Chem. Commun.*, 1998, 457-458.

197. T. A. Van der Knaap, F. Bickelhaupt, J. G. Kraaykamp, G. Van Koten, J. P. C. Bernards, H. T. Edzes, W. S. Veeman, E. De Boer and E. J. Baerends, *Organometallics.*, 1984, **3**, 1804-1811.

198. G. Becker, *Z. Anorg. Allg. Chem.*, 1976, **439**, 121-133.

199. R. Appel, B. Laubach, and M. Siray, *Tetrahedron Lett.*, 1984, **25**, 4447-4448.

200. A. Jouaiti, M. Geoffroy, and G. Bernardinelli, *Tetrahedron Lett.*, 1992, **33**, 5071-5074.

201. T. C. Klebach, R. Lourens and F. Bickelhaupt, *J. Am. Chem. Soc.*, 1978, **100**, 4886–4888.

202. N. Trathen, V. K. Greenacre, I. R. Crossley and S. M. Roe, *Organometallics*., 2013, **32**, 2501–2504.

203. M. Regitz and P. Binger, *Angew. Chem.*, 1988, **100**, 1541-1565.

204. T. E. Gier, *J. Am. Chem. Soc.*, 1961, **83**, 1769-1770.

205. M. Regitz, *Chem. Rev.*, 1990, **90**, 191-213.

206. L. N. Markovski and V. D. Romanenko, *Tetrahedron.*, 1989, **45**, 6019-6090.

207. H. E. Hosseini, H. W. Kroto and J. F. Nixon, *J. Chem. Soc., Chem. Commun.*, 1979, 653-654.

208. M. Yam, C-W. Tsang and D. P. Gates, *Inorg. Chem.*, 2004, **43**, 3719-3723.

209. C. J. Herbert, PhD Thesis, University of Manchester, 2010.

210. J. C. Hierso, *Chem. Rev.*, 2014, **114**, 4838-4867.

211. K. Ohtsuki, H. T. G. Walksgrove, Y. Hayashi, S. Kawauchi, B. O. Patrick, D. P. Gates and S. Ito, *Chem. Commun.*, 2020, **56**, 774-777.

212. V. G. Becker, M. Rössler, and W. Uhl, *Z. Anorg. Allg. Chem.*, 1981, **473**, 7.

213. N. Muller, P. C. Lauterbur and J. Goldenson, *J. Am. Chem. Soc.*, 1956, **78**, 3557-3561.

214. J. D. Masuda and R. T. Boere, *Dalton Trans.*, 2016, **45**, 2102-2115.

215. N. G. Petrochko, J. M. Ash, M. M. Choate, J. Spott and R. Peters, *Inorg. Chimi. Acta.*, 2013, **402**, 116-122.

216. C. G. Barlow, D. L. Miller and R. A. Newmark, *Magn. Reson. Chem.*, 2000, **38**, 38-42.

217. V. D. Romanenko, M. Sanchez, T. V. Sarina, M. Mazieres and R. Wolf, *Tetrahedron Lett.*, 1992, **33**, 2981-2982.

218. C. Cesari, L. Ciabatti, C. Femoni, M. C. Lapalucci, F. Mancini and S. Zacchini, *Inorg. Chem.*, 2017, **56**, 1655-1668.

219. K. B. Dillon, A. E. Goeta, P. K. Monks ad H. J. Shepherd, *Polyhedron.*, 2010, **29**, 606-612.

220. W. R. Dolbier Jr, Guide to fluprine NMR for Organic Chemists, Second Edition, John Wiley & Sons, Chichester, 2016, Chapter 4, 133-186.

221. G. K. S. Prakash, P. V. Jog, P. T. D. Batamack and G. A. Olah, *Science.*, 2012, **338**, 1324-1327.

222. S. Wang, J. Han, C. Zhang and H. Qin, *Tetrahedron Lett.*, 2015, **56**, 6219-6222.

223. K. G. Pearce, A. M. Borys, E. R. Clark and H. J. Shepherd, *Inorg. Chem.*, 2018, **57**, 11530-11536.

224. S. A. Garatt, R. P. Hughes, I. Kovacik, A. J. Ward, S. Willemsen and D. Zhang, *J. Am. Chem. Soc.*, 2005, **127**, 15585-15594.

225. D. J. Burton, S. Shinya and R. D. Howells, *J. Am. Chem. Soc.*, 1979, **101**, 3689-3690.

226. J. G. Cordaro, D. Stein and H. Grutzmacher, *J. Am. Chem. Soc.*, 2006, **128**, 14962-14971.

227. K. Toyota, S. Kawasaki and M. Yoshifuji, *J. Org. Chem.*, 2004, **69**, 5065-5070.

228. J. Guillemin, T. Janati and J. Denis, *J. Org. Chem.*, 2001, **66**, 7864-7868.

229. L. L. Liu, J. Zhou, L. L. Cao and D. W. Stephan, *J. Am. Chem. Soc.*, 2019, **141**, 16971-16982.

230. P. Payard, L. A. Perego, L. Grimaud and L. Ciofini, *Organometallics.*, 2020, **39**, 3121-3130.

231. V. K. Greenacre, N. Trathen and I. R. Crossley, *Organometallics.*, 2015, **34**, 2533-2542.

232. G. B. Kauffman, *J. Chem. Educ.*, 1983, **60**, 185-186.

233. Togni, A.; Halterman, R. L. Metallocenes: Synthesis, Reactivity, Applications; Wiley-VCH: New York, 1998; Vols. 1 and 2.

234. D. Zhang, J. Meng and S. Tian, *J. Organomet. Chem.*, 2015, **798**, 341-346.

235. S. Chen, D. Yan, M. Xue, Y. Hong, Y. Yao and Q. Shen, *Org. Lett.*, 2017, **19**, 3382-3385.

236. B. M. Day, F. Guo and R. A. Layfield, *Acc. Chem. Res.*, 2018, **51**, 1880-1889.

237. M. A. Angadol, D. H. Woen, C. J. Windorff, J. W. Ziller and W. J. Evans, *Organometallics.*, 2019, **38**, 1151-1158.

238. O. T. Summerscales and F. G. N. Cloke, *Coord. Chem. Rev.*, 2006, **250**, 1122-1140.

239. A. L. Wayda, S. Cheng and I. Mukerji, *J. Organomet. Chem*., 1987, **330**, 17-19.

240. A. Vega and J. Y. Saillard, *Inorg. Chem.*, 2007, **46**, 3295-3300.

241. C. Li, D. Lu and C. Wu, *Sci. Rep.*, 2018, **8**, 7284.

242. N. Maigrot, N. Avarvari, C. Charrier and F. Mathey, *Angew. Chem. Int. Ed. Engl.*, **1995**, 34, 590-592.

243. C. Fish, M. Green, J. C. Jeffery, R. J. Kilby, J. M. Lynam, C. A. Russell and C. E. Willians, *Organometallics.*, 2005, **24**, 5789-5791.

244. A. S. Ionkin, W. J. Marshall, B. M. Fish, A. A. Marchione, L. A. Hower, F. Davidson and C. N. McEwen, *Eur. J. Inorg. Chem.*, 2008, 2386-2390.

245. V. A. Miluykov, O. G. Sinyashin, O. Scherer and E. Hey-Hawkins, *Mendeleev Commun.*, 2002, **12**, 1-2.

246. L. S. H. Dixon, P. D. Matthews, S. A. Solomon and D. S. Wright, *Eur. J. Inorg. Chem.*, 2015, 2041-2045.

247. L. S. H. Dixon, S. Hanf, J. E. Waters, A. D. Bond and D. Wright, *Organometallics.*, 2018, **37**, 4465-4472.

248. I. Jevtovikj, M. B. Sarosi, A. K. Adhikari, P. Lonnecke, and E. Hey-Hawkins, *Eur. J. Inorg. Chem.*, 2015, 2046-2051.

249. C. P. Butts, M. Green, T. N. Hooper, R. J. Kilby, J. E. McGrady, D. A. Pantazis and C. A. Russell, *Chem. Commun.*, 2008, 856-858.

250. J. Bresien, D. Michalik, A. Schulz, A. Villinger and E. Zander, *Angew. Chem. Int. Ed.*, 2020.

251. D. Usharani, A. Poduska, J. F. Nixon and E. D. Jemmis, *Chem. Eur. J.*, 2009, **15**, 8429-8442.

252. A. Steffen, R. M. Ward, W. D. Jones and T. B. Marder, *Coord. Chem. Rev.*, 2010, **254**, 1950-1976.

253. D. A. Loginov, D. V. Muratov, Y. V. Nelyubina, J. Laskova and A. R. Kudinov, *J. Mol. Cat. A.*, 2017, **426**, 393-397.

254. I. R. Crossley, *Personal Communication.*

255. R. Bohra, P. B. Hitchcock, M. F. Lappert and W. Leung, *J. Chem. Soc. Chem. Commun.*, 1989, 728-730.

256. A. M. Arif, A. H. Cowley, M. Pakulski and J. M. Power, *J. Chem. Soc., Chem. Commun.*, 1986, 889-890.

257. S. Hap, L. Szarvvas, M. Nieger and D. Gudat, *Eur. J. Inorg. Chem.*, 2001, 2763-2772.

258. X. Jie, Q. Sun, C. G. Daniliuc, R. Knitsch, M. R. Hansen, H. Eckert, G. Kehr and G. Erker, *Chem. Eur. J.*, 2020, **26**, 1269-1273.

259. E. G. Cox, D. W. J. Cruickshank and J. A. S. Smith, *Nature.*, 1955, **175**, 766.

260. R. C. Fortenberry, C. M. Novak, T. J. Lee, P. P. Bera and J. E. Rice, *ACS Omega 2018.,* **3**, 16035-16039.

261. K. Issleib, J. H. Deylig, *Chem. Ber.*, 1964, **97**, 946–951.

262. M. Gartner, H. Gorls and M. Westerhausen, *Inorg. Chem.*, 2008, **47**, 1397-1405.

263. W. Schlenk and W. Schlenk, Jr, *Chem. Ber*., 1929, **62**, 920-924.

264. R. M. Peltzer, O. Eisentein, A. Nova and M. Cascella, *J. Phys. Chem. B.*, 2017, **121**, 4226-4237.

265. R. A. Anderson, G. Wilkinson, M. F. Lappert and R. Pearce, *Inorg. Synth.*, 1979, **19**, 262−264.

266. P. R. Schleyer, C. Maerker, A. Dransfield, H. Jiao and N. J. R. E. Hommes, *J. Am. Chem. Soc.*, 1996, **118**, 6317-6318.

267. R. Edge, R. J. Less, V. Naseri, E. J. L. McInnes, R. E. Mulvey and D. S. Wright, *Dalton. Trans.*, 2008, 6454-6460.

268. J. D. Masuda, A. J. Hoskin, T. W. Graham, C. Beddie, M. C. Fermin, N. Etkin and D. W. Stephan, *Chem. Eur. J.*, 2006, **12**, 8696-8707.

269. R. C. Compton and C. E. Banks, Understanding Voltammetry, Imperial College Press, London, 2nd Edition, 2011.

270. V. V. Pavlishschuk and A. W. Addison, *Inorg. Chim. Acta.*, 2000, **298**, 97-102.

271. J. A. Bard, B. Parsons and J. Jordon, Standard Potentials in Aqueous Solutions, Dekker: New York, 1985.

272. E. P. Kyba, S. Liu and R. L. Harris, *Organometallics.*, 1983, **2**, 1877-1879.

273. W. A. Munzeiwa, B. Omondi and V. O. Nyamori, *Beilstein J. Org. Chem.*, 2020, **16**, 362-383.

274. M. Yamashita, Y. Suzuki, Y. Segawa and K. Nozaki, *J. Am. Chem. Soc.*, 2007, **129**, 9570-9571.

275. H. J. Reich, J. P. Borst, R. R. Dykstra and P. D. Green, *J. Am. Chem. Soc.*, 1993, **115**, 8728-8741.

276. E. R. Clark, A. M Borys, K. G. Pearce, *Dalton. Trans.*, 2016, **45**, 16125-16129.

277. H. Schumann, G. Rodewals, J. L. Lefferts and J. J. Zuckerman, *J. Organomet. Chem.*, 1980, **190**, 53-63.

278. Y. Li, S. Chakrabarty, C. Muck-Lichtenfeld and A. Studer, *Angew. Chem.*, 2016, **55**, 802-806.

279. B. M. Cossairt and C. C. Cummins, *New J. Chem.*, 2010, **34**, 1533-1536.

280. J. Arras, K. Eichele, B. Maryasin, H. Schubert and C. Ochsenfeld, *Inorg. Chem.*, 2016, **55**, 4669-4675.

281. E. C. Y. Tam, PhD Thesis, University of Sussex, 2012.

282. P. B. Johnson, S. Almstatter, F. Dielmann, M. Bodensteiner and M. Scheer, *Z. Anorg. Allg. Chem*., 2010, **636**, 1275-1285.

283. H. Ranaivonjatovo, J. Escudié, C. Couret, and J. Satge*, J. Chem. Soc., Chem. Commun*., 1992, 1047-1048.

284. K. R. Dixon, In Multinuclear NMR, Plenum Press: New York, 1987, 369-402

285. J. J. Durkin, M. D. Francis, P. B. Hitchcock, C. Jones and J. F. Nixon, *J. Chem. Soc., Dalton Trans.*, 1999, 4057-4062.

286. A. L. Balch and D. E. Oram, *Organometallics.*, 1986, **5**, 2159–2161

287. W. Zhou, R. H. Platel, T. T. Tasso, T. Furuyama, N. Kobayashi and D. B. Leznoff, *Dalton Trans.*, 2015, **44**, 13955-13961.

288. F. Mathey, *Coord. Chem. Rev.*, 1994, **137**, 1-52.

289. E. Madl, E. Peresypkina, A. Y. Timoshkin and M. Scheer, *Chem. Commun.*, 2016, **52**, 12298-12301.

290. C. L. Campion, W. Li and B. L. Lucht, *J. Elec. Chem. Soc.*, 2005, **152**, A2327-A2334.

291. H. Noth and B. Wrackmeyer, *Nuclear Magnetic Resonance Spectroscopy of Boron Compounds.*, Springer: Berlin Heidelberg, 1978, 16-65.

292. I. R. Crossley, M. R. J. Foreman, A. F. Hill, A. J. P. White and D. J. Williams, *Chem. Commun.,* 2005, 221-223.

293. A. J. Marinolich, R. F. Higgins, M. P. Shores and J. R. Neilson, *Chem. Mater.*, 2016, **28**, 1854-1860.

294. J. H. Nelson, *Concepts Mag. Res.*, 2002, **14**, 19-78.

295. O. Kuhl, Phosphorus-31 NMR spectroscopy – A Concise Introduction for the Synthetic Organic and Organometallic Chemist, Springer, 2008.

296. D. E. Koshland, S. E. Myers and J. P. Chesick, *Acta Cryst. B.*, 1977, **33**, 2013-2019.

297. C. W. Tate, P. B. Hitchcock, G. A. Lawless, Z. Benko, L. Nyulaszi and J. F. Nixon, *C. R. Chimie.*, 2010, **13**, 1063-1072.

298. T. Moeller, The Chemistry of the Lanthanides. New York: Reinhold Publishing Corporation, 1963.

299. K. Chen, L. Ouyang, H. Zhong, J. Liu, H. Wang, H. Shao, Y. Zhang and M. Zhu, *Green Chem.*, 2019, **21**, 4380-4387.

300. A. F. Kilpatrick and F. G. N. Cloke, *Dalton Trans.*, 2017, **46**, 5587-5597.

301. A. Streitwieser Jr and U. Mueller-Westerhoff, *J. Am. Chem. Soc.*, 1968, **90**, 7364.

302. N. Tsoureas, *Personal Communication.*

303. J. A. Osborn and G. Wilkinson, *Inorg. Synth.*, 1967, **10**, 68−70.

304. C. Schade, W. Bauer, P. V. R. Schleyer, *J. Organomet. Chem.*, 1985, **295**, c25-c28.

305. G. M. Sheldrick, *Acta Crystallogr. A: Found. Adv.*, 2015, **71**, 3-8.

306. G. M. Sheldrick, *Acta Crystallogr. C: Struct. Chem.*, 2015, **71**, 3-8.

307. O. V. Dolomanov, L. J. Bourhis, R. J. Gildea, J. A. Howard, H. Puschmann, *J. Appl. Crystallogr.*, 2009, **42**, 339-341.

308. M. J. Frisch, G. W. Trucks, H. B. Schlegel, G. E. Scuseria, M. A. Robb, J. R. Cheeseman, G. Scalmani, V. Barone, B. Mennucci, G. A. Petersson, H. Nakatsuji, M. Caricato, X. Li, H. P. Hratchian, A. F. Izmaylov, J. Bloino, G. Zheng, J. L. Sonnenberg, M. Hada, M. Ehara, K. Toyota, R. Fukuda, J. Hasegawa, M. Ishida, T. Nakajima, Y. Honda, O. Kitao, H. Nakai, T. Vreven, J. A. Montgomery Jr., J. E. Peralta, F. Ogliaro, M. Bearpark, J. J. Heyd, E. Brothers, K. N. Kudin, V. N. Staroverov, T. Keith, R. Kobayashi, J. Normand, K. Raghavachari, A. Rendell, J. C. Burant, S. S. Iyengar, J. Tomasi, M. Cossi, N. Rega, J. M. Millam, M. Klene, J. E. Knox, J. B. Cross, V. Bakken, C. Adamo, J. Jaramillo, R. Gomperts, R. E. Stratmann, O. Yazyev, A. J. Austin, R. Cammi, C. Pomelli, J. W. Ochterski, R. L. Martin, K. Morokuma, V. G. Zakrzewski, G. A. Voth, P. Salvador, J. J. Dannenberg, S. Dapprich, A. D. Daniels, O. Farkas, J. B. Foresman, J. V. Ortiz, J. Cioslowski and D. J. Fox, Gaussian 09, Revision D.01, Gaussian, Inc., Wallingford CT, 2013.

309. N. M. O'Boyle, A. L. Tenderhold and K. M. Langner, *J. Comp. Chem.*, 2008, **29**, 839–845.

310. A. D. Groman, J. A. Bailey, N. Fey, T. A. Young, H. A. Sparkes, P. G. Pringle, *Angew. Chem. Int. Ed.*, 2018, **57**, 15802-15806.

311. V. G. Fritz, W. Holderich, *Z. Anorg. Allg. Chem.*, 1977, **431**, 61-75.

312. K. G. Pearce, A. M. Borys, E. R. Clark and H. J. Shepherd, *Inorg. Chem.*, 2018, **57**, 11530-11536.

313. R. Martes, W. Mont, *Chem. Ber.*, 1992, **125**, 657-658.

314. K. Bourumeau, A. Gaumont and J. Denis, *J. Organomet. Chem.*, 1997, **529**, 205-213.

315. J. A. Bailey, M. Ploeger, P. G. Pringle, *Inorg. Chem.*, 2014, **53**, 7763-7769.

316. Y. Takeda, T. Nishida, S. Minakata, *Chem. Eur. J.*, 2014, **20**, 10266-10270.

317. X. Duan, C. Wu, S. Xiang, W. Zhou, T. Yildirim, Y. Cui, Y. Yang, B. Chen and G. Qian, *Inorg. Chem.*, 2015, **54**, 4377-4381.

318. R. Zogota, L. Kinena, C. Withers-Martinez, M. J. Blackman, R. Bobrovs, T. Pantelejevs, I. Kanepe-Lapsa, V. Ozola,K. Jaudzems, E. Suna and A. Jirgensons, *Eur. J. Med. Chem.*, 2019, **163**, 344-352.

319. R. Gatri, I. Ouerfelli, M. L. Efrit, F. Serein-Spirau, J. Lere-Porte, P. Valin, T. Roisnel, S. Bivaud, H. Akdas-Kilig and J. Fillaut, *Organometallics.*, 2014, **33**, 665-676.

320. C. Heim, A. Affeld, M. Nieger and F. Voegtle, *Helv. Chim. Acta*, 1999, **82**, 746-768.

321. K. Jaudzems, K. Tars, G. Maurops, N. Ivdra, M. Otikovs, J. Leitans, I. Kanepe-Lapsa, L. Domraceva, I. Mutule, P. Trapencieris, M. J. Blackman and A. Jirgensons, *ACS Med. Chem. Lett.*, 2014, **5**, 373-377.

322. D. Zhao, X. Rao, J. Yu, Y. Cui, Y. Yang and G. Qian, *Inorg. Chem.*, 2015, **54**, 11193-11199.

323. J. F. Eubank, F. Nouar, R. Luebke, A. J. Cairns, L. Wojtas, M. Alkordi, T. Bousquet, M. R. Hight, J. Eckert, J. P. Ems, P. A. Georgiev and M. Eddaoudi, *Angew. Chem. Int. Ed.*, 2012, **51**, 10099-10103.

324. G. Liu,W. Zhang, S. Zhou, X. Wang and Y. Wang, *RSC Adv.*, 2016, **6**, 68942-68951.

325. C. Song, Y. Ling, Y. Feng, W. Zhou, T. Yildirim and Y. He, *Chem. Commun.*, 2015, **51**, 8508-8511.

326. S. Zulfiqar, S. Awan, F. Karadas, M. Atilhan, C. T. Yavuz and M. I. Sarwar, *RSC Adv.*, 2013, **3**, 17203-17213.

327. K. J. Wicht, J. M. Combrinck, P. J. Smith, R. Hunter and T. J. Egan, *J. Med. Chem.*, 2016, **59**, 6512-6530.

328. J. Morgan and J. T. Pinhey, *J. Chem. Soc., Perkin Trans. 1.*, 1990, 715-720.

329. J. D. Odom, T. F. Moore, R. Goetze, H. Noth and B. Wrackmeyer, *J. Organomet. Chem.*, 1979, **173**, 15-32.

330. C. C. Hsu and R. A. Geanangel, *Inorg. Chem.*, 1980, **19**, 110-119.